



Rüngeler, Elena Elisabeth (2016) *The regulation of cancer cell invasive behaviour by Chloride Interacellular Channel 3 (CLIC3) and Transglutaminasae 2*. PhD thesis.

<http://theses.gla.ac.uk/7379/>

Copyright and moral rights for this work are retained by the author

A copy can be downloaded for personal non-commercial research or study, without prior permission or charge

This work cannot be reproduced or quoted extensively from without first obtaining permission in writing from the author

The content must not be changed in any way or sold commercially in any format or medium without the formal permission of the author

When referring to this work, full bibliographic details including the author, title, awarding institution and date of the thesis must be given

Enlighten:Theses  
<http://theses.gla.ac.uk/>  
theses@gl.a.ac.uk

# **The regulation of cancer cell invasive behaviour by Chloride Intracellular Channel 3 (CLIC3) and Transglutaminase 2**

Elena Elisabeth Rüngeler (BSc, MSc)

Thesis submitted to the University of Glasgow for the degree of  
Doctor of Philosophy

May 2016

CRUK Beatson Institute for Cancer Research

College of Medical, Veterinary and Life Science (MVLS)

## Abstract

A study into the role of secreted CLIC3 in tumour cell invasion

The initiation and progression of cancers is thought to be linked to their relationship with a population of activated fibroblasts, which are associated with tumours. I have used an organotypic approach, in which plugs of collagen I are preconditioned with fibroblastic cells, to characterise the mechanisms through which carcinoma-associated fibroblasts (CAFs) influence the invasive behaviour of tumour cells. I have found that immortalised cancer-associated fibroblasts (iCAFs) support increased invasiveness of cancer cells, and that this is associated with the ability of CAFs to increase the fibrillar collagen content of the extracellular matrix (ECM). To gain mechanistic insight into this phenomenon, an in-depth SILAC-based mass proteomic analysis was conducted, which allowed quantitative comparison of the proteomes of iCAFs and immortalised normal fibroblast (iNFs) controls. Chloride Intracellular Channel Protein 3 (CLIC3) was one of the most significantly upregulated components of the iCAF proteome. Knockdown of CLIC3 in iCAFs reduced the ability of these cells to remodel the ECM and to support tumour cell invasion through organotypic plugs. A series of experiments, including proteomic analysis of cell culture medium that had been preconditioned by iCAFs, indicated that CLIC3 itself was a component of the iCAF secretome that was responsible for the ability of iCAFs to drive tumour cell invasiveness. Moreover, addition of soluble recombinant CLIC3 (rCLIC3) was sufficient to drive the extension of invasive pseudopods in cancer cell lines, and to promote disruption of the basement membrane in a 3D *in vitro* model of the ductal carcinoma *in situ* (DCIS) to invasive ductal carcinoma (IDC) transition.

My investigation into the mechanism through which extracellular CLIC3 drives tumour cell invasiveness led me to focus on the relationship between CLIC3 and the ECM modifying enzyme, transglutaminase-2 (TG2). Through this, I have found that TG2 physically associates with CLIC3 and that TG2 is necessary for CLIC3 to drive tumour cell invasiveness.

These data identifying CLIC3 as a key pro-invasive factor, which is secreted by CAFs, provides an unprecedented mechanism through which the stroma may drive cancer progression.

# Table of Contents

Abstract .....	1
List of Figures .....	5
List of Tables .....	7
Acknowledgements .....	8
Author's Declaration .....	9
Abbreviations .....	10
<b>1 Introduction .....</b>	<b>12</b>
1.1 Cancer cell invasion and metastasis .....	12
1.1.1 The hallmarks of cancer .....	12
1.1.2 Cancer metastasis .....	16
1.1.3 Modes of cell migration .....	19
1.2 The nature of the extracellular matrix .....	25
1.2.1 ECM deposition and remodelling in wound healing .....	26
1.2.2 Parallels between wound healing and cancer .....	28
1.2.3 The ECM and its components in cancer .....	28
1.2.4 Role of the ECM in cancer progression .....	30
1.3 Transglutaminases .....	32
1.3.1 Transglutaminase 2 .....	35
1.3.2 Structure and function .....	35
1.3.3 TG2 and signalling .....	40
1.3.4 Transglutaminase 2 in cancer .....	41
1.4 CLIC proteins .....	43
1.4.1 Phylogeny and structural conservation of CLICs .....	43
1.4.2 The structure of CLIC3 .....	45
1.5 CLICs as membrane inserted proteins .....	48
1.5.1 Ion conductance .....	49
1.5.2 CLICs as glutathione transferases .....	51
1.5.3 CLICs and their role in cancer .....	54
1.6 Project aims .....	57
<b>2 Material and Methods .....</b>	<b>58</b>
2.1 Materials .....	58
2.1.1 Reagents and solutions .....	58
2.1.2 Antibodies and dyes .....	60
2.1.3 Enzyme and kits .....	60
2.1.4 Tissue culture plastic ware .....	61
2.2 Methods .....	61

2.2.1	RNA extraction .....	61
2.2.2	cDNA Synthesis .....	62
2.2.3	Primers for real time PCR.....	63
2.2.4	Real time PCR .....	63
2.2.5	Cloning and DNA manipulation.....	64
2.2.6	Recombinant protein production .....	67
2.2.7	Mammalian cell culture techniques.....	67
2.2.8	Inverted invasion assay.....	71
2.2.9	Generation of cell derived matrix.....	72
2.2.10	Migration assay.....	73
2.2.11	Conditioned Media Experiments .....	73
2.2.12	Fixing and staining cells on CDM.....	74
2.2.13	Protein isolation.....	74
2.2.14	Determination of protein concentration .....	75
2.2.15	SDS-PAGE and Coomassie staining .....	75
2.2.16	Western blotting.....	75
2.2.17	Secretion experiments .....	76
2.2.18	Preparation of collagen I from rat tail tendons .....	76
2.2.19	Organotypic assay.....	77
2.2.20	Determination of Collagen amount .....	78
2.2.21	Three-dimensional basement membrane cultures .....	78
2.2.22	Immunofluorescence of mammary epithelial cells.....	79
2.2.23	Statistics.....	79
<b>3</b>	<b>CLIC3 is secreted by iCAFs to promote the invasive behaviour of tumour cells</b>	<b>81</b>
3.1	Introduction .....	81
3.2	<i>Results</i> .....	83
3.3	<i>iCAFs</i> enhance invasiveness of tumour cells.....	83
	<i>iCAFs</i> influence collagen remodelling in organotypic matrices and increase tumour cell migration and invasion .....	83
	CLIC3 is highly expressed in cancer-associated, but not normal fibroblasts .....	89
3.4	Expression of CLIC3 in <i>iCAFs</i> is required for the generation of a highly fibrillar ECM that supports tumour cell invasion .....	91
	CLIC3 is a component of the CAF secretome that is necessary and sufficient to promote cancer cell invasiveness .....	94
	Characterisation of the pro-invasive attributes of extracellular CLIC3.....	96

Mutation of cysteine residues in CLIC3's thioredoxin fold opposes its ability to drive pseudopod extension.....	104
Extracellular CLIC3 drives tumour cell invasion .....	106
Other CLIC family members elongate invasive pseudopods .....	111
rCLIC3-driven pseudopod extension is $\alpha 5\beta 1$ integrin and RCP-dependent .....	113
3.5 Discussion.....	115
<b>4 Secreted CLIC3 regulates ECM remodelling via TG2 to generate a pro-invasive stroma.....</b>	<b>118</b>
4.1 Introduction .....	118
4.2 Results.....	120
CLIC3 influences transglutaminase-2 behaviour in a redox-dependent manner .....	120
TG2 and CLIC3 collaborate to promote ECM remodelling.....	125
CLIC3-driven tumour cell invasion is TG2 dependent.....	131
4.3 Discussion.....	135
<b>5 General Discussion .....</b>	<b>138</b>
5.1 Summary .....	138
5.2 The function of extracellular CLIC3 in the tumour stroma .....	138
5.3 Secreted CLIC3 regulates ECM remodelling via TG2 to generate a pro-invasive stroma	140
Future Directions .....	144
<b>Bibliography .....</b>	<b>148</b>

## List of Figures

Figure 1.1: The hallmarks of cancer and its emerging hallmarks and enabling characteristics.....	15
Figure 1.2: Cancer metastasis .....	18
Figure 1.3: Schematic overview of some important molecules important in actin polymerisation. ....	20
Figure 1.4: Graphical representation of the different modes of cell migration.....	24
Figure 1.5: X-ray structure of TG2 complexed with Adenosine triphosphate (ATP).....	36
Figure 1.6: The transamidating functions of transglutaminases.....	38
Figure 1.7: Transglutaminase2 exists in 3 different conformations and has several functions. ....	40
Figure 1.8: Crystal structures of the human CLIC proteins (CLIC1 – CLIC4).....	45
Figure 1.9: X-ray structure of CLIC3. ....	47
Figure 1.10: Conserved cysteines in CLIC3 crystallised in the reduced state.....	47
Figure 3.1: The influence of iCAFs on the fibrillar collagen content of organotypic plugs. ....	86
Figure 3.2: Invasion of PDAC cells into organotypic matrices preconditioned with iCAFs or iNFs.....	87
Figure 3.3: iCAF-derived matrix increases the length of invasive pseudopods extended by A2780 cells .....	88
Figure 3.4: CLIC3 is highly expressed in iCAFs by comparison to iNFs.....	90
Figure 3.5: CLIC3 knockdown reduces collagen remodelling by iCAFs.....	92
Figure 3.6: Invasion of PDAC cells into organotypic matrices is opposed by siRNA of CLIC3 expression in the iCAFs used to precondition the plugs. ....	93
Figure 3.7: Identification of CLIC3 as a key pro-invasive component of the iCAF secretome.....	98
Figure 3.8: CLIC3 is secreted from iCAFs and MDA-MB-231 cells. ....	99
Figure 3.9: Production of recombinant CLIC3 and GST. ....	100
Figure 3.10: Response of pseudopod extension to various concentrations of rCLIC3....	101
Figure 3.11: rCLIC3's ability to drive pseudopod extension is ablated by boiling the protein. ....	102
Figure 3.12: Pseudopod extension becomes apparent 5 minutes following rCLIC3 addition.....	103

Figure 3.13: The cysteine residues in CLIC3's thioredoxin domain are required for its ability to drive the extension of invasive pseudopods.....	105
Figure 3.14: Extracellular rCLIC3 promotes tumour cell invasion .....	107
Figure 3.15: Extracellular rCLIC3 leads to a disruption of comedo-like structures formed by MCF10DCIS.com cells.....	109
Figure 3.16: The circularity of MCF10DCIS.com cells was disrupted by extracellular rCLIC3 but not by rGST or the rCLIC3 <sup>C22A</sup> mutant.....	110
Figure 3.17: A comparison of the ability of rCLIC3, rCLIC1 and rCLIC4 to drive pseudopod extension in A2780 cells. ....	112
Figure 3.18: $\alpha 5\beta 1$ integrin and RCP are required for extracellular rCLIC3 to drive the extension of invasive pseudopods. ....	114
Figure 4.1: Thioredoxin is capable of driving extension of invasive pseudopods, but with approximately 30-fold less potency than CLIC3. ....	122
Figure 4.2: Production of recombinant purified TG2.....	123
Figure 4.3: CLIC3 influences the polarised fluorescence signal emanating from the Mant-GMPPNP/rTG2 complex in GSH dependent fashion. ....	124
Figure 4.4: Knockdown of TG2 in iCAFs reduces the fibrillar collagen content of organotypic plugs preconditioned with these cells.....	127
Figure 4.5: Transglutaminase-2 inhibitor Z-DON inhibits CLIC3-driven pseudopod extension, .....	128
Figure 4.6: Knockdown of TG2 in the ECM producing fibroblasts opposes CLIC3-driven pseudopod extension by tumour cells.....	129
Figure 4.7: Addition of soluble rTG2 restores CLIC3-driven pseudopod extension when A2780 cells are plated onto cell-derived matrices generated by TG2 knockdown fibroblasts. ....	130
Figure 4.8: The TG2 small molecule inhibitor Z-DON opposes rCLIC3-driven invasiveness. ....	132
Figure 4.9: CLIC3-promotes disruption of the basement membrane and this is reversed by Z-DON.....	133
Figure 4.10: rCLIC3 and Z-DON do not alter the proliferation rate of MCF10DCIS.com cells.....	134
Figure 4.11: Proposed model for CLIC3's influence on cancer. Adapted from Hernandez, Ruengeler et al., submitted.....	136
Figure 5.1: CLIC3 is a secreted factor from cancer-associated fibroblasts and has the potential to activate TG2. ....	143
Figure 5.2: CLIC3 interacts with TG2 and drives invasion via two possible mechanisms. ....	144

## List of Tables

Table 1.1: Properties of the 9 transglutaminase proteins. ....	34
Table 1.2: The functional diversity of the CLIC proteins. ....	53
Table 2.1: The oligo-dT/template thermal denaturation was performed at first. ....	62
Table 2.2: Reverse transcription reaction setup. ....	62
Table 2.3: Primers used for real time PCR. ....	63
Table 2.4: Reagents which were mixed for PCR assembling. ....	63
Table 2.5: The real time PCR reaction setup. ....	64
Table 2.6: Sequences for mutagenesis primers ....	65
Table 2.7: PCR setup ....	66
Table 2.8: Program used for PCR setup. ....	66

## Acknowledgements

I am grateful for Prof. Jim Norman to take me on as a student during my second year of my PhD. Thank you for the guidance and supervision throughout the last 3 years. I would also thank my advisor Prof. Peter Adams for his support during the more difficult times and his helpful discussions and continuous encouragement. I would also like to thank exR21 for easing my life into the Beatson with lots of cake and helpful discussions. I would also like to thank R20 for taking me on and making the Beatson an enjoyable place to work. Thanks Cat for helping me and I am happy that you joined the lab. Also I would like to thank Dr. Sara Zanivan and Juan Hernandez for being such good collaborators and helping me a lot as well. Thanks Juan for all the discussions. I would also like to thank the Beatson support staff for invaluable help. Thanks to Cancer Research UK for generous funding, which made it possible to conduct this PhD.

I have made very good friends at the Beatson, whom I would like to thank as well. I would have not made it without them. I would like to especially thank Max for his invaluable help, everyday encouragement and for bearing with me every day when times were rough. I would also like to thank Christine and Steven for being very good friends and having an open ear for everything and playing Badminton every week. I would also like to thank Sarah, who was always there when things got hard and always going for a swim throughout the last years. Also I would like to thank Hannah a lot for always being there.

I would further like to thank my family and friends in Scotland and in Germany. Especially, I would like to thank my parents and for their never ending encouragement and for helping me to believe in myself. I am very lucky to have you as parents. I would also like to thank my brother and his family for always being there for me. Finally, I would like to thank my boyfriend Christopher for his invaluable love, encouragement, help and believing in me when I did not. You make me laugh every day and my world is better with you in it.

I dedicate the thesis to my parents.

## Author's Declaration

I, Elena Ruengeler, declare that I am the sole author of this thesis. The work presented here is entirely my own, unless otherwise stated.

A handwritten signature in blue ink, consisting of a stylized 'E' followed by 'R' and 'U' with a long horizontal stroke extending to the right.

Elena Rüngeler

## Abbreviations

ANOVA	Analysis of variance
ATP	Adenosine triphosphate
CAF	Cancer-associated fibroblast
CAM	Cell adhesion molecules
CAT	Collective to amoeboid transition
CDM	Cell-derived matrix
CLIC3	Chloride intracellular channel 3
CM	Conditioned medium
Ctl	Control
DAPI	4',6-Diamidino-2-Phenylindole, Dihydrochloride
DMEM	Dulbecco's Modified Eagle Medium
DMSO	Dimethyl sulphoxide
DCIS	Ductal carcinoma <i>in situ</i>
DNA	Deoxyribonucleic acid
ECM	Extracellular matrix
EDTA	Ethylenediaminetetraacetic acid
EGF	Epidermal growth factor
EMT	Epithelial-mesenchymal transition
ER	Endoplasmic reticulum
FAK	Focal adhesion kinase
FBS	Foetal Bovine Serum
FITC	Fluorescein isothiocyanate
FN	Fibronectin
FRET	Förster resonance energy transfer
GAG	Glycosaminoglycan
GAPDH	Glyceraldehyde-3-phosphate dehydrogenase
GDP	Guanosine diphosphate
GSH	Glutathione
GSSG	Glutathione disulphide
GST	Glutathione S-transferase
GTP	Guanosine triphosphate
IAA-94	Indayloxyacetic acid 94
kDa	Kilodalton

LB	Luria-Bertani medium
LOX	Lysyl oxidase
MAT	Mesenchymal to amoeboid transition
MMP	Matrix Metalloproteinase
MT1-MMP	Membrane-type 1 matrix metalloproteinase
NF	Normal fibroblasts
OD	Optical density
PAGE	Polyacrylamide gel electrophoresis
PBS	Phosphate buffered saline
PBS-T	Phosphate buffered saline - Tween20
PDAC	Pancreatic Ductal Adenocarcinoma
PIP <sub>2</sub>	Phosphatidylinositol 4,5-biphosphate
PG	Proteoglycans
PTEN	Phosphatase and tensin homolog
PCR	Polymerase chain reaction
RCP	Rab-coupling protein
RNA	Ribonucleic acid
RPM	Rotations per minute
SDS	Sodium Dodecyl sulphate
sec	Seconds
siRNA	Short interfering RNA
TBS	Tris-buffered Saline
TBS-T	Tris-buffered Saline- Tween 20
TCF	Transcription factor
TGF- $\beta$	Transforming growth factor $\beta$
TG	Transglutaminase
TIFF	Telomerase immortalised foetal fibroblasts
TIMP	Tissue Inhibitors of Metalloproteinases
TEM	transendothelial migration
Tween20	Polyoxethylene sorbitan monolaurate
U	Units
V	Volts
$\alpha$ -SMA	$\alpha$ - Smooth Muscle Actin
3D	Three-dimensional

# 1 Introduction

## 1.1 Cancer cell invasion and metastasis

### 1.1.1 The hallmarks of cancer

Cancer is a very heterogeneous disease and it was believed that cells only acquired mutations over time, allowing these cells ultimately to change morphology and start proliferating. The cells were found to form insular masses, which spread over lymph nodes to form metastasis at distal sites. This is still valid. However, now it is thought that cancer is composed of complex tissues. They consist of various cell types that cooperate in heterotypic interactions with one another. In the year 2000, Hanahan and Weinberg published the first version of the hallmarks of cancer (Hanahan and Weinberg 2000). As cancer research has evolved in following 11 years, they published an updated version of the hallmarks of cancer in 2011 (Hanahan and Weinberg 2011).

As the **first hallmark** it was established that cancer cells acquire the trait to sustain chronic proliferation (Figure 1.1). They are able to control their own fate by the production of mitogenic signals, which are mostly growth factors that bind to the cell-surface receptors. Mostly, these receptors contain an intracellular tyrosine kinase domain. The signalling through these receptors elicits intracellular signalling cascades that regulate cell cycle progression, cell growth, cell survival and energy metabolism. Cancer cells are able to produce the growth factor ligands themselves and secrete them in an autocrine manner. The other option is that cancer cells interact with the tumour-associated stroma, which then supplies cancer cells with a variety of growth factors. Moreover, cancer cells either produce more receptors or they produce receptors that do not need ligand binding to be active. In addition, the intracellular signalling pathways promoting cell growth and proliferation can be deregulated in cancer cells. Underlying these hallmarks of cancer are the somatic mutations in cancer cells, which were shown mostly by high-throughput methods such as DNA sequencing analysis. Some activating mutations of downstream signalling pathways deregulate cell cycle control as well as cell growth. Furthermore, inactivation of negative-feedback mechanisms that reduce proliferative

signalling are counted as an underlying hallmark. A prominent example is the PI3-kinase antagonist PTEN phosphatase. The phosphatase expression is in many cases mutated. Therefore, PI3-kinase is constantly active. Its product phosphatidylinositol-3,4,5- triphosphate (PIP<sub>3</sub>) is thus not degraded. This leads to constant active downstream signalling and an increase in cell growth and proliferation. However, excessive cell proliferation identifies the cell as inappropriate, thus it either enters the senescence state or these cells undergo apoptosis. For instance, the cells which express very high levels of oncogenic RAS may enter senescence, which is a viable but non-proliferative state. These cells have an inflated cytoplasm, they express the β-galactosidase enzyme and they show upregulation of tumour suppressors and an absence of proliferation markers. For cancer cells to continue proliferating they can either reduce the amount of oncoproteins or they adapt to the high levels of oncogene expression and deactivate either apoptosis or senescence.

The **second hallmark** of cancer is described as evading the tumour suppressors. When cancer cells undergo indefinite cell proliferation they need to evade very strong negative cell proliferation regulation mechanisms. The two most well-known tumour suppressor genes encode the retinoblastoma (RB) and TP53 proteins. These are important to determine whether cells enter the cell cycle or whether they go towards the senescence programme. RB is important in deciding whether cells enter the cell cycle and thus proliferate or not (Burkhardt and Sage 2008). TP53 is important in transducing inputs from stress signals from intracellular systems. When DNA damage arises, it stops cell cycle progression and only allows continuation of the cell cycle program once the DNA has been repaired. However, experiments show that, when some cells do not express these tumour suppressors, the body shows normal homeostasis and experimental animals do not necessarily acquire cancer. Therefore, redundant mechanisms avoiding cell proliferation must exist. Moreover, cells stop proliferating when touching other cells and this mechanism is called contact-inhibition. A lot of research has identified several proteins which interact with signalling receptors blocking these for their agonists. Thus proliferation is inhibited and the cells stay in a quiescent state.

Yet **another hallmark** of cancer is that the cells acquire the ability to overcome programmed cell death such as apoptosis which is a tightly regulated mechanism where cells are killed (Lowe, Cepero et al. 2004; Adams and Cory 2007).

In addition, replicative immortalisation of cancer cells is described as being one **hallmark** of cancer. Most cells' replicative potential is exhausted after a certain number of cell duplications due to telomere shortening. However, when cells become immortalised the telomeres are not shortened, because of an active telomerase enabling the cells to divide indefinitely. For several years now, replicative senescence has emerged as a tumour suppressor mechanism.

The penultimate of the **hallmarks** comprises the increase in vascularisation of tumours to provide the cancer cells with nutrients. Moreover, the cancer cells are supplied with oxygen whereas CO<sub>2</sub> and other metabolic products are removed. Early on, it was postulated that a certain "angiogenic switch" takes place. During tumour progression the normally quiescent vasculature becomes proliferative and new vessels sprout (Hanahan and Folkman 1996).

The **last cancer hallmark** comprises the ability of cancer cells to invade and spread to distant sites of the body. The cancer cells can establish there and grow in a secondary tumour, which is called the formation of metastasis.

In addition to the major 6 hallmarks of cancer, Hanahan and Weinberg have defined other enabling characteristics and emerging hallmarks ((Hanahan and Weinberg 2011), not yellow coloured hallmarks). Tumour cells need to survive, proliferate and disseminate. However, depending on the tumour type, cells use different mechanisms. Therefore, one enabling characteristic is the acquisition genomic instability, which includes random mutations as well as chromosome rearrangements. The second enabling hallmark denotes the inflammatory state of premalignant as well as malignant lesions. These 2 hallmarks orchestrate other hallmark capabilities.

Moreover, two emerging hallmarks have been proposed. One of them describes the reprogramming of cellular energy metabolism, which supports continued cell

growth and proliferation. The second one which becomes very important for cancer cells is avoidance of the immune system.

In the last few years it has become clear that cancer cells need assistance from neoplastic tumour stroma cells, which accumulate around cancer cells in order to invade and metastasise. The tumour as well as the tumour stroma consists of cancer cells, cancer stem cells and cancer-associated fibroblasts. In addition, the tumour stroma consists of other cells such as endothelial cells, pericytes and immune inflammatory cells. I will describe in more detail the tumour microenvironment as well as the formation of cancer metastasis at different sites.

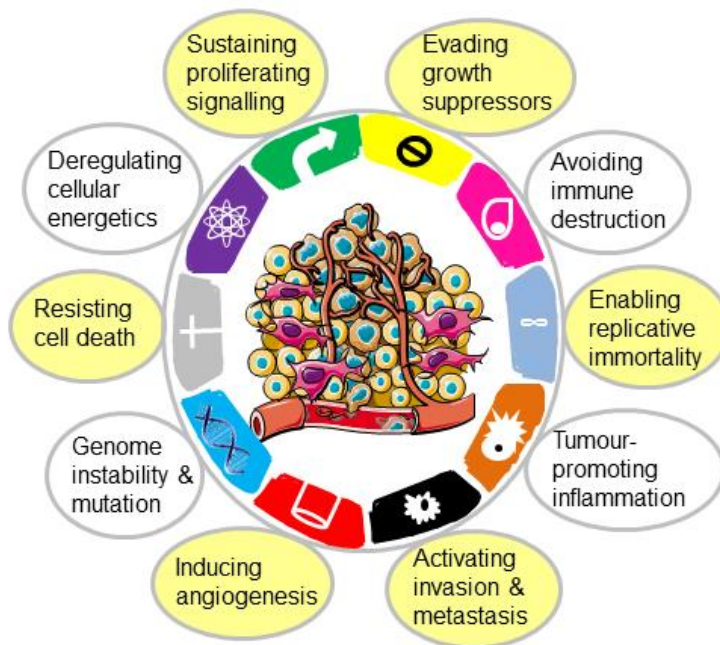


**Figure 1.1: The hallmarks of cancer and its emerging hallmarks and enabling characteristics.**

The six established hallmarks are shown in yellow. The two hallmarks classified as enabling hallmarks are genome instability and mutation as well as the tumour-promoting inflammation. The other two hallmarks that are considered as emerging hallmarks are deregulation of cellular energetics as well as avoidance of the immune system. Adapted from (Hanahan and Weinberg 2011).

### 1.1.2 Cancer metastasis

At the beginning of the 21st century the mechanisms of invasion and metastasis were mostly unknown. Research in the past 15 years has helped to increasingly understand that the formation of cancer metastasis is a multistep process involving loss of cell-cell adhesion, followed by local cell invasion allowing the cells then to undergo intravasation, a process during which cancer cells migrate into the blood stream or the lymphatic system. At a distant site, cancer cells can escape the vessels and settle in tissues (extravasation). They form small nodules of cancer cells as they micrometastasise, followed by the formation of macrometastatic tumours, which is termed 'colonisation' (Hanahan and Weinberg 2011). For cells to become more invasive, they undergo so called 'epithelial-mesenchymal transition' (EMT). EMT is epitomised by transformed epithelial cells, which become resistant to apoptosis and which acquire the ability to invade and disseminate (Barrallo-Gimeno and Nieto 2005; Klymkowsky and Savagner 2009; Polyak and Weinberg 2009). One of the major characteristics of EMT is the loss of cell-cell attachment as well as the cell-to-extracellular matrix (ECM) attachment. E-cadherin, which is one of the most important cell-to-cell adhesion molecules (CAMs), forming bridges between epithelial cells, holding them together and stopping cells from proliferating by signalling through the downstream effectors  $\beta$ -catenin and transcription factor (TCF). The loss of E-cadherin protein expression or mutations are implicated in human cancers (Cavallaro and Christofori 2004; Berx and van Roy 2009; Hanahan and Weinberg 2011). A basement membrane underlies the epithelial cell layers and presents a physical barrier to cancer cell invasion. The membrane consists of a thick layer of glycoproteins and proteoglycans (such as laminins and type IV collagens), which prevent cancer cells from invading into the surrounding stroma. However, when cancer cells acquire invasive and metastatic capabilities, matrix-degrading enzymes or proteases allow dissemination through the basement membrane and the associated ECM (Egeblad and Werb 2002; Palermo and Joyce 2008; Kessenbrock, Plaks et al. 2010). The proteases are usually tightly controlled either by autoinhibition or secreted inhibitors. However, in tumours pro-carcinogenic metalloproteinases are upregulated, and this allows cells to migrate through the basement membrane to reach the vasculature (Kessenbrock, Plaks et al. 2010). To undergo intravasation cells must penetrate the tumour-

associated vasculature. As the tumour needs a supply of oxygen and nutrients, blood vessels grow and surround the tumour. These blood vessels usually grow towards chemoattractants which are secreted from cancer cells and can be, amongst others, either vascular endothelial growth factor (VEGF) or basic fibroblast growth factor (bFGF). The vasculature grows at a fast rate, with these vessels often displaying a dilated and irregular shape. The cancer cells enter the blood vessels by crossing through the endothelial cell (EC) junctions. Once the cancer cells have entered the blood vessel, they need to avoid being killed by the immune system. They need to oppose shear forces, which could lead to physical damage and they need to evade programmed cell death. The cells do survive can extravasate into their hostile microenvironment. They extravasate through the vascular ECs via cell adhesion and chemokine-related processes. During this process several ligands and receptors expressed on cancer cells and ECs allow the cells to adhere to endothelial walls. The cancer cells then migrate through the endothelial wall, via a process called 'transendothelial migration' (TEM), followed by invasion into the basement membrane surrounding the blood vessels. Following extravasation, cells can stay in a quiescent state followed by cell proliferation, the establishment of interactions with the microenvironment as well as initiation of new angiogenic sprouting. Cancer cells then start proliferating to form micrometastasis and thereafter establishing macrometastatic lesions.

For many cancer types it has been identified to which organ they preferably metastasise. In the case of breast cancer disseminated cancer cells preferably metastasise to the lymph nodes, the bone, the liver, the lung and the brain (Kennecke, Yerushalmi et al. 2010; Vona-Davis, Rose et al. 2014). Ovarian carcinoma cells preferably metastasise to the liver and the peritoneum (Lengyel 2010; Kumar, Gilks et al. 2013). However, the organs to which cancer cells ultimately metastasise depend also on the individual patient.

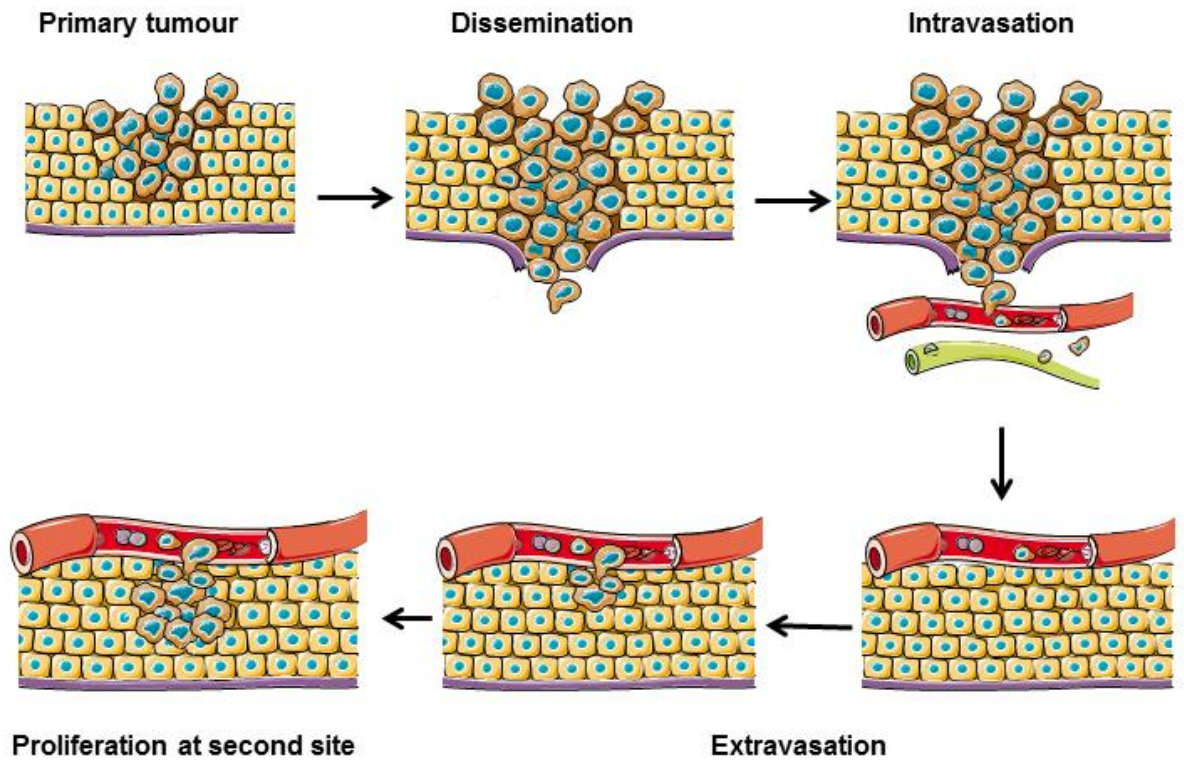


**Figure 1.2: Cancer metastasis**

The formation of cancer metastasis is a multistep process. Cancer cells disseminate from the primary tumour followed by entering the blood stream, which is called intravasation (Friedl and Wolf 2003). This allows them to travel to distant sites where they could then undergo extravasation. These cancer cells form a niche, where they can proliferate forming the so-called metastasis. (Figure adapted from <http://www.servier.co.uk/content/servier-medical-art>.)

### 1.1.3 Modes of cell migration

The migration of non-neoplastic cells during processes such as wound healing, immune cell trafficking or embryonic morphogenesis is very similar to the migration of neoplastic cells. Cancer cells need to acquire locomotory capacity to move from the primary tumour to distant sites, where they can establish metastases (Friedl and Brocker 2000; Friedl and Wolf 2003). For cancer cells to move and undergo EMT several transcriptional alterations have to take place. The most well-known are the repression of Snail and Slug, which keep cells in an epithelial cell shape. Moreover, Twist up-regulation allows cells to become mesenchymal (Wushou, Hou et al. 2014; Grzegorzolka, Biala et al. 2015). In addition, cancer cells can use transforming growth factor  $\beta$  (TGFB) as a cytokine to increase cancer progression (Massague 2008). When the cells diffuse from the primary tumour, they can use several types of migration. In the following sections I will describe the different kinds of movement cells can undergo to disperse from the initial tumour (Friedl and Wolf 2003).

#### 1.1.3.1 Individual cell migration

Several studies both *in vitro* and *in vivo* have shown that individual cells are motile (Enterline and Coman 1950; Wood 1958; Thiery 2002). Friedl *et al.* described, that single cell migration occurs in diverse morphologies. One of them is described as mesenchymal migration, one as amoeboid migration and the final one is known as mesenchymal cell migration in cell chains (Friedl and Wolf 2003).

Mesenchymal cell migration is characterised by cell polarisation at the front of the cell. This migration type is separated into a so-called 5-step migration cycle (Lauffenburger and Horwitz 1996). When cells migrate in a mesenchymal way in 3D environments, they form protrusions at the leading edge. During the second step, cells interact with the ECM and form focal contacts. Throughout this process, integrins at the outside of the cell come into contact with ECM ligands and they form integrin clusters (Cress, Rabinovitz et al. 1995; Cukierman, Pankov et al. 2001). The integrins can convey messages into the cells via their cytoplasmic tails. During the third step, the surface proteases recruited to ECM contacts allow focalised proteolysis. These focal adhesions can transmit the

actomyosin contractile force to the ECM. In the final step the cell body moves forward - following the leading edges - and this allows detachment of the trailing edge. The cell's velocity is relatively slow and in the range of 0.1 - 1  $\mu\text{m}/\text{min}$ . In many cases, mesenchymal cell migration is triggered by receptor tyrosine kinases, such as EGFR or c-Met. This is followed by the generation of  $\text{PIP}_3$  at the cell front. There, the Rac GTPase further undergoes activation and recruits other components such as the Scar/WAVE complex and Actin related protein (Arp2/3) complex. Arp2/3 then nucleates actin branched networks (G-actin into F-actin) (Figure 1.3: Schematic overview of Figure 1.3). In addition, this mode of migration can be initiated via Cdc42 or by oncogenic RAS, which increases the presence of  $\text{PIP}_3$  by activating PI-3 kinase. PTEN as a tumour suppressor can reverse this process (Sahai 2005). RhoA and its effector activities are downregulated in mesenchymal cell migration and in turn RhoA can activate Rac-driven polarised F-actin-rich protrusions (Vial, Sahai et al. 2003).

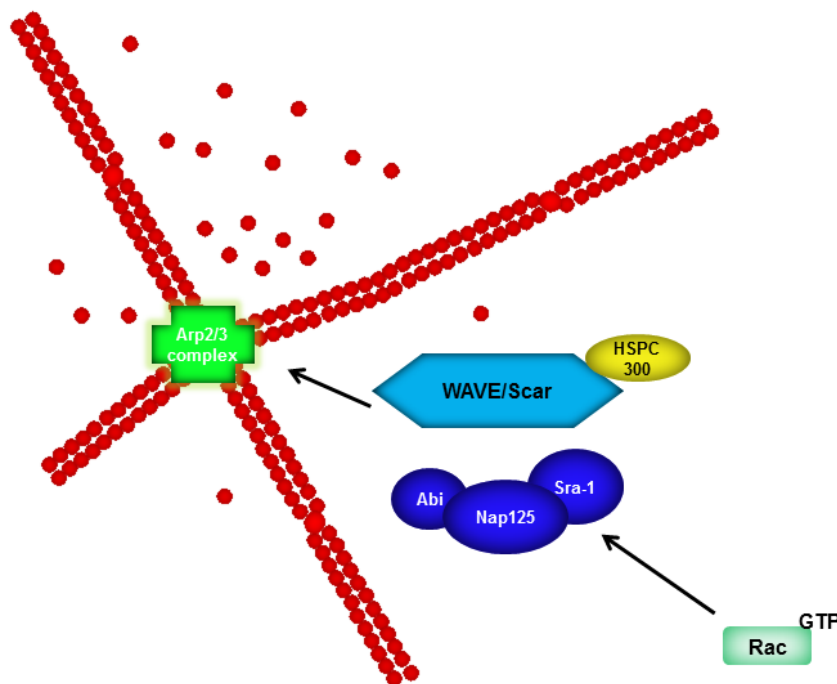


**Figure 1.3: Schematic overview of some important molecules important in actin polymerisation.**

The Arp2/3 complex can bind to existing actin strands. This starts the elongation of the filaments, which causes actin branches (Machesky and Gould 1999). The control of polymerisation or branching of actin by the Arp2/3 complex is taken by the nuclear-promoting factor WAVE/Scar-Abi or Wasp complex (Robinson, Turbedsky et al. 2001). The WAVE complex consists of several proteins including, Nap 125, Abi, Sra-1 and HSPC-300. This complex can be activated by the small GTPase Rac being responsible for the dissociation of the Abi, Nap125 and the Sra-1 from the WAVE. Adapted from (Vicente-Manzanares, Webb et al. 2005).

Mesenchymal cell migration is mostly found in cells present in gliomas and fibrosarcomas, which are connective-tissue tumours (Paulus, Baur et al. 1996; Wolf, Mazo et al. 2003). These cells have a fibroblast-like spindle shaped morphology and use integrins as adhesion molecules. In addition, a chain like migration has been observed for cells from these varieties of tumour. This type of migration occurs in melanomas and non-neoplastic neural crest cells or myoblasts (Jacques, Relvas et al. 1998; El Fahime, Torrente et al. 2000). Specifically in melanoma cells, it has been shown that they move one cell after the other in a chain-like fashion. Even following transplantation of these cells in clumps in 3D collagen they form streams, which move along tracks of remodelled ECM (Friedl, Maaser et al. 1997; Jacques, Relvas et al. 1998). These cells form cell-cell contacts and their communication between one another is thus maintained. Cancer cells form single cell chains and are particularly present in epithelial neoplasms such as breast carcinoma and ovarian carcinoma. Single cell chain migration has been described to be very effective. This might be due to a very effective infiltration mechanism that leads to a high metastatic potential and possibly a poor prognosis (Page and Anderson 1987; Pitts, Rojas et al. 1991; Sood, Seftor et al. 2001; Seftor, Meltzer et al. 2002).

Amoeboid cell migration originates from the single-cell amoeba *Dictyostelium discoideum*. A fair amount of tumour cell lines as well as leukocytes do not follow the mesenchymal cell migration, but the amoeboid migration pattern (Enterline and Coman 1950; Wolf, Mazo et al. 2003). These cells form elongated actin-rich filopodia at the leading edge, but they show a poor interaction with the substrate (Yoshida and Soldati 2006; Smith, Aranda-Espinoza et al. 2007). They rely on the activity of the RhoA-ROCK pathway and they do not require ECM proteolysis in order to penetrate the ECM, but squeeze through existing holes in the ECM. Moreover, due to the few focal contacts and the cells' high deformability, they move at a velocity, which is 10 - 30 fold higher than mesenchymal migration mechanism (Friedl, Zanker et al. 1998; Friedl, Borgmann et al. 2001). However, switching from amoeboid to mesenchymal migration modes is possible. A second form of amoeboid migration is used by zebrafish macrophages as well as some stem cells. They form blebby-like actin rich cytoskeleton structures and move a little slower than other amoeboid cells. They have low polarity and are poorly adhesive. These cells can change migration

behaviour from amoeboid blebby to amoeboid pseudopodal (Blaser, Reichman-Fried et al. 2006).

### **1.1.3.2 Collective tumour cell migration and motility mode switching**

Single-cell and collective cell migration serve different purposes during morphogenesis. Collective cell migration has been described to contribute to cancer progression by local invasion. In addition, collective cell migration takes part in shaping, building and remodelling of complex tissues and compartments such as epithelia, vessels ducts and glands. For collective cell migration, it is important that cell-cell adhesions can form within these cell groups. The cells form a cortical actin filament along cell junctions (Hegerfeldt, Tusch et al. 2002). This leads to the formation of larger sized contractile bodies. The cell at the leading edge generates traction via pseudopod activity (Friedl, Noble et al. 1995; Hegerfeldt, Tusch et al. 2002). These 'leading cells' bind to and cluster  $\beta 1$  integrins at the front protrusion closest to the ECM, and they have an increased expression of MT1-MMP and MMP-2 which leads to ECM degradation (Klinowska, Soriano et al. 1999; Nabeshima, Inoue et al. 2000; Hegerfeldt, Tusch et al. 2002). Therefore, cells migrating in a collective fashion are sensitive to integrin antagonists and susceptible to protease inhibition. The latter has been shown in angiogenesis as well as branching morphogenesis (Hiraoka, Allen et al. 1998; El Fahime, Torrente et al. 2000; Simian, Hirai et al. 2001; Collen, Hanemaaijer et al. 2003). In collective migration, the cells in the inner body or at the trailing edge are dragged passively behind the leading cells (Friedl, Noble et al. 1995).

In cancers two types of collective cell migration exist. In colon, mammary and oral squamous cell carcinoma cells form sheets and perform local invasion without losing contact with the primary tumour (Bell and Waizbard 1986; Page and Anderson 1987; Nabeshima, Inoue et al. 1999). In epithelia carcinomas and melanomas cells detach as a cluster from the primary tumour and form long interstitial tissue gaps as they move along a path, which gives the least resistance (Page and Anderson 1987). Collective cell migration gives selective advantage to the tumour as, during this process, the tumour cells secrete promigratory factors and matrix proteases and the topography of the migrating cell mass protects the inner cells from immunological attacks. Thus, although collective migration is slower than single cell modes of movement, this type of

migration protects cells from immune attack and apoptosis, thus increasing the probability of the tumour to metastasise successfully.

When the tumour progresses, the cells dedifferentiate and epithelial cells can change their migration pattern. In this case, they change from collective invasion to a disseminated cell migration mechanism, and this type of migratory mode-switching conforms roughly to EMT. During the switch from epithelial to mesenchymal-type migration, cells usually lose their cell-cell junctions. However, they keep the expression of promigratory proteins such as integrins (Lochter, Navre et al. 1999; Thiery 2002).

Tumour cells may also switch their migratory mode from mesenchymal to amoeboid-type migration and this has been termed the mesenchymal amoeboid transition (MAT) (Wolf, Mazo et al. 2003). MAT is in many cases followed changes in cell morphology. These changes can be from a fibroblast-like form to rounded shape. Moreover, integrin expression and distribution as well as actin cytoskeletal organisation changes dramatically. It is thought that amongst the factors that are capable of driving MAT are inhibition or proteolysis and the weakening of cell-ECM linkages.

Finally, cells may switch from collective to amoeboid-type migration, and this is termed 'collective to amoeboid transition (CAT). CAT includes breakage of cell-cell contacts and the resulting amoeboid cell migration is  $\beta$ 1-integrin independent. CAT has been reported in small-lung cell carcinoma, as it leads to increased resistance to cytostatic drugs and irradiation (Kraus, Ferber et al. 2002). This switch may also be triggered by upregulation of integrins and increased substrate adhesion.

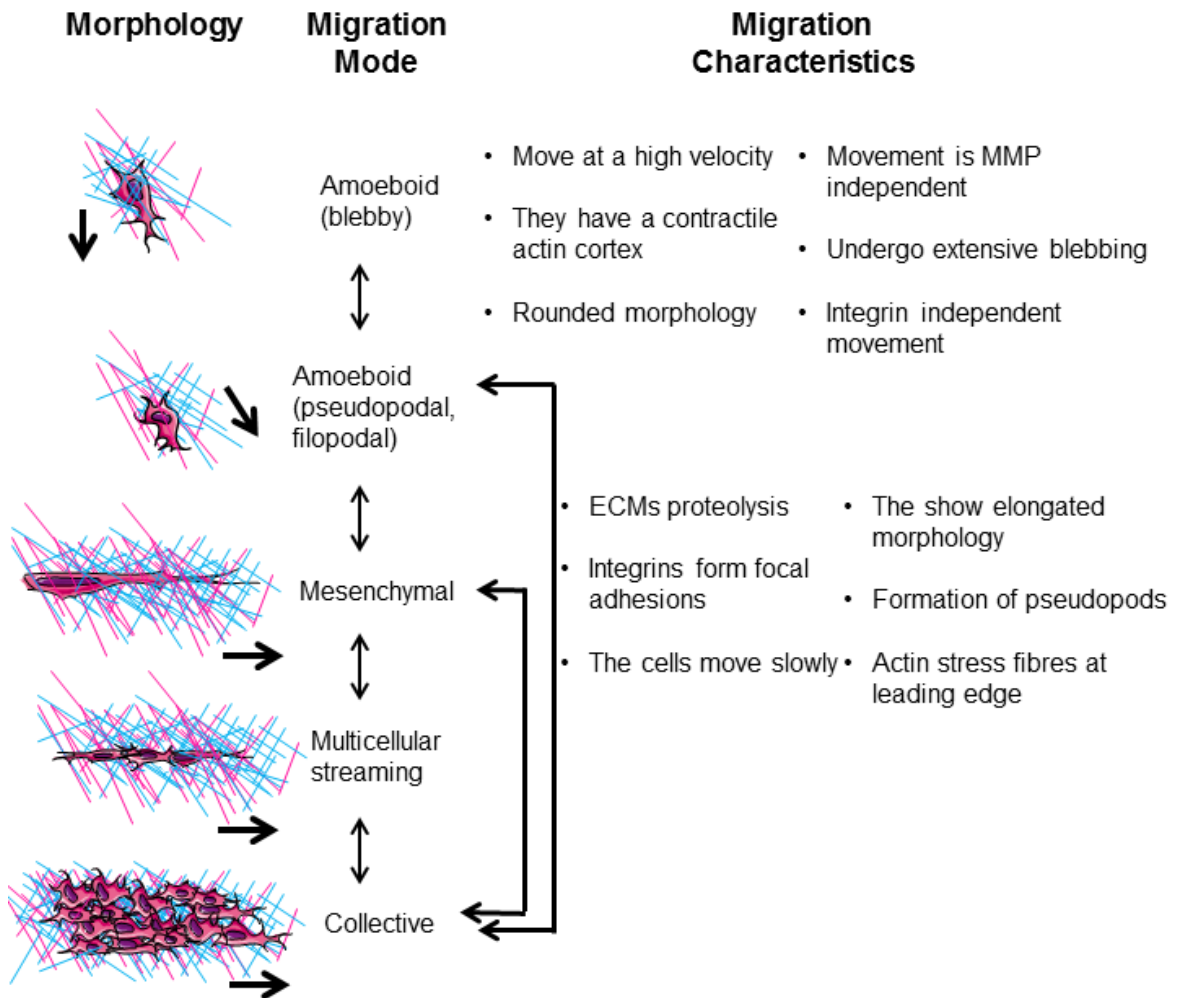


**Figure 1.4: Graphical representation of the different modes of cell migration.**

Individual cell migration shows only very low control of cell-ECM contacts. However, when cells move collectively the cell-ECM control is increased and this provided by matrix-metalloproteinases and integrins. Moreover, when cells move collectively they show characteristics of cadherin expression and gap junctions. Leukaemia, lymphoma and small-cell lung carcinoma cells migrate in an amoeboid-like behaviour. Mesenchymal cell migration is used by fibrosarcomas, glioblastomas and anaplastic tumours. Epithelial cancers which show a high level of differentiation such as breast cancers, prostate cancers and melanoma migrate in a collective cluster. The ECM is represented with blue and pink lines. This figure was adapted from Friedl and colleagues (Friedl and Wolf 2010).

## 1.2 The nature of the extracellular matrix

Most cells need a substrate in order to migrate. The ECM amongst having other functions represents the substrate upon which cells exert force in order to migrate. The ECM consists of a complex variety of macromolecules, which fill a substantial amount of the extracellular space of tissues. Two main classes of biomolecules constitute the ECM; one class is represented by the proteoglycans (PG) and the other class is the fibrous proteins, including laminin, different types of collagen, elastin and fibronectin. PGs are composed of glycosaminoglycan (GAG) chains, which are unbranched polysaccharide chains made of repeating disaccharide units (Krusius and Ruoslahti 1986; Dammer, Popescu et al. 1995). Furthermore, these molecules are largely hydrophilic and present as highly extended proteins, allowing the ECM to withstand massive compressive forces. The fibrous proteins can be further categorised into either structural or specialised proteins. The structural proteins are represented by different classes of collagens, elastin and fibrillins. The specialised proteins, on the other hand, are represented by fibronectin, integrins and several laminins. The collagens to date make up a group comprising 28 different types. Collagens constitute about 30% of the total protein mass of most metazoans, and they give the ECM structure, regulate cell adhesion, provide a substrate for cell migration and thus permit tissue development (Rozario and DeSimone 2010). Collagens and the other ECM components are produced and secreted by fibroblasts which reside in the stroma or by fibroblasts that migrate from nearby tissues. Following secretion from fibroblasts, ECM proteins assemble and are organised in a meshwork by integrin-dependent events which promote fibrillogenesis and deposition (De Wever, Demetter et al. 2008). Additionally, by putting pressure and tension on the matrix, fibroblasts can organise collagen fibrils into sheets and long ropes. In most tissues, one type of collagen is predominant, despite the fact that most collagen fibrils are heterogeneous (Frantz, Stewart et al. 2010). Collagen also associates with the fibrous ECM protein elastin. The precursor of elastin is secreted as proelastin and this assembles into fibres which are, in turn, cross-linked by lysyl oxidase (LOX) family members (Lucero and Kagan 2006). Fibronectin (FN) is another fibrous protein and this is involved in the organisation of the ECM. FN is very important in directing cell attachment and can be stretched to several times its original length (Smith, Gourdon et al.

2007). This in turn allows disclosure of integrin binding sites leading to pleiotropic changes and rendering fibronectin to function as a mechanoregulator (Smith, Gourdon et al. 2007).

## **1.2.1 ECM deposition and remodelling in wound healing**

### ***1.2.1.1 ECM deposition in normal tissue homeostasis***

Normal epithelia comprise a single layer of epithelial cells that are present with apical-basal polarity. The apical face is exposed to a fluid filled lumen and the basal side is in most cases in contact with a single layer of basement membrane or myoepithelial cells (Barsky and Karlin 2005). The basement membrane is a specialised and very compact ECM. It is composed of mostly collagen IV, fibronectin, laminins and other linker proteins, connecting collagens with other proteins (Egeblad, Rasch et al. 2010). For normal tissue homeostasis, it is important to have controlled tissue organisation and communication with the surrounding normal stroma, which consists of non-activated fibroblasts. These fibroblasts secrete collagen I and collagen III, fibronectin, elastin and some PGs. These secreted proteins all maintain the functional integrity of the interstitial ECM. This meshwork is embedded in a glycosaminoglycan-chain containing a PG network (Bosman and Stamenkovic 2003). The ECM, as it is functionally very versatile, needs to be in control of its unique biochemical, physical and biomechanical properties in order to maintain tissue homeostasis. These properties ensure that its spatial arrangement, porosity, rigidity and insolubility are maintained allowing the ECM to act as a scaffold. Additionally, the ECM is indirectly or directly involved in signal transduction cascades, as the cells need to communicate with their environment. One example of such communication involves the accessibility to growth factors. The ECM is a charged protein network with many polysaccharides and their modifications can bind to certain growth factors, such as WNT, FGFs and hedgehogs (Hynes 2009). The ECM, due to its charged protein meshwork, is rich in polysaccharide modifications and is able to limit the accessibility of growth factors to their receptors (Hynes 2009; Lu, Takai et al. 2011). The restrictions that the ECM puts on growth factor signalling are important in regulating cell growth and migration (Hynes 2009). Additionally, despite the fact that the ECM can resist a lot of physical and

chemical insults, it needs to undergo remodelling in order to stay healthy (Kass, Erler et al. 2007). The remodelling is carried out by matrix metalloproteinases (MMPs) and these are inhibited by their counterparts, the so-called, tissue inhibitors of metalloproteinases (TIMPs) (Docherty, Lyons et al. 1985; Carmichael, Sommer et al. 1986). Additionally, LOX proteins and transglutaminase crosslinking activities are used to stiffen the ECM during remodelling (Lucero and Kagan 2006).

### ***1.2.1.2 ECM remodelling in wound healing***

When a tissue has been wounded, the wound healing machinery needs to be activated. At first, when the vasculature has been damaged and a fibrin clot has formed, monocyte infiltration to the damaged ECM is stimulated. The immune response is thereby intensified as monocytes bind to ECM-degradation products and cytokines, leading to a differentiation of monocytes into macrophages (Clark 2001). The macrophages in turn stimulate the release of several metalloproteinases, growth factors and cytokines, resulting in angiogenesis, fibroblast migration and proliferation (Schultz and Wysocki 2009). The fibroblasts present at the wound are then responsible for ECM secretion, which entails the deposition of collagens I and III, fibronectin and hyaluronic acid. This ECM deposition leads to increased mechanical stress at the wound, which in turn can lead to fibroblast activation into myofibroblasts. The tissue is then stiffened by these myofibroblasts, whose main characteristic is to be highly contractile. The secreted ECM components consist of rigid collagen bundles, which are cross-linked by LOX enzymes and thus are much stiffer, compared to unwounded ECM (Szauter, Cao et al. 2005). This now wounded and stiffer microenvironment results in basement membrane disruption and the apical- basal polarity of the destabilised epithelial cell-cell adhesions is lost. Additionally, the wound and the remodelled ECM cause cells to migrate towards the injured tissue (Schafer and Werner 2008). Once the wound has been closed, tissue homeostasis is restored and fibrosis inhibited by specific feedback mechanisms (Schultz and Wysocki 2009; Velnar, Bailey et al. 2009).

## **1.2.2 Parallels between wound healing and cancer**

The ECM has always been seen as a structural support for the maintenance of tissue morphology, but the notion that the ECM can be a supportive milieu for cancer progression, has only recently been established and is now considered to be a hallmark of cancer (Hynes 2009). Cancers are conspicuous by the complete loss of tissue organisation and this is a characteristic that they share with unhealable wounds (Bissell and Radisky 2001; Schafer and Werner 2008). Indeed, like scar tissue, tumours tend to be stiffer than the surrounding normal tissue, and this is due to many of the same processes, such as inflammation, fibroblast activation and ECM deposition and cross-linking that occur during wound healing (Tan and Coussens 2007; Butcher, Alliston et al. 2009; Levental, Yu et al. 2009).

## **1.2.3 The ECM and its components in cancer**

As described above, there are some parallels between the ECM deposited around tumours and wounds. The so called tumorigenic ECM makes the cancer cells more permissive to move from primary tumours to distant sites. Following malignant transformation, changes in the normal amount of ECM deposition and composition, alter the biochemical properties of the ECM and thus have the potential to increase many growth factor signalling pathways. Additionally, the physical properties of the ECM are important in the tumour-associated ECM. The arrangement of the collagen I fibres has been shown to be important in this regard. In normal tissues the collagen I fibrils are arranged in a non-oriented loose meshwork. However, in breast cancer they are aligned in highly linearized collagen I fibrils, which are either arranged perpendicularly into the tissue or oriented adjacently to the epithelium (Provenzano, Eliceiri et al. 2006; Levental, Yu et al. 2009). The enzymes which remodel the ECM are also very often deregulated in human cancers. Metalloproteinases, cysteine cathepsins and heparanases are upregulated in many tumour types (Ilan, Elkin et al. 2006; Kessenbrock, Plaks et al. 2010). As mentioned before, the tumour stroma is often stiffer than the normal stroma. Indeed, in breast cancer the stroma is 10 times stiffer than the normal breast stroma (Levental, Yu et al. 2009; Lopez, Kang et al. 2011). Some of this could be due to an increased activity of lysyl oxidase (LOX). The oxidase cross-links the collagen fibres and other ECM

components, and has been shown to be upregulated in head and neck cancer and breast cancer (Le, Harris et al. 2009; Barker, Chang et al. 2011). Furthermore, in mice the increased expression of LOX stiffens the ECM and promotes tumour cell migration and invasion (Levental, Yu et al. 2009). The overexpression of LOX alone, however, is not enough to promote tumorigenesis in normal breast epithelium (Holloosi, Yakushiji et al. 2009). Therefore, it seems clear that ECM remodelling is not the only cause for cancer initiation, but likely is a key factor that contributes to tumour aggressiveness. ECM dynamics, are dictated by the cells within the tumour microenvironment, and these cell types include; cancer cells, cancer stem cells, immune inflammatory cells, pericytes and endothelial cells (Hanahan and Weinberg 2011). These specialised cell types need to be studied to understand the multistep process of tumour progression. I will focus on cancer-associated fibroblasts as they secrete many factors that constitute the tumour permissive ECM.

### ***1.2.3.1 Fibroblast activation and cancer-associated fibroblasts***

Two different types of fibroblasts are present within the tumour environment; normal fibroblasts and myofibroblast-like cancer-associated fibroblasts (CAFs). The myofibroblast-like CAFs can be characterised by the expression of  $\alpha$ -smooth muscle actin ( $\alpha$ -SMA), account for a considerable fraction of the stroma of tumours (Sappino, Skalli et al. 1988), and they rarely appear in healthy tissue. They do appear, however, in wound healing as well as in chronic inflammation. These myofibroblast-like CAFs can arise via activation of normal fibroblasts. The myofibroblast-like CAFs secrete extracellular matrix components such as collagens and fibronectins. Specifically, they have been shown to have an increased deposition of collagen I, II, III, V and IX (Zhu, Risteli et al. 1995; Kauppila, Stenback et al. 1998; Huijbers, Iravani et al. 2010). As these activated fibroblasts change the ECM and make it more permissive for cancer cells to grow, it was proposed that their ablation might reduce cancer growth. To test whether ablating myofibroblast-like CAFs has an effect on tumour growth, a knockout mouse was generated which was devoid of  $\alpha$ -SMA positive CAFs. Unexpectedly, these mice were more prone to develop pancreatic cancer indicating that ablation of myofibroblasts promoted cancer emergence (Ozdemir, Pentcheva-Hoang et al. 2014). Therefore, the research in this area

rather focuses on targeting and examining secreted factors which influence the deposition of an ECM microenvironment, which is permissive for cancer progression. The ECM fibres deposited by myofibroblasts are remodelled and cross-linked not only by LOX, but also by transglutaminases, which increases their stiffness. The studies which test the effect of depletion of enzymatic components of the ECM, such as lysyl oxidase, have shown reduced angiogenesis (Baker, Bird et al. 2013), reduced tumour growth (Levental, Yu et al. 2009) and increased drug delivery (Provenzano, Cuevas et al. 2012). Vascular endothelial growth factor (VEGF) is able to increase vascular permeability, which increases vessel sprouting and growth. This has been shown to be particularly true for stiff breast cancer tumours, which are very invasive and highly vascularised (Levental, Yu et al. 2009; Baker, Bird et al. 2013). All of these characteristics constitute a vicious cycle, which acts to drive tumour aggressiveness. This includes tumour-associated ECM stiffening and reciprocal ECM resistance induced by resident tumour cells and myoepithelial cells. This generates contractility which increases tumour growth, survival, angiogenesis, tumour cell invasion and metastasis (Paszek and Weaver 2004; Paszek, Zahir et al. 2005; Butcher, Alliston et al. 2009; Erler and Weaver 2009).

#### **1.2.4 Role of the ECM in cancer progression**

The formation of cancer metastasis is a multistep process as described above. It is characterised by local invasion, intravasation at the primary tumour, movement through the blood stream, extravasation at the distant site and proliferation forming the metastasis (Paget 1989). It seems that the ECM supports the cell proliferation, colonisation, and the expansion necessary to form macrometastasis in the metastatic niche in a similar manner as it does in the primary tumour niche. Support of this hypothesis has been provided by a study in mammary carcinoma cells. These carcinoma cells have a low survival rate when they do not express the hyaluronan receptor CD44 on their surface. However, when these mammary carcinoma cells express the CD44 surface marker they have a higher survival rate (Yu, Toole et al. 1997). The obtained data suggest that possibly hyaluronan as part of the ECM promotes survival of cancer cells in the metastatic niche. Additionally, in the primary tumour ECM, the activity of the lysyl oxidase was higher and this has also been reported for

the metastatic niche. The action of LOX in the secondary organs has been shown to promote the seeding of cancer cells into metastatic niches (Erler, Bennewith et al. 2009). Additionally, as in the primary tumour site, ECM stiffening could promote infiltration of immune cells as well as triggering the angiogenic switch at the metastatic site.

Furthermore, in the distant pre-metastatic niche fibronectin secretion is increased. This is important for the VEGF receptor 1-positive hematopoietic progenitor cells, which express the fibronectin-binding integrin  $\alpha 4\beta 1$  and migrate and adhere to niches in the lung (Kaplan, Riba et al. 2005). Once the VEGFR1-positive hematopoietic cells are resident in the metastatic niche they secrete MMP9, which has a potential role in lung-metastasis (Hiratsuka, Nakamura et al. 2002). This would imply that the ECM is a significant player to form distant metastasis.

## 1.3 Transglutaminases

Transglutaminases are cross-linking enzymes and are thought to play a role in ECM stiffness and cancer progression. The transglutaminase (TG) family consists of 9 members in humans, namely TG 1 - 7, factor XIII and band 4.2 (Griffin, Casadio et al. 2002). One of the functions of the transglutaminases is to catalyse thiol- and calcium-dependent transamidation reactions. It was first described by Pisano et al, that a primary amine group and a carboxamide group of a peptide bound glutamine residue can form a covalent bond and this is called a transamidation reaction. An amine donor in the reaction can be  $\epsilon$ -amino group of the peptide bound lysine. Therefore, a transamidation reaction entails formation of a crosslink of covalent nature between an  $\epsilon$ -amino group of a lysine and the  $\gamma$ -carboxamide of the glutamine (Pisano, Finlayson et al. 1968). Furthermore, the transglutaminases possess a GTPase and G-protein function. However, recent reports suggest that these functions are mutually exclusive. The transglutaminase family members can be discriminated by their tissue distribution, localisation, physical properties and mechanisms of action (Table 1.1). Transglutaminases have also been described to be involved in wound healing and in stiffening of the erythrocyte membrane (Aeschlimann and Paulsson 1994). Transglutaminase-2 (TG2) and fXIIIA are secreted proteins, but they lack the amino-terminal hydrophobic leader sequence that is typical of secreted proteins, thus must be released from the cell via unconventional mechanisms. They are structurally and functionally related proteins. Therefore, it has been suggested that they originate from duplication of a single transglutaminase gene. These genes probably evolved early in evolution, because primitive organisms such as bacteria also have transglutaminase enzymes (Yokoyama, Nio et al. 2004). However, in lower vertebrates only one transglutaminase exists. It was therefore suggested that gene duplication gave rise to the transglutaminase family, and this view is further supported by the sequence similarity in the genes encoding these enzymes (Grenard, Bates et al. 2001). Furthermore, they are known to catalyse  $\text{Ca}^{+}$ -dependent posttranslational modifications of proteins. This can be for example that free amine groups are covalently linked, which is called a transamidating/deaminating function as described above. The transamidation (catalytic active site) domain is retained in all transglutaminases, except band 4.2 as this protein is mostly involved in

scaffolding (Satchwell, Shoemark et al. 2009). They further possess a GTPase/G-protein function and they have therefore the potential to function as a signalling protein (Begg, Carrington et al. 2006).

Gene [Protein]	Molecular Mass kDa	Main function	Tissue distribution	References
TGM1 [TG1]	90	Forming cell envelopes during keratinocyte differentiation	Membrane bound keratinocytes	(Kalinin, Marekov et al. 2001)
TGM2 [TG2]	80	Apoptosis, cell adhesion, matrix stabilisation, signal transduction	Many tissues: cytosolic nuclear, membrane, and extracellular	(Chen and Mehta 1999)
TGM3 [TG3]	77	Forming cell envelopes during keratinocyte differentiation	Hair follicle, epidermis, brain	(Kalinin, Marekov et al. 2001)
TGM4 [TG4]	77	Reproduction	Prostate	(Williams-Ashman, Notides et al. 1972)
TGM5 [TG5]	81	Cell formation in keratinocytes	Foreskin keratinocytes, epithelial barrier lining, skeletal muscular striatum	(Candi, Oddi et al. 2001; Candi, Oddi et al. 2002; Cassidy, van Steensel et al. 2005)
TGM6 [TG6]	78	Not known	Testis and lung	
TGM7 [TG7]	81	Not known	Ubiquitous, but predominantly in testis and lung	
fXIII subunit A	83	Platelets, astrocytes, dermal dendritic cells, chondrocytes, placenta, plasma coagulation, synovial fluid, bone growth	Cytosolic, extracellular	(Lorand 2001), (Wozniak, Fausto et al. 2000)
Band 4.2	72	membrane skeletal component, signal transduction	Red blood cells, bone marrow, foetal liver and spleen	(Ideguchi, Nishimura et al. 1990)

**Table 1.1: Properties of the 9 transglutaminase proteins.**

This table is mostly taken from Eckert et al. (Eckert, Kaartinen et al. 2014).

### 1.3.1 Transglutaminase 2

The first transglutaminase, nowadays known as TG2, was identified in 1987 in guinea pig liver extracts (Achyuthan and Greenberg 1987). TG2 has been detected in many tissues and cell types. It has been shown to be mostly present in the cytosol, but also in the nucleus and plasma membrane. Therefore, it was named tissue transglutaminase. TG2's functions as a GTPase, as it hydrolyses GTP, and it is also able to catalyse a  $\text{Ca}^{2+}$ -dependent posttranslational modification of proteins (Lorand and Graham 2003). Additionally, TG2 has several proposed functions which were published. Therefore, it was proposed that it can act as a protein scaffold (Akimov and Belkin 2001; Akimov and Belkin 2001), as protein disulphide isomerase (PDI) (Hasegawa, Suwa et al. 2003; Mastroberardino, Farrace et al. 2006), as protein kinase (Mishra and Murphy 2004; Mishra, Saleh et al. 2006), and as DNA hydrolase (Takeuchi, Ohashi et al. 1998). Moreover, TG2 interacts with several proteins such as  $\beta$ -integrins, fibronectin, osteonectin, RhoA, multilineage kinases, PTEN, I $\kappa$ B $\alpha$  and the retinoblastoma protein. In mice, TG2 loss leads to viable offspring, but delays wound healing and results in a poor response to stress (Murtaugh, Mehta et al. 1983).

### 1.3.2 Structure and function

#### 1.3.2.1 Structure of TG2

The multifunctional enzyme TG2 consists of 4 domains, namely the N-terminal  $\beta$ -sandwich domain (AA1-140), the catalytic core ranging from amino acid residues 141-460 and 2 C-terminal  $\beta$ -barrel domains, which range from amino acid residues 461-589 and 587-687. Additionally, three different structures of TG2 have been resolved, giving invaluable insight into the possible functions of TG2. TG2 was crystallised in a complex with ATP rendering it in the closed form (Figure 1.5) (Han, Cho et al. 2010). It was also co-crystallised with GDP and rendering it in a closed form (Liu, Cerione et al. 2002). Finally, it was complexed in an open conformation, with a TG2 inhibitor (Pinkas, Strop et al. 2007). TG2's catalytic site (transamidating site) is composed of cysteine proteases, namely cysteine C277, histidine 335 (H335) and aspartate 358 (D358) (Liu, Cerione et al.

2002). The mutation of cysteine C277 renders the transamidation domain inactive. In addition, this cysteine mutation C277S is able to reduce the GTP/GDP binding due to changes in the conformation of the protein (Begg, Carrington et al. 2006). Next to this catalytic active site, two conserved tryptophan residues (W241 and W332) have been shown to stabilise a thiol intermediate, which forms during catalysis (Murthy, Iismaa et al. 2002; Pinkas, Strop et al. 2007). The mutation of W241A results in loss of the TG2 transamidase activity, but the GTP/GDP binding capability is not impaired. Mutation of W332F, however, impairs GTP/GDP binding (Murthy, Iismaa et al. 2002; Gundemir and Johnson 2009). Additionally, the tyrosine residue at position 516 (Y516) has been shown to form a hydrogen bond with the cysteine 277. This seems to keep TG2 in a more closed conformation, but when Y516 was mutated to a phenylalanine, TG2 was observed to be in an open conformation (Begg, Carrington et al. 2006).

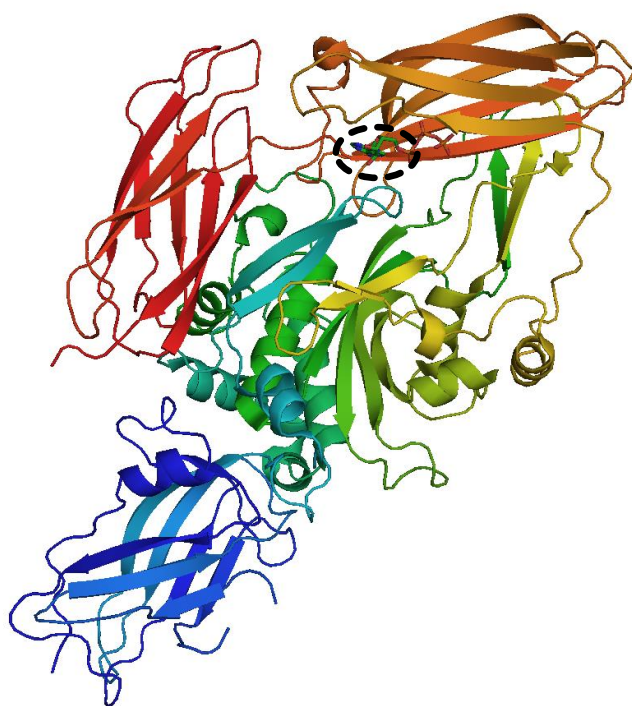


**Figure 1.5: X-ray structure of TG2 complexed with Adenosine triphosphate (ATP).**

This structure was crystallised by Han and colleagues and downloaded from the RCSB PDB website (<http://www.rcsb.org/pdb>) (PDB code: 3LY6) (Han, Cho et al. 2010). The structure was generated in PYMOL (<https://www.pymol.org/>). The black dotted line indicates the ATP molecules in its binding site. The  $\beta$ -barrels are indicated in red and orange, the catalytic core is indicated in yellow, turquoise and green. The dark blue is one  $\beta$ -strand.

Unfortunately, TG2 has not yet been crystallised in the presence of calcium. Therefore, the crystallised structures of TG3 and factor XIII (Fox, Yee et al. 1999; Ahvazi, Boeshans et al. 2003; Ahvazi, Boeshans et al. 2004) were used to predict the calcium binding sites for TG2. From calorimetric studies and site directed mutagenesis it has been detected that six calcium binding sites exist. When mutating three of them, the transamidation activity did not change. However, when mutating all six of the calcium binding sites the transamidation activity was blocked, but the GTP/GDP binding capacity was not changed (Kiraly, Csoz et al. 2009).

### **1.3.2.2 *Transamidating/deaminating function***

The reactions catalysed by TG2 have been studied to date in great detail. It has been shown in experiments that one  $\gamma$ -carbon of a peptide glutamine side chain can be nucleophilically attacked by sulphur of an active site cysteine of TG2 (C277). Ammonia is the product being released after the formation of a thioester bond (active site cysteine and substrate). For the transglutaminase to detach, an amine (transamidation) or  $H_2O$  (deamination) (acyl-acceptor) attacks the thioester bond. The transamidation reaction has two possible outcomes. The result of the first reaction occurs after adding an amine to the protein. The amine can be the attacking group and this leads to isopeptide bond formation between the glutamine side chain and the amine (Figure 1.6 C). This has been regarded as a posttranslational modification. Furthermore, the properties of both proteins are changed. An isopeptide bond forms between two amino acids, such as glutamine and lysine (Figure 1.6 B). It has been described that this isopeptide bond functions to increase the ECM stability and it has also been described that it stops the release of cell contents of apoptotic cells (Nicholas, Smethurst et al. 2003). The result of the second reaction occurs upon the presence of an amine. This amine can form an indirect cross-link during its incorporation as a cross-linker (Figure 1.6 D).

When a deamination reaction occurs a glutamine residue is transformed to a glutamate residue (Figure 1.6 A). In 2002 it was shown that the deamination reaction only took place under specific conditions, such as low pH (Fleckenstein, Molberg et al. 2002). However, in 2006 it was shown that one glutamine residue

## Chapter 1

in Hsp20 was specifically deaminated by transglutaminases and not transamidated (Boros, Ahrman et al. 2006), and this was subsequently shown to be the case for other proteins too (Stamnaes, Fleckenstein et al. 2008).

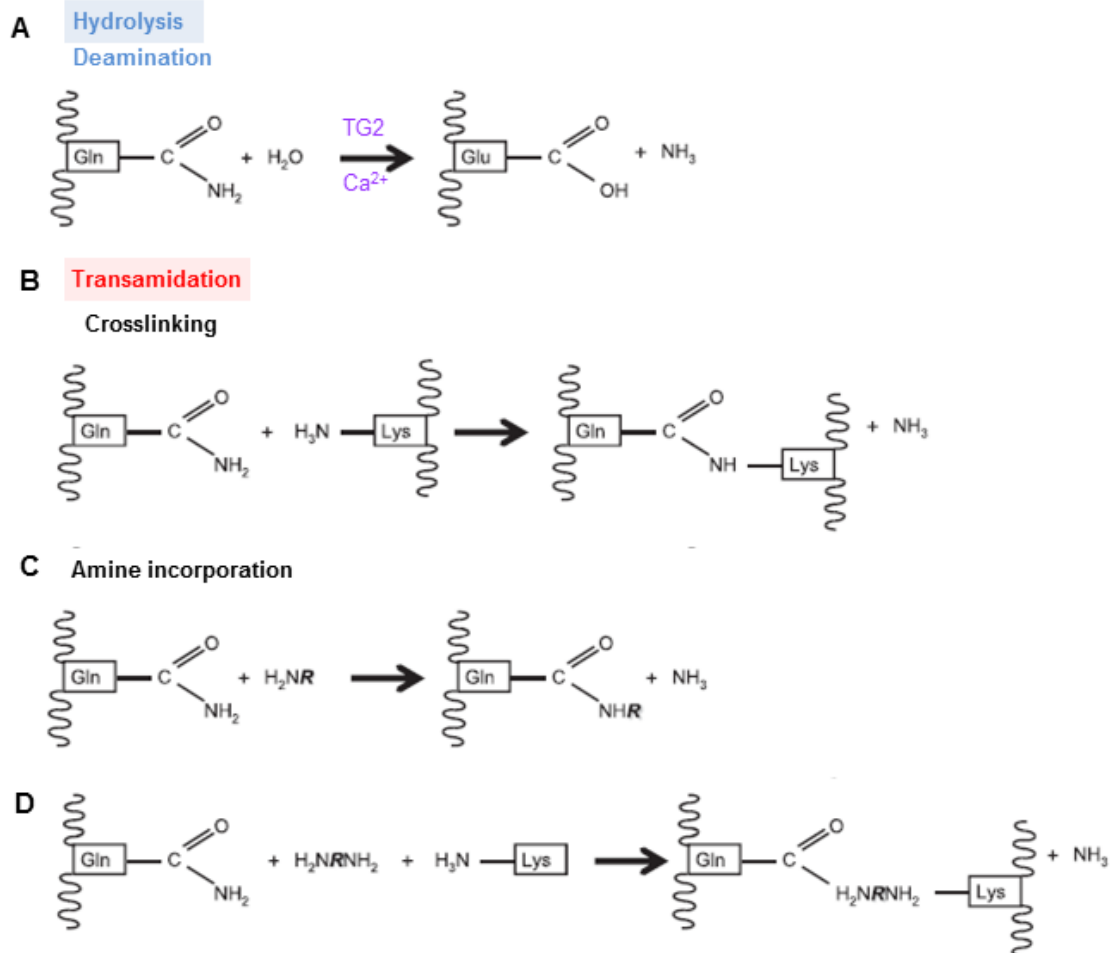


**Figure 1.6: The transamidating functions of transglutaminases.**

(A) Deamination of a peptide-bound glutamine to a glutamate residue by TG2. The water in this case functions as an acyl-acceptor for the deamination process. (B) Isopeptide bond formation to crosslink two proteins. In this case it is shown the  $\epsilon$ -group of the peptide bound lysine as the acyl-acceptor. (C) Posttranslational modification. In this case a primary amine (acyl-acceptor) and the glutamine residue is modified. (D) An alternative for an isopeptide bond can be a primary amine which acts in this case as a cross-linker of 2 proteins. This figure was adapted from Gundemir and colleagues (Gundemir, Colak et al. 2012).

### 1.3.2.3 GTPase/G-protein function

Transglutaminase 2 was first shown to hydrolyse GTP in 1987 (Achyuthan and Greenberg 1987). In these experiments it was also shown that GTP binding to TG2 and calcium binding to TG2 were competitive. When TG2 is bound to GTP, TG2 acquires a closed conformation (Figure 1.7). In addition, they showed that the mutation of the active site cysteine (277) did not abolish GTP hydrolysis.

One research group has categorised TG2 as  $G\alpha_h$ , which belongs to a family of heterotrimeric guanosine triphosphate (GTP)-binding proteins. TG2 was further shown to associate with the  $\alpha_1$ -adrenergic receptor and increase its signalling capacity (Nakaoka, Perez et al. 1994).

The binding affinity of TG2 to GTP has been determined. It has, however, proven more laborious to determine the affinity of calcium ions to TG2, as the protein has several binding  $Ca^{2+}$ -binding sites. These binding sites have different binding affinities. However, it seems quite likely that the GTP/calcium ratio in the cell (~150  $\mu$ M/~100 nM), ensures that cytosolic TG2 will be in the GTP-bound state thus maintaining intracellular TG2's transamidase activity at relatively low levels. In addition, some GTP-binding defective TG2 mutants have been shown to promote apoptosis, suggesting that uncontrolled cytosolic TG2 activity may be pro-apoptotic (Datta, Antonyak et al. 2007; Gundemir and Johnson 2009; Tee, Marshall et al. 2010). Finally, a study has shown that different TG2 isoforms change cell differentiation in diverse ways. When a GTP-binding short isoform of TG2 is present the neuroblastoma cells differentiate more compared to the long isoform as this inhibits neuroblastoma cell differentiation. As TG2 inhibitors are able to inhibit neuroblastoma differentiation induced by the short form of TG2, this suggests, that differentiation is induced by TG2's transamidating activity (Tee, Marshall et al. 2010).

#### **1.3.2.4 TG2 and other functions**

As described above it seems that increased calcium concentrations increase TG2's transamidation activity, and when the GTP/GDP concentration is high TG2 assumes a closed GTP-bound conformation (Figure 1.7). However, even though the extracellular calcium concentration is significantly higher than extracellular GTP levels, TG2's transamidation function is not necessarily high outside the cell. It is thought that activation of TG2's transamidation activity outside the cell may be triggered by exposure to outside stresses (Siegel, Strnad et al. 2008), indicating that in addition to the influence of calcium other potential factors that control TG2's transamidase activity need to be considered. Observations that the five intramolecular disulphide bonds in TG2 were presumed to be able to form under oxidising conditions suggested the possibility

that the redox state of the environment may to have an impact on TG2's transamidase activity (Hasegawa, Suwa et al. 2003). More recently it has been shown that disruption of the disulphide bond between C370 and C371 inhibits transamidase activity in the presence of calcium (Stamnaes, Pinkas et al. 2010).

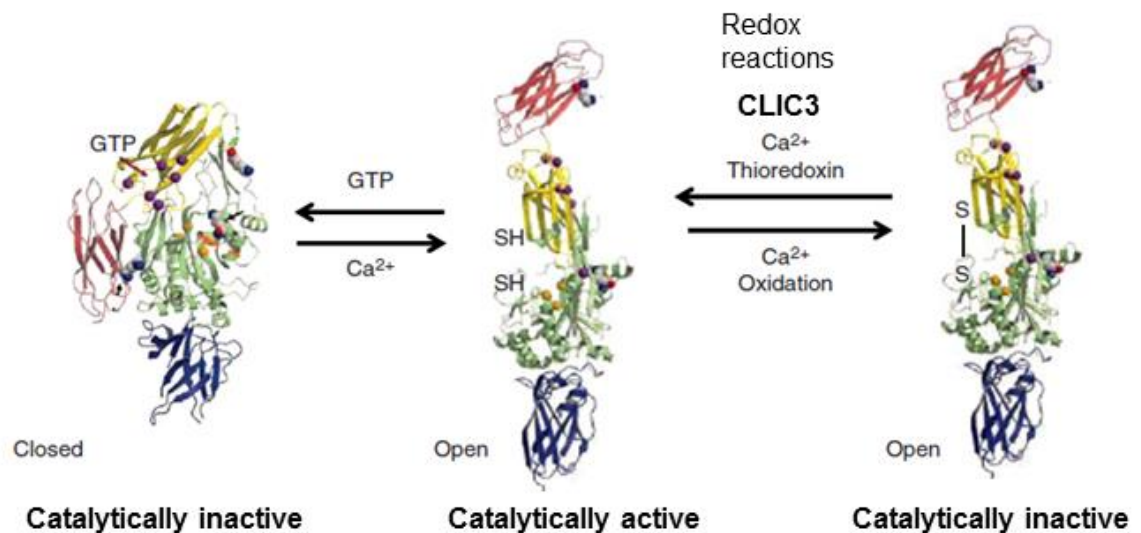


**Figure 1.7: Transglutaminase2 exists in 3 different conformations and has several functions.** This figure shows TG2 in the two catalytic inactive forms and in its catalytic active conformation. TG2 can be present in the GTP/GDP bound catalytically inactive conformation. When TG2 is present in its catalytically active and open conformation, it performs transamidation and deamidation reactions. The  $\text{Ca}^{2+}$  bound crystal structure of TG2 has not been resolved thus far. However, the putative  $\text{Ca}^{2+}$  binding sites are homologous to those of the FXIIIa domain. Upon GTP/GDP binding  $\text{Ca}^{2+}$  can no longer bind to TG2. TG2 domain 3 and 4 are altered and expose the catalytic domain, upon binding to  $\text{Ca}^{2+}$ . When the protein is present in the open active form in oxidising conditions, the catalytic activity is lost. In the presence of thioredoxin the open and active site can exist. The red indicated fold is the COOH-terminal and the blue is the  $\text{NH}_2$  domain. This figure was adapted from *Eckert* and colleagues (Eckert, Kaartinen et al. 2014).

### 1.3.3 TG2 and signalling

Despite the fact that TG2 was initially discovered as a cross-linking enzyme, nowadays it seems that TG2 also has several signalling functions. TG2 has been shown to interact with several target proteins located on the ECM, in the cytoplasm, in the nucleus and in mitochondria (Lorand and Graham 2003; Park, Choi et al. 2010). I will concentrate on TG2's function in enhancing integrin-mediated signalling and crosslinking of ECM proteins. TG2 is released via a poorly understood non-classical secretion pathway, where it covalently modifies ECM proteins to enhance their stability by forming homo- or heteropolymers (Aeschlimann and Thomazy 2000; Lorand and Graham 2003). This has been

described to increase the rigidity of fibronectin (Nelea, Nakano et al. 2008) and collagen (Spurlin, Bhadriraju et al. 2009). This increase in ECM stiffness promotes fibroblast and osteoblast adhesion (Chau, Collighan et al. 2005; Forsprecher, Wang et al. 2009) and is further able to enhance cell growth, survival, migration and differentiation, by having an impact on integrin-related mechanosensing pathways (Bershadsky, Kozlov et al. 2006). Additionally, it has been described that fibrinogen  $\alpha$ C, once cross-linked by TG2, allows endothelial cell adherence and increases integrin clustering. This then leads to the formation of focal adhesions and extracellular signal-regulated kinase (ERK) 1/2 activity (Belkin, Tsurupa et al. 2005).

Integrins have a transmembrane domain and act as signalling and adhesion receptors. However, they do not possess an intrinsic enzymatic activity. ECM proteins can activate integrins (Hynes 2002). As described above, TG2 can interact with the ECM, enhancing cell adhesion and integrin-mediated signalling via interaction with  $\beta$ 1,  $\beta$ 3 and  $\beta$ 5 integrin (Zemskov, Janiak et al. 2006; Belkin 2011). Additionally, in cancer cells and during metastasis TG2 has been shown to enhance the affinity of certain integrins for fibronectin, which increases cell attachment to the matrix and in can lead to an activation of integrin signalling (Satpathy, Cao et al. 2007; Belkin 2011; Piercy-Kotb, Mousa et al. 2012). TG2-induced integrin clustering increases integrin-dependent signalling. This is for example the activation of FAK and Src. Furthermore, this leads to increased levels of GTP-bound RhoA and its downstream target ROCK. The outcome of this can be actin stress fibre formation, which leads to enhanced actomyosin contractility to promoted further ECM remodelling (Toth, Garabuczi et al. 2009; Torocsik, Szeles et al. 2010).

### **1.3.4 Transglutaminase 2 in cancer**

TG2 is highly expressed in several cancers including breast (Agnihotri, Kumar et al. 2013), pancreatic (Iacobuzio-Donahue, Maitra et al. 2003), colon (Miyoshi, Ishii et al. 2010), non-small cell lung cancers (NSCLC) (Choi, Jang et al. 2011) and melanoma (Fok, Ekmekcioglu et al. 2006). TG2 overexpression can confer transformed characteristics such as enhanced survival capacity and anchorage-independent growth on normal fibroblasts and epithelial cells (Verma, Wang et

al. 2006; Yakubov, Chelladurai et al. 2013). However, TG2 cannot transform fibroblasts by itself. It has therefore been proposed to collaborate with other factors to transform fibroblasts. TG2 expression has been associated as a negative prognostic marker. The expression of TG2 is usually detectable in advanced cancer (Mehta, Fok et al. 2004; Fok, Ekmekcioglu et al. 2006; Herman, Mangala et al. 2006; Mehta, Fok et al. 2006).

Cells in primary tumours can change their cell migration behaviour from epithelial to mesenchymal migration. This goes hand in hand with extensive remodelling of the ECM. The remodelling is carried out in some cases by matrix metalloproteinases (MMPs). TG2 seems very important in laying down ECM and increasing its stiffness. Moreover, several studies show that TG2 is also important in inflammation and wound healing (Chau, Collighan et al. 2005; Collighan and Griffin 2009; Fisher, Jones et al. 2009; Mehta, Kumar et al. 2010). Additionally, the ability of TG2 to cross-link ECM proteins has not only been associated with the desmoplastic response, but also with kidney scarring, atherosclerosis and diabetic nephropathy (Johnson, El-Koraie et al. 2003; Cho, Kim et al. 2008; Schelling 2009). Moreover, it has been demonstrated that TG2 overexpression in the tumour stroma is associated with a high risk of recurrence in invasive ductal carcinomas of the breast (Assi, Srivastava et al. 2013). The extracellular pool of TG2 has also been shown to cross-link secreted fibronectins and to stabilise the ECM as it has been found to bind to the gelatin-binding domain of fibronectin. This then increases the association between the fibronectin and integrins on the cell surface, enabling TG2 to impact characteristics of cancer cells (Akimov, Krylov et al. 2000; Chau, Collighan et al. 2005; Mangala and Mehta 2005; Collighan and Griffin 2009; Fisher, Jones et al. 2009; Mehta, Kumar et al. 2010). TG2 can impact on FAK, Akt, NF- $\kappa$ B, PI3K, focal adhesion kinase or phospholipase C signalling via its cross-linking or signalling functions (Verma, Wang et al. 2006; Verma, Guha et al. 2008; Mehta, Kumar et al. 2010; Yakubov, Chelladurai et al. 2013). Some of these pathways have been associated with epithelial-mesenchymal transition. The TG2 expression is increased upon high protein level of inflammatory cytokines, such as TGF- $\beta$  in fibroblasts and epithelial cancer cells. This leads to enhanced production of both collagen and fibronectin. This dense material presents at the clinical diagnosis as a lump or dense stroma (Walker 2001; Apte and Wilson 2012).

TG2 has also been shown to be involved in the process of EMT in cancer cells. These cancer cells therefore acquired a more stem-cell phenotype. MCF-7 breast cancer cells were treated with doxorubicin and the cell population which survived were considered to be cancer stem cells. These cells also had high TG2 expression (Calcagno, Salcido et al. 2010). Additionally, in ovarian carcinoma it has been shown that TGF- $\beta$  is secreted which increases the expression and enzymatic function of TG2, leading to the acquisition of the stem cell-like phenotype (Cao, Shao et al. 2012).

TG2 has been shown to be up-regulated in drug resistant cancer cells. Upon inhibition of TG2 expression, certain cancer cells acquire drug sensitivity. However, the mechanisms that TG2 uses to mediate drug resistance have not been completely understood, and it depends on the cancer tissue, as well as drug in question (Antonyak, McNeill et al. 2003; Herman, Mangala et al. 2006). In one case it has been shown that doxorubicin-resistant breast cancer cells displayed upregulation of TG2. This is partly because TG2 can activate the EGF signalling pathway, contributing to oncogenic breast cancer potential and promoting chemoresistance against doxorubicin (Antonyak, Miller et al. 2004).

## 1.4 CLIC proteins

### 1.4.1 Phylogeny and structural conservation of CLICs

The CLIC family of proteins have a high sequence similarity and appear very early in evolution. CLIC proteins are conserved throughout metazoa. Lower organisms such as *Hydra magnipapillata* (phylum Cnidaria), *Schistosoma mansoni* (phylum Platyhelminthes), *Drosophila melanogaster* (phylum Arthropoda) and *Ciona intestinalis* (phylum Chordata) express a single CLIC. In *Drosophila melanogaster* the CLIC proteins are represented by DmCLIC. Nematodes express two CLIC-like proteins, which are EXC-4 and EXL-1. The crystal structure of the (DmCLIC) and EXC-4 reveal that a potassium ion is bound in what would be part of the glutathione (GSH) site. The urochordate *Ciona intestinalis* CLIC protein has a sequence identity with vertebrate paralogues of 45%. There is some variation in CLIC proteins from different species as, for example, teleost fish

have a second copy of CLIC5. However, lizards and birds do not contain CLIC1. Choanoflagellates also have a CLIC-like gene. The human CLIC family of proteins consists of 6 paralogues namely CLIC1 to CLIC6, with CLIC2, CLIC5 and CLIC6 existing in alternative splice forms (Littler, Harrop et al. 2010). The six family members have a high sequence identity ranging from 47 to 76 % (Singh 2010). A characteristic of the CLIC proteins is a ~240 amino acid stretch forming the glutathione S-transferase (GST) fold. The most divergent CLICs are CLIC5B and CLIC6, as they are longer in sequence and have an N-terminal domain, which is attached to the GST-fold (Shanks, Larocca et al. 2002; Griffon, Jeanneteau et al. 2003). These domains often include repetitions and are not very well conserved in sequence. In addition, the size of the protein is also not well conserved.

In addition, CLIC5 and CLIC6 are not as widely expressed in human tissues compared to the other CLICs and their function is most likely far more diverse. The crystal structure of CLIC1, CLIC2, CLIC3 and CLIC4 has been resolved in their soluble, globular state. They have a very high structural homology as they all contain 10  $\alpha$ -helices and 4  $\beta$ -sheets. Between helix 5 and 6 they possess a highly negatively charged loop, which extrudes from the globular domain and is positioned between Pro147 and Gln 164 in CLIC1 (Singh, Cousin et al. 2007). Due to sequence and structural similarities the human CLIC proteins have probably arisen from one single CLIC protein through duplication events (Littler, Harrop et al. 2010). CLIC proteins in vertebrates are highly conserved which would suggest that these proteins have a very similar function. However, it has not been validated in science so far and needs further investigation.

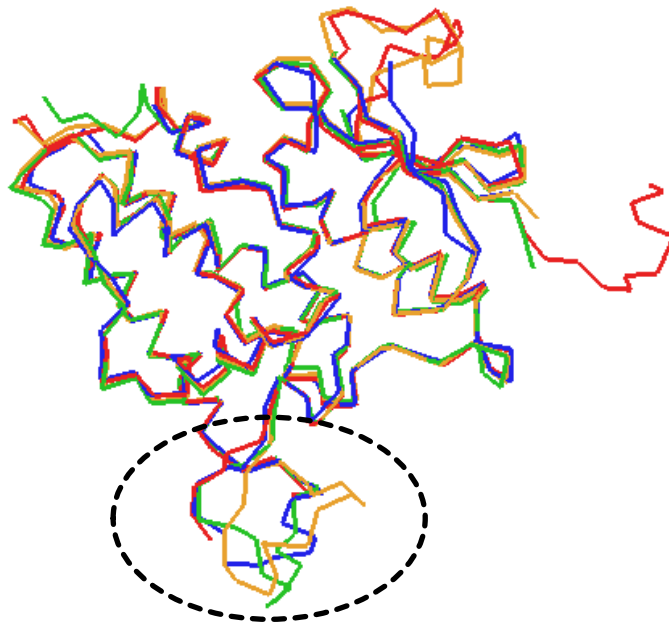


**Figure 1.8: Crystal structures of the human CLIC proteins (CLIC1 – CLIC4).**

The protein structures were downloaded from the RCSB Protein Data Bank (<http://www.rcsb.org/pdb>). The CLIC protein structures were visualised and aligned in PYMOL (<https://www.pymol.org/>). The orange structure represents CLIC1 (PDB structure 1K0M), the green structure represents CLIC2 (PDB structure 2PER), the blue structure represents CLIC3 (PDB structure 3FY7) and the red structure represents CLIC4 (PDB structure 2D2Z). The divergent loop is encircled with the black dotted line. I generated the Figure myself but the idea was from Marta Dozynkiewicz.

### 1.4.2 The structure of CLIC3

The CLIC3 protein was first identified in a yeast two hybrid screen binding to ERK7. ERK7 is part of the mitogen-activated protein kinase family of signal transducers. CLIC3 interacted with the COOH-domain of ERK7, which was used as a bait. Qian and colleagues showed via Northern blot analysis that CLIC3 is expressed in the heart, the lung and the placenta. Finally, they showed the association of ERK7 with CLIC3 via co-immunoprecipitation and found that the protein is mainly localised to the nucleus, but it was also detected in the cytoplasm (Qian, Okuhara et al. 1999).

In 2010 the crystal structure of CLIC3 was resolved at a 2 Å resolution by Littler and colleagues (Figure 1.9) (Littler, Brown et al. 2010). The crystal structure of CLIC3 revealed that it can be present in the oxidised and reduced state. CLIC3 was identified as being monomeric in solution. In addition, it possesses a GST-

like form, with a more open and polar active site compared to the other CLIC proteins. This might open the possibility to form distinct interactions with other proteins during specific cellular processes. The foot loop region is more flexible in the other CLIC family members compared to CLIC3. This might suggest that CLIC3 is functionally divergent. The GST-fold in the CLICs consists of two domains: the C-terminal all helical domain and an N-terminal thioredoxin-like domain. The N-terminal thioredoxin domain is thought to be the active site and comprises two active cysteines. These are able to form an internal disulphide bond within a thioredoxin-like CxxC motif (Figure 1.10) (Littler, Brown et al. 2010). This cysteine motif is homologous to that of the GST-fold and serves to fine-tune the reactivity and enzymatic action towards the substrate. Moreover, the soluble GST-like state of the CLICs has been well characterised, but the structural transition into a membrane spanning ion channel remains unknown. Therefore, in CLIC3 a disulphide bond might form between the CxxC motif (Cysteine 22 and Cysteine 25) (Figure 1.10). With the formation of a disulphide bond it could reduce other proteins which have a formed disulphide bond, thus acting as an enzyme. This hypothesis relies on the observations which were made with CLIC1, CLIC2 and CLIC4 as they can act as an enzyme (Al Khamici, Brown et al. 2015). Furthermore, whether CLIC3 is a secreted protein or only acts within the cells has not been evaluated.

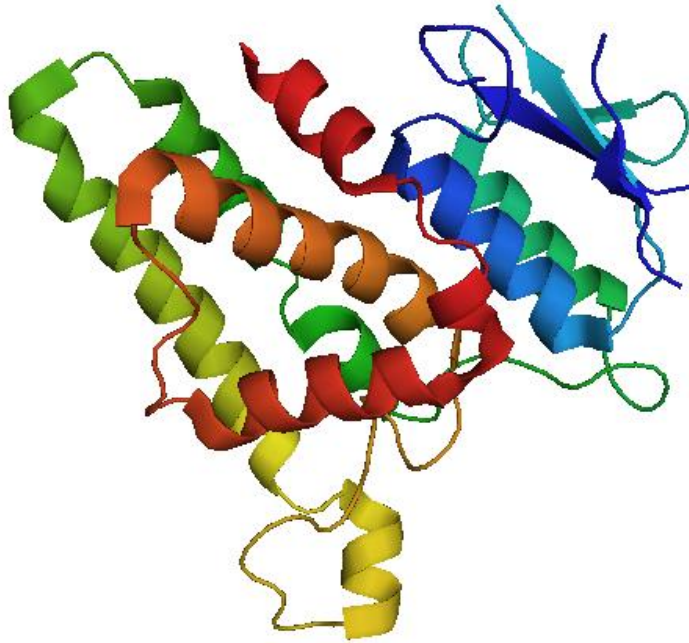


**Figure 1.9: X-ray structure of CLIC3.**

CLIC3 (PDB structure 3FY7) was crystallised by Littler and colleagues and the structure was downloaded from the RCSB Protein Data Bank (<http://www.rcsb.org/pdb/home>). The structures were then visualised by PYMOL (<https://www.pymol.org/>). The arrows indicate the  $\beta$ -sheets and the curls represent the  $\alpha$ -helices.

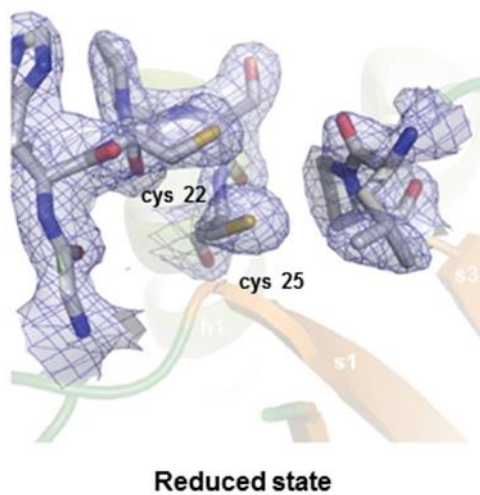


**Figure 1.10: Conserved cysteines in CLIC3 crystallised in the reduced state.**

Electron cloud of the potential active site of CLIC3 protein. A potentially disulphide bond can form between the two cysteines. Adapted from Littler and colleagues (Littler, Brown et al. 2010).

## 1.5 CLICs as membrane inserted proteins

The sequence similarity between the CLICs and other well-characterised ion channels is negligible. In addition, CLICs do not possess a region that could conform to a transmembrane domain.

Nevertheless, there is evidence that the CLICs can insert into membranes. The crystal structure of CLIC1 was solved in reducing and oxidising environments by Littler and colleagues (Littler, Harrop et al. 2004). This indicated that under reducing conditions CLIC1 exists as a soluble, GST-like protein with a glutaredoxin-like active site. However, when CLIC1 is present in an oxidative environment it is present in a non-covalent dimeric state. This is due to the formation of an intramolecular disulphide bond between cysteine 24 and cysteine 59. The assumption of the dimeric state entails dramatic structural changes, where most of the N-terminal domain appears in a different secondary and tertiary structure. It was shown that CLIC1 undergoes a conformational change to insert into artificial bilayers. To further evaluate the membrane insertion of CLIC1, Förster resonance energy transfer (FRET) spectroscopy was used to measure the distances between the tryptophan on position 35 located in the N-terminal domain (suggested to be transmembrane domain) and the three conserved cysteines (Cysteine 89, Cysteine 178 and cysteine 223) on the C-terminus in the presence of membranes or in aqueous solution. This indicated that in the presence of a lipid bilayer conformational unfolding occurs between the N- and C-terminus, which was not observed in aqueous solution (Goodchild, Howell et al. 2010). Consistent with this, EXC-4 - the CLIC protein found in *C. elegans* - can localise to luminal intracellular apical membranes and a 66 amino acid residue of the N-terminal domain is required for this. This N-terminal helical portion of the protein has, therefore, been termed a putative transmembrane helix (Berry, Bulow et al. 2003; Berry and Hobert 2006). Studies on CLIC1 suggested that CLIC proteins might only insert into lipid bilayers in oxidising conditions. However, Singh and colleagues have found that CLIC4 inserts into membranes under both oxidising and reducing conditions (Singh and Ashley 2007). Additionally, CLIC2 inserts into membranes at lower pH and in a way that is insensitive to redox state (Cromer, Gorman et al. 2007). Therefore, further studies need to be conducted to identify under which conditions specific

CLIC family members insert into the lipid bilayers and whether the insertion into the membrane has any physiological role *in vivo*.

### 1.5.1 Ion conductance

Prior to the publication of crystallographic studies, which have now indicated that the CLICs are (at physiological pH and cytosolic redox conditions) soluble globular proteins lacking transmembrane domains, it was thought that the CLICs were ion channels - and this accounts for their, perhaps, rather anachronistic name. It is interesting to consider the history of the discovery of the CLICs as this sheds light on why they have been considered to be chloride conductors. In the 1980s Al-Awaqati and colleagues screened compounds derived from three classes: indanyloxyacetic acid (IAA), anthranilic acid (AA), and ethacrynic acid in order to look for pharmacological tools to manipulate chloride channels in the bovine kidney. This led to the discovery of IAA-94 as a potent inhibitor of chloride conductance. Subsequently, these workers used an expression cloning approach to identify the molecular targets of IAA-94, which led to the cloning of a gene for a protein that they termed p64 and which is now known as CLIC5B. Thus, because p64/CLIC5B was identified as a target of IAA-94, there was considerable pressure to show that it was a chloride channel, despite the fact that its primary sequence argued against it being a membrane protein (Redhead, Edelman et al. 1992; Landry, Sullivan et al. 1993). Indeed, patch clamp and whole cell current experiments were executed on mammalian cells endogenously expressing bona fide chloride channels and on those overexpressing CLIC paralogues. However, 25 years later the chloride conducting properties of CLIC proteins have not been proven convincingly.

Following the discovery of p64/CLIC5B, the human sequences for CLIC1 (Valenzuela, Martin et al. 1997) and CLIC4 (Howell, Duncan et al. 1996; Duncan, Westwood et al. 1997) were cloned. This revealed that neither of these proteins contains an N-terminal extension that might mediate insertion into membranes. In addition, structural analysis showed that they exist in a globular form and not as a transmembrane protein. Nevertheless, the potential channel activity of CLICs 1 & 4 was further investigated because it is similar to p64 (Landry, Sullivan et al. 1993). Initially, localisation studies indicated that CLIC1 was present in the

nucleus and the cytoplasm and it was therefore termed, NCC27 (nuclear chloride channel - 27) (Valenzuela, Martin et al. 1997). Tonini *et al.* showed with electrophysiological experiments that CHO-1 cells transfected with CLIC1 showed higher Cl<sup>-</sup> channel activity. In addition, they tagged CLIC1 at the N- or C-terminal with a FLAG-tag and identified that CLIC1 was inserted into the plasma membrane, with the C-terminal end extending into the cytoplasm. This was identified with a FLAG antibody (Tonini, Ferroni et al. 2000). Furthermore, CLIC1 and CLIC4 channel activity have been measured using isolated membranes. Berryman and colleagues used purified CLIC1 and CLIC4 proteins and added these to artificial liposomes. This resulted in a dose-dependent chloride efflux from the liposomes that were sensitive to IAA-94. Additionally, they showed that CLIC5A was stably expressed in placental choriocarcionma cells and localised with ezrin in apical microvilli. The efflux of iodide was not influenced by CLIC5A expression. It was therefore reasoned, that the channel activity might be restricted to intracellular membrane compartments (Berryman, Bruno et al. 2004). A study shows that macrophages from CLIC1 knockout mice display defective phagosome acidification and this is the only physiologically relevant experimental setting where CLIC proteins function as ion channels so far (Tulk, Kapadia et al. 2002).

There is evidence that CLIC proteins might not so much act as selective chloride ion channels, but rather as non-selective ion channels. Indeed, CLIC2 can suppress the cardiac ryanodine receptor calcium release (Board, Coggan et al. 2004; Jalilian, Gallant et al. 2008), and this was consistent with a role for this CLIC in reducing the electrochemical gradient across the ER membrane. Additionally, Singh *et al.* described CLIC4 insertion into membranes and showed that this increases the conductance of the bilayer, but not in a way that is specific for chloride ions (Singh and Ashley 2007), CLIC1 and CLIC5 have been shown to transport anions other than chloride (Valenzuela, Martin et al. 1997; Singh and Ashley 2007; Ponsioen, van Zeijl et al. 2009). Although these studies generally support the CLIC's ability to insert into or associate with cellular membranes, the capacity for the CLICs to act as ion channels (whether more or less specific for chloride) is still under debate.

## 1.5.2 CLICs as glutathione transferases

The first GSTs were enzymes identified because they were associated with xenobiotic metabolism. However, since the whole genomes have been encoded, more and more proteins belong to the GST fold superfamily. This includes the identification of several other GSTs. The CLIC proteins belong to the GST superfamily despite their weak sequence homology (15%) with the newly discovered GST omega (GSTO) proteins (Dulhunty, Gage et al. 2001). An important characteristic of GSTs is that they are able to catalyse the conjugation of a tripeptide (glutamine, cysteine, glycine) glutathione (GSH) to electrophilic regions of other molecules (Wilce and Parker 1994). The reaction occurs through activation of the thiol group of GSH, which allows non-covalent, but high-affinity binding to the substrate. A GST-fold is made of two different domains. One of the two domains is made up of the  $\alpha$ -helical C-terminal domain. The second domain has been described as the N-terminal thioredoxin fold. Most of the thioredoxin proteins have an active site in which a redox-active cysteine is located. This specific site is not present in all GST proteins (Wilce and Parker 1994).

The CLICs comprise a ~240 residue that adopts a GST superfamily fold (Dulhunty, Gage et al. 2001; Harrop, DeMaere et al. 2001). A single conserved cysteine is part of all CLIC proteins. Structural analyses reveal that the cysteine sits within a putative enzymatic active site. Furthermore, this putative 'active site cysteine' seems to become activated by the protein itself and thereafter is capable of forming disulphide bridges with GSH (Ponsioen, van Zeijl et al. 2009; Littler, Harrop et al. 2010). Moreover, in CLICs 2 & 3 the 'active site cysteine' is adjacent to another cysteine, thus forming a possible di-cysteine motif (Cys-X-X-Cys).

Experiments in which 2-hydroxyethyl disulphide was used as a substrate have recently indicated that CLIC1, 2 and 4 have a "glutaredoxin-like glutathione-dependent oxidoreductase enzymatic activity" (Al Khamici, Brown et al. 2015), which was ablated by mutation of the putative 'active site cysteine'. Moreover, the indanyloxyacetic acid (IAA) and ethacrynic acid compounds (IAA-94, A9C) that had been previously identified as CLIC-binding molecules in the 1990s and

(perhaps erroneously) termed 'chloride channel blockers', inhibit the glutathione-dependent oxidoreductase activity of CLIC1. Conversely, 4,4'-Diisothiocyano-2,2'-stilbenedisulfonic acid (DIDS), which is well-established to be a *bona fide* chloride channel antagonist had no effect on CLIC1's oxidoreductase activity. Taken together with structural observations that the GST-like active site fold is not present in the membrane-inserted form of the CLIC1, these studies suggest that the CLICs are metamorphic proteins that can assume at least two distinct structures. One is a globular soluble enzyme possessing glutarredoxin-like activity that is inhibited by IAA compounds, and which is neither a channel nor a membrane-associated protein. The other one is a membrane inserted/associated conformer, which lacks a GST fold, does not bind to IAA compounds, and that may have some influence on the ion permeability of biological membranes in a way that is unrelated to the enzymatic activity of the soluble CLIC conformers. To conclude, I think that the evidence that CLICs are chloride conductance channels is not persuasive, and that the primary role of the CLICs is to function as oxidoreductases. Moreover, the conclusions that compounds such as IAA-94 act as chloride channel blockers is likely based on circular argument that relied on the likely false assumption that the CLICs were chloride channels. However, the metamorphic nature of the CLICs cannot be ignored, and the ability of these proteins to switch between soluble-globular enzymes and membrane inserted proteins likely contributes to their biological roles. For instance, many CLICs localise to cellular membranes - CLIC3 is present at late endosomes and lysosomes and CLIC4 localises to the plasma membrane - and the ability of these proteins to insert into membranes may contribute to this. Thus the membrane inserted forms of the CLICs may form a reservoir of catalytically inactive CLIC within a particular cellular locale. Then, upon dissociation from these membranes, the CLIC may assume its globular conformer and act as oxidoreductase. Finally, the ability of the CLICs to insert into membranes is likely to form part of the mechanism allowing them to cross the plasma membrane to exit the cell via an unconventional secretion mechanism, and the role of secreted CLICs, in particular CLIC3, is the primary focus of this thesis (Al Khamici, Brown et al. 2015). CLICs and their various biological functions are summarised in Table 1.2.

Protein	AA length	Function	References
CLIC1	241	Involved in cell cycle regulation	(Valenzuela, Mazzanti et al. 2000)
		Modulation of amyloid- $\beta$ phagocytosis	(Paradisi, Matteucci et al. 2008)
		Regulation of osteoblast differentiation	(Yang, Jung et al. 2009)
		Apoptosis	(Kang and Kang 2008)
		Involved in cancer	(Wang, He et al. 2012)
		Functioning as an enzyme	(Al Khamici, Brown et al. 2015)
CLIC2	247	Interacts with the RyR1 receptor and modulates its activity	(Meng, Wang et al. 2009)
		it modulates RyR2 channel activity	(Board, Coggan et al. 2004; Dulhunty, Pouliquin et al. 2005)
CLIC3	236	Associates with the COOH-domain of ERK7	(Qian, Okuhara et al. 1999)
		Expressed in tumour cells of ER-negative breast cancers and the cancer aggressiveness is likely attributable to its ability recycle MT1-MMP back to the plasma membrane	(Macpherson, Rainero et al. 2014)
		Expressed in pancreatic adenocarcinomas leading to poorer survival due to control of the recycling of lysosomally-targeted $\alpha$ 5B1 integrin back to the plasma membrane	(Dozynkiewicz, Jamieson et al. 2012)
		Expressed in the placenta	(Money, King et al. 2007; Murthi, Stevenson et al. 2012)
		The absence of CLIC3 functioning as a chloride channel makes cells more prone to Listeria infections	(Kim, Choi et al. 2013)
		Expressed in bladder cancer and a peptide (CLT1) is able to kill bladder cancer cells through integrin $\alpha$ 5B1 integrin and CLIC3	(Knowles, Zewe et al. 2013)
CLIC4	253	Tubulogenesis	(Ulmasov, Bruno et al. 2009)
		Myofibroblast conversion	(Ronnov-Jessen, Villadsen et al. 2002)
		Association with Schnurri-2, apoptosis Regulates TGF- $\beta$ - dependent myofibroblast differentiation and produces cancer stroma	(Shukla, Malik et al. 2009; Shukla, Edwards et al. 2014)
		Affects RhoA and Rac1 activation and cell motility	(Spiekerkoetter, Guignabert et al. 2009)
		Capillary sprouting and endothelial proliferation	(Tung, Hobert et al. 2009)
		Acts as an enzyme	(Al Khamici, Brown et al. 2015)
CLIC5A	251	Ezrin-CLIC5-Podocalyxin co-expression increases migration and invasion in HCC	(Flores-Tellez, Lopez et al. 2015)
		Associates with the actin cytoskeleton	(Berryman, Bruno et al. 2004)
CLIC5B	410	Interacts with AKAP350	(Shanks, Larocca et al. 2002)
		Regulates myoblast proliferation and differentiation	(Li, Yin et al. 2010)
CLIC6	704	Interacts with a dopamine $D_2$ -like receptors	(Griffon, Jeanneteau et al. 2003)

**Table 1.2: The functional diversity of the CLIC proteins.**

### 1.5.3 CLICs and their role in cancer

The CLICs 1, 3, 4 have been shown, in one way or another, to contribute to the initiation and/or progression of cancer. In the following section I will focus on the roles played by individual CLICs in a cancer:

**CLIC1.** CLIC1 is expressed in several cancers including ovarian carcinoma (Tang, Beer et al. 2012), hepatocellular carcinoma, high grade gliomas (Wang, He et al. 2012), human breast ductal carcinoma (Wulfkühle, Sgroi et al. 2002), gastric cancers (Chen, Wang et al. 2007), gallbladder metastasis (Wang, Peng et al. 2009) and nasopharyngeal carcinoma (Chang, Wu et al. 2009). In 2004, CLIC1 was found to be expressed in liver cancer and it was thought to alter cell division and/or apoptotic signalling, resulting in cellular transformation. CLIC1 was found to be upregulated in mouse hepatocellular carcinoma and this was further associated with cell migration and invasion (Song, Tang et al. 2010; Li, Zhang et al. 2012). The presence of CLIC1 in cancer cells has been associated with increased ROS production by NADPH oxidase, and this can lead to CLIC1 translocation as well as alterations to chloride fluxes (Milton, Abeti et al. 2008). ROS levels are fundamental for cell cycle progression. Therefore, at high ROS levels CLIC1 has the potential to insert into the membrane, or conversely CLIC1 insertion into the membrane is associated with increased ion flux which keeps ROS levels high. This could promote cell cycle progression (Peretti, Angelini et al. 2014).

CLIC1 has been suggested to be important in the development of glioblastoma. CLIC1 is highly expressed at the mRNA and protein level in glioblastoma, and is higher expressed in high grade tumours than low grade tumours (Wang, He et al. 2012; Setti, Savalli et al. 2013). In addition, silencing of CLIC1 in cancer stem cells injected into immunodeficient mice reduced their self-renewal capacity as well as their proliferation and migration. (Peretti, Angelini et al. 2014).

**CLIC3.** Our group has discovered and described an intracellular role of CLIC3 in cancer cells. We have shown that CLIC3 is highly expressed in tumour cells of ER-negative breast cancers and in pancreatic adenocarcinomas, and that high CLIC3 levels are associated with reduced survival in these cancer types (Dozynkiewicz,

Jamieson et al. 2012; Macpherson, Rainero et al. 2014). These studies found that CLIC3's association with tumour aggressiveness is likely attributable to its ability to control the recycling of lysosomally-targeted  $\alpha 5\beta 1$  integrin and MT1-MMP back to the plasma membrane. Since then some other studies have been published associating CLIC3 with renal carcinoma and bladder cancer. In bladder cancer an antiangiogenic peptide CLT1 forms complexes with fibronectin killing proliferating cells through the  $\alpha 5\beta 1$  and CLIC3 pathway (Knowles, Zewe et al. 2013). The other study indicated that the plasma membrane sialidase NEU3 regulates the malignancy of renal carcinoma cells by controlling  $\beta 1$  integrin internalisation and recycling. Silencing of *NEU3* upregulates the Ras-related protein RAB25. RAB25 directs internalised integrins to lysosomes. *NEU3* silencing also downregulates CLIC3 which induces the recycling of internalised integrins to the plasma membrane. Therefore, silencing of *NEU3* increased the  $\beta 1$  integrin endocytosis, but blocked recycling and thus reduced  $\beta 1$  levels at the plasma membrane (Tringali, Lupo et al. 2012).

**CLIC4.** CLIC4 is likely to be relevant in cancer and has been shown to be present in the tumour profiling of glioma (Zhong, Kong et al. 2012), melanoma (Alonso, Tracey et al. 2007), uterine leiomyoma (Bae, Kim et al. 2004) and bladder cancer (Dyrskjot, Kruhoffer et al. 2004). CLIC4 expression varied considerably in these tumours. Moreover, CLIC4 expression has been associated with a poor prognosis in colon cancer, and it is expressed in colon cancer stem cells (Deng, Tang et al. 2014). Furthermore, CLIC4 has been identified as a circulating biomarker in patients with ovarian carcinoma (Tang, Beer et al. 2013), and has been shown to be released in exosomes from ovarian cancer cells (Liang, Peng et al. 2013; Sinha, Ignatchenko et al. 2014). Moreover, the level of circulating exosomes in ovarian carcinoma is correlated with disease progression (Szajnik, Derbis et al. 2013). Therefore, CLIC4 might be an ideal biomarker to measure tumour progression.

CLIC4 has two opposing functions in cancer. When expressed at high levels in the tumour cells it functions as a tumour suppressor, but when it is expressed in the myofibroblast stroma, it is associated with tumour progression.

CLIC4 downregulation in osteosarcoma cells *in vitro* and *in vivo* increased apoptosis and decreased cell proliferation, and this was enhanced following TNF $\alpha$  administration (Suh, Crutchley et al. 2007). However, in this study the antisense mRNA that was used to suppress CLIC4 levels also targeted CLIC1 and CLIC5, and thus the reduction of tumour cell proliferation may be attributed to multiple CLIC protein loss. In addition, other experiments showed that CLIC4 was lost in many tumours, but that its high expression in the tumour stroma led to malignant progression. CLIC4 is lost early in the evolution of tumours (Suh, Malik et al. 2012) and the re-expression of exogenous CLIC4 in the tumour inhibited growth. CLIC4 might act as a tumour suppressor, because its presence makes cells responsive to TGF- $\beta$ -mediated growth inhibition, which in turn functions through keeping SMAD in a dephosphorylated state (Shukla, Malik et al. 2009). From these studies it becomes clear that CLIC4 loss leads to tumour progression. Recently, a few studies have shown that following TGF- $\beta$  treatment, CLIC4 is one of the most upregulated proteins in myofibroblast stroma of breast cancer patients (Ronnov-Jessen, Villadsen et al. 2002). Finally, CLIC4 has a role in angiogenesis and this may be important to the stromal contribution to tumour growth (Ulmasov, Bruno et al. 2009).

## 1.6 Project aims

The goal of my project was to determine the characteristics of stromally-derived extracellular CLIC3 and the effect that this has on cancer cells. It has been shown that CLIC3 is expressed in fibroblastic cell types, but the impact of stromal CLIC3 on tumour aggressiveness has not yet been investigated.

1. I will characterise the effect of extracellular/secreted CLIC3 on cell migration and invasion.
2. I intend to investigate CLIC3's function as an enzyme and its role in collaborating with TG2 to promote ECM re-modelling, cell migration and invasion.

## 2 Material and Methods

### 2.1 Materials

#### 2.1.1 Reagents and solutions

Solution	Details	Company	Catalogue Number
2 % gelatine	diluted in PBS	Sigma	
Albumin Standard		Pierce	23209
Ammonium hydroxide solution		Sigma	318612-500ml
Ampicillin			
Amphotericin B solution	final concentration: 0.25 µg/ml	Sigma	A2942-100ml
Ascorbic acid		Sigma	A4403-100mg
Bovine Serum Albumin (BSA)			40-00-410
Comassie stain	Instant Blue	Expedeon	I5BIL
Cyclo(-Arg-Ala-ASP-D-Phe-Val) (cRADfV)	final concentration 2.5 µM	Bachem	H-4088
Cyclo(-Arg-Gly-Asp-D-Phe-Val) (cRGDFV)	final concentration 2.5 µM	Bachem	H-2574
DNase I	final concentration: 50	Roche	11284932001
dNTP		Promega	
Dulbecco's Modified Eagle Medium (DMEM)		Gibco	21969-035
Advanced DMEM/F-12 (Dulbecco's Modified Eagle Medium/Ham's F-12)		Gibco	12634-010
Epidermal growth factor Receptor (EGF)	50 ng/ml	Sigma	
Fibronectin	final concentration 25 µg/ml	Sigma	1141 -5MG
Glutaraldehyde		Sigma	G6257
Foetal Bovine Serum (FBS)		Gibco	
Geltrex LDEV-Free Reduced Growth Factor Basement membrane Matrix		Life technologies	A14132-02
IPTG	Isopropyl β-D-1-thiogalactopyranoside		
1 x IF Wash	1 x PBS, NaN <sub>3</sub> , BSA, Triton-X, Tween		

<b>Matrigel</b>		BD Biosciences	354230
<b>Methanol</b>		VWR chemicals	
<b>Millipore-P PVDF membrane</b>		GE Healthcare	
<b>L-Glutamine (200 mM)</b>		Gibco	
<b>Penicillin/Streptomycin</b>	10 U/mL penicillin and 10 ug/mL streptomycin	Gibco	
<b>NDLB cell lysis buffer</b>	150 mM NaCl, 50 mM Tris, 10 mM NaF, 1 mM Na <sub>3</sub> VO <sub>3</sub> , 5 mM EDTA, 5 mM EGTA, 1%Triton X-100, 0.5%Igepal		
<b>NuPAGE MOPS Running buffer (20x)</b>		Life Technologies	NP0001
<b>NuPAGE Pre-cast gels</b>		Life Technologies	NP8323BOX
<b>NuPAGE LDS Sample Buffer (4x)</b>		Life Technologies	NP0007
<b>NuPAGE Transfer buffer (20x)</b>		Life Technologies	NP0006-1
<b>Parafilm wrap</b>			
<b>PBS containing Calcium and Magnesium</b>			Sigma
<b>PBS/EDTA (PE)</b>	PBS + 1mM EDTA	Beatson Institute Central Services	
<b>PBS-T</b>	PBS+0.1%Triton X-100		
<b>Precision Plus Protein Standard All Blue</b>		Biorad	161-0373
<b>BL21 pLys(DE) E.coli</b>		Life Technologies	
<b>Roswell Park Memorial Institute (RPMI) 1640 Medium</b>		Gibco	31870-025
<b>SOC medium</b>		Life Technologies	
<b>SYBR green PerfeCTa®</b>		Quanta	
<b>One Shot® TOP10</b>		Life Technologies	
<b>Trypsin</b>	0.25 % final concentration		Gibco
<b>Triton-X</b>		Sigma	
<b>VECTASHIELD Antifade Mounting Medium with DAPI - non-hard set</b>	3 drops of the mounting medium used every well/dish	Vectorlaboratories	H-1200
<b>Z-DON</b>	Inhibitor used at 40 µM and 20 nM	Zedira	Z006

### 2.1.2 Antibodies and dyes

Antigen	Details	Dilution for WB	Source
TG2	rabbit	1:1,000, 5% milk	Sigma, HPA021019
Calcein, AM, cell-permanent Dye			Life Technologies, C1430
Phalloidin	Alexa Fluor 546	1:200	Life Technologies, A22283
Vincullin	mouse		
secondary IR Dye 680	goat - anti-rabbit	1:10,000, TBS-T	Licor: 926-32221
secondary IR Dye 680	donkey - anti - mouse	1:10,000, TBS-T	Licor 926-68072
secondary IR Dye 800	donkey - anti - rabbit	1:10,000, TBS-T	Licor: 926-32213
secondary IR Dye 800	donkey - anti - mouse	1:10,000, TBS-T	Licor: 926-32212
Laminin 5 $\gamma$ -chain	mouse, Lot: D4B5	1:200	Millipore, MAB19562
Integrin $\beta$ 4	mouse anti-human	1:200	BD555722
FITC	goat - anti - mouse	1:200	southern Biotec, 1031 - 02
Phalloidin 546		1:200	Life technologies, A22283

### 2.1.3 Enzyme and kits

Kit	Supplier	Catalogue Number
AMAXA Nucleofection Kits	Lonza	VCA-1001 VCA-1002
Glutathione Sepharose beads	GE Healthcare	17-0756-01
Improm II Reverse Transcription Kit	Promega	A3800
PreScission Protease	GE Healthcare	27-0843-01
Pierce <sup>®</sup> BCA Protein Assay Kit	Thermo Fisher Scientific	23227
QIAquick <sup>®</sup> PCR purification Kit	Qiagen	28104
Quick Change <sup>®</sup> Site-Directed Mutagenesis Kit	Stratagene	200518

### 2.1.4 Tissue culture plastic ware

Kit	Supplier
Cryotubes	NUNC
3 cm glass bottom dishes	MatTek
6-well plates	Falcon
10 cm dishes	Corning
15 cm dishes	NUNC
Transwell Permeable Support; pore size of 8 $\mu$ m diameter	Corning

## 2.2 Methods

### 2.2.1 RNA extraction

Total cellular RNA from cells was isolated using the RNeasy kit, according to manufacturer's instructions. The medium was removed from plates. Plates were transferred onto ice and washed twice with ice-cold PBS (pH 7.4). The cells were lysed in 1 ml of RLT buffer supplemented with  $\beta$ -mercaptoethanol (10  $\mu$ l per 1 ml of buffer). The samples were filtered using Qias shredder columns and RNA was extracted and purified. DNA was removed by an on column DNase I digestion. RNA was eluted from the column in 50  $\mu$ l H<sub>2</sub>O and snap-frozen on dry ice and stored at -80°C.

The RNA concentration was measured using the Nanodrop (Spectrophotometer, Thermo, NANODROP 2000c).

### 2.2.2 cDNA Synthesis

cDNA was synthesised using the Promega kit according to manufacturer's instructions to a final reaction volume of 20  $\mu\text{l}$ .

Reagent	Amount
Oligo-dT primer (500 $\mu\text{g}/\text{ml}$ )	1 $\mu\text{l}$
1 $\mu\text{g}$ RNA	x $\mu\text{l}$ as determined from the RNA concentration
H <sub>2</sub> O	make up to a final of 10 $\mu\text{l}$

**Table 2.1: The oligo-dT/template thermal denaturation was performed at first.**

The samples were heated up to 70°C for 10 minutes in the Biorad DNA (Dyad) Engine Peltier Thermal Cycler and transferred to ice for one minute. The reverse transcription reaction was then added to the samples.

Reagent	Amount
imProm-II 5 x reaction buffer	4 $\mu\text{l}$
MgCl <sub>2</sub> (25mM)	3 $\mu\text{l}$
dNTP mix (10 mM)	1 $\mu\text{l}$
RNasin (40U/ml)	0.5 $\mu\text{l}$
IMProm-II Reverse Transcriptase	1 $\mu\text{l}$
H <sub>2</sub> O	0.5 $\mu\text{l}$

**Table 2.2: Reverse transcription reaction setup.**

The samples were incubated at 25°C for five minutes, which allowed initial annealing, and the elongation proceeded at 42°C for 1 hour. When the first strand synthesis was completed, the reaction was terminated by incubation of the samples at 70°C for ten minutes and the samples subsequently cooled to 4°C.

### 2.2.3 Primers for real time PCR

These are the two primer sets for real time PCR.

Description	Sequence
TG2 Fw	CCGTAAGGCAGTCACGGTAT
TG2 Rev	TCAGCTACAATGGGATCTTGG
GAPDH Fw	AGGTGAAGGTCCGGAGTCAAC
GAPDH Rev	AATGAAGGGGTCATTGATGG

**Table 2.3: Primers used for real time PCR.**

### 2.2.4 Real time PCR

PerfeCTa® SYBR® Green SuperMix was used to perform quantitative PCR on a BioRAD C1000 Thermal Cycler CFX96 BioRAD Real time System. As a programme the Bio-Rad CFX manager was used. A standard curve was prepared from cDNA starting at a dilution of 1:2 down to 1:256. The real time PCR reactions were assembled as follows:

Reagent	Amount
2 x PerfeCTa® SYBR® Green SuperMix	5 µl
Primer forward	0.5 µl (100 pm/µl)
Primer reverse	0.5 µl (100 pm/µl)
cDNA	0.5 µl
H <sub>2</sub> O	3.5

**Table 2.4: Reagents which were mixed for PCR assembling.**

The real time PCR reaction was performed according to the protocol shown below Table 2.5.

<b>Initial denaturation</b>	95 °C	10 min
<b>40 cycles</b>		
Denaturation	95 °C	30s
Annealing	55 °C	30s
Extension	72 °C	30s
<b>Plate read</b>		
Final extension	72 °C	5 min
Dissociation curve	70 °C to 90 °C in 0.3 °C increments	
Final hold	4 °C	

Table 2.5: The real time PCR reaction setup.

The data was analysed with the Bio-Rad CFX manager with the help of the  $\Delta\Delta C(t)$  method and GAPDH served as a reference gene (Livak and Schmittgen 2001).

## 2.2.5 Cloning and DNA manipulation

### 2.2.5.1 Bacterial strains

OneShot® BL21 (DE3) pLysS *E.coli* competent cells were used for protein production and One Shot® TOP10 *E.coli* DH5 $\alpha$  were used for all other cloning procedures.

### 2.2.5.2 Bacterial transformation

The pGEX-6-P1 fusion plasmid (GE Healthcare) was transformed into OneShot® BL21 (DE3) pLysS *E.coli* competent cells. All other plasmids, which were used for sequencing, were transformed by using the One Shot® TOP10 *E.coli* DH5 $\alpha$  chemically competent cells. 1  $\mu$ g of the corresponding plasmid was added to 50  $\mu$ l of (thawed on ice) competent cells, incubated for 15 min and heat shocked at 42 °C for 10 sec. Subsequently, 450  $\mu$ l of SOC medium were added and the cells incubated at 37 °C, shaking at 350 rpm. *E.coli* cells were then plated on LB containing soft agar in Petri dishes containing 100  $\mu$ g/ml of ampicillin. Plates were further incubated overnight at 37 °C. The next day single colonies were picked and cultured for protein production overnight in 20 ml of LB

supplemented with 100 ug/ml ampicillin. Plasmids for sequencing were cultured in 5 ml LB medium containing 100 µg/ml Ampicillin shaking overnight at 37°C.

### 2.2.5.3 Plasmid preparation

The overnight cultures were pelleted by centrifugation at 3,000 rpm for 10 minutes using the Beckmann Coulter centrifuge. Central Services then used the QIAprep Spin Mini-Prep Kit followed by sequencing the samples. Sequences were analysed using the CLC Genomic Workbench. If large scale plasmid preparations were used, 200 ml were cultured overnight in LB media with 100 µg/ml ampicillin. The cells were pelleted by centrifugation as described above for a duration of 10 minutes. Maxipreps were performed by Central services. The DNA was quantified with a Biophotometer at 260 nm absorbance.

### 2.2.5.4 Site-directed mutagenesis

The GST-TG2 plasmid was a kind gift from Dr. Jeffery Keillor (Roy, Smith et al. 2013). The coding region of CLIC3 with flanking restriction sites was amplified and subcloned into a pGEX-6P-1 vector by Marta Dozynkiewicz. The GST-CLIC3<sup>C22A</sup> and GST-CLIC3<sup>C22A C25A</sup> were generated by mutating the cysteines of CLIC3 in the position 22 and 22 and 25 to alanine using site directed mutagenesis, according to the manufacturer's instructions (Stratagene). The following primers were generated to perform these mutations.

Description	Sequence
CLIC3 C22/A22 Fw	GAGAGCGTGGGTACGCCCCCTCCTGCCAGCGGCTC TTCATG
CLIC3 C22/A22 Rev	CATGAAGAGCCGCTGGCAGGAGGGGGCGTGACCCA CGCTCTC
CLIC3 C22/A22 C25/A25 Fw	GAGAGCGTGGGTACGCCCCCTCCGCCAGCGGCTC TTCATG
CLIC3 C22/A22 C25/A25 Rev	CATGAAGAGCCGCTGGGCGGAGGGGGCGTGACCCA CGCTCTC

Table 2.6: Sequences for mutagenesis primers

## Chapter 2

In short, the plasmid (pGEX-6-P-1) was denatured and the designed primers were annealed. The plasmid was then further extended using the *PFU Turbo DNA polymerase*, incorporating the mutagenic primers. This resulted in nicked circular strands.

Reagent	Amount
10× reaction buffer	5 µl
pGEX-6P-1 - CLIC3	10 ng
oligonucleotide primer #1	125 ng
oligonucleotide primer #2	125 ng
dNTP mix	1 µl of 10 mM dNTPs
ddH <sub>2</sub> O	make a final volume of 50 µl
PFU Turbo DNA Polymerase	1 µl

**Table 2.7: PCR setup**

The Polymerase chain reaction was performed in the DNA Engine Thermal Cycler (Biorad).

Initial denaturation	95° C	60 s
<b>18 cycles</b>		
Denaturation	95° C	50 s
Annealing	60° C	50 s
Extension	68° C	7 min
	68	7 min

**Table 2.8: Program used for PCR setup.**

Afterwards, the non-mutated methylated parental DNA template was digested with *DpnI*. For this, 1 µl of *DpnI* was added to the samples and incubated for 60 minutes at 37° C. The new formed plasmid was subjected to transformation and sequencing.

## 2.2.6 Recombinant protein production

### 2.2.6.1 Protein expression

One litre of sterile LB media with 100 µg/ml ampicillin was inoculated with 10 ml of overnight culture, grown under shaking/agitation at 37°C until an OD<sub>600</sub> of 0.4 - 0.6 was reached. At that point, 1 ml of sample was taken as an uninduced control and then protein expression induced with 0.25 mM of IPTG. After 2 hours, 1 ml of the solution was taken as a sample for immunoblotting. The rest was pelleted at 4,000 rpm for 30 minutes at 4°C. The pellets were frozen at -80°C. After thawing on ice, the pellets were resuspended in 10 ml of PBS (pH 7.4) and 0.1 % Triton X-100. After the cells were resuspended, 1M of Benzamidine and 1 mg/ml of PALA (Pepststin, Antipain, Leupeptin and Aprotinin protease inhibitors) were added. The cells were sonicated on ice, with three cycles of 30 seconds ON and 30 seconds OFF at 50 mAmp (Sonicator: Sonics, Vibra Cell). The sonicated cells were then spun at 11,000 rpm for 30 minutes at 4°C. The supernatant was transferred to a 50 ml Falcon tube and kept on ice. 250 µl of pre-swollen 50% glutathione agarose beads were added. The tubes containing the samples were incubated on a roller mixer at 4°C for two hours. The lysate with the glutathione beads was spun at 1,000 rpm for 10 minutes at 4°C and then transferred to 1.5 ml tube. The beads were washed three times in 1 x PBS (pH 7.4) and spun for 5 minutes at 500 x g. The beads were then washed with cleavage buffer, which contained 50 mM Tris-HCL pH 7.0 (at 25°C), 150 mM NaCl, 1 mM EDTA, 1 mM DTT and 0.01% Triton X-100. Finally, the PreScission Protease (20 U) was added to the PreScission Protease buffer. The samples were further incubated overnight at 4°C with slow rotation. The following day the samples were centrifuged at 500 x g for 5 minutes, the supernatant was collected in a fresh 1.5 ml tube and the protein concentration was determined using the BCA assay.

## 2.2.7 Mammalian cell culture techniques

### 2.2.7.1 Cell origin

Stable clones of A2780-DNA3 cells were a kind gift from Gordon Mills and were generated as described previously (Cheng, Lahad et al. 2004). The originators of

the A2780 cell line have not defined to which histological ovarian carcinoma subtype they belong. However, it is up to now the second most common high-grade serous ovarian carcinoma (HGSOC) cell line used (according to PubMed). Whether the A2780 ovarian carcinoma cell line resembles HGSOC or another histological ovarian carcinoma subtype, was recently analysed by Domcke and colleagues (Domcke, Sinha et al. 2013). They have published a study in which they analysed 47 ovarian carcinoma cell lines and identified those that have the highest genetic similarity to ovarian carcinoma (Domcke, Sinha et al. 2013). To do this they made use of The Cancer Genome Atlas (TCGA) in which more than 500 tissue samples per tumour were characterised. They also used a collection of genomic profiles of about 1000 cell lines which are used as model systems for various tumours and this collection is called The Broad-Novartis Cancer Cell Line Encyclopaedia. They compared these databases and identified that typical signs for HGSOC are a mutation in TP53 and flat copy number alterations. The A2780's have been shown not to be the best cell line to study HGSOC carcinoma as they lack a TP53 mutation. Moreover, the A2780 cell line mutations per million bases was correlated with the copy number alterations of HGSOC tumour samples and this resembles only 20%. Therefore, this analysis stands in contrast to the frequently used cell lines as models for this subtype. Therefore, to study HGSOC specifically another cell line is certainly better such as KURAMOCHI cell line. In this thesis I partly follow up on the work which was previously done in the lab and this is the reason I have used the A2780 cell line (Dozynkiewicz, Jamieson et al. 2012). In the future it would be better to consult the study first and pick the best suited cell line.

MCF10DCIS.com cells were a kind gift from Chavier Philippe. Telomerase-immortalised foetal fibroblasts (TIFFs) (Munro, Steeghs et al. 2001) were obtained from Deborah Gardner, immortalised cancer-associated fibroblasts (iCAFs) and immortalised normal fibroblasts (iNFs) (Orimo, Gupta et al. 2005; Polanska and Orimo 2013) from Juan Hernandez. These two cell lines were generated from healthy human breast tissue. Fibroblasts were isolated from the breast tissue and transfected with a retroviral pMIG (MSCV-IRES-GFP) vector which expressed hTERT and GFP. These cells were cultured and then FACS sorted for GFP positive cells. Afterwards these cells were transfected with a pBabe-puro retroviral vector. Following a few days in culture the GFP positive cells were selected for puromycin resistance. These cells were selected and thus are

called immortalised mammary fibroblasts. The immortalised mammary fibroblasts were mixed with MCF-7-ras human breast carcinoma cells and injected into an immunodeficient mouse. To generate normal fibroblasts the immortalised mammary fibroblasts were injected into an immunodeficient mouse without mixing them with MCF7-ras cells. After 42 days of incubation the breast cancer xenograft was isolated and a single cell culture prepared. These cells are from hereon called immortalised cancer-associated fibroblasts (iCAFs). The normal fibroblasts were also isolated at the site of injection and a single cell culture prepared. These cells are called immortalised normal fibroblasts (iNFs). The cells were selected for puromycin resistant cells. Both of these cell lines were again injected into mice and incubated for 242 days. This was done as described above. The iCAFs were co-injected with MCF-7-ras cells into an immunodeficient mouse and this was done because they wanted to increase the activated myofibroblastic phenotype. The iNFs were injected alone into an immunodeficient mouse. The tissues were again isolated and a single cell suspension was prepared from both cell lines. The cells were selected again for puromycin resistance. Finally, these are the iCAFs and iNFs I used (Polanska, Acar et al. 2011). MDA-MB-231 breast cancer cells, as well as PDAC (*Pdx1-Cre*, *KRas<sup>G12D/+</sup>*, *p53<sup>R172H/+</sup>*) (Morton, Timpson et al. 2010) were obtained from Max Nobis.

### **2.2.7.2 Cell maintenance**

A2780 DNA3 cells was cultured in in RPMI-1640 supplemented with 10% (v/v) FBS, 2 mM L-glutamine, 10 U/ml penicillin, 10 µg/ml streptomycin and 0.25 µg/ml amphotericin B in an incubator at 37°C and 5% CO<sub>2</sub>. The iCAFs, TIFFs, iNFs, PDAC cells and MDA-MB-231 breast cancer cells were cultured in DMEM supplemented with 10% (v/v) FBS, 2 mM L-glutamine, 100 U/ml penicillin, 100 µg/ml streptomycin and 0.25 µg/ml Amphotericin B in an incubator at 37°C and 5% CO<sub>2</sub>. The DCIS.com cells were cultured in Advanced DMEM/F12 supplemented with 5% (v/v) horse serum, 2 mM L-glutamine, 100 U/ml penicillin, 100 µg/ml streptomycin and 0.25 µg/ml Amphotericin B in an incubator at 37°C and 5% CO<sub>2</sub>.

The cells were passaged once they reached 80 - 90% confluence. The cells were washed with 1 x PBS. 0.25% Trypsin/PE was added and the cells were put in the

incubator to detach. The cells were resuspended in fresh medium and spun at 1,000 rpm for five minutes followed by resuspension in fresh medium and seeding at the desired density.

### **2.2.7.3 Freezing of cells for long term storage**

For long term storage the cells were washed once in 1 x PBS and then trypsinized in Trypsin/PE at 37°C. The cells were resuspended in fresh culture medium followed by a five minute spin at 1,000 rpm. The cell pellet was resuspended in freezing medium (10% DMSO in FBS) and aliquoted into cryo vials. The cells were frozen at -80°C and then transferred to the liquid nitrogen.

### **2.2.7.4 Nucleofection®**

Nucleofection® was used to transfect siRNAs into A2780, iCAF, iNF and TIFF cells. The cells were passaged the day before and were about 80% confluent at the day of transfection. The cells were trypsinized, re-suspended in the corresponding growth media and centrifuged for 5 minutes at 1,000 rpm. The cells were washed in PBS, followed by another centrifugation step. The resulting cell pellet was resuspended in 100 µl of the corresponding Nucleofactor solution R for iCAFs, TIFFs, and iNFs and solution T for A2780 cells. The cells in the Nucleofactor solution were mixed with 5 µl of 20 µM siRNA (1 µM final siRNA concentration) and transferred to a Nucleofection® cuvette and inserted into the Amaxa Nucleofactor®. The transfected cells were suspended in 500 µl of warm media and added to tissue culture dishes.

### **2.2.7.5 Cell proliferation assays**

For the cell proliferation assay 10,000 cells were seeded in 6-well plates. They were seeded in the morning and allowed to settle on the plate. In the afternoon, inhibitors or recombinant proteins were added to the cells. The next day, the cells were counted using the CASY® counter. The cells were counted every day either for four or six consecutive days.

### 2.2.8 Inverted invasion assay

Geltrex™ inverted invasion assay was performed as described previously (Hennigan, Hawker et al. 1994). Pure growth factor reduced Geltrex™ (LDEV-Free Reduced Growth Factor Basement Membrane Matrix, Cat. No. A1413202) was thawed on ice and mixed with equal volume of ice-cold PBS and supplemented with 25 µg/ml soluble fibronectin. The sample was additionally supplemented with either 2.5 µM cRADfv, 2.5 µM cRGDfv, 25 ng/ml GST, 25 ng/ml CLIC3 C22A or 25 ng/ml CLIC3 with or without 20 nM Z-DON (Benzyloxycarbonyl-(6-Diazo-5-oxonorleucinyl)-L-Valinyl-L-Prolinyl-L-Leucinmethylester). Z-DON functions as a TG2 inhibitor by functioning as an analogue of TG2's substrate, glutamine (McConoughey, Basso et al. 2010). Transwells (Corning, pore size of 8.0 µm diameter) were inserted into wells of a 24-well cell culture dish, followed by the addition of 100 µl of the Geltrex™-PBS mixture and this was left at 37°C to solidify. A2780 cells were washed in PBS and trypsinized. After resuspension in media and centrifugation for 5 minutes at 1,000 rpm, the cells were counted and  $4 \times 10^4$  cells were seeded on top of the then inverted transwell. The cells on the bottom of the filter were covered with the base of the 24-well cell culture plate so that they made contact with the cell droplets. The cell attachment was allowed to take place at 37°C, 5% CO<sub>2</sub> for 4 hours. The wells were again inverted and non-adherent cells were washed off by two sequential washes in 1 ml of 0.5 % FBS-RPMI medium. The transwells were then placed in 1 ml of 0.5 % FCS-RPMI supplemented with 2.5 µM cRADfv, 2.5 µM cRGDfv, 25 ng/ml GST, 25 ng/ml CLIC3 C22A or 25 ng/ml CLIC3 with or without 20 nM Z-DON, respectively. In the upper chamber, 10 % FBS-RPMI was supplemented with 50 ng/ml EGF and 2.5 µM cRADfv, 2.5 µM cRGDfv, 25 ng/ml GST, 25 ng/ml CLIC3 C22A or 25 ng/ml CLIC3 with or without 20 nM Z-DON, respectively. The cells were allowed to invade towards the serum-EGF gradient for 72 hours at 37°C and 5 % CO<sub>2</sub>. To visualise cells that migrated into the Geltrex™ matrix, 4 µM Calcein-AM (acetoxymethyl ester calcein) was used. The transwells were transferred to a new 24-well plate and 1 ml of the Calcein-RPMI mixture was added into the top chamber of the transwell ontop of the Geltrex™ matrix. After one hour of incubation at 37°C, the transwells were imaged by confocal microscopy using the Olympus FV1000 with a 20x/0.75 NA objective at an excitation wavelength of 488 nm and emission wavelength at 515 nm. Starting

at the bottom of the transwell 10  $\mu\text{m}$  slices upwards in the direction of cell invasion were taken. The resulting images were analysed and quantified using the Image J. The threshold fluorescence intensity of the images was set to register only cells which are present in the individual slice. The sum of the resulting fluorescence at 30  $\mu\text{m}$  and above was divided by the total fluorescence of all the sections. This gave the invasion index of 30  $\mu\text{m}$  and above. The data were generated from at least 3 independent experiments, with each individual experiment encompassing three transwells per condition and three different optical sections acquired at different 3 areas of the transwell.

### **2.2.9 Generation of cell derived matrix**

The cell derived matrix (CDM) (Cukierman, Pankov et al. 2001; Bass, Roach et al. 2007) was generated as described before. Tissue culture plates were coated with 0.2 % gelatine for one hour at 37°C. Afterwards, the tissue culture dishes were washed 2 times with PBS followed by crosslinking with 1 % of sterile glutaraldehyde for 30 minutes at 37°C. Subsequently, the wells were washed twice with PBS and the cross-linker quenched with 1 M of sterile glycine in PBS (pH 7) for 20 minutes at room temperature. Following 2 more PBS washes, the tissue culture wells were equilibrated with DMEM containing 100 U/ml penicillin, 100  $\mu\text{g}/\text{ml}$  streptomycin, 2 mM L-glutamine and 10% (v/v) FBS for 30 minutes at 37°C. iNFs, iCAFs or TIFs were grown up to 70 - 80 % confluence and then transfected with final 1  $\mu\text{M}$  siRNA concentration. The cells were transfected with a control (siNT) or with a siRNA targeting CLIC3 or TG2. After transfection cells were seeded near confluence and cultured for 8 to 9 days in DMEM containing 100 U/ml penicillin, 100  $\mu\text{g}/\text{ml}$  streptomycin, 2 mM L-glutamine and 10 % FBS (v/v) and 50  $\mu\text{g}/\text{ml}$  ascorbic acid. Every second day the medium was refreshed. The ascorbic acid induces collagen production and renders the cell-derived matrix adherent to the cell culture wells. To denude the matrix from intact cells, PBS containing 20 mM  $\text{NH}_4\text{OH}$  and 0.5 % TritonX-100 was added to the cell culture wells and left for about 2 minutes. Once all the cells had died, the cell-derived matrix was washed twice with PBS containing  $\text{MgCl}_2$  and  $\text{CaCl}_2$ . During this step the remaining DNA was digested with 10  $\mu\text{g}/\text{ml}$  DNase I in the PBS containing 0.1 g/L  $\text{MgCl}_2$  and 0.133 g/L  $\text{CaCl}_2$  for 30 minutes at 37°C in 5 %  $\text{CO}_2$ . Afterwards, the CDM was washed twice with PBS containing 0.1 g/L  $\text{MgCl}_2$  and

0.133 g/L CaCl<sub>2</sub> and stored in PBS with 0.1 g/L MgCl<sub>2</sub> and 0.133 g/L CaCl<sub>2</sub> supplemented with 100 U/ml penicillin and 100 µg/ml streptomycin.

### **2.2.10 Migration assay**

A2780 ovarian carcinoma cells or MDA-MD-231 cells were plated onto CDM in a 6-well plate at a density of  $1 \times 10^5$  cells/well. Two hours later, recombinant CLIC proteins were added at different concentrations ranging from 0.3 ng/ml up to 25 ng/ml. Another three hours later the timelapse was started. The cells were transferred to an incubator attached to the microscope (37°C, 5 % CO<sub>2</sub>). Every five minutes pictures were taken of the cells over a 22 hour period at a 10x/NA:0.25 magnification with a Nikon Z6012. The analysis of pseudopod lengths was carried out with Image J. The pseudopod length was measured from the nucleus to the front tip of the cell. 30 cells per movie were measured and six images were taken per each well. In total, 180 pseudopod lengths were measured per condition per experiment.

### **2.2.11 Conditioned Media Experiments**

80% confluent 15 cm culture dishes of iCAFs or iNFs were nucleofected, using Amaxa Kit R and programme T-20 (Amaxa Nucleofector®), with 1 µM final siRNA concentration. One siRNA was used as a non-targeting control (siNT) and another to target CLIC3 (siCLIC3 oligo #3). The cells were allowed to recover for 24 hours and then seeded at  $1.5 \times 10^6$  cells per 10 cm dish. After 72 hours at 37°C and 5 % CO<sub>2</sub> incubation, the supernatant was sequentially spun at 300 x g for 10 minutes, 2,000 x g for 10 minutes and 10,000 x g for 30 minutes. The remaining medium was mixed (1:1) with fresh DMEM (10% FBS). MDA-MB-231 cells were trypsinized and resuspended in 10 ml DMEM and counted.  $1 \times 10^5$  cells were seeded per well in the respective conditioned medium from iNF siNT, iCAF siNT, iCAF siCLIC3 cells or MDA-MB-231 in DMEM containing 10 % (v/v) FBS, 100 U/ml penicillin, 100 µg/ml streptomycin and 2 mM L-glutamine. Before, the timelapse was started either 1 ng/ml GST or 1 ng/ml CLIC3 was added.

### **2.2.12 Fixing and staining cells on CDM**

A2780 DNA3 cells were seeded on 3 cm glass bottom dishes (MatTek), with CDM laid down. The cells were allowed to settle on the dish for two hours followed by stimulation with CLIC3 (1 ng/ml) for 2 hours. Afterwards the cells were fixed with 4 % Paraformaldehyde (PFA) for 15 minutes followed by permeabilisation of the cells with 0.2 % Triton in PBS for 5 minutes. The cells were washed in PBS twice and then blocked with 1 % BSA for one 1 hour, followed by 1 x PBS wash. The cells were stained with fibronectin antibody (1:100 diluted in PBS) for 1 hour. Afterwards, the cells were washed again three times with PBS and stained with FITC, and the excess staining was washed off two times with PBS. Finally, the cells were stained with Phalloidin 546 (1:200 in PBS) for 10 minutes. Afterwards, excess stain was washed off two times PBS and one time dH<sub>2</sub>O. In the end, nuclei were stained with DAPI (VECTASHIELD Antifade Mounting Medium with DAPI - non-hard set). The cells were imaged by confocal microscopy using the Olympus FV1000 with a 60x (oil) /NA: 1.4 objective. Starting at the bottom of the cell, a Z-stack with 0.3 µm slices upwards in the direction of the cells, with at least 20 slices, were acquired. The images were merged using the Image J software.

### **2.2.13 Protein isolation**

Cells were cultured until they reached a confluence between 70 or 80 %. The medium was aspirated and the plates were transferred onto ice and washed twice with ice-cold PBS (pH 7.4). The cells were lysed with 1.5 x NDLB buffer which contained protease inhibitors: 1 mM AEBSF (4-[2-Aminoethyl] benzenesulphonyl fluoride), 50 µg/ml Leupeptin and 50 µg/ml Aprotinin. The cell lysates were scraped with a cell lifter, homogenised with a 25 gauge syringe and transferred to a 1.5 ml tubes. After centrifugation at 13,000 rpm for 10 minutes (4 °C), and the cleared cell lysate was transferred to a fresh tube. The samples were snap frozen with dry ice and stored at -80 °C.

### **2.2.14 Determination of protein concentration**

The protein concentration was measured using the Pierce BCA Protein Assay Kit according to manufacturer's instructions. The BSA standard had a working range of 20 - 2,000 µg/ml. The samples were pipetted in duplicate to reduce pipetting errors. To identify protein concentrations a working reagent was made up consisting of a solution A and solution B, with a ratio of 50:1. 200 µl of the working reagent was pipetted into each well containing either the BSA standard or samples (96-well plate). The mixtures in the plate were mixed and incubated at 37°C for 30 minutes. The plate was cooled and the absorbance was measured at a wavelength of 562 nm in a plate reader (Molecular Devices). The individual protein concentrations were determined by correlation to the BSA-standard curve.

### **2.2.15 SDS-PAGE and Coomassie staining**

Sodium-dodcyl sulphate (SDS) - poly acrylamide gels were used to resolve the protein samples. 40 µg of each protein sample was mixed with 1 x sample buffer (NuPAGE LDS Sample Buffer with freshly added 50 mM DTT). The samples were heated for 5 minutes up to 95°C and afterwards briefly spun before being loaded onto a 4 - 12 % gradient gel (NuPAGE, Life Technologies). Gel electrophoresis was performed by adding 1 x MOPS running buffer (NuPAGE, Life Technologies) and run at 150 V for 1.5 hours. To identify the size of the protein molecular weight markers (Precision Plus Protein Standard All Blue, BioRad) were loaded next to the samples. The gel was either stained with Simply Blue Coomassie stain (Expedeon) or subjected to Western blotting.

### **2.2.16 Western blotting**

The gel was transferred onto a PVDF-membrane in blotting buffer (NuPAGE Transfer buffer (20x)) at 100 V for one hour using a BioRAD wet transfer. Afterwards, PVDF membrane was blocked in 5 % milk overnight at 4°C to block the excess protein sites. The membranes were then incubated overnight with primary antibodies at the corresponding concentrations at 4°C. The membranes were washed three times for 5 minutes in TBS-T, followed incubation with the

corresponding LICOR fluorophore conjugated secondary antibody at a 1:10,000 dilution for 30 minutes at room temperature. The membrane was then washed three times in TBS-T followed by scanning the membrane with an infrared imaging system (Licor CLx Odyssey).

### **2.2.17 Secretion experiments**

The cells were plated at a density of  $1.5 \times 10^6$  cells/10 cm dish and left for 48 hours at 37°C and 5 % CO<sub>2</sub>. The medium was then changed to 7 ml/10 cm dish of serum-free DMEM (100 U/ml penicillin, 100 µg/ml streptomycin and 2 mM L-glutamine). After 24 hours the supernatant and cells were harvested. The supernatant was harvested and transferred into Beckmann spinning tubes. The samples were spun sequentially at 300 x g for 10 min, at 2,000 x g for 10 min and at 10,000 x g for 30 minutes. The supernatant was then transferred to a 15 ml falcon tube and Trifluoroacetic acid (TFA, 10%) was used to reduce the pH to 5. Afterwards, 70 µl of Streptavidin beads were used for each supernatant. The tube containing the beads was vortexed for 1 minute and then rotated in the cold room overnight. The beads were pelleted by centrifugation at 2,000 x g for 1 minute. The beads were mixed in with 35 µl of 4 x loading buffer containing 50 mM DTT. The samples were boiled before being loaded onto SDS PAGE gels.

### **2.2.18 Preparation of collagen I from rat tail tendons**

The method has been precisely described (Timpson, McGhee et al. 2011). Briefly, twelve adolescent frozen rat tails were used to prepare collagen. The tails were thawed and washed in 70 % ethanol. The skin on the tails was removed by slicing through from the top of the tail to the bottom of the tail with a scalpel and the tendons were detached using toothed forceps from the core of the proximal region of the tail. Once the tendons were removed, they were placed in a petri dish with 70% ethanol as they needed to be kept hydrated. Subsequently, the tendons were extracted for 48 hours in ice-cold 0.5 M acetic acid and stirred at 4°C. The solution was centrifuged at 7500 x g for 30 minutes and the pellet discarded. The cold supernatant was kept in a beaker on ice. Afterwards, 10 % (w/v) of NaCl was added to the solution in the beaker and this was stirred again for 60 minutes.

The solution was then further centrifuged at 10,000 x g for 30 minutes. The pellet was resuspended in 0.25 M acetic acid (in about 300 ml) and resolubilized by stirring for 24 hours at 4°C. The collagen was finally dialysed to remove the NaCl and highly concentrated acetic acid. Two dialysis tubes (BioDesignDialysis Tubing™ (14,000 MWCO, Fisher Scientific) (around 40 cm each) were put in the microwave in dH<sub>2</sub>O for one minute. On one side a knot was made and the collagen was poured in from the other side. The top was closed and air bubbles were avoided. The collagen was dialysed against millipore water containing 17.5 mM acetic acid for 4 days at 4°C with the solution being changed two times daily. The dialysed collagen was then centrifuged at 30,000 x g for 1.5 hours to remove any remaining debris. The supernatant was removed and placed in a fresh sterile flask. The collagen I solution was adjusted to about 0.5 mg/ml with acetic acid at 4°C. The collagen concentration was measured with the BCA assay described previously.

### 2.2.19 Organotypic assay

The 3D matrix consisting of collagen I preconditioned with fibroblasts was prepared as described previously (Timpson, McGhee et al. 2011). Rat tail collagen I (approx. 0.5 mg/ml) was mixed with 10 x MEM and the pH adjusted to 7.2 with 0.22 M NaOH. To this sample, 1-2 x 10<sup>6</sup> fibroblasts (iCAFs or iNFs) resuspended in 3 ml FBS were added. The preconditioned collagen I with fibroblasts was allowed to set and then fresh culture medium (DMEM, 10 % FBS) was added and the collagen was detached from the sides. The iCAFs and iNFs were allowed to contract. To analyse the invasion of primary invasive pancreatic tumour cell line that was derived from a primary tumour of a *Pdx1-Cre*, *KRas*<sup>G12D/+</sup>, *p53*<sup>R172H/+</sup> expressing KPC mouse (Morton, Timpson et al. 2010). The cells were stably transduced with pMSCV-IRES-EGFP (Addgene), thus expressing EGFP and seeded at a density of 1 x 10<sup>5</sup> cells onto each plug. The following day the plugs were transferred onto a metal mesh grid and fresh medium was added to the bottom of the dish. The PDAC cells were allowed to invade for eight to nine days and the area of invading cells was identified by the amount of GFP signal, quantified by the area calculator plug-in using Image J.

### **2.2.20 Determination of Collagen amount**

Collagen second harmonic images were collected using a Trim-scope (LaVision Biotec) fitted with a Ti:Sapphire femtosecond pulsed laser (Coherent Chameleon). An excitation wavelength of 890 nm was used so that the second harmonic generation (SHG) would be generated at a wavelength of 445 nm. The beam was focused to the sample plane by a long working distance 20x/NA:0.95 water immersion objective (Olympus). A 150  $\mu\text{m}$  deep stack was imaged over a region of 500  $\mu\text{m}$  by 500  $\mu\text{m}$  in 5  $\mu\text{m}$  increments and three regions of interest per sample were acquired. Image analysis was performed using Image J. The images were loaded into ImageJ. A threshold was manually adjusted to remove background. Afterwards, the plugin Area calculator was loaded. The threshold was put in and the algorithm determines the total area, the threshold area and the region of interest. The region of interest is determined by dividing the threshold area by the total area and multiply it by 100. This gives the final value of the amount of fibrillar collagen per slice.

### **2.2.21 Three-dimensional basement membrane cultures**

The three-dimensional basement membranes cultures were performed as described before (Debnath, Muthuswamy et al. 2003; Macpherson, Rainero et al. 2014). 10  $\mu\text{l}$  of Growth Factor Reduced Matrigel was evenly spread on each well of an eight-well glass chamber. The glass bottom chambers were incubated at 37°C and 5 % CO<sub>2</sub> for at least 15 minutes. In the meantime the MCF10DCIS.com cells were trypsinized using Trypsin/PE and resuspended in DMEM F12 complete medium. The cells were spun at 900 rpm for 3 minutes and then resuspended in 3 ml of fresh medium. Afterwards a stock medium containing 2 % Matrigel, 5 ng/ml EGF and 25 ng/ml CLIC3, CLIC3 C22A, GST or CLIC3 respectively with 20 nM Z-DON was prepared. The cells were counted and diluted in the prepared stock medium to achieve a final concentration of 12,500 cells/ml. The 8-well chamber was removed from the incubator and 400  $\mu\text{l}$  of cell suspension was added into each well on top of the solidified Matrigel. The final concentration of cells was then 5,000 cells/well. The cells were grown in the incubator for 6 days. Brightfield images were taken from day three until day six and analysed

for circularity of the spheres formed by using Image J. On day three the stock medium was changed. Fresh stock medium containing 2 % Matrigel, 5 ng/ml EGF and 25 ng/ml CLIC3, CLIC3 C22A, GST-CLIC3 respectively, with 20 nM Z-DON was added. At day six the cells were fixed and stained using immunofluorescence.

### **2.2.22 Immunofluorescence of mammary epithelial cells**

The cells were fixed with 2 % paraformaldehyde (PFA) for 20 minutes at room temperature. Afterwards the cells were washed 1 x in PBS and stored in 500 µl/well PBS overnight. The next morning the cells were permeabilised with 0.5 % Triton in PBS for 10 minutes at room temperature. Afterwards the wells were rinsed three times in 1 x PBS-glycine for 10 minutes each. The wells were then incubated with 200 µl of primary block (IF wash plus 1 % BSA) for 1 hour. The primary block was then removed and the wells were incubated with the primary antibody diluted (1:100, used 100 µl/well) in IF wash and 1 % BSA overnight at 4 °C.

The following day the chamber slides were brought up to room temperature, as the Matrigel hardens again at higher temperatures. The wells were washed three times with IF wash each for 20 minutes with gentle rocking. Afterwards, the secondary antibody was added in IF Wash and 1 % BSA for one hour at room temperature. All the steps from the secondary antibody were performed in the dark. The secondary antibody was washed once in IF wash for 20 minutes. Afterwards, it was rinsed 2 x in PBS for ten minutes each. The F-actin cytoskeleton was then stained with Phalloidin toxin at 1:100 (in PBS) for 30 minutes at room temperature. The remaining, unbound antibody was washed off with PBS and then 3 drops of DAPI Vectorshield, were added into each well. The cells were imaged by confocal microscopy using the Olympus FV1000 and the 60x objective (oil). Twenty images were taken per condition and per antibody staining.

### **2.2.23 Statistics**

Graph Pad Prism 5 was used for statistical analysis. When comparing more than two groups the Kruskal-Wallis test with the Dunn's post test was used. If two groups were used the Mann-Whitney U test was used. The statistical tests used

## Chapter 2

were stated in the figure legends. Experiments were performed 3 times if not stated otherwise. A significant difference was defined with a p-value of  $< 0.05$ .

## **3 CLIC3 is secreted by iCAFs to promote the invasive behaviour of tumour cells**

### **3.1 Introduction**

Cancer-associated-fibroblasts (CAF) are the predominant cell population of the tumour stroma. They consist of at least two different cell types. The first type is represented by normal fibroblasts, which constitute the foundation of the structure supporting normal epithelium. The second type of cells are the myofibroblasts, which account for a considerable fraction of the stroma of tumours (Sappino, Skalli et al. 1988) and their presence constitutes one of the key hallmarks of cancer (Hanahan and Weinberg 2011). These myofibroblast-like CAFs have the ability to render the tumour stroma more permissive to tumour cell invasion, metastasis, angiogenesis, recruitment of immune/infiltrating cells and drug resistance (Desmouliere, Guyot et al. 2004; Orimo, Gupta et al. 2005; Kalluri and Zeisberg 2006; Tsujino, Seshimo et al. 2007; Hanahan and Weinberg 2011; Mao, Keller et al. 2013). Myofibroblast-like CAFs also contribute to aggressiveness of tumours by producing a number of categories of molecules, including those of the extracellular-matrix (ECM). The ECM is made of fibrillar collagen and fibronectin-rich fibres, which are secreted by fibroblasts. Additionally, it consists of proteins, water and non-cellular components making up a 3D matrix. The ECM is present within all tissues and organs providing a physical scaffold, which also initiates biochemical and biomechanical functions (Cukierman, Pankov et al. 2001). The increased mechanical stiffness of the ECM has been exploited to detect cancer (Sinkus, Lorenzen et al. 2000; Butcher, Alliston et al. 2009). The high stiffness of the ECM is important in cell growth, survival of tumour cells (Lo, Wang et al. 2000) and tumour cell invasion, and the latter process in turn is  $\beta 1$  integrin-dependent (Levental, Yu et al. 2009). Moreover, increased ECM stiffness contributes to angiogenic sprouting (Mason, Starchenko et al. 2013), and in mice the stiffness of breast tumours is thought to dictate their invasiveness and their degree of vascularity (Levental, Yu et al. 2009; Baker, Bird et al. 2013). Furthermore, removal or inhibition of ECM components that are known to increase stiffness, such as lysyl oxidase, leads to reduced tumour angiogenesis (Baker, Bird et al. 2013), reduction in tumour growth (Levental, Yu et al. 2009) and increased drug delivery (Provenzano,

Cuevas et al. 2012). Thus, it is clear that inhibition of certain key proteins expressed in myofibroblast-like CAFs (such as lysyl oxidase) can reduce ECM stiffness and influence tumour growth and invasion. However, this is controversial as Özdemir and colleagues have shown that, in a mouse model of pancreatic cancer, depletion of  $\alpha$ -SMA-positive CAFs (the cells that are responsible for stiffening tumours) can lead to faster disease progression (Ozdemir, Pentcheva-Hoang et al. 2014). So far a number of studies have looked at factors expressed or secreted explicitly from CAFs (Bronisz, Godlewski et al. 2012; Torres, Bartolome et al. 2013), but the complexity of signalling that is orchestrated by these secreted factors, in the context of cancer progression, has not yet been fully elucidated.

CLIC3 belongs to a subgroup of the glutathione S-transferase (GST) superfamily, which is comprised of six members (CLIC1 - CLIC6). The CLIC proteins have been associated with several biological processes such as angiogenesis, macrophage activation, cancer invasiveness and response to DNA damage (Valenzuela, Martin et al. 1997; Berry, Bulow et al. 2003; Ulmasov, Bruno et al. 2009; Shukla, Edwards et al. 2014). As they can adopt more than one three-dimensional structure, CLICs have been named metamorphic proteins (Murzin 2008; Bryan and Orban 2010). The study of crystallographic structures of the CLICs has shown that they can adopt a structure which conforms to a soluble monomer with a GST-fold, and without any obvious hydrophobic stretch that could form a transmembrane domain (Harrop, DeMaere et al. 2001; Littler, Assaad et al. 2005; Littler, Brown et al. 2010). Biophysical studies have shown that the N-terminal domain of CLIC1 is conformationally plastic with its structural stability reducing at low pH and under oxidising conditions (Fanucchi, Adamson et al. 2008; Stoychev, Nathaniel et al. 2009; Achilonu, Fanucchi et al. 2012; Legg-E'Silva, Achilonu et al. 2012). The possibility that CLIC1 spontaneously integrates into membranes has been demonstrated in artificial lipid bilayers, but the physiological relevance of this CLIC property is still not established (Tulk, Kapadia et al. 2002; Warton, Tonini et al. 2002; Singh and Ashley 2006; Singh and Ashley 2007). Furthermore, the conditions under which membrane insertion takes place has not been resolved because CLIC4 can insert into lipid bilayers under oxidising and reducing conditions (Singh and Ashley 2007). For CLIC2 the situation is somewhat different, because redox conditions do not influence its

capability to insert into lipid bilayers (Cromer, Gorman et al. 2007). Thus further work is needed to identify the mechanism(s) through which CLICs can insert into lipid bilayer and to determine the physiological relevance of this phenomenon.

The cellular function of the CLICs has been evaluated to some extent. CLIC1 is crucial to macrophage function as it modulates phagosomal acidification (Jiang, Salao et al. 2012) and CLIC4 is known to be an important factor in TGF- $\beta$  signalling during cancer cell growth (Shukla, Malik et al. 2009; Shukla, Edwards et al. 2014). In the Norman group, we have shown that CLIC3 is highly expressed in tumour cells of ER-negative breast cancers and in pancreatic and ovarian adenocarcinomas, and high CLIC3 levels are associated with reduced survival in these cancer types (Dozynkiewicz, Jamieson et al. 2012; Macpherson, Rainero et al. 2014). These studies found that CLIC3's association with tumour aggressiveness is likely attributable to its ability to control recycling of lysosomally-targeted  $\alpha 5\beta 1$  integrin and MT1-MMP back to the plasma membrane. However, CLIC3 is also expressed in fibroblastic cell types, and the impact of stromal CLIC3 on tumour aggressiveness has not been investigated. Furthermore, it is interesting to note that CLICs are found extracellularly in the blood plasma of patients (Chang, Wu et al. 2009), but any potential role of this extracellular pool of CLIC3 has not yet been described.

In this chapter I will describe data indicating that expression of CLIC3 is strongly upregulated in fibroblasts that undergo myofibroblastic conversion to CAFs, and that expression of CLIC3 in CAFs is necessary for these stromal cells to support the invasiveness of tumour cells. Furthermore, I will describe how CLIC3 is secreted from CAFs and that it is this secreted pool of CLIC3, which is responsible for many of the pro-invasive properties of the CAF secretome.

## **3.2 Results**

### **3.3 iCAFs enhance invasiveness of tumour cells**

#### **iCAFs influence collagen remodelling in organotypic matrices and increase tumour cell migration and invasion**

To investigate the role of stromal fibroblasts in tumour progression, Orimo *et al.* (2005) developed two immortalised cell lines; one derived from breast cancer-associated fibroblasts and one from normal mammary fibroblasts. These lines

were generated by injecting immortalised human breast fibroblasts into mice in the presence or absence of Ras-transformed MCF-7 cells. These fibroblasts were then recovered from the mice. Those that had been injected in the absence of tumour cells were termed immortalised normal fibroblasts (iNFs) and those that had been co-injected with MCF-7-Ras cells were termed immortalised cancer-associated fibroblasts (iCAFs) (as described in the Materials and Methods section). (Orimo, Gupta et al. 2005; Polanska, Acar et al. 2011). These workers then went on to show that these iCAFs were more potent than iNFs in promoting tumorigenesis in xenograft models of breast cancer.

To determine whether iCAFs are capable of altering the ECM microenvironment in a way that might promote cell migration and invasion, I used an organotypic system (Timpson, McGhee et al. 2011), in which matrices of collagen I were preconditioned with either iNF or iCAF. To do this, collagen I was allowed to polymerise in the presence of either iNFs or iCAFs. Following a period of four to eleven days, during which the preconditioned collagen contracted, I used second-harmonic generation microscopy (SHG) to determine the amount of fibrillar collagen in these matrices. The collagen is illuminated using a near infrared (>800 nm) femtosecond pulsed laser with a very high intensity. Due to the noncentrosymmetric structure of fibrillar collagen in the matrix, the light emitted is exactly half the wavelength and double the frequency (400 nm, blue light) of the excitation source. I first recorded the fibrillar collagen content of matrices that were preconditioned with either iNF or iCAF (Figure 3.1 A). iCAF-preconditioned plugs remodelled the ECM in a way that yielded a higher proportion of fibrillar collagen than those preconditioned with iNFs (Figure 3.1 B). One possible consequence of increased fibrillar collagen is that it may enhance the invasive capacity of cells that migrate through it. Indeed, the aggressiveness of cancer is closely linked to the fibrillar collagen content of the tumour stroma (Provenzano, Eliceiri et al. 2006). To investigate this, I looked at the ability of a primary pancreatic tumour cell line *Pdx1-Cre*, *KRas<sup>G12D/+</sup>*, *p53<sup>R172H/+</sup>* (PDAC) that was derived from a primary mouse pancreatic adenocarcinoma (Morton, Timpson et al. 2010) to invade plugs of collagen I that were preconditioned with either iCAF, or iNFs (Figure 3.2 A). The PDAC cells invaded into iCAF-preconditioned collagen plugs with many tumour cells penetrating the plug to a depth of 75  $\mu\text{m}$  or more (Figure 3.2 B). The proportion of PDAC cells that were able to invade into the iCAF-preconditioned collagen I to

distances of 50  $\mu\text{m}$  and deeper was significantly greater than that recorded for PDAC cells migrating into collagen I plugs preconditioned with iNFs (Figure 3.2 C).

These experiments indicate that iCAFs are able to influence the amount of fibrillar collagen in a 3D microenvironment, and that this is associated with increased invasiveness of tumour cells. I now wished to determine, whether the ability of iCAFs to remodel the ECM was causally linked to the invasive process. When many tumour cell types, including MDA-MB-231 breast cancer cells and A2780 ovarian carcinoma cells, are plated onto preparations of cell-free ECM, or cell-derived matrix, the invasiveness of these cells is manifested by extension of protrusions called invasive pseudopods at the front of the cell (Caswell, Spence et al. 2007; Caswell, Chan et al. 2008; Rainero, Caswell et al. 2012). To determine the contribution of the matrix-depositing cells in this index of tumour cell invasiveness, I generated cell-derived matrices from iCAFs and iNFs and measured the ability of tumour cells to extend invasive protrusions into these ECM preparations. Time-lapse microscopy videos were analysed by measuring the pseudopod length from the middle of the nucleus to the front of the cell in the direction of movement using Image J. The green arrows indicate the direction of movement and the red brackets denote the length of the invasive pseudopod. When A2780 cells were plated onto cell-free ECM derived from iCAFs, they extended significantly longer invasive pseudopods than when they were plated onto ECM from iNFs (Figure 3.3). This indicates that the ability of iCAFs to support tumour cell invasion is due, at least in part, to differences in their ability to remodel the ECM.

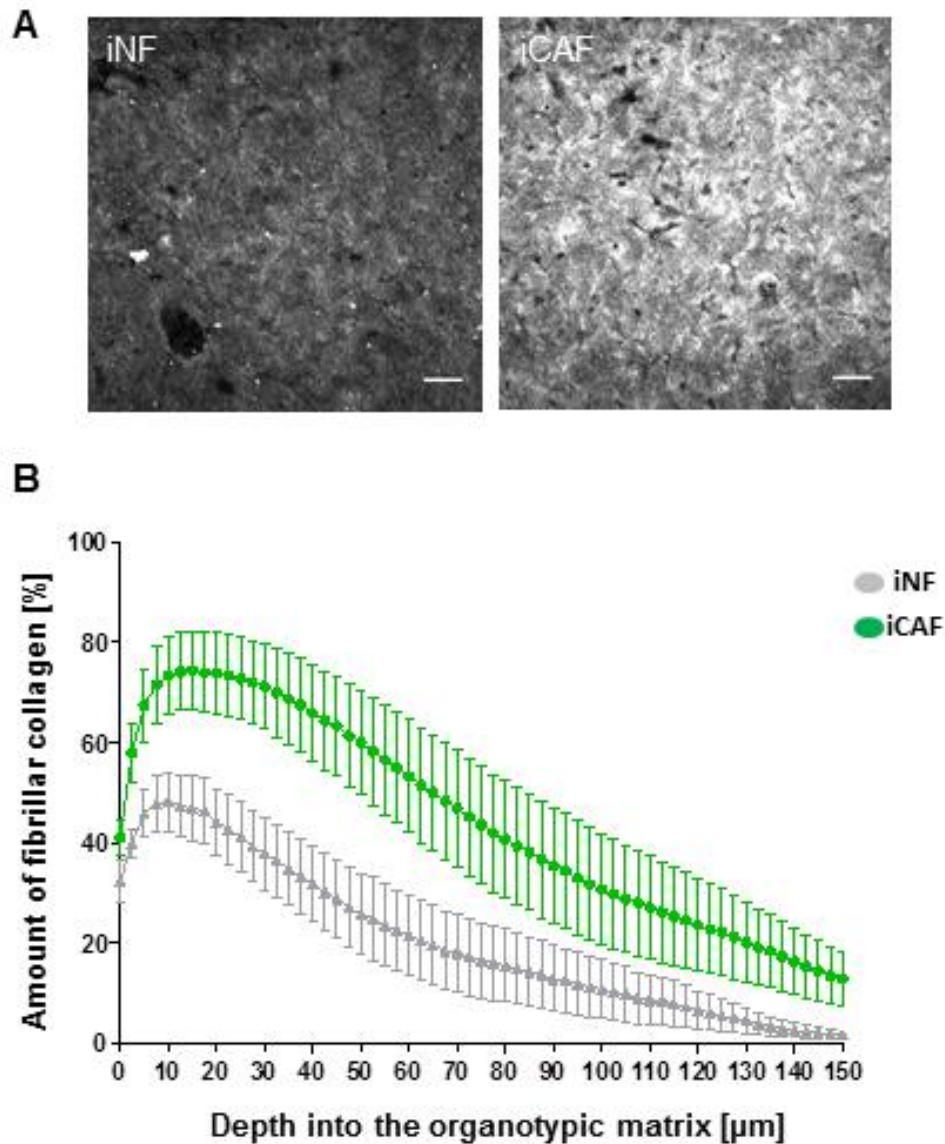


**Figure 3.1: The influence of iCAFs on the fibrillar collagen content of organotypic plugs.**

(A) Collagen I was mixed with either iNFs or iCAFs and plugs were allowed to contract until they reached equivalent size, and second-harmonic generation microscopy (SHG) was used to determine the amount of fibrillar collagen in these matrices. The dimensions of the image stacks acquired were 500 x 500 x 150 µm. A single slice at a depth of 22.5 µm was used as a representative image; scale bar: 50 µm (B) SHG was used to determine the percentage of fibrillar collagen throughout the whole depth of the collagen plug. Values are mean ± s.e.m., n = 3, \*\*\*\*p<0.0001 Mann-Whitney.

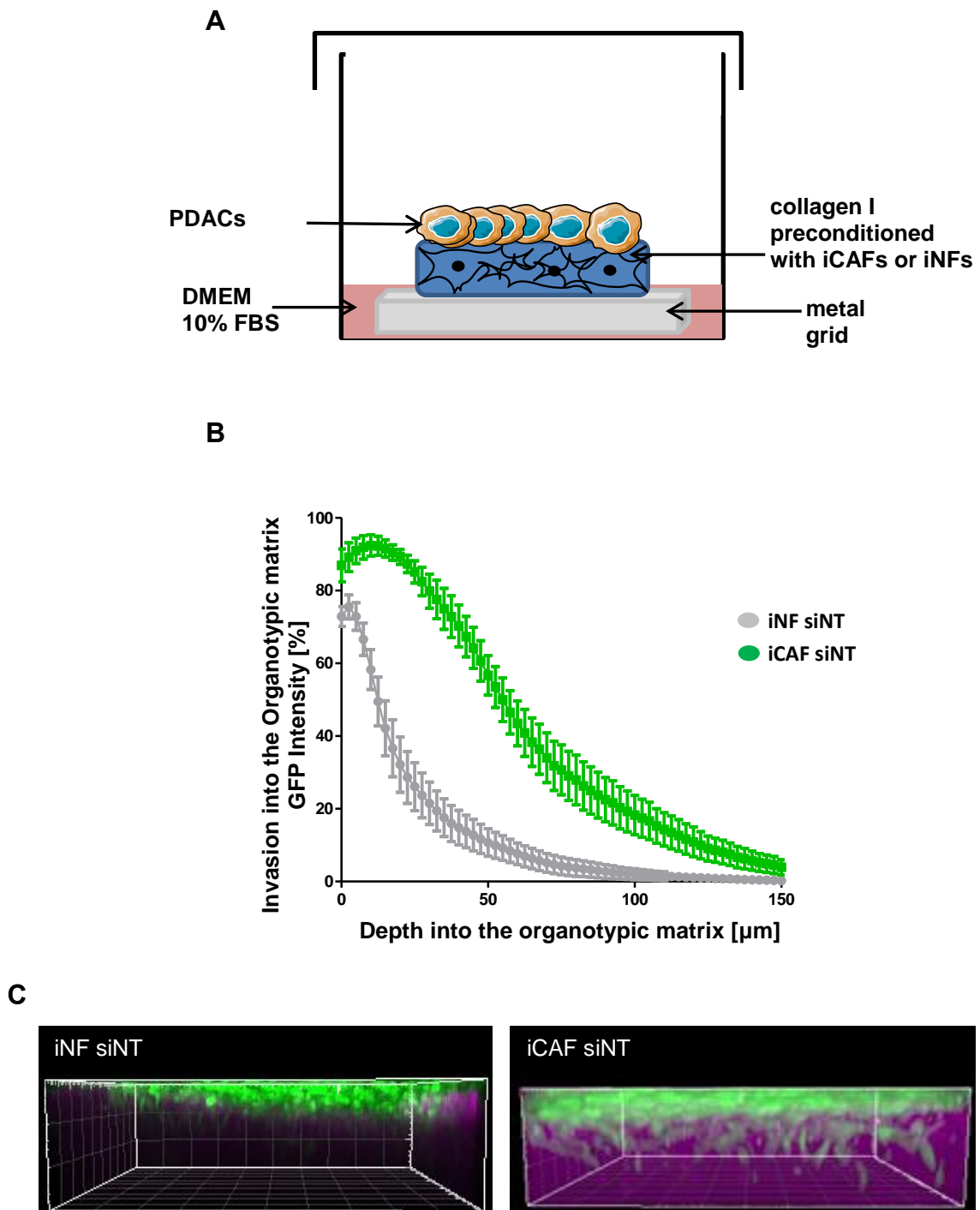


**Figure 3.2: Invasion of PDAC cells into organotypic matrices preconditioned with iCAFs or iNFs**

(A) Schematic set-up of an organotypic assay. Collagen I was preconditioned with fibroblasts. After contraction, cancer cells were seeded onto the top of the organotypic plug. The cancer cells were then allowed to invade (Timpson, McGhee et al. 2011). (B) Collagen I was mixed with iCAF or iNF cells and was allowed to contract. Following this, EGFP-expressing PDAC cells were seeded on top. The PDAC cells were then allowed to invade for 8 days. The invasion of PDAC cells into organotypic matrices was measured by multiphoton imaging, and these data are expressed as a function of distance into the organotypic plug. Values are mean  $\pm$  s.e.m.,  $n=3$  independent experiments. \*\*\*\* $p<0.0001$  Mann-Whitney. (C) Representative images for the invasion of EGFP-expressing PDAC cells (green, EGFP) into organotypic matrices. The purple colour scale represents the SHG signal of fibrillar collagen I.

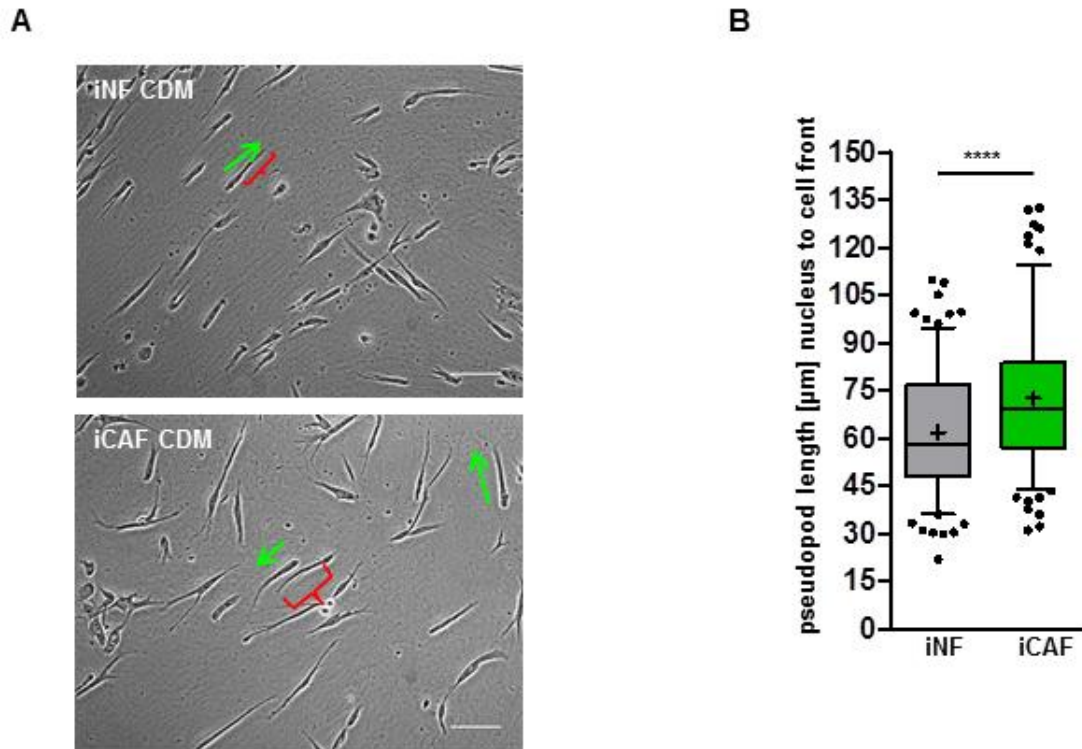


**Figure 3.3: iCAF-derived matrix increases the length of invasive pseudopods extended by A2780 cells**

(A) Representative images of A2780 seeded on iNF- and iCAF-derived cell-derived matrices (CDM). Time-lapse microscopy was used to visualise invasive protrusions at the front of the cell. The green arrow indicates the direction of movement and the red bracket an example of an invasive pseudopod. (B) A2780 cells were plated on iNF- and iCAF-derived cell-derived matrices. Time-lapse videos were recorded over a period of 22 hours. The pseudopod length was measured from the middle of the nucleus to the front of the cell in the direction of migration and analysed using Image J. One biological replicate is shown. Three biological replicates were performed. Values are mean  $\pm$  s.e.m.,  $n = 1$  (counted 180 cells per experiment), \*\*\*\* $p < 0.0001$  Mann-Whitney. The data were plotted as a Box and Whisker 5 – 95% plot. The median is presented as a black line and the mean as a black cross, scale bars: 100  $\mu\text{m}$ .

### **CLIC3 is highly expressed in cancer-associated, but not normal fibroblasts**

To identify candidate proteins that might be responsible for the increased ability of iCAFs to deposit an ECM which is highly supportive of tumour cell invasion, we compared the proteome and secretome of iNFs and iCAFs. Cells were subjected to Stable Isotope Labelling with Amino Acids in cell culture (SILAC)-based mass-spectrometry (MS). iNFs and iCAFs were labelled with light and heavy SILAC amino acids respectively (forward experiment), and with heavy and light amino acids respectively (reverse experiment). We then prepared cell extracts from which proteomes were detected using an LTQ-Orbitrap and MS data were analysed with the MaxQuant computational platform (Cox and Mann 2008), which identified proteins in the proteome with high correlation between forward and reverse experiments. In Fig. 3.4 A, the proteins upregulated in the iCAFs in both (forward and reverse) experiments are presented in the top right hand corner and are within the region shaded in blue. The proteins downregulated in the iCAFs in both (forward and reverse) experiments are presented in the bottom left corner and indicated by the region shaded in red (Figure 3.4 A). As expected, there were a number of differences between the proteomes of iNF and iCAF. The myofibroblast-like iCAFs showed a myoCAF signature in which proteins such as  $\alpha$ -SMA and TGF- $\beta$  were upregulated and mesenchymal markers were downregulated. In addition, many ECM components such as collagens, fibronectin, laminins, lysyl oxidase and transglutaminase 2 (TG2), most of which would be expected to influence tumour cell invasion, were upregulated (data not shown). Interestingly, CLIC3 was identified as a protein that was expressed at significantly higher levels in iCAFs than in iNFs (Figure 3.4 A). This result was confirmed by Western blotting (Figure 3.4 B). CLIC2 was not detected in the proteome, and the other CLIC family members (CLIC1, CLIC4, CLIC5 and CLIC6) were present in similar quantities in both iCAFs and iNFs (Figure 3.4 C).

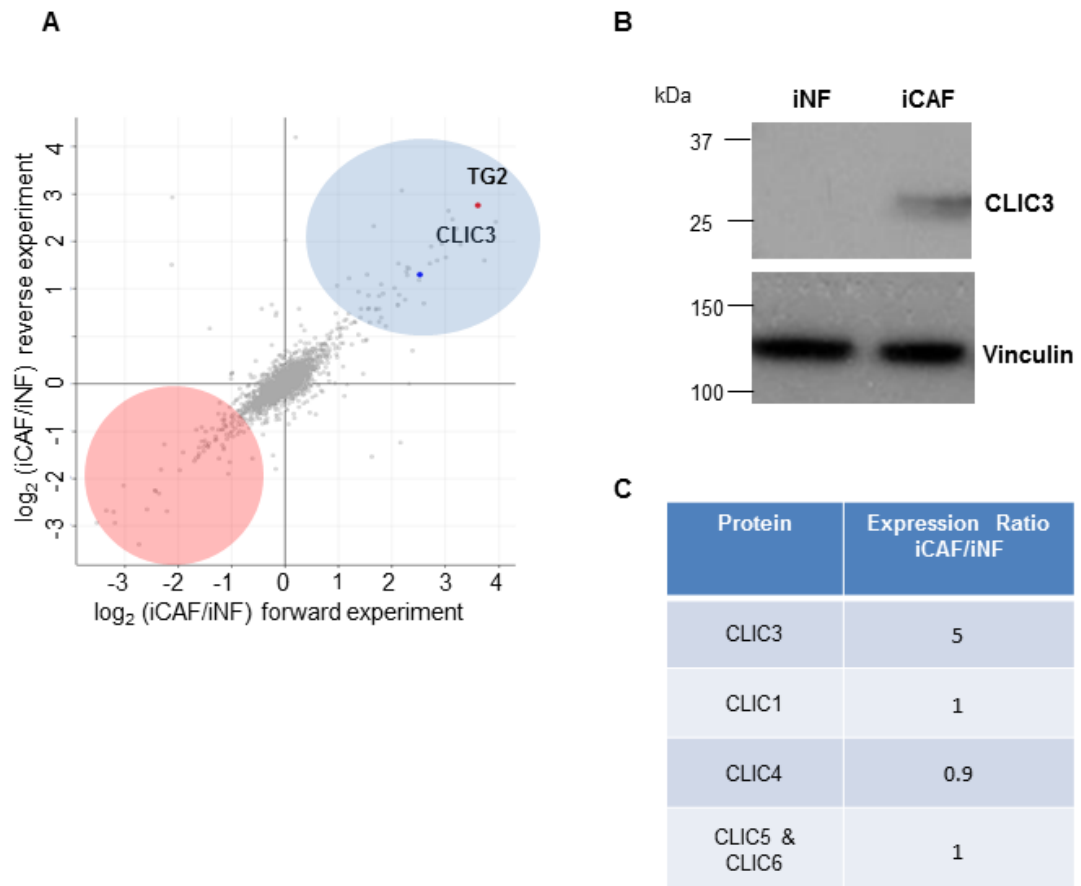


**Figure 3.4: CLIC3 is highly expressed in iCAFs by comparison to iNFs.**

(A) The plot shows the  $\log_2$  of the iCAF proteome over the iNF proteome. They are two experiments, with one being termed as forward and the other as reverse. The iCAFs were labelled first with heavy isotope amino acids and the iNFs were labelled with light isotope amino acids. The heavy and light labelling was reversed in the “reverse experiment”. The results were analysed using the MaxQuant computational platform (Cox and Mann 2008). The resulting graph shows the proteins which were upregulated in the iCAF proteome in the top right square (blue region). The proteins in the left bottom quadrant were downregulated in the iCAFs (red region). (B) The expression of the CLIC proteins was calculated by inverting the logarithm of 2 and correcting for loading errors. (C) Western blot analysis shows that iCAFs express CLIC3 at higher levels than iNFs. The data of the proteomic screen were produced by Juan Hernandez. The Western blot was performed by myself.

### **3.4 Expression of CLIC3 in iCAFs is required for the generation of a highly fibrillar ECM that supports tumour cell invasion**

As described above, CLIC3 is highly expressed in iCAFs and this might be linked to the ability of these cells to remodel the ECM in way that generates a pro-invasive stroma. Therefore, I used siRNA to investigate whether CLIC3 expression is required for iCAFs to generate a pro-invasive microenvironment that is rich in fibrillar collagen. CLIC3 knockdown (siCLIC3) significantly reduced the ability of iCAFs to increase the fibrillar collagen content of organotypic plugs (Figure 3.5). Consistent with this, PDAC cells were less able to invade into plugs preconditioned with CLIC3-knockdown iCAFs by comparison with plugs preconditioned with control knockdown (siNT) iCAFs (Figure 3.6 A-C). Taken together, these data indicate that CLIC3 expression in iCAFs is required for these cells to increase the fibrillar collagen content of organotypic matrices and to support the invasion of tumour cells into this stromal-like microenvironment.

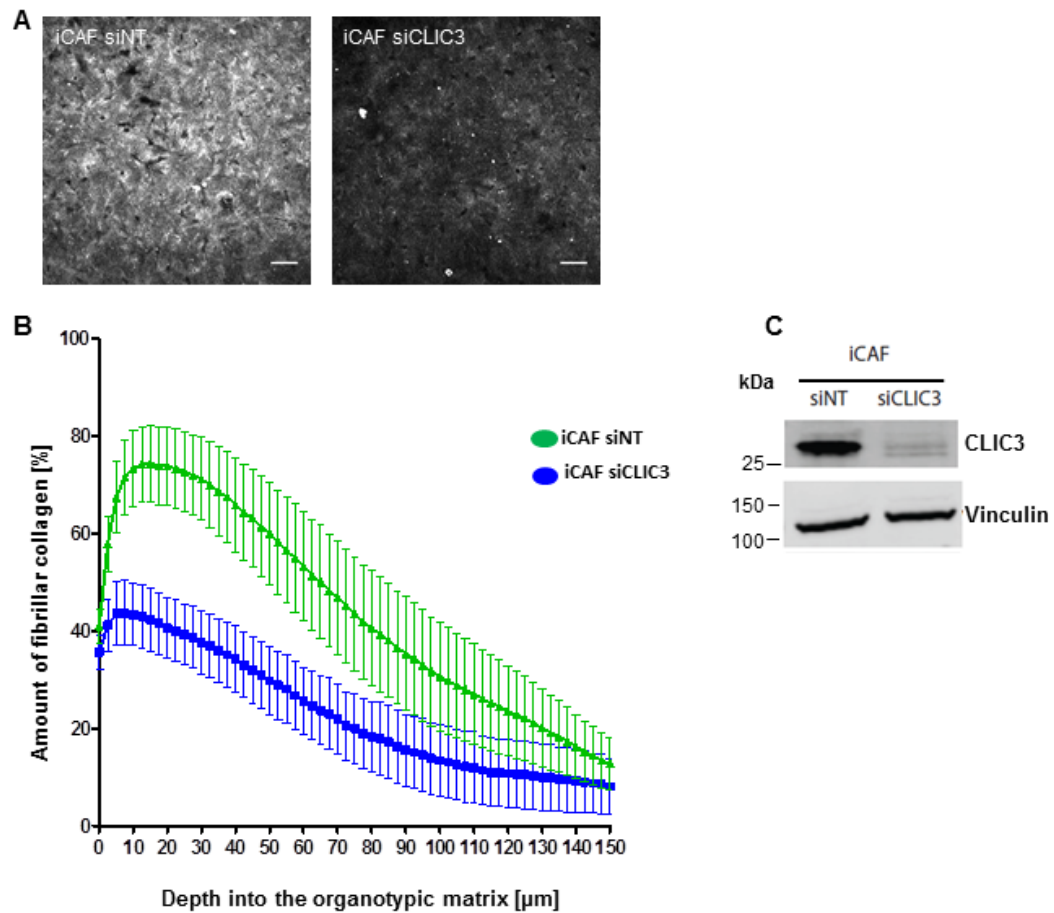


**Figure 3.5: CLIC3 knockdown reduces collagen remodelling by iCAFs.**

Collagen was mixed with iCAFs transfected with a non-targeting (siNT) siRNA or one that targets CLIC3 (siCLIC3), and second-harmonic generation microscopy (SHG) was used to determine the amount of fibrillar collagen in these matrices. The dimensions of the image stacks acquired were 500 x 500 x 150 µm. (A) A single slice at a depth of 22.5 µm was taken as a representative image, scale bars: 50 µm. (B) The percentage of fibrillar collagen was analysed throughout the whole depth of the organotypic plug. Values are mean ± s.e.m., n = 3, \*\*\*\*p < 0.0001 Mann-Whitney. (C) Western blot of cellular extracts from iCAFs transfected with control (siNT) or CLIC3 siRNA (siCLIC3) were probed with CLIC3 antibody, with the expression of vinculin being used as loading control.

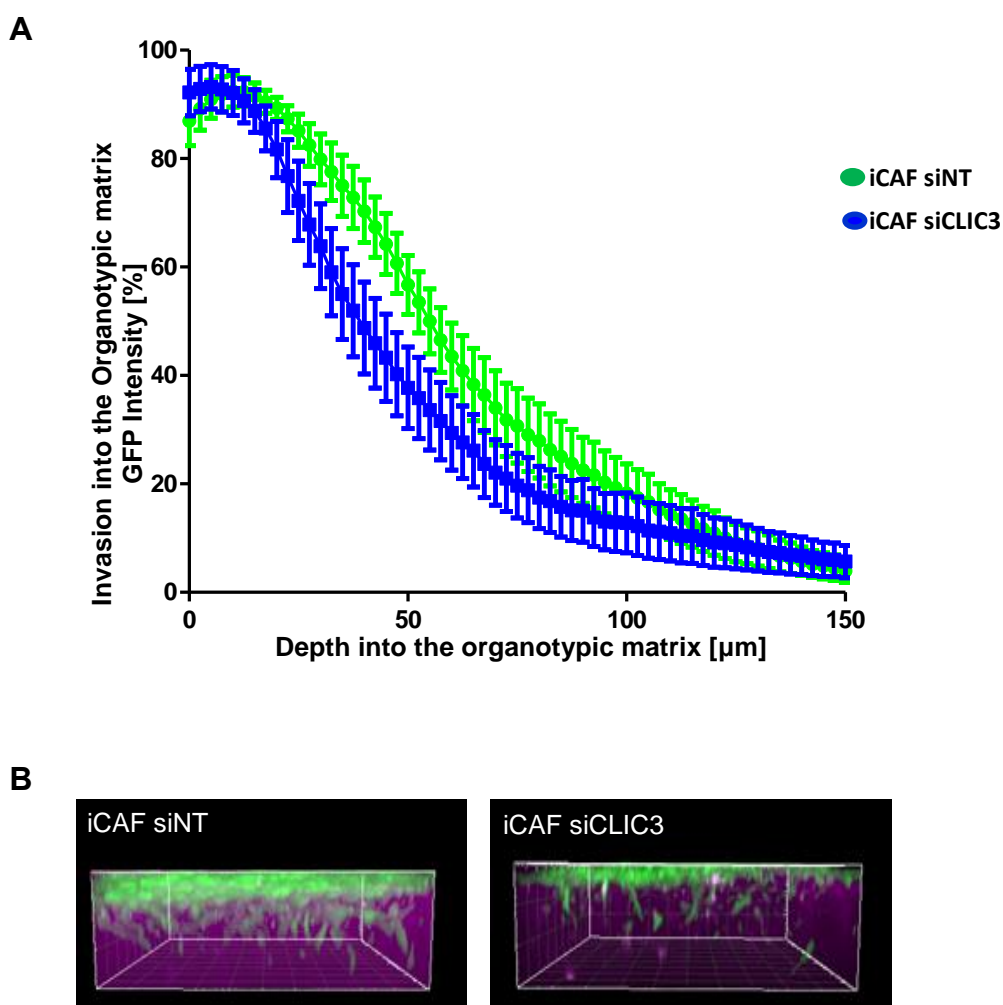


**Figure 3.6: Invasion of PDAC cells into organotypic matrices is opposed by siRNA of CLIC3 expression in the iCAFs used to precondition the plugs.**

Collagen was mixed with iCAFs transfected with a non-targeting (siNT) siRNA or one that targets CLIC3 (siCLIC3). Following plug contraction, PDAC cells were seeded onto the top of the organotypic plug. The cancer cells were then allowed to invade for 8 days (Timpson, McGhee et al. 2011). (A) The invasion of PDAC cells into organotypic matrices was measured by multiphoton imaging, and these data are expressed as a function of distance into the organotypic plug. Values are mean  $\pm$  s.e.m.,  $n = 3$ , \*\*\*\* $p < 0.0001$  Mann-Whitney. (B) 3D rendering of multiphoton images of the invading PDAC cells (EGFP, green) into the organotypic matrix (SHG, magenta). The images have a dimension of  $500 \times 500 \times 150 \mu\text{m}$ .

### **CLIC3 is a component of the CAF secretome that is necessary and sufficient to promote cancer cell invasiveness**

Expression of CLIC3 in iCAFs is required for their ability to increase the fibrillar collagen I content of organotypic plugs, and for iCAFs to generate an ECM that is strongly supportive of cancer cell invasiveness. The enhanced ability of iCAFs to remodel the ECM may be either due to alterations in their ability to physically manipulate the ECM, or to differences in the profile of proteins secreted (the secretome) by iCAFs and iNFs. To determine whether differences in the secretome were responsible for iCAF's ability to foster increased invasiveness, I investigated the ability of MDA-MB-231 breast cancer cells to extend invasive pseudopods in the presence of conditioned medium (CM) from either iCAFs or iNFs. This clearly indicated that MDA-MB-231 cells extend significantly longer invasive pseudopods when cultured in the presence of CM from iCAFs than they did in the presence of CM from iNFs. Moreover, the ability of iCAFs to produce CM that supported increased pseudopod extension was reversed by siRNA of CLIC3 in the iCAFs (Figure 3.7 A, B). Taken together, these data indicate that the ability of iCAFs to support tumour cell invasiveness can be attributed to the composition of their secretome, and that CLIC3 expression is required to increase the pro-invasive characteristics of the iCAF secretome.

I then hypothesised that CLIC3 itself might be a component of the secretome from iCAFs. I first looked at the coding region of CLIC3. The coding region of CLIC3 does, however, not contain any sequences that conform to a canonical signal peptide that would aid its translocation into the lumen of the endoplasmic reticulum. Thus, one would not necessarily propose that CLIC3 would be a secreted protein. However, our mass spectrometry analyses have consistently indicated that CLIC3 is a component of the iCAF secretome, and that CLIC3 is incorporated into ECM deposited by these cells (data not shown). Moreover, there is evidence that proteins of the CLIC family are found in plasma and in other biological fluids (Chang, Wu et al. 2009; Tang, Beer et al. 2013), indicating the possibility that these proteins may be able to leave the cell to perform extracellular functions. Proteins may be released from cells by mechanisms other than those that involve canonical signalling peptides (Nickel and Seedorf 2008). To investigate this possibility, I used a secretome prediction programme

developed by workers at the University of Denmark (<http://www.cbs.dtu.dk/services/SecretomeP>), (Bendtsen, Jensen et al. 2004; Bendtsen, Kiemer et al. 2005). This programme is based on a feed forward neural network. For the neural network to function properly it needs to be trained. This is done by using a positive and a negative control. The authors would have liked to use proteins which are secreted via the non-classical secretion pathway as a positive control. However, only thirteen secreted proteins via the non-classically pathway (such as FGF1, IL1 or CNTF all human) are available. Instead they used 3321 extracellular mammalian proteins which were imported from Swiss-Prot as a positive control. The N-terminal signal peptide was removed as the network was trained to identify proteins secreted based on the sequence, the number of atoms, number of positively charged residues or transmembrane helices. Furthermore, as a negative control they used 3654 mammalian proteins also imported from Swiss-Prot which were present in the nucleus or cytoplasm. They removed all proteins from other locations and also the transmembrane proteins. Based on the protein features and sequences they could identify ten of the thirteen known protein which are secreted via the non-classical pathway reaching a secretion score above 0.6. Based on test results the programme generates this score (a SecP score) which indicates the likelihood of it being secreted by a non-canonical pathway - a SecP score in excess of 0.6 indicates a high likelihood of the protein being a secretome component. The protein coding sequence of CLIC3 generates a SecP score of 0.838, indicating a high probability that it may be secreted via a non-canonical mechanism.

Based on these observations, I used Western blotting to determine whether CLIC3 is released from cells, and whether it is incorporated into the ECM. Indeed, Western blotting indicated that iCAFs secrete CLIC3 and that it physically associates with the cell-free preparations of cell-derived matrix (Figure 3.8 A). In addition to the presence of CLIC3 at its expected molecular weight, we noticed that there was a band of immunoreactive CLIC3 at a higher molecular weight in the preparations of the cell free fibroblast-derived matrix, indicating the possibility that CLIC3 is covalently associated with other ECM proteins. Moreover, CLIC3 is secreted from MDA-MB-231 breast cancer cells (Figure 3.8 B). Since CLIC3 has late endosomal localization (Dozynkiewicz, Jamieson et al. 2012; Macpherson, Rainero et al. 2014), I explored a well-

characterized cellular mechanism for unconventional secretion, which involves late endosome/multivesicular body (MVB) exocytosis as a possible export mechanism (Malhotra 2013). However, CLIC3 release is not dependent on Rab GTPases that control such a mechanism, for instance Rab27a/Rab27b (Figure 3.8 B), consistent with a non-exocytic route for CLIC3 release.

These observations that CLIC3 is secreted from iCAFs prompted us to test whether CLIC3 might act extracellularly to influence ECM remodelling and tumour cell invasion. Therefore, I prepared recombinant, soluble purified CLIC3 (rCLIC3) and a control protein (rGST) (Figure 3.9 A, B) and added these to the extracellular milieu to determine whether this was capable of rescuing the ability of CM from CLIC3 knockdown cells to drive invasive pseudopod extension (Figure 3.7 B). Clearly, addition of rCLIC3 to CM from CLIC3 knockdown iCAFs yielded a CM that supported pseudopod extension to the same extent as did CM from control iCAFs. Furthermore, addition of soluble rCLIC3 drove pseudopod extension in MDA-MB-231 cells even in the absence of CM (Figure 3.7 B). Taken together, these data indicate that CLIC3 is a component of the iCAF secretome that is necessary and sufficient to promote invasive behaviour of tumour cells.

### **Characterisation of the pro-invasive attributes of extracellular CLIC3**

The measurement of pseudopod extension from cells plated onto cell-derived matrix is a quick and convenient way of obtaining a quantitative read-out of invasiveness.

I used Western blotting to estimate the concentration of CLIC3 in the cell-exposed medium. This indicated that iCAFs released CLIC3 at levels sufficient to attain a concentration which was in the low pM range (11.26 - 22.52 pM or 0.3 - 0.6 ng/ml) (not shown). I therefore, wished to determine whether the concentration of rCLIC3, which is required to drive the extension of invasive pseudopods, was approximately within this concentration range. I plated A2780 and MDA-MB-231 cells onto cell-derived matrices, added rCLIC3 to achieve final concentrations in the range of 0.3 ng/ml up to 25 ng/ml (11.26 - 938.16 pM) and measured the length of invasive pseudopods (Figure 3.10: Response of pseudopod extension to various concentrations of rCLIC3. Figure 3.10). In A2780 cells significant elongation of invasive pseudopods was seen at an rCLIC3

concentration of 0.3 ng/ml and this increased in a dose-dependent fashion to reach a maximum at approximately 25 ng/ml. In MDA-MB-231 cells maximal pseudopod extension was achieved following addition of 0.3 ng/ml rCLIC3.

rGST, which like CLIC3, possesses a glutathione-like fold, does not drive any significant extension of invasive pseudopods - indicating that there is a degree of specificity in regard of the invasive response to CLIC3. Despite this, I wished to perform an additional control to assess whether CLIC3 must be in its appropriate conformation to evoke pseudopod extension. To do this, I boiled rCLIC3 and tested the ability of this (presumably) denatured protein to drive pseudopod extension. Clearly, boiled rCLIC3 was unable to promote the extension of invasive pseudopods, indicating that CLIC3 must be in its proper folded conformation to function as a pro-invasive molecule (Figure 3.11).

I also wanted to determine the timeframe over which rCLIC3-driven pseudopod extension takes place. To do this, I seeded A2780 cells onto cell-derived matrix and initiated time-lapse microscopy. I added rCLIC3 and measured pseudopod length at 5 minute intervals following this. The data indicate that maximal pseudopod extension was achieved within 5 minutes of rCLIC3 addition (Figure 3.12).

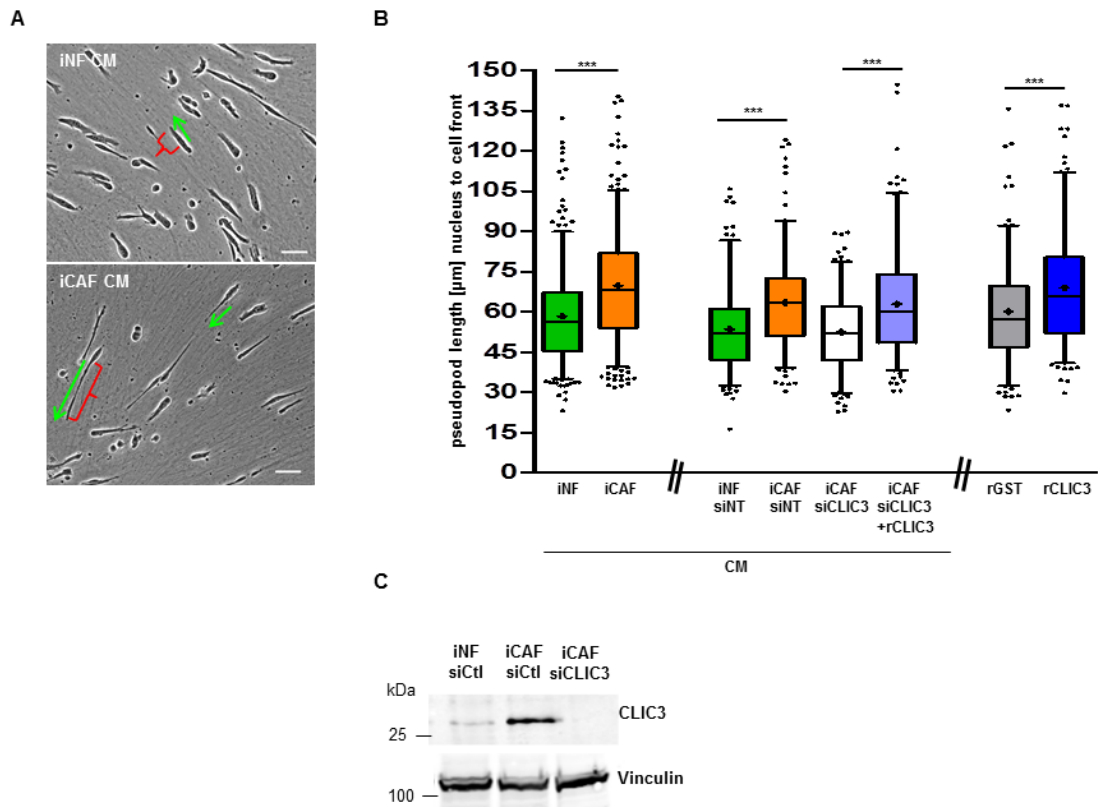


**Figure 3.7: Identification of CLIC3 as a key pro-invasive component of the iCAF secretome.**

(A) MDA-MB-231 cells were plated onto fibroblast-derived matrix in the presence of either iNF or iCAF cell-exposed medium (CM). Representative images of cells migrating in the presence of iNF CM or iCAF CM are presented. The green arrow indicates the direction of migration of the cells and the red bracket indicates the length of the invasive pseudopod. The pseudopod length was measured from the middle of the nucleus to the tip of the cells in the direction of migration. Scale bars, 50  $\mu\text{m}$ . (B) Invasive pseudopods of MDA-MB-231 cells were measured in the presence of iNF CM or iCAF CM or CM from iCAFs that had been transfected with siRNA targeting CLIC3 (siCLIC3) or a non-targeting control (siNT). rCLIC3 (1 ng/ml) was added to CM where indicated. One biological replicate is shown. However, three independent experiments were performed. Values are mean  $\pm$  s.e.m.,  $n = 1$ , \*\*\* $p < 0.001$  Mann-Whitney. Plots are Box and Whisker 5 – 95% plots. The mean is indicated with a cross and the median with the line through the plot. (C) Cell lysates from iNFs and iCAFs transfected with a control siRNA and iCAFs transfected with a siRNA targeting CLIC3. Western blot was used to assess the CLIC3 knockdown. Vinculin was used as the loading control.

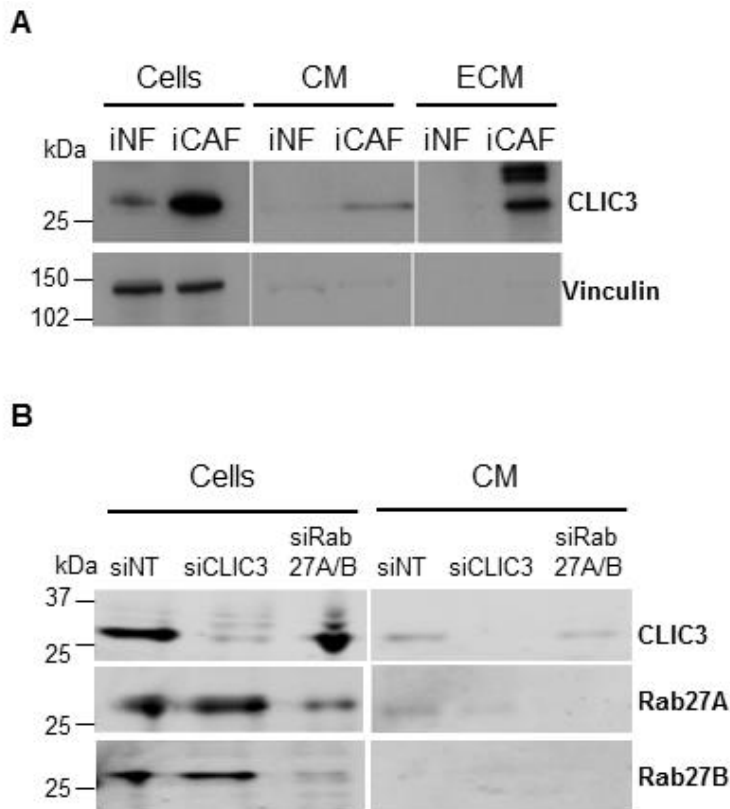


**Figure 3.8: CLIC3 is secreted from iCAFs and MDA-MB-231 cells.**

(A) iNFs and iCAFs were seeded at  $1.5 \times 10^6$  cells/dish in a 10 cm dish. The medium was changed for serum-free medium after 48 hours. The cell-exposed medium and cells were then harvested after a further 24 hours. The cell-exposed medium was centrifuged to remove cell debris. Following this, the cell-exposed medium was incubated with StrataClean beads to concentrate the proteins, which were present in the cell-exposed medium. The beads were resuspended in sample buffer supplemented with DTT and boiled to remove the proteins from the beads. The Western blot indicates that CLIC3 was expressed in iCAFs and that it was secreted into the cell-exposed medium. The ECM was also harvested and CLIC3 was detected to be bound to the ECM. (B) MDA-MB-231 cells were transfected with siRNAs targeting CLIC3 (siCLIC3), a non-targeting control (siNT), or a siRNA targeting Rab27A and Rab27B and plated onto 10 cm dishes. The cells were incubated for 48 hours. Afterwards, the cell-exposed medium was changed to serum-free medium for further 24 hours. The cells and the cell-exposed medium were harvested and concentration of the supernatant was performed as described in (A).

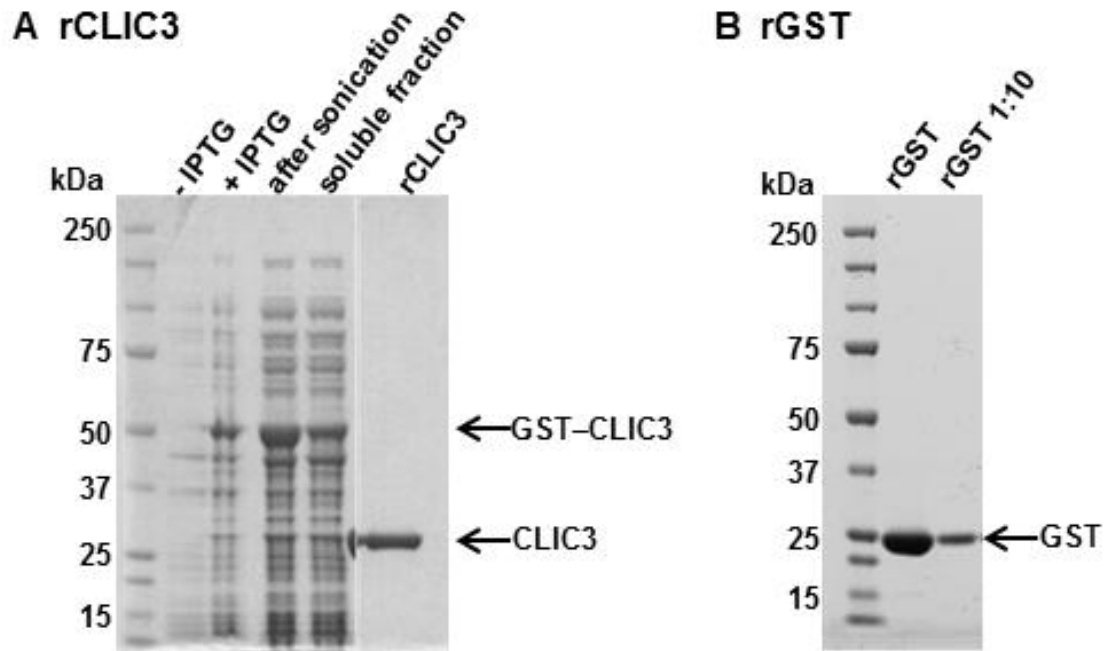


**Figure 3.9: Production of recombinant CLIC3 and GST.**

(A) The left hand lane show samples of the BL21 (DE3) pLysS *E.coli* cells transformed with CLIC3–GST expression vector, but before induction with IPTG. The second lane shows the lysate after IPTG induction. Following this, the bacteria were sonicated and an aliquot of this is shown in the third lane. Thereafter, the lysates were centrifuged and the supernatant incubated with glutathione agarose beads. Finally, the purified rCLIC3 was cleaved from GST using PreScission protease. (B) The migration of GST for comparison. Gels were stained with Coomassie brilliant blue.

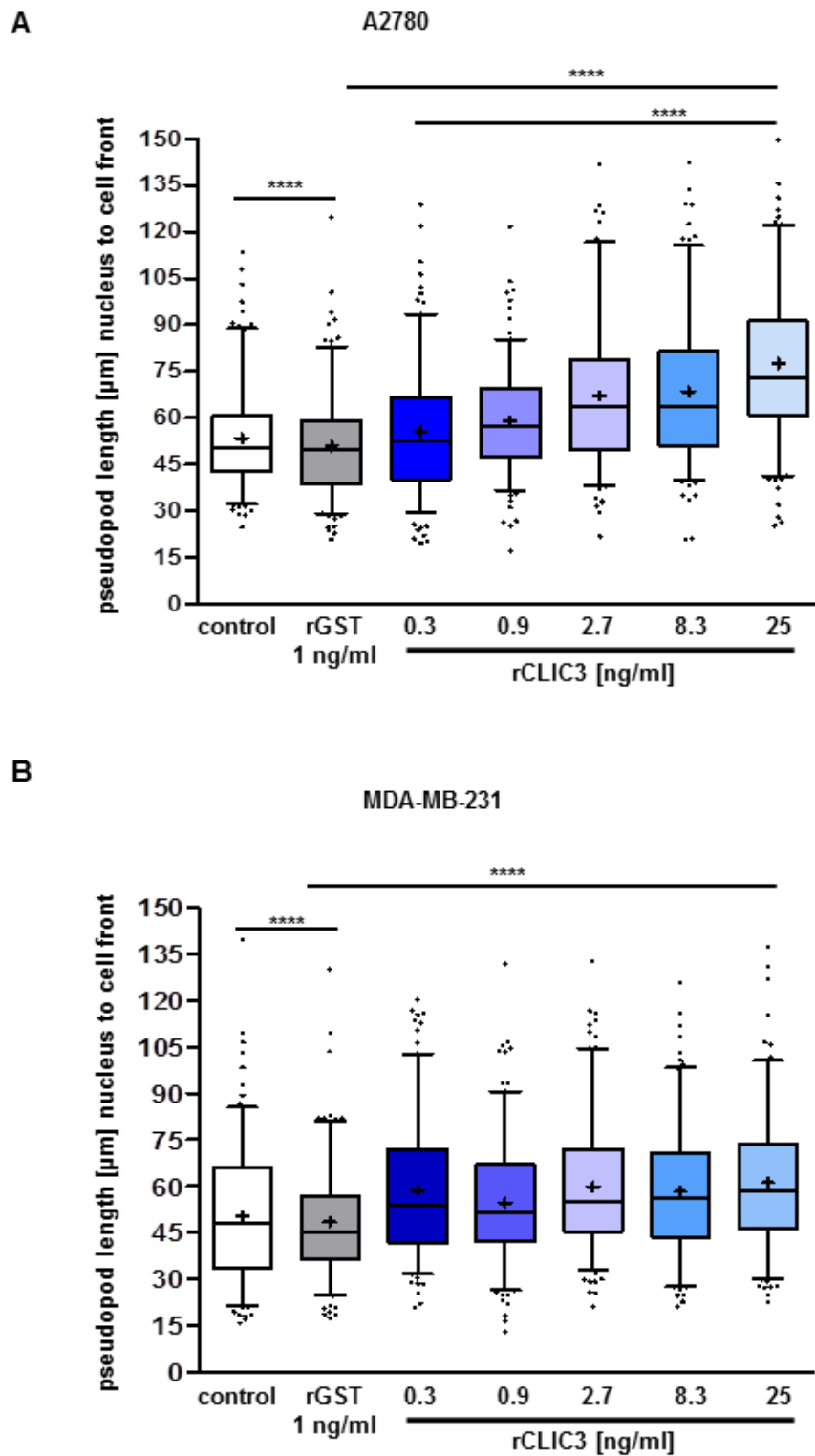


**Figure 3.10: Response of pseudopod extension to various concentrations of rCLIC3.**

A2780 ovarian carcinoma cells (A) and MDA-MB-231 breast cancer cells (B) were plated onto fibroblast-derived matrix. Time-lapse videos were recorded (over a time period of 22 hours) in the presence of no protein, rGST (1 ng/ml) or the indicated concentrations of rCLIC3. Pseudopod elongation was measured from the middle of the nucleus to the tip of the cell in the direction of movement using ImageJ. One biological replicate is shown and three independent biological replicates were performed. The median is shown as a black line and the mean as a cross. Values are mean  $\pm$  s.e.m.,  $n = 1$ , \*\*\*\* $p < 0.0001$  Mann-Whitney. The data are represented as Box and Whisker 5 – 95% plots.

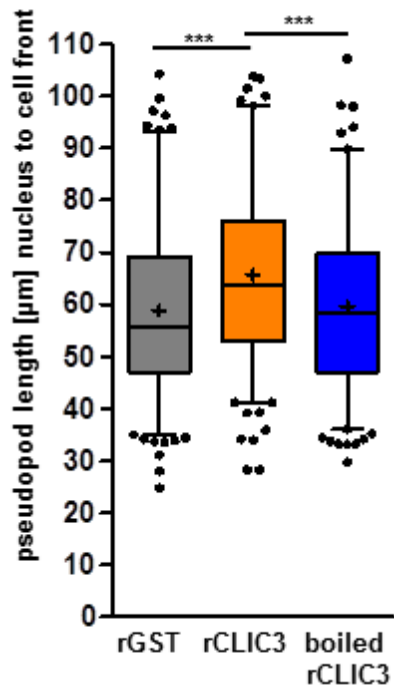


**Figure 3.11: rCLIC3's ability to drive pseudopod extension is ablated by boiling the protein.** A2780 cells were plated on fibroblast-derived matrices. Time-lapse videos were recorded in the presence of rCLIC3, rGST, or boiled rCLIC3 (all proteins at 1 ng/ml). The distance between the middle of the nucleus to the tip of the cell in the direction of movement was measured using ImageJ. One biological replicate is shown but three independent biological replicates were performed. Values are mean  $\pm$  s.e.m.,  $n = 1$ , \*\*\* $p < 0.001$  Kruskal-Wallis test with a Dunns post-test. The data are represented as a Box and Whisker 5 – 95% plots. The mean is indicated with a cross and the median with the line through the plot.

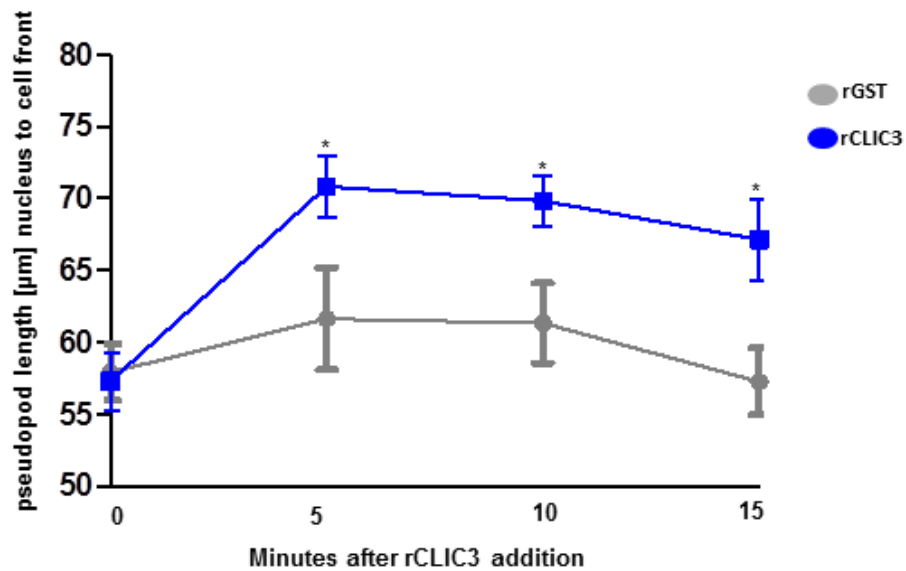


**Figure 3.12: Pseudopod extension becomes apparent 5 minutes following rCLIC3 addition.** A2780 cells were plated onto fibroblast-derived matrix. Time-lapse microscopy was started and after 1 hour rCLIC3 (1 ng/ml, blue) was added and the pseudopod length was measured every 5 minutes afterwards for 15 minutes. A minimum of 540 cells were measured. Values are mean  $\pm$  s.e.m.,  $n = 3$ , \* $p < 0.05$ , Mann-Whitney.

### **Mutation of cysteine residues in CLIC3's thioredoxin fold opposes its ability to drive pseudopod extension**

CLIC proteins have been proposed to function in a number of ways including as Cl<sup>-</sup> channels and molecular scaffolds (Littler, Brown et al. 2010), but evidence that their primary role in the cell is to function as oxidoreductases is now accumulating. A recent study has clearly demonstrated that CLIC1, -2 and -4 have glutaredoxin-like activity, with a cysteine in the GST fold acting as a key catalytic residue (Al Khamici, Brown et al. 2015). To investigate the functionality of the putative active cysteine at position 22 within the thioredoxin domain of CLIC3, I generated a mutant CLIC3 (rCLIC3<sup>C22A</sup>) in which this cysteine was replaced with an alanine. Moreover, CLIC3 is unique amongst the CLICs as it possesses an additional cysteine close to position 22 at position 25. I therefore constructed a double cysteine mutant of CLIC3 by mutating both cysteine 22 and cysteine 25 to alanine (rCLIC3<sup>C22/25A</sup>). Both rCLIC3<sup>C22A</sup> and rCLIC3<sup>C22/25A</sup> were completely unable to drive extension of invasive pseudopods in A2780 or MDA-MB-231 cells (Figure 3.13 B, C). These data indicate the possibility that a functional thioredoxin domain is essential for extracellular CLIC3 to drive invasive protrusions, and suggest that the oxido-reductase activity of the CLIC3 is required for its pro-invasive function.

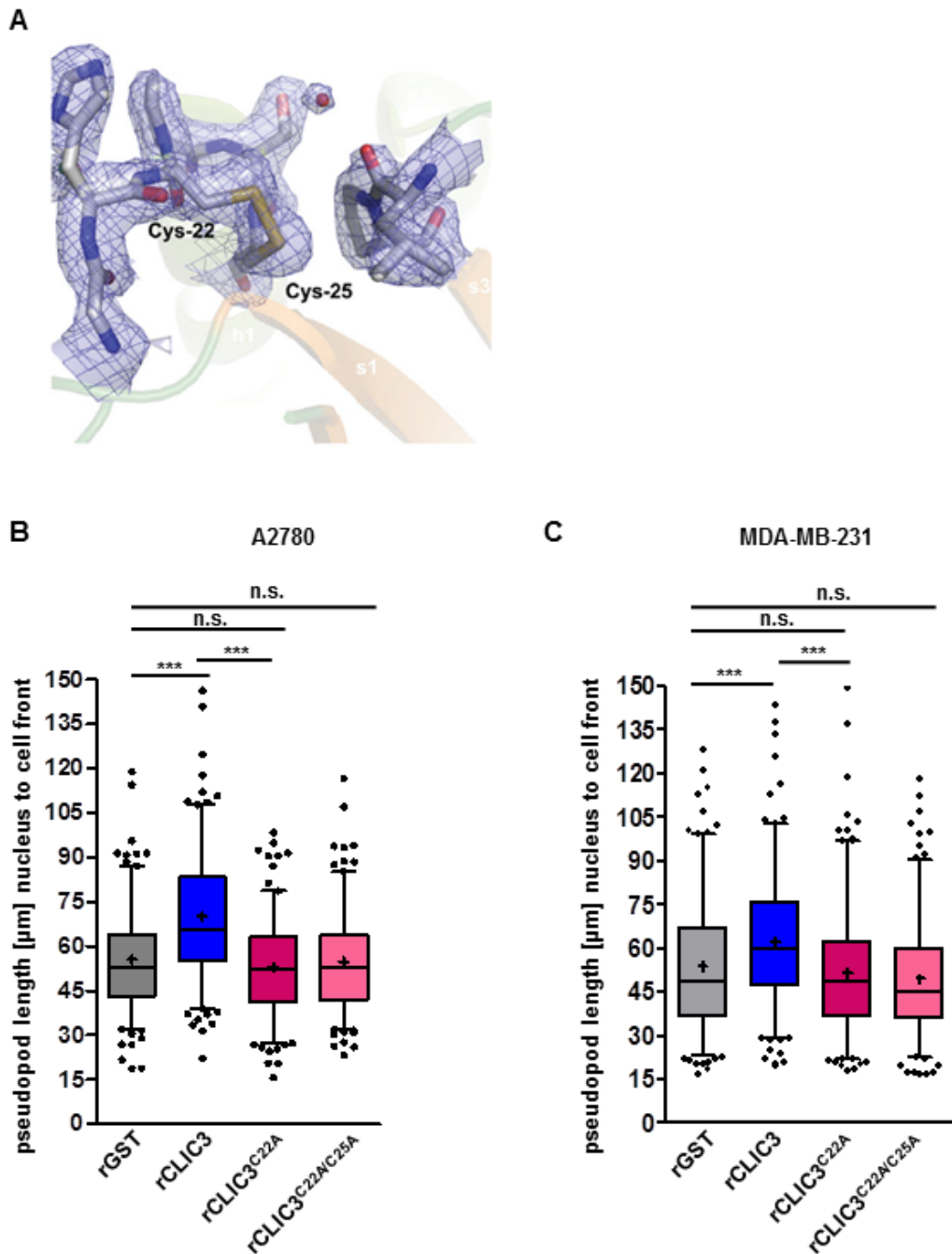


**Figure 3.13: The cysteine residues in CLIC3's thioredoxin domain are required for its ability to drive the extension of invasive pseudopods.**

(A) Crystal structure of the thioredoxin fold of CLIC3 indicating the position of the proposed 'active site' cysteines (Littler, Brown et al. 2010). (B & C) A2780 adenocarcinoma (B) and MDA-MB-231 (C) cells were plated onto fibroblast-derived matrix. Time-lapse videos were recorded in the presence of rGST, rCLIC3, rCLIC3<sup>C22A</sup> and rCLIC3<sup>C22/25A</sup> (25 ng/ml). The distance between the centre of the nucleus and the cell front was measured (with respect to the direction of migration). Image J was used to measure pseudopod length. rCLIC3<sup>C22A</sup> and rCLIC3<sup>C22/25A</sup> do not lead to pseudopod extension in A2780 cells or MDA-MB-231 cells. One biological replicate is shown but three independent replicates were performed. Values are mean  $\pm$  s.e.m.,  $n = 1$ , \*\*\* $p < 0.01$ , Kruskal-Wallis test with a Dunns post-test. The data are represented as Box and Whisker 5 – 95% plots. The mean is indicated with a cross and the median with the line through the plot.

### **Extracellular CLIC3 drives tumour cell invasion**

The pseudopod extension assay provides evidence that extracellular CLIC3 can drive some of the morphological changes that are associated with the invasive process. To determine whether extracellular CLIC3 can activate a complete invasive programme, I used an inverted invasion assay, which measures the ability of invading tumour cells to translocate considerable distances into a Matrigel plug. A2780 cells were seeded on the bottom of a transwell (0.8  $\mu\text{m}$  pore size) and were then allowed to migrate through these pores into a Matrigel plug towards a chemoattractant, which consisted of full medium supplemented with EGF in the presence or absence of rCLIC3 (Figure 3.14 A). The addition of rCLIC3 to the chemoattractant medium significantly promoted invasion of A2780 cells into Matrigel (Figure 3.14). Moreover, the degree of invasiveness observed in the presence of rCLIC3 was comparable to that evoked by cRDGfV - an  $\alpha\text{v}\beta\text{3}$  integrin blocking peptide, which is routinely used as a positive control in these inverted invasion assays (Caswell, Chan et al. 2008).

It is thought that estimates of invasiveness using assays such as the inverted Matrigel assay may be influenced by the proliferation rate of cells plated into the assay. I, therefore, determined whether addition of rCLIC3 to the extracellular milieu altered the growth of A2780 cells. However, A2780 cells proliferated at identical rates irrespective of whether they were treated with rCLIC3 or with rGST control (Figure 3.14 D).

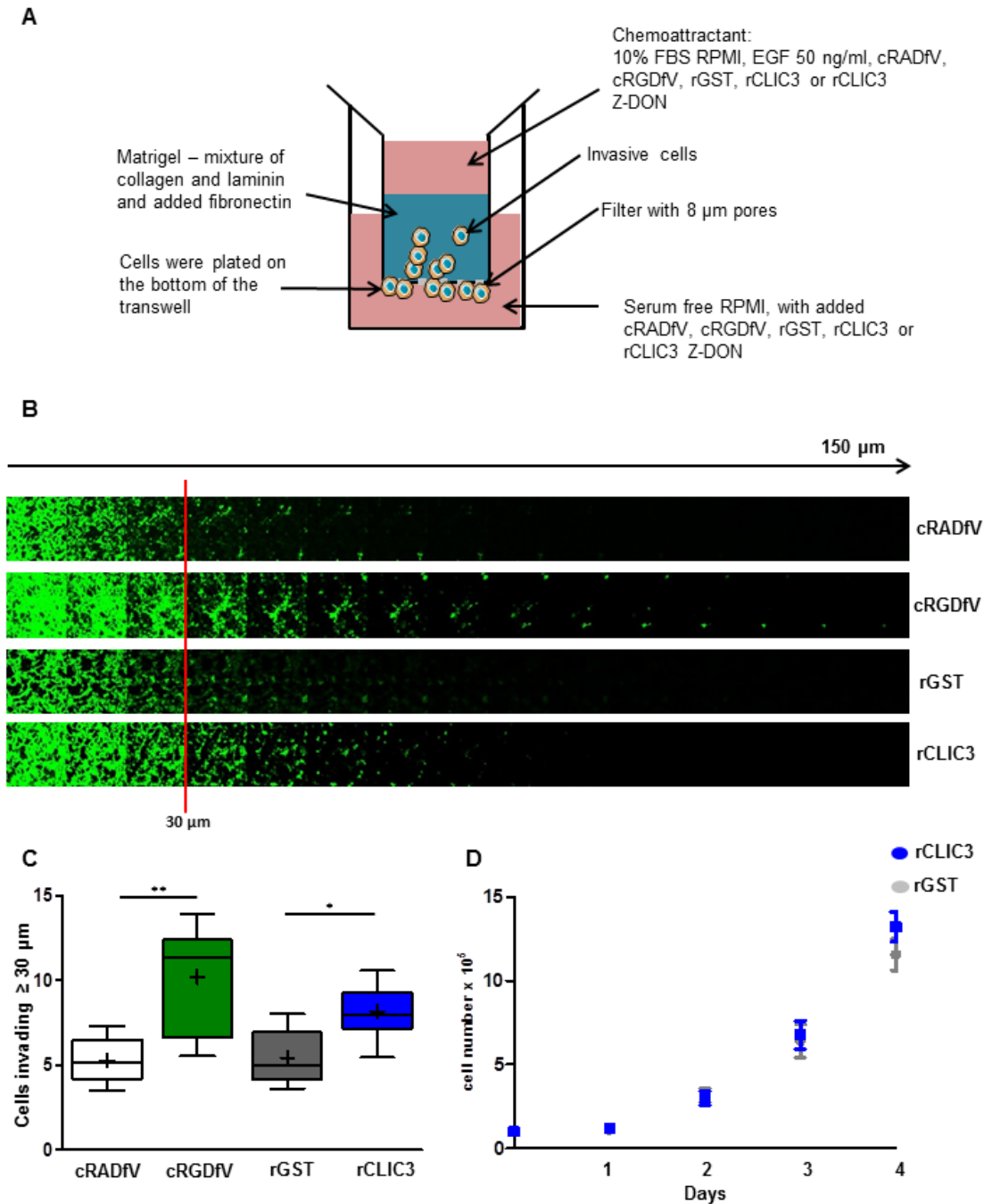


**Figure 3.14: Extracellular rCLIC3 promotes tumour cell invasion**

(A) Schematic representation of the set-up of an inverted invasion assay. A2780 ovarian adenocarcinoma cells were seeded on the bottom of Matrigel plugs (transwell with a 0.8 µm pore size). The Matrigel plugs were formed in the presence of 25 µg/ml fibronectin. The cells were allowed to invade for 72 hours towards a gradient of 10% FBS, 50 ng/ml EGF and cRADfV (2.5 µM), cRGDfV (2.5 µM), rGST(25 ng/ml) and rCLIC3 (25 ng/ml). (B) Cells were stained with calcein acetoxymethyl ester and visualised by confocal microscopy. Serial optical slices were captured at 10 µm intervals. They are presented as a sequence in which the individual optical sections are placed alongside one another with increasing depth from left to right as indicated. (C) The relative invasion was measured by quantification of the fluorescence intensity of cells penetrating the Matrigel to a depth of 30 µm and greater. cRGDfV is a well-established pro-invasive positive control in this assay. The addition of rCLIC3 increased invasion by comparison with the rGST control. Values are mean  $\pm$  s.e.m.,  $n = 3$ ,  $**p < 0.01$ ,  $*p < 0.05$  Kruskal-Wallis test with a Dunns post-test. Plots are Box and Whisker 5 – 95% plots. The mean is indicated with a cross and the media with the line through the plot. (D) A2780 cell proliferation was measured over 4 days in the presence of rCLIC3 (1 ng/ml, blue) or rGST (1 ng/ml, grey). The cells were plated at a density of  $1 \times 10^5$  cells/well in a 6 well dish and were treated with either rGST or rCLIC3. The cells were counted using a CASEY® counter every day for 4 days, Values are mean  $\pm$  s.e.m.,  $n = 3$ .

In many types of carcinoma, the acquisition of malignant phenotype is associated with the progression from a relatively non-invasive form of the disease, in which tumour cells acquire the ability to proliferate inappropriately - but do not disseminate because they are confined by an intact basement membrane - to a more aggressive phenotype in which the basement membrane is disrupted and the carcinoma cells can then spread into the surrounding tissue. In breast cancer this progression is characterised by transition from the relatively non-invasive ductal invasive carcinoma *in situ* (DCIS) to the more aggressive invasive carcinoma. Experimentally, this transition may be modelled using the MCF10DCIS.com breast cancer cell line. MCF10DCIS cells are ER-negative premalignant mammary carcinoma cells which are derived from the 'normal' MCF10A cell line and are known to form well-defined comedo-like DCIS structures when injected as subcutaneous or intraductal xenografts. However, with time these lesions spontaneously progress to invasive carcinoma characterised by disruption of their surrounding basement membrane, and the development of invasive outgrowth (Miller, Santner et al. 2000; Hu, Yao et al. 2008; Behbod, Kittrell et al. 2009). Elements of this progression may be recapitulated in 3D culture (Jedeszko, Victor et al. 2009; So, Lee et al. 2012). When MCF10DCIS.com cells were cultured for up to 6 days in Matrigel they formed comedo-like structures, which were surrounded by basement membranes evidenced by immunofluorescence staining for the basolateral marker  $\beta 4$  integrin and the basement membrane component laminin-5 (Figure 3.15 A, B). I used an algorithm to quantitatively assess the shape of these organoids and found that MCF10DCIS.com cells formed structures that were roughly spherical - as reflected by high index of circularity of a cross sectional focal plane - and this sphericity was maintained for up to 6 days in culture (Figure 3.16 A, B). However, when rCLIC3 (but not rGST or the inactive CLIC3 mutant, rCLIC3<sup>C22A</sup>) was added extracellularly to this assay, structures with high degree of sphericity were able to initially form, but their symmetry became significantly disrupted during the following few days (Figure 3.16 B). Consistently, immunofluorescence staining for  $\beta 4$  integrin and laminin-5 indicated that addition of rCLIC3 (but not rCLIC3<sup>C22A</sup>) drove substantial disruption of the basement membrane surrounding the comedo-like structure and MCF10DCIS.com cells can be seen to migrate out of the organoid (Figure 3.16 A).

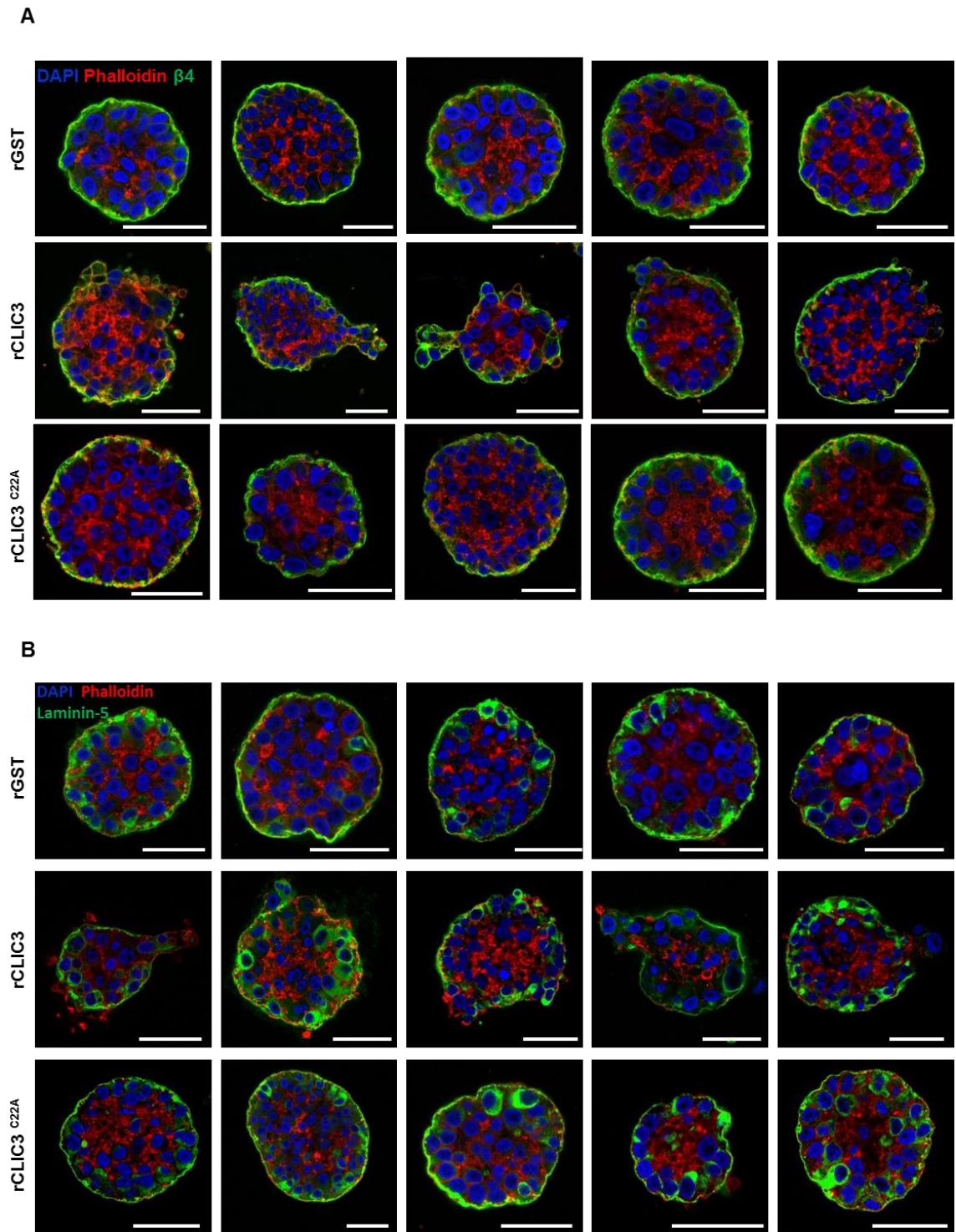


**Figure 3.15: Extracellular rCLIC3 leads to a disruption of comedo-like structures formed by MCF10DCIS.com cells.**

(A, B) MCF10DCIS.com cells were plated on a thin layer of Matrigel in the presence of rGST, rCLIC3 or rCLIC3<sup>C22A</sup> (25 ng/ml). The cells were fixed after 6 days in culture and stained for basement membrane, the nuclei and the actin cytoskeleton. To visualise the basement membrane acini were stained for  $\beta 4$  integrin (A, green) or Laminin-5 (B, green). The nuclei were visualised with DAPI (blue). The actin cytoskeleton was visualised with phalloidin-Alexa-Fluor-546 (red), scale bars: 50  $\mu$ m.

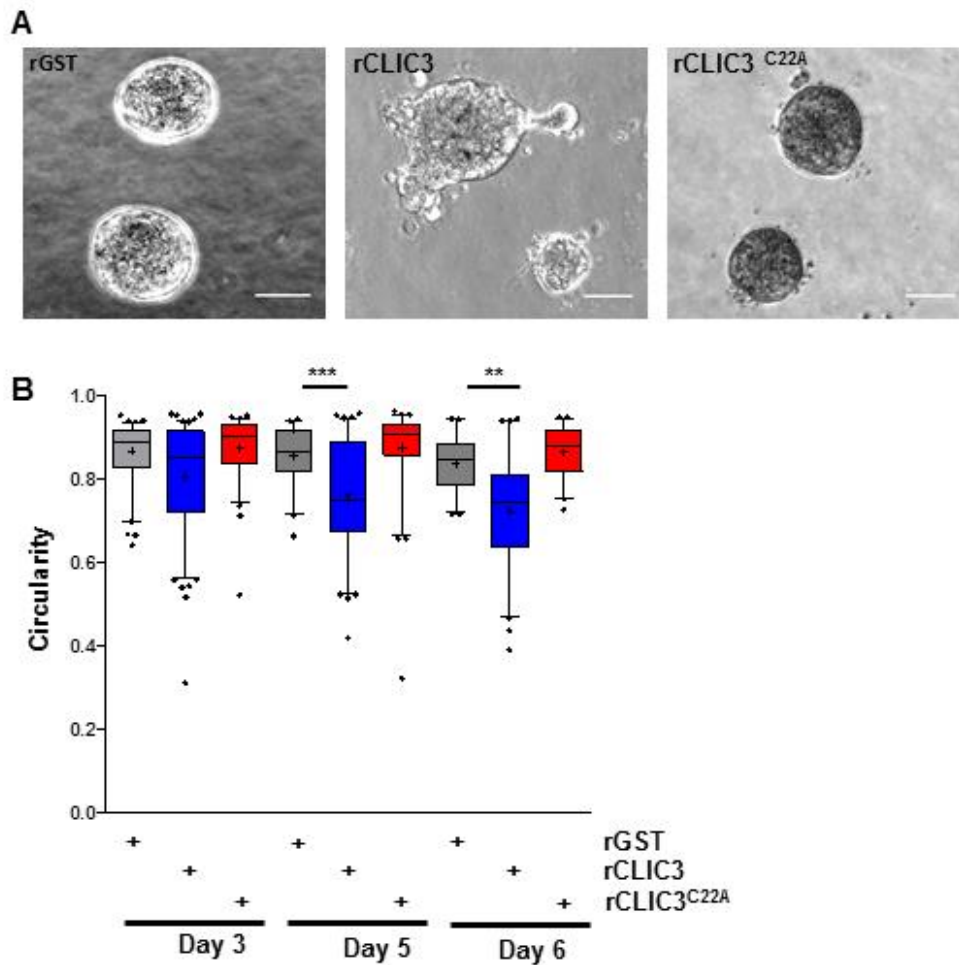


**Figure 3.16: The circularity of MCF10DCIS.com cells was disrupted by extracellular rCLIC3 but not by rGST or the rCLIC3<sup>C22A</sup> mutant.**

(A) MCF10DCIS.com cells were plated on a thin layer of Matrigel in the presence of rGST, or rCLIC3 or rCLIC3<sup>C22A</sup> (25 ng/ml). The recombinant proteins were refreshed every other day and phase contrast images were captured at day 3, 5 and 6 days after plating. Scale bars: 50  $\mu$ m. (B) Individual comedo-like structures were delineated and their circularity was determined using Image J. An Image J algorithm was used to determine the circularity. The value of 1 describes perfect circularity. Crosses are mean  $\pm$  s.e.m., n=3, \*\*\*p<0.001, \*\* p<0.01 Kruskal-Wallis test with a Dunn's post-test Plots are Box and Whisker 5 – 95%. The bars represent the median.

### **Other CLIC family members elongate invasive pseudopods**

CLIC1 and CLIC4 display 50 % and 45 % sequence homology to CLIC3, respectively. I, therefore, wanted to determine whether the rCLIC3-induced increase in pseudopod length is a particular characteristic of this CLIC family member, or whether rCLIC1 and rCLIC4 are also able to promote the elongation of invasive protrusions. I generated rCLIC1 and rCLIC4 (Figure 3.17 A, B) in *E.coli*, purified these proteins as previously described for rCLIC3, and evaluated their ability to drive pseudopod extension in A2780 cells. When added to the extracellular milieu, rCLIC1 and rCLIC4 increased pseudopod length to a very similar extent as CLIC3 did (Figure 3.17 C). This indicates that these three CLIC family members have similar biological activities with respect to the ability to drive pseudopod extension in A2780 target cells.

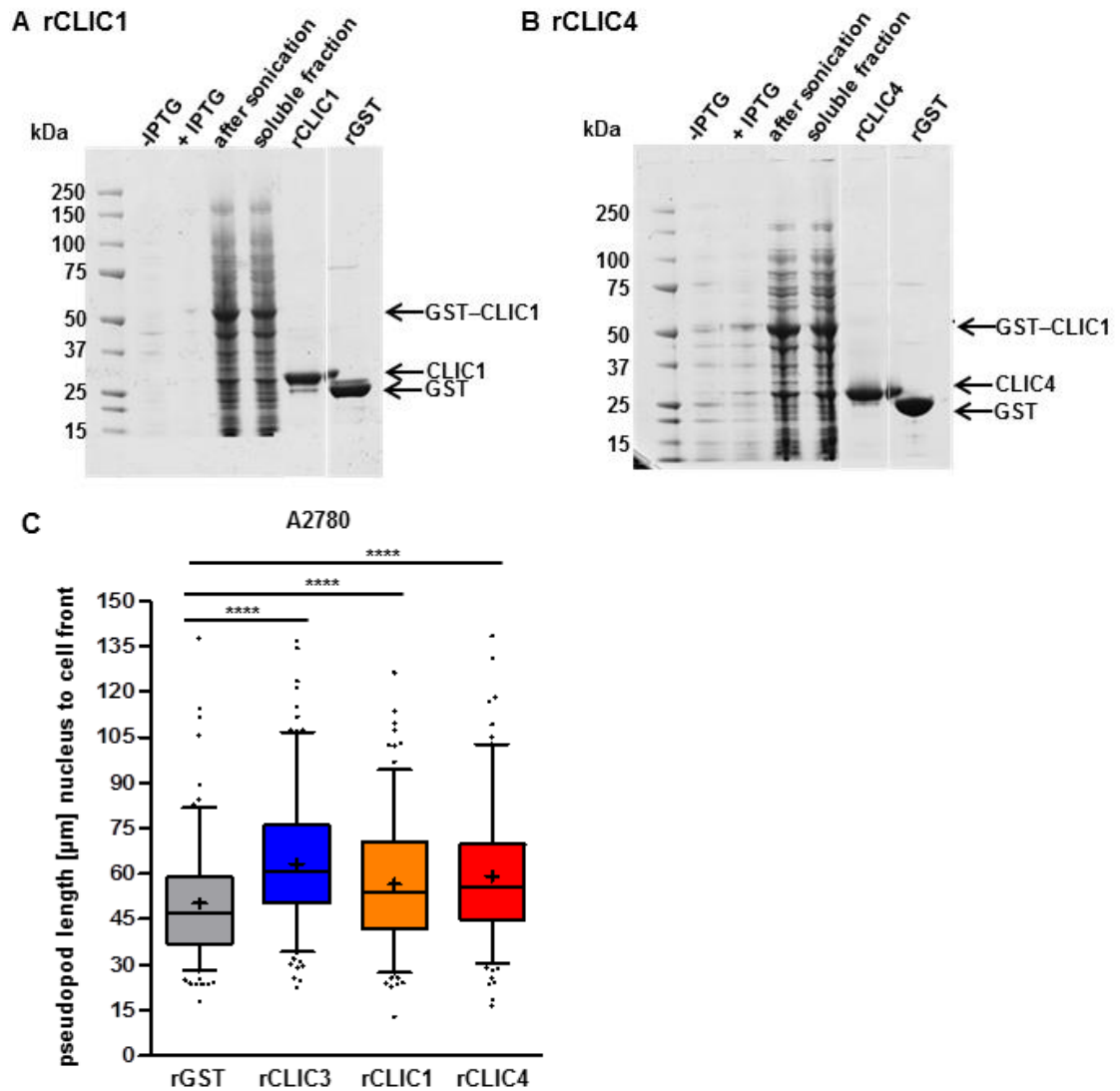


**Figure 3.17: A comparison of the ability of rCLIC3, rCLIC1 and rCLIC4 to drive pseudopod extension in A2780 cells.**

(A+B) Recombinant rCLIC1 (A) and rCLIC4 (B) were produced, purified and then visualised using Coomassie staining of an SDS-PAGE gel, as for Figure 3.9. (C) A2780 cells were plated on fibroblast-derived matrix and rGST, rCLIC1, rCLIC3 and rCLIC4 proteins (25 ng/ml) were added to the medium. rGST was used as a control protein and did not drive pseudopod extension. One biological replicate is shown and three independent biological replicates were performed. Values are mean  $\pm$  s.e.m.,  $n = 3$ , \*\*\*\* $p < 0.0001$  Mann-Whitney. Plots are Box and 5 – 95% Whisker plots. The mean is indicated with a cross and the median with the line through the plot.

### **rCLIC3-driven pseudopod extension is $\alpha 5\beta 1$ integrin and RCP-dependent**

Previous work has indicated that certain drivers of cell invasiveness, including blockade of  $\alpha v\beta 3$  integrin with cRGDfV and the expression of certain mutants of p53, are associated with increased recycling of  $\alpha 5\beta 1$  integrin.  $\alpha 5\beta 1$  recycling is controlled by Rab11 effector, Rab-coupling protein (RCP) and, consistently, a number of aspects of mutant p53-driven invasiveness (including the extension of invasive pseudopods) are dependent on  $\alpha 5\beta 1$  integrin and RCP (Muller, Caswell et al. 2009; Rainero, Caswell et al. 2012). I used siRNA of RCP and a blocking antibody that targets  $\alpha 5$  integrin to test whether the ability of rCLIC3 to drive pseudopod extension requires  $\alpha 5\beta 1$  integrin and its RCP-dependent recycling. Clearly, both the blockade of  $\alpha 5$  integrin (using mAb16, 2  $\mu\text{g}/\text{ml}$ ) or suppression of RCP levels (using either a SMARTPool or a single siRNA oligonucleotide targeting RCP) completely ablated the ability of extracellular rCLIC3 to drive the extension of invasive pseudopods in A2780 cells (Figure 3.18 A, B). Taken together, these data indicate that extracellular CLIC3 relies on RCP-dependent trafficking of  $\alpha 5\beta 1$  integrin in order to drive the extension of invasive protrusions.

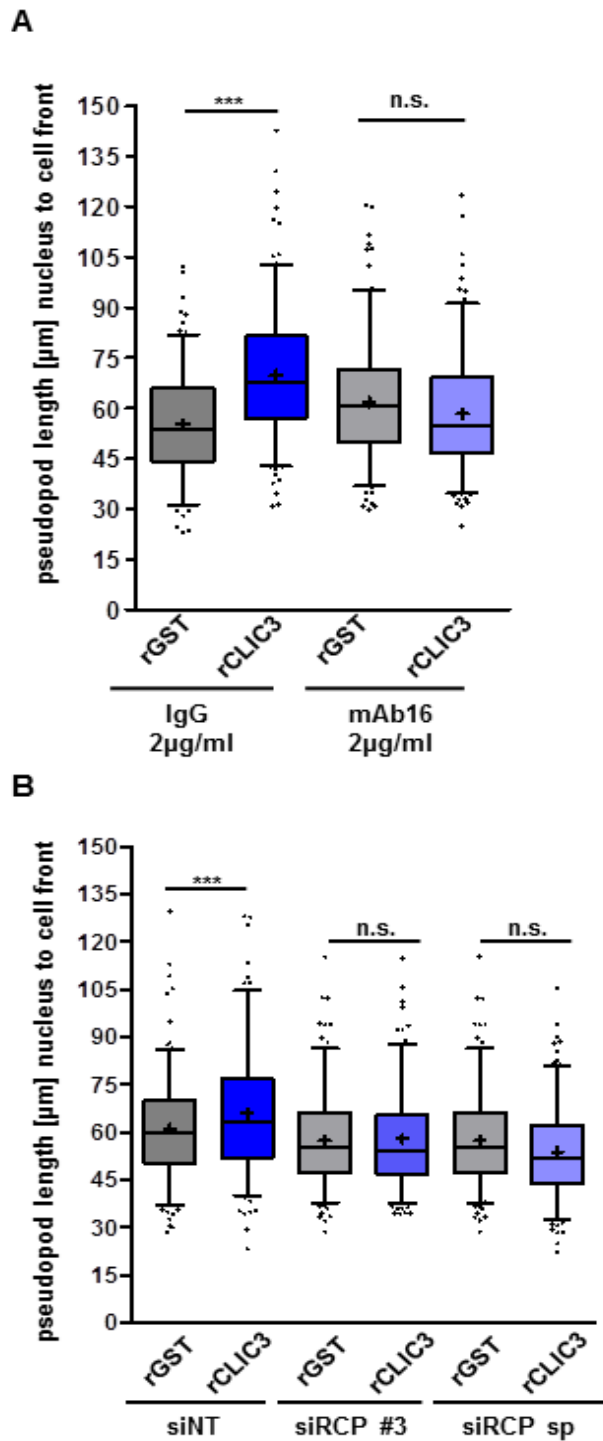


**Figure 3.18:  $\alpha 5\beta 1$  integrin and RCP are required for extracellular rCLIC3 to drive the extension of invasive pseudopods.**

(A) A2780 cells were plated onto fibroblast-derived matrix and allowed to attach. Following this an  $\alpha 5$  integrin blocking antibody (mAb16, 2  $\mu\text{g/ml}$ ) or an isotype matched control antibody (IgG, 2  $\mu\text{g/ml}$ ) were added and pseudopod extension determined using time-lapse microscopy and Image J analysis as for Figure 3.3. (B) A2780 cells were transfected with an siRNA targeting RCP (siRCP #3), a SMARTPool of siRNAs targeting RCP (siRCP sp) or a non-targeting control (siNT). Pseudopod extension was determined as in (A). One biological replicate is shown and three independent biological replicates were performed. Values are mean  $\pm$  s.e.m.,  $n = 1$ ,  $***p < 0.001$ , Kruskal-Wallis test with a Dunn's post-test. Plots are Box and 5 – 95% Whisker plots. The mean is indicated with a cross and the median with the line through the plot.

### 3.5 Discussion

The tumour stroma is important for tumour cell invasion and angiogenesis. CAFs are a major component of the tumour stroma and they can render tumour cells more permissive to undergo EMT as well as helping tumour cells to establish metastases at distant sites. Despite these observations, a recent study has shown that when CAFs are genetically deleted in a genetic mouse model of pancreatic adenocarcinoma, tumour progression is accelerated and the survival of the animals is significantly reduced (Ozdemir, Pentcheva-Hoang et al. 2014). This indicates that the relationship between the tumour stroma and tumour progression is far from straightforward, and that at least some CAF-generated factors may be tumour suppressive. This conflict highlights the need to understand what particular stromal factors promote tumour aggressiveness, so that these may be selectively targeted. Indeed, it has been discussed in the literature that neutralisation of certain CAF-secreted factors may be sufficient to yield better patient outcomes (Orimo, Gupta et al. 2005; Yu, Xiao et al. 2014). I have found that CAFs increase the amount of fibrillar collagen and stiffen (not shown) the ECM. Consistently, CAFs increase invasion of pancreatic adenocarcinoma cells into organotypic matrices. Mass spectrometry revealed CLIC3 to be one cohort of proteins with markedly higher expression in CAFs than iNFs, and CLIC3 knockdown reverses a number of CAF-specific attributes - such as the ability to generate a pro-invasive stroma with increased levels of fibrillar collagen. Thus, simply suppressing CLIC3 levels renders CAFs to be more akin to normal fibroblasts.  $\alpha 5\beta 1$  integrin has a well-established role in helping tumour cells to respond to the stromal environment and, in particular, this integrin is key to sensing altered stiffness and transducing these mechanical cues into increased tumour growth and invasiveness (Levental, Yu et al. 2009). Consistent with this, I have found that the ability of tumour cells to respond to the secreted stromal factor, CLIC3, requires them to express  $\alpha 5\beta 1$ . Moreover, my observations that RCP is also required for tumour cells to respond to extracellular CLIC3 indicates that not only must  $\alpha 5\beta 1$  be present, but that it must traffic appropriately to enable tumour cells to respond to the stroma.

CLIC family members are known to be highly expressed in tumours and the tumour stroma. Specifically, CLIC4 drives tumour cell growth (Shukla, Edwards

et al. 2014) via alterations in TGF- $\beta$  signalling, and CLIC3 increases invasiveness by driving integrin recycling (Dozynkiewicz, Jamieson et al. 2012). However, the pathways by which stromal CLICs might drive tumour progression are not yet clear. As discussed by Shulka and colleagues CLIC4 might act within stromal cells to influence TGF- $\beta$  signalling (Shukla, Edwards et al. 2014), but our data indicate that it is the extracellular pool of CLIC3 that drives tumour cell invasion. Indeed, I have shown that factor(s) that drive invasiveness are present in CAF-conditioned medium. Knockdown of CLIC3 in CAFs yields conditioned medium that is incapable of driving extension of invasive pseudopods and that, strikingly, the pro-invasive attributes of iCAF-conditioned medium may be restored by adding purified rCLIC3. From this and other experiments, I have been able to deduce that CLIC3 is a *bona fide* CAF-secreted factor that is necessary and sufficient to support invasiveness of tumour cells through Matrigel and to accelerate DCIS to invasive carcinoma transition in a 3D model of breast cancer invasiveness.

It has been previously suggested, that CLICs might be secreted (Chang, Wu et al. 2009; Wojciak-Stothard, Abdul-Salam et al. 2014). However, as none of the CLICs possess a canonical signal sequence to guide the protein to the endoplasmic reticulum, an unconventional mechanism seems to be more probable to move CLIC3 from the cytosol to the extracellular space. As shown before, CLIC3 has a late endosomal location (Dozynkiewicz, Jamieson et al. 2012; Macpherson, Rainero et al. 2014) and I explored whether CLIC3 release was linked to exocytosis of multivesicular bodies. However, upon knocking-down the levels of Rab GTPases controlling this process (Rab27A/Rab27B), I found that CLIC3 is still secreted into the extracellular environment, consistent with a non-exocytic route for CLIC3 release. Structural studies have identified that CLIC3 can exist in two different conformations; a soluble globular form comprising a GST-fold, that most likely possesses a thioreductase activity; and another confirmation displaying amphiphatic helical regions, capable of inserting into lipid bilayers. It has been suggested that the amphiphatic membrane insertion conformers enable Cl<sup>-</sup> transport across membranes. However, the CLICs can switch between the soluble globular and the membrane-inserted confirmation very quickly, suggesting that this change in confirmation might be a mechanism via which

CLIC3 permeates the plasma membrane and leaves the cell (Littler, Harrop et al. 2004; Littler, Assaad et al. 2005).

CLIC proteins are highly conserved throughout their family (with 6 CLIC family members) and throughout evolution. It is thought that most of the CLIC proteins are highly expressed in tumours and increase angiogenesis (Ulmasov, Bruno et al. 2009; Tang, Beer et al. 2013; Deng, Tang et al. 2014; Shukla, Edwards et al. 2014). Therefore, it was thought that in terms of tumour cell migration they all have a similar outcome and indeed I was able to show this. The precise molecular mechanisms through which CLIC proteins achieve their biological effects are still not clear. Littler and colleagues demonstrated that CLICs might have several different functions ranging from  $\text{Cl}^-$  channels, to molecular scaffolds, to functioning as oxidoreductases enzymes (Littler, Brown et al. 2010). A recent study showing that CLIC1, -2 and -4 have a glutaredoxin-like activity, with a cysteine in the GST-fold acting as a key catalytic residue, has increased awareness that the enzymic activity of CLICs may be biologically more relevant as the channel activity (Al Khamici, Brown et al. 2015). Indeed, our results indicate that mutation of the putative 'active site' cysteine in CLIC3 completely ablates its pro-invasive capacity, which suggests that extracellular CLIC3 functions as an oxidoreductase to promote ECM remodelling and tumour cell invasion.

In the following chapter, I will show that extracellular CLIC3 acts via TG2 to drive invasive processes and I will argue the possibility that this may be linked to the CLIC's ability to function as oxidoreductases.

## 4 Secreted CLIC3 regulates ECM remodelling via TG2 to generate a pro-invasive stroma

### 4.1 Introduction

In the previous chapter I demonstrated that CLIC3 is a secreted protein which increases both the stiffness of the ECM and the amount of fibrillar collagen in organotypic plugs. These changes in the tumour microenvironment are associated with increased tumour cell migration and invasion. However, how CLIC3 changes the behaviour of the tumour stroma to drive tumour cell invasion has not yet been established. A mass spectrometry screen provided an insight into which secretory proteins might be co-regulated with CLIC3 during fibroblast activation. Indeed, one abundant secreted protein whose levels increase in parallel with CLIC3 is transglutaminase 2 (TG2).

Transglutaminases are multifunctional enzymes catalysing the  $\text{Ca}^{2+}$ -dependent posttranslational modification of proteins by introducing covalent bonds between free amine groups and  $\gamma$ -carboxamide groups of peptide-bound glutamines (Folk and Finlayson 1977; Eckert, Kaartinen et al. 2014). They have been shown to be upregulated in several tumours as well as in the tumour stroma (Assi, Srivastava et al. 2013), and are found both within cells and as secreted proteins in the extracellular milieu. TG2 - the most studied transglutaminase - is upregulated in many cancers, and it is reported to perform many functions within and outwith cells, including protein cross-linking and the regulation of a number of intracellular signalling pathways (Oh, Ko et al. 2011; Leicht, Kausar et al. 2014). It has been shown that the desmoplastic response involves interplay between invading tumour cells and altered ECM (Apte and Wilson 2012) and, as TG2 alters the ECM, it is thought to be likely that this enzyme impacts on tumour cell behaviour. Indeed, it is possible that the  $\gamma$ -glutamyl cross-links, which are potentially generated by TG2, contribute to stiffening of the ECM - in much the same way as has been reported for the lysyl cross-links generated by lysyl oxidase (Levental, Yu et al. 2009). Therefore, I hypothesised that the reduction of the amount of fibrillar collagen that was observed upon CLIC3 knockdown could be due to the reduced activity of TG2.

A role for intracellular CLIC3 in tumour cell migration and invasion has been previously described by our group (Dozynkiewicz, Jamieson et al. 2012; Macpherson, Rainero et al. 2014). However, the mechanisms through which CLIC3 acts extracellularly to promote ECM remodelling and tumour cell invasion are yet to be described. Structural studies have shown that the CLIC proteins belong to the GST superfamily (Dulhunty, Gage et al. 2001; Harrop, DeMaere et al. 2001). GST proteins can be divided in at least 12 classes of proteins. They are multifunctional enzymes that exist mostly in a dimeric form in the cytosol (Hayes, Flanagan et al. 2005). GSTs are cytosolic proteins which can catalyse the conjugation of a tripeptide (glutamine, cysteine, glycine) glutathione (GSH) to electrophilic regions of other molecules (Wilce and Parker 1994). This reaction can occur through activation of the thiol group of GSH, which allows non-covalent, but high-affinity binding to the substrate. Moreover, GSTs have been reported to be upregulated in tumour cells and can contribute to anticancer drug resistance (Booth, Boyland et al. 1961; Kanaoka, Ago et al. 1997; Harrop, DeMaere et al. 2001).

The CLIC proteins have been shown to exist in a globular form consisting of an N-terminal thioredoxin domain which contains four  $\beta$ -strands in between three  $\alpha$ -helices which contain the conserved glutaredoxin monothiol or dithiol motif (Board, Coggan et al. 2000). Experiments in which 2-hydroxyethyl disulphide was used as a substrate have recently indicated that CLIC1, 2 and 4 have glutaredoxin-like glutathione-dependent oxidoreductase enzymatic activity (Al Khamici, Brown et al. 2015), which was inhibited by mutation of the putative 'active site cysteine'. Moreover, the indanyloxyacetic acid (IAA) and ethacrynic acid compounds (IAA-94, A9C) that had been previously identified as CLIC-binding molecules in the 1990s and (perhaps erroneously) termed 'chloride channel blockers', inhibit the glutathione-dependent oxidoreductase activity of CLIC1. In contrast, 4,4'-Diisothiocyano-2,2'-stilbenedisulfonic acid (DIDS), which is a well-established chloride channel antagonist had no effect on CLIC1's oxidoreductase activity (Al Khamici, Brown et al. 2015).

Given the recent work describing CLIC1's thioredoxin activity, and studies indicating that thioredoxin activates TG2 (Jin, Stammaes et al. 2011), I proposed that CLIC3 might be able to reduce the disulphide bonds of the enzyme TG2 to influence its activity. Therefore, in this chapter I investigate how TG2 is required for CLIC3 to perform its extracellular pro-invasive function.

## 4.2 Results

### **CLIC3 influences transglutaminase-2 behaviour in a redox-dependent manner**

As discussed above, TG2's activity is sensitive to its redox state. Indeed, TG2 possesses cysteine residues that need to be reduced for the protein to display full enzymatic activity. Moreover, thioredoxin - a protein that is involved in a number of redox signalling events - can function as an activator of oxidised TG2. This is likely to be mediated via the ability of thioredoxin to catalyse the reduction of cysteine residues within oxidised TG2. Indeed, the activation of TG2 by thioredoxin is inhibited by a small molecule inhibitor, which reduces thioredoxin (Jin, Stammaes et al. 2011). In addition, structural analysis of CLIC3 revealed a thioredoxin-like CxxC motif and, as for CLIC2, these two cysteines are capable of forming an intramolecular disulphide bond (Littler, Brown et al. 2010). Therefore, if thioredoxin was to be capable of evoking similar cellular responses as does the addition of extracellular CLICs, then this might implicate a redox-like mechanism in CLIC3's function, and also indicate a possible involvement of TG2 in the function of extracellular CLIC3. I determined the ability of a range of concentrations of recombinant, purified thioredoxin (rThx) to drive pseudopod extension in A2780 cells plated onto cell-derived matrices. rThx was capable of driving pseudopod extension, but this occurred at an approximately 30-fold higher concentration that is necessary for CLIC3 to evoke a similar response (Figure 4.1). Taken together with data from the previous chapter demonstrating the requirement for CLIC3's putative active site cysteine in its pro-invasive function, this observation suggests that a redox reaction is involved in CLIC3's extracellular role, and that this might be mediated via activation of TG2.

I then determined whether CLIC3 and TG2 are capable of interacting physically, and whether the redox context is important to this. To do this, I expressed TG2 as a GST-tagged fusion protein in *E.coli* and purified this using affinity chromatography (Figure 4.2). We then used a fluorescence polarisation assay (Lorand and Graham 2003) which exploits the fact that TG2 is a GTP/GDP-binding protein. First we confirmed the capability of recombinant TG2 to bind to the fluorescently-labelled non-hydrolysable GTP analogue, Mant-GMPPNP (Figure

4.3 - point (a) on graph). Then we explored CLIC3's interaction with TG2. We observed a transient increase in the polarisation signal from the Mant-GMPPNP-TG2 complex following addition of rCLIC3, but not rCLIC3<sup>C22A</sup> (Figure 4.3 - point (c) on graph). This increase was observed in the presence of reduced-glutathione, but not its oxidised form (Figure 4.3 - point (b) on graph). Furthermore, this effect could not be seen using dithiothietol (DTT) indicating the specificity of the effect toward reduced glutathione (not shown). Since TG2 was at a sub-saturating concentration, the increase in polarisation signal could indicate either that rCLIC3 physically interacts with Mant-GMPPNP-TG2 or that it regulates the affinity between TG2 and Mant-GMPPNP.

TG2 binds to Ca<sup>2+</sup> ions and this is known to control its affinity for GTP. Thus, at sub-millimolar calcium concentrations, such as would be encountered in the cytosol, TG2 binds to GTP and is thought to function intracellularly as a GTP-binding protein. Conversely, when the free calcium concentration is in the low millimolar range, as found in the extracellular milieu, the affinity of TG2 for GTP is reduced. Consistent with this, our data indicate that addition of 5 mM Ca<sup>2+</sup> led to a marked reduction in the Mant-GMPPNP fluorescence polarisation signal indicating that GTP was released from TG2 at high free calcium concentrations (Figure 4.3 - point (e) on graph). Interestingly, in the combined presence of rCLIC3 (but not rCLIC3<sup>C22A</sup>) and GSH (but not GSSH) the Mant-GMPPNP fluorescence polarisation signal did not reduce following addition of 5 mM Ca<sup>2+</sup>, indicating that CLIC3 is able to oppose the Ca<sup>2+</sup>-induced release of GTP from TG2. These results are consistent with recent evidence that several CLIC proteins are glutaredoxin-like enzymes (Al Khamici, Brown et al. 2015), hence we conclude that CLIC3 may be an oxidoreductase with glutathione-dependent activity and that TG2 is a likely CLIC3 substrate.

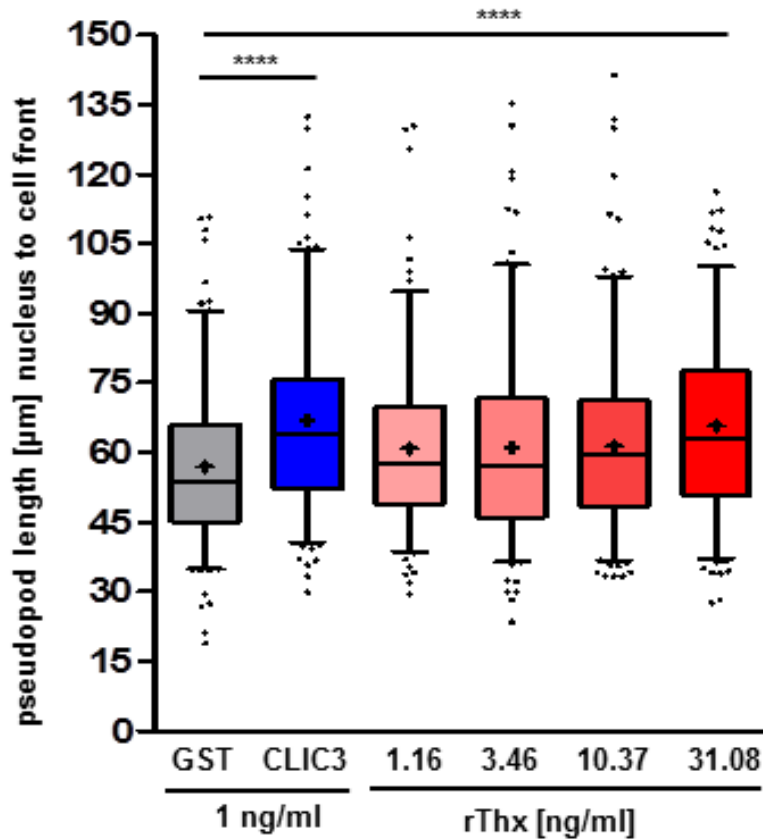


**Figure 4.1: Thioredoxin is capable of driving extension of invasive pseudopods, but with approximately 30-fold less potency than CLIC3.**

A2780 cells were plated onto CDMs. Time-lapse videos were recorded in the presence of 1 ng/ml rGST, 1 ng/ml rCLIC3 or increasing concentration (1.16 ng/ml, 3.46 ng/ml, 10.7 ng/ml and 31.08 ng/ml) of thioredoxin. The distance between the centre of the nucleus and the cell front was measured (with respect to the direction of migration). Image J was used to measure the pseudopod length. One biological replicate is shown and three independent biological replicates were performed. Values are mean  $\pm$  s.e.m,  $n = 1$ . 180 pseudopods were measured per experiment, \*\*\*\* $p < 0.0001$ , Mann-Whitney test. The data are represented as box and Whisker 5 – 95 % plots (the median are shown with lines and the mean as a cross).

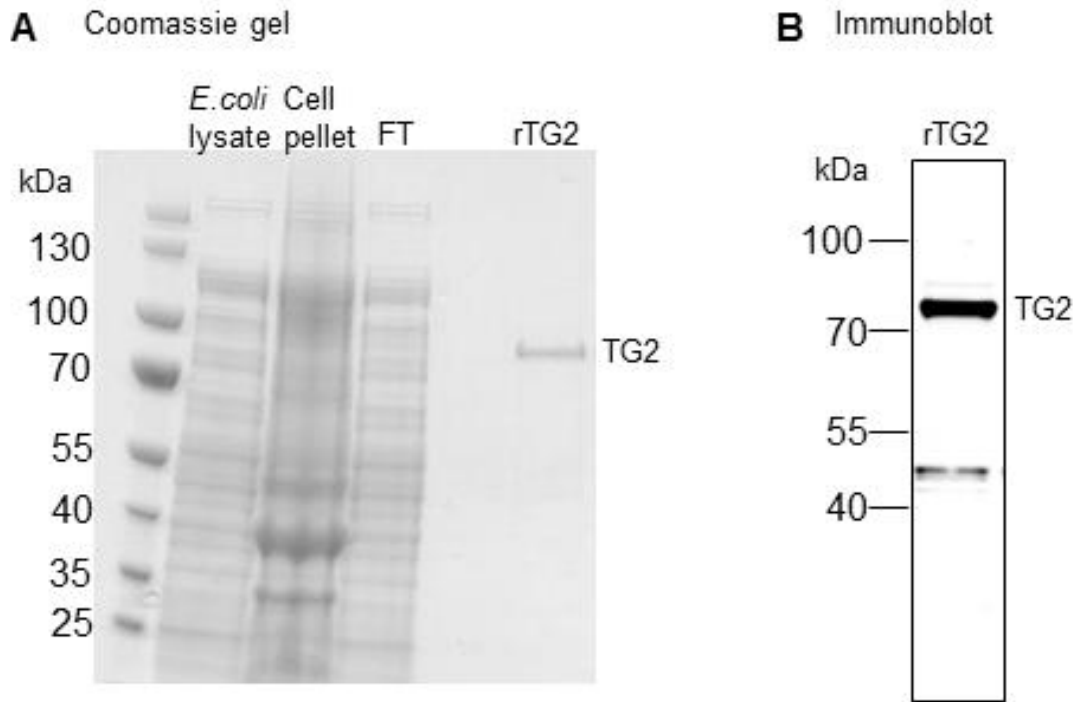


**Figure 4.2: Production of recombinant purified TG2.**

(A) The left hand lane shows the lysate of the BL21 (DE) pLysS *E.coli* cells which were transformed with TG2-GST expression vector (*E. coli* lysate). The lysates were filtered and centrifuged. The second lane shows the pellet which was remaining after centrifugation (cell pellet). The supernatant was loaded onto a GSTrap column. Afterwards, the column was washed with lysis buffer to remove proteins which were not bound to the column. An aliquot of this was loaded in lane three and was called flow through (FT). Finally, rTG2 with a size of 77 kDa was cleaved from GST using PreScission protease. The protein was concentrated and frozen in liquid nitrogen. The gel was stained with Coomassie brilliant blue. (B) The Western blot confirms that the 77 kDa band is rTG2 protein; an immunoreactive degradation product is visible at approximately 45 kDa.

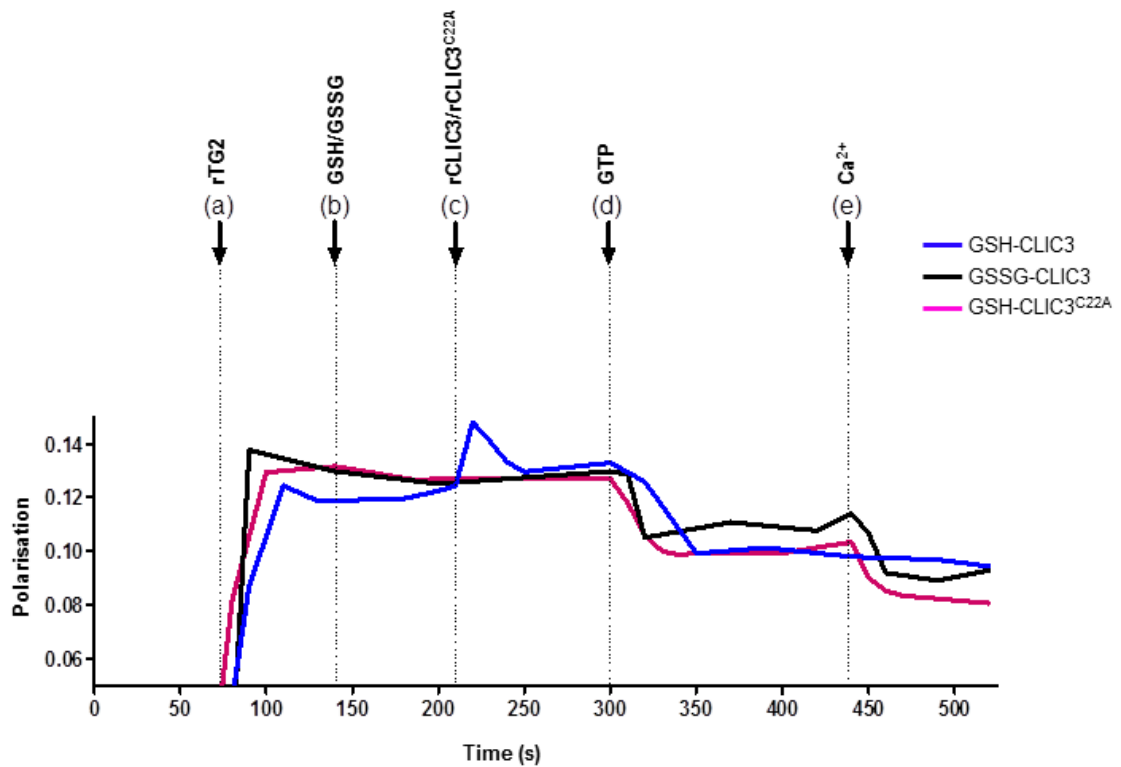


**Figure 4.3: CLIC3 influences the polarised fluorescence signal emanating from the Mant-GMPPNP/rTG2 complex in GSH dependent fashion.**

Mant-GMPPNP (2  $\mu$ M) was added to the cuvette of a polarised fluorimeter. rTG2 was then added and the fluorescence measurement increased as rTG2 bound to Mant-GMPPNP (a). The following were then added in sequence: Reduced (GSH) or oxidised glutathione (GSSG) (1 mM) (b); rCLIC3 or rCLIC3<sup>C22A</sup> (8  $\mu$ M) (c); GTP (2  $\mu$ M) (d); and CaCl<sub>2</sub> (5 mM) (e). In the presence of reduced glutathione and rCLIC3 polarised fluorescence from Mant-GMPPNP/rTG2 increased transiently, but oxidised glutathione or rCLIC3<sup>C22A</sup> were ineffective in this regard (d). Unlabelled GTP (2  $\mu$ M) was added to displace some Mant-GMPPNP from rTG2. This experiment was performed by Juan Hernandez.

## TG2 and CLIC3 collaborate to promote ECM remodelling

In view of the indications provided by our fluorescence polarisation analysis that CLIC3 and TG2 might be physically and mechanistically linked, I determined the requirement for TG2 in the ability of extracellular CLIC3 to promote ECM remodelling and cell invasiveness. Initially, I used either control or TG2-knockdown iCAFs to precondition organotypic collagen plugs, and multiphoton microscopy to quantify their fibrillar collagen content. siRNA of TG2 in the iCAFs led to significant reduction in the proportion of fibrillar collagen present in the organotypic plugs, indicating clearly that TG2 expression is required for CAFs to efficiently remodel the ECM (Figure 4.4).

Next I wanted to determine whether ability of extracellular rCLIC3 to drive pseudopod extension in cancer cells is TG2 dependent. Initially, I used a well-characterised TG2 inhibitor (Z-DON (Benzyloxycarbonyl-(6-Diazo-5-oxonorleucinyl)-L-Valinyl-L-Prolinyl-L-Leucinmethylester)) to test whether TG2 activity is needed for CLIC3-driven pseudopod extension. This inhibitor is an analogue of TG2's substrate, glutamine. When TG2's active site cysteine attacks Z-DON's carbonyl group, this leads to alkylation at the active site of the transglutaminase thus irreversibly inhibiting the enzyme (McConoughey, Basso et al. 2010). Low concentrations (20 nM) of Z-DON are reported to selectively inhibit extracellular transglutaminases, whereas higher concentrations (40  $\mu$ M) can act on both the intracellular and extracellular pool of transglutaminases (Schaertl, Prime et al. 2010). Addition of Z-DON at concentrations of either 20 nM or 40  $\mu$ M completely opposed the ability of rCLIC3 to drive extension of invasive pseudopods, indicating a clear requirement for a transglutaminase (and most likely an extracellular one) in extracellular CLIC3 function (Figure 4.5 A). The amounts of Z-DON inhibitor used did not affect proliferation of A2780 ovarian carcinoma cells (Figure 4.5 B).

TG2 is expressed in both A2780 cells and fibroblasts and mass spectrometry indicated that considerable quantities of TG2 are associated with the cell-free ECM deposited by iCAFs. In view of this, I was particularly interested in which of these two potential sources of TG2 (from the tumour cells or from the fibroblasts) might play a role in the function of extracellular CLIC3. TG2 knockdown in A2780 tumour cells did not compromise the ability of extracellular

rCLIC3 to drive pseudopod extension (Figure 4.6). However, when A2780 cells were plated onto cell-derived matrix generated by TG2 knockdown fibroblasts, CLIC3-driven pseudopod extension was strongly suppressed (Figure 4.6 C, D). Extension of invasive pseudopods may be driven by a number of stimuli including addition of rCLIC3, inhibition of  $\alpha\beta 3$  using cRGDfV, and expression of mutant p53 or the Rab11 GTPase, Rab25. To test whether TG2 expression in the matrix-producing cells was required for one of these other drives to pseudopod extension I plated Rab25-expressing A2780 cells onto cell-derived matrices generated by control and TG2 knockdown fibroblasts. Consistent with previous reports, Rab25-expressing A2780 cells had longer invasive pseudopods than control A2780 cells (Caswell, Spence et al. 2007) and, interestingly, the length of these was unaffected by knockdown of TG2 in the matrix-generating fibroblasts (Figure 4.5 C). These data indicate that the requirement for ECM-derived TG2 in pseudopod extension depends on the stimulus used to evoke the invasive response.

To provide confirmation of the requirement for extracellular TG2 in the invasive process, I determined whether the ability of rCLIC3 to drive pseudopod extension could be restored by addition of soluble rTG2 to cell-derived matrices derived from TG2 knockdown fibroblasts. Addition of rTG2 to A2780 cells plated onto cell-derived matrices did not significantly influence pseudopod extension in the absence of rCLIC3. Furthermore, rTG2 did not enhance rCLIC3's ability to drive pseudopod extension when A2780 cells were plated onto cell-derived matrices generated by control fibroblasts. However, rTG2 restored the ability of CLIC3 to drive pseudopod extension when A2780 cells were plated onto cell-derived matrices generated by TG2 knockdown fibroblasts (Figure 4.7). Taken together these data provide evidence that an extracellular pool of TG2 (which may be either soluble or ECM-associated) is necessary for CLIC3 to evoke the extension of invasive pseudopods.

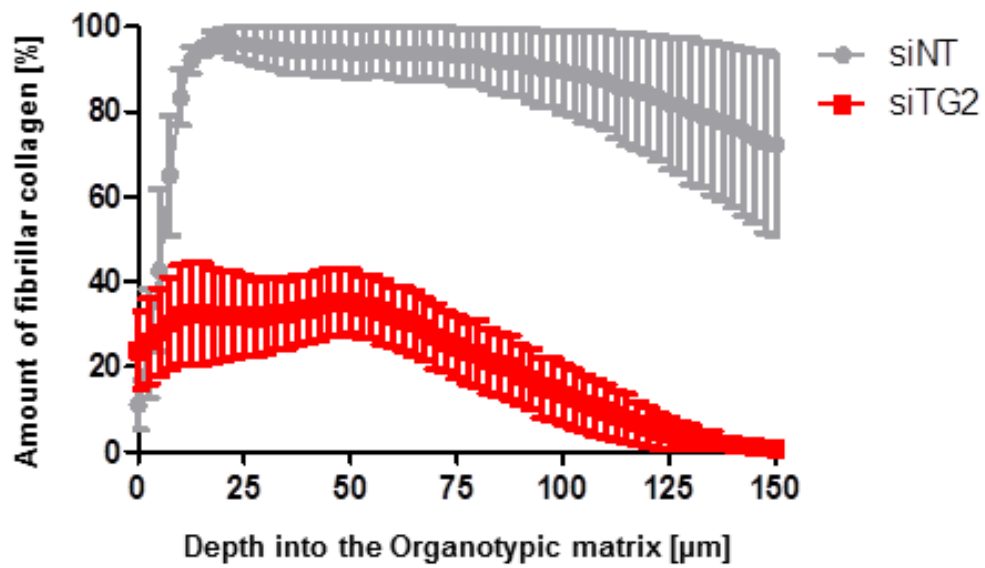


**Figure 4.4: Knockdown of TG2 in iCAFs reduces the fibrillar collagen content of organotypic plugs preconditioned with these cells.**

Plugs of collagen I were preconditioned with iCAFs that had been transfected with siRNAs targeting TG2 (siTG2) or a non-targeting control (siNT). The SHG signal was then measured using multiphoton microscopy followed by application of the Image J area calculator plug-in to measure the fibrillar collagen content at the indicated depth into the plug. Values are mean  $\pm$  s.e.m,  $n = 1$ ,  $p < 0.0001$ , Mann-Whitney test.

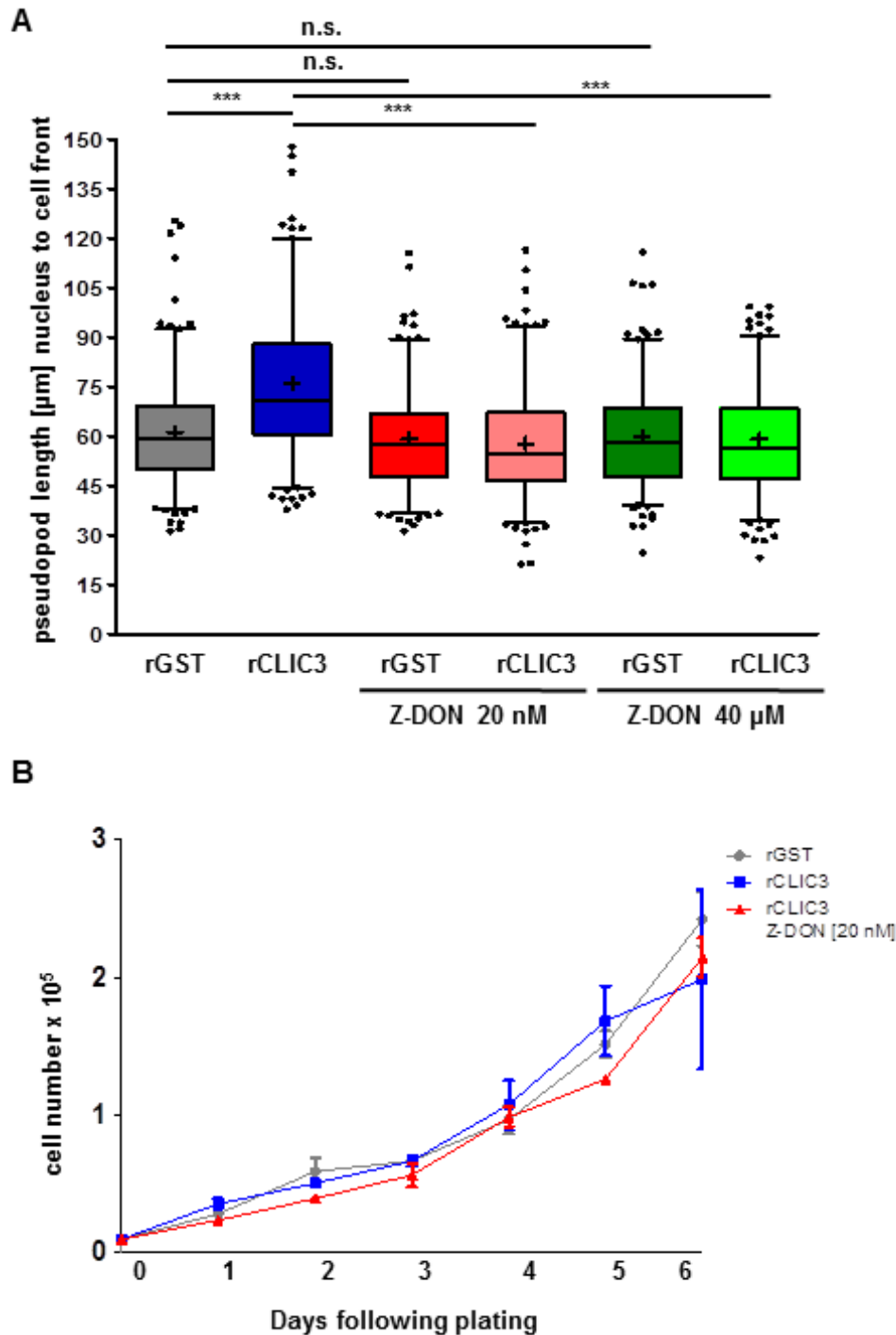


**Figure 4.5: Transglutaminase-2 inhibitor Z-DON inhibits CLIC3-driven pseudopod extension,** (A) A2780 adenocarcinoma cells were seeded on fibroblast-derived cell-derived matrices. Following attachment the Z-DON inhibitor was added at 20 nM or 40  $\mu$ M. 30 minutes later either rGST (1 ng/ml) or rCLIC3 (1 ng/ml) were added. Time-lapse videos were started after the addition of either CLIC3 or GST. The distance between centre of the nucleus to the front of the cell was measured (in the direction of movement) using Image J. One biological replicate is shown but three independent biological replicates were performed. Values are mean  $\pm$  s.e.m,  $n = 1$  and 180 pseudopods were measured per experiment, \*\*\* $p < 0.001$ , Kruskal-Wallis test with a Dunns post-test. The data are represented as box and Whisker 5 – 95 % plots (the median are shown with lines and the mean as a cross). (B) The cells were seeded at 10,000 cells per well. They attached to the plastic dish. rGST, rCLIC3 and rCLIC3 in the presence of Z-DON was added (all proteins at 1 ng/ml). Every day the cells were counted with the CASY® counter. The treatments were refreshed every 2 days in fresh culture medium.  $n = 2$ .

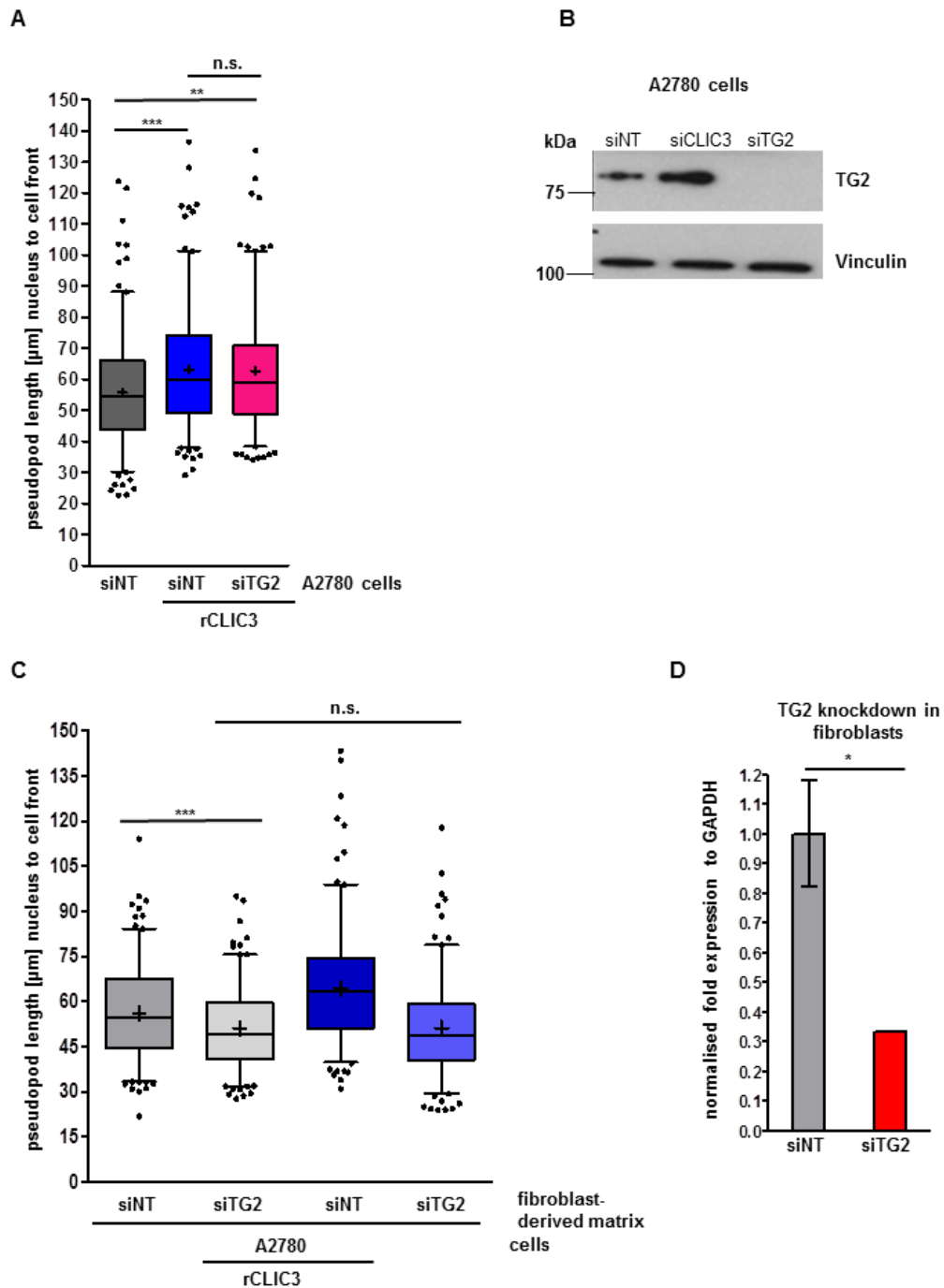


**Figure 4.6: Knockdown of TG2 in the ECM producing fibroblasts opposes CLIC3-driven pseudopod extension by tumour cells.**

(A) A2780 cells transfected with a siRNA targeting TG2 (siTG2) or a non-targeting control (siNT) and seeded on fibroblast-derived matrices. Pseudopod elongation in the presence and absence of rCLIC3 (1 ng/ml) was determined in the same manner as for Figure 4.1. The siRNA of TG2 in the A2780 cells was confirmed using Western blotting (B). (C) A2780 cells were plated onto cell-derived matrix. The fibroblasts producing the cell-derived matrices had been transfected with a siRNA targeting TG2 (siTG2) or a non-targeting siRNA (siNT). The siRNA of TG2 in the fibroblasts was confirmed using qPCR in (D). Pseudopod length in the presence or absence of rCLIC3 (1 ng/ml) was determined in the same manner as for Figure 4.1. One biological replicate of the pseudopod extension assays is shown and three biological replicates were performed. Values are mean  $\pm$  s.e.m,  $n = 1$  experiments and 180 pseudopods were measured per experiment, \*\*\* $p < 0.001$ , \*\* $p < 0.01$ , Kruskal-Wallis test with a Dunns post-test. The data are represented as box and Whisker 5 – 95 % plots (the median are shown with lines and the mean as a cross).

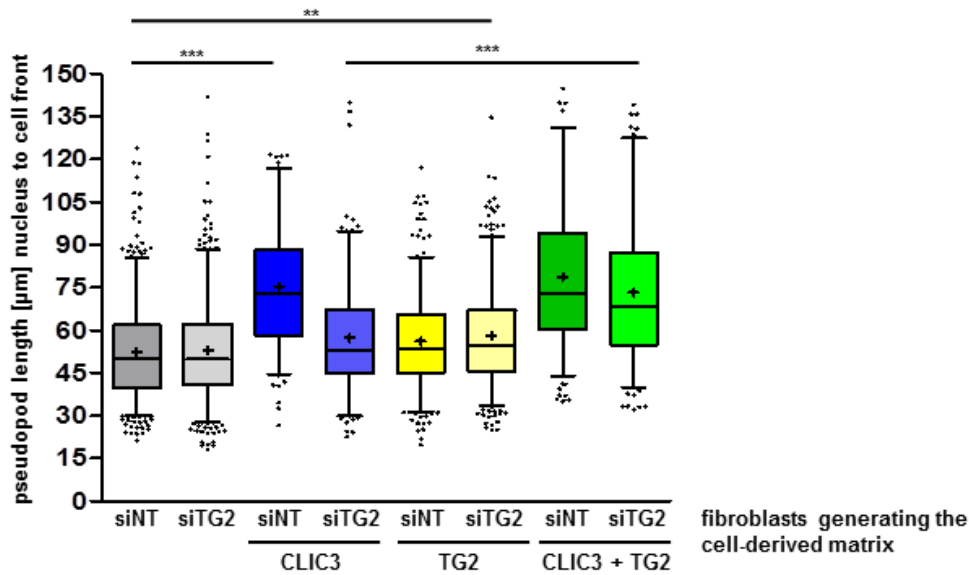


**Figure 4.7: Addition of soluble rTG2 restores CLIC3-driven pseudopod extension when A2780 cells are plated onto cell-derived matrices generated by TG2 knockdown fibroblasts.** A2780 cells were plated on fibroblast-derived matrices. The fibroblasts producing the cell-derived matrices has been transfected with a siRNA targeting TG2 (siTG2) or a non-targeting control (siNT). Pseudopod length in the presence and absence of rCLIC3 (1 ng/ml) and/or siTG2 (0.9 ng/ml) was determined in the same manner as for Figure 4.1. One biological replicate is shown but three independent biological replicates were performed. Values are mean  $\pm$  s.e.m,  $n=1$  experiments and 180 pseudopods were measured per experiment, \*\*\* $p<0.001$ , \*\* $p<0.01$ , Kruskal-Wallis test with a Dunns post-test. The data are represented as box and Whisker 5 – 95 % plots (the median are shown with lines and the mean as a cross).

## **CLIC3-driven tumour cell invasion is TG2 dependent**

The previous section makes extensive use of the pseudopod extension assay to pinpoint the source of TG2 that is necessary for CLIC3's ability to drive invasive behaviour. To determine whether TG2 plays a role in CLIC3's ability to evoke a comprehensive programme of invasive behaviour, I investigated the consequences of TG2-inhibition on CLIC3-driven invasiveness in the inverted Matrigel assay (Figure 4.8) and on the morphology of spheroids formed by MCF10DCIS.com cells plated into Matrigel (Figure 4.9).

Firstly, Z-DON was used to determine whether CLIC3-driven invasion into Matrigel was TG2 dependent. A2780 cells were allowed to invade into fibronectin-containing Matrigel plugs in the presence and absence of 20 nM Z-DON. Z-DON significantly opposed CLIC3-driven invasion into Matrigel plugs (Figure 4.8 A, B). Furthermore, I used MCF10DCIS.com breast cancer cells, as described in the previous chapter, to investigate the role of TG2 in CLIC3-driven invasiveness. As before, addition of rCLIC3 drove extensive disruption of the basement membrane that formed around MCFDCIS.com cell spheroids, and this led to a significant loss of circularity and extension of invasive protrusions. Addition of Z-DON significantly opposed this rCLIC3-driven basement membrane disruption and loss of circularity indicating that TG2 is required for CLIC3 driven invasiveness. Furthermore, Z-DON did not affect proliferation of MCF10DCIS.com cells (Figure 4.10).

Taken together, these data indicate that extracellular CLIC3 functionally associates with TG2, and that CLIC3 acts via TG2 to promote collagen I remodelling and tumour cell invasion.

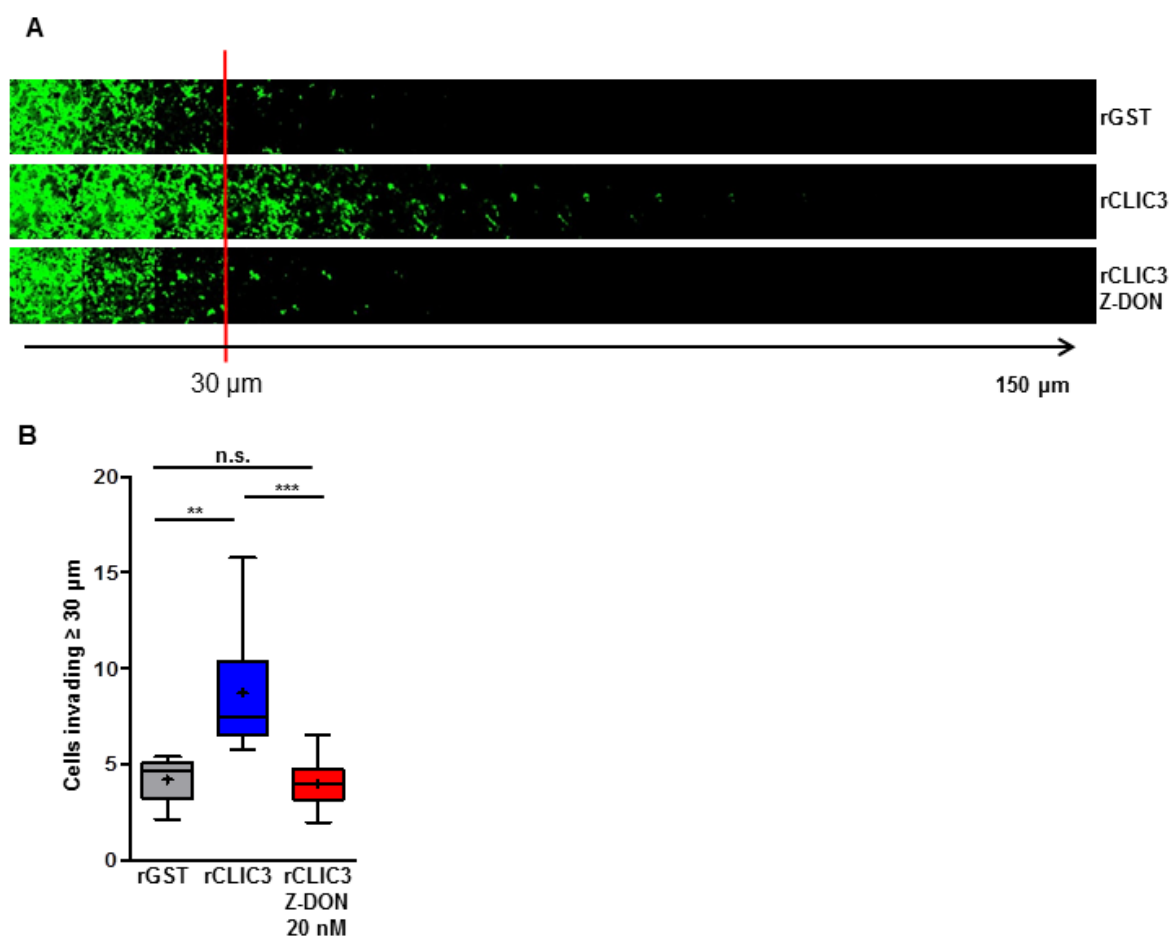


**Figure 4.8: The TG2 small molecule inhibitor Z-DON opposes rCLIC3-driven invasiveness.**

(A) A2780 cells were allowed to invade into fibronectin-supplemented Matrigel plugs. Cells were stained with calcein acetoxymethyl ester and visualised by confocal microscopy. Serial optical slices were captured at 10  $\mu\text{m}$  intervals. They are presented as a sequence in which the individual optical sections are placed alongside one another with increasing depth from left to right as indicated. The invasion behaviour was measured by quantification of the fluorescence intensity of cells penetrating the Matrigel to a depth of 30  $\mu\text{m}$  and above. Recombinant proteins and the inhibitor were present in the Matrigel plug as well as in the medium. (B) The proportion of cells that invaded to point of 30  $\mu\text{m}$  or above was determined. The addition of rCLIC3 increased invasion by comparison with the rGST control (rGST). The TG2 inhibitor Z-DON reduced rCLIC3-dependant invasion. Values are mean  $\pm$  s.e.m,  $n=4$ , \*\*\* $p<0.001$ , \*\* $p<0.01$  Kruskal-Wallis test with a Dunns post-test. The data are represented as box and Whisker 5 – 95 % plots (the median are shown with lines and the mean as a cross).

## Chapter 4

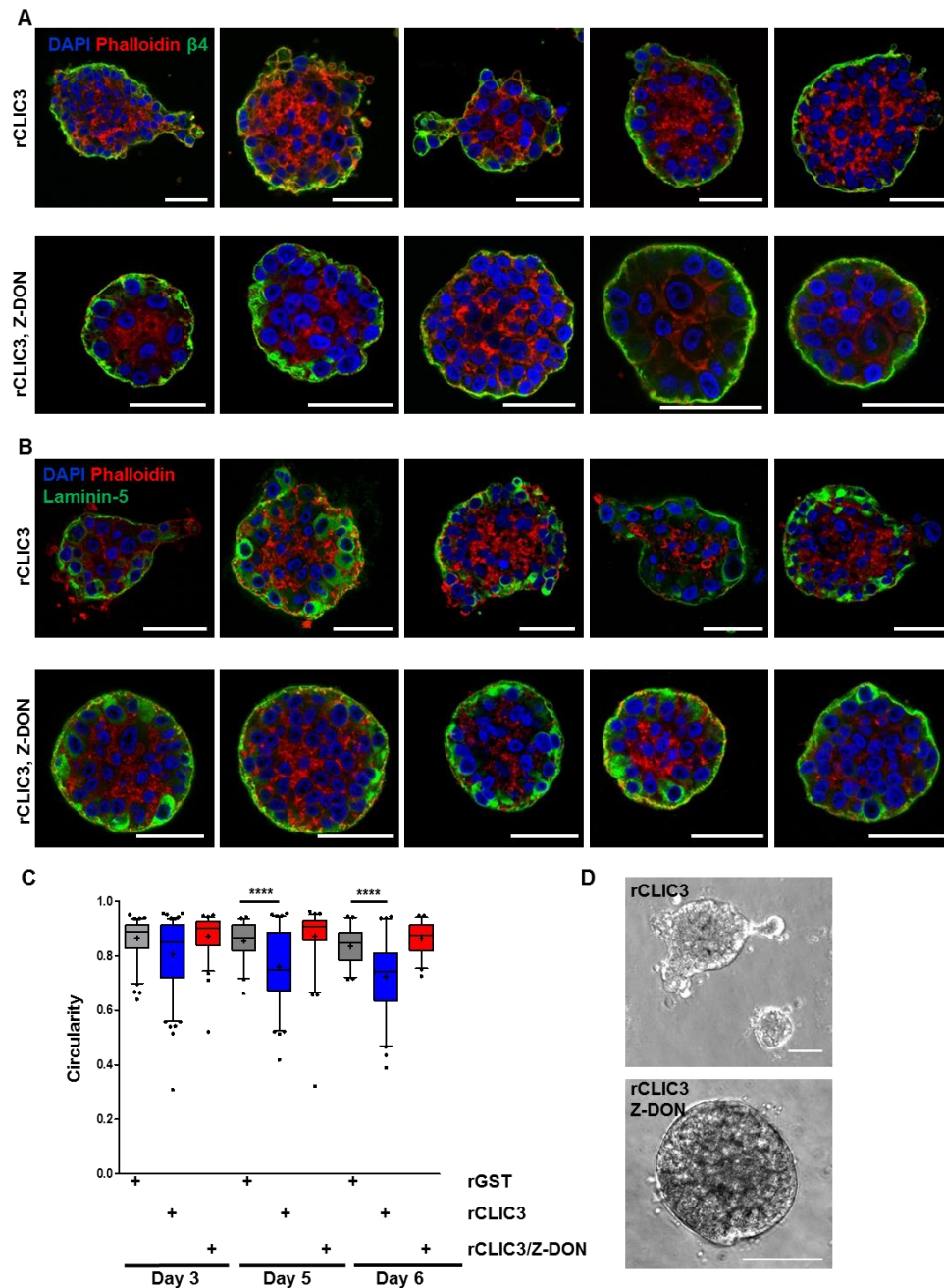


**Figure 4.9: CLIC3-promotes disruption of the basement membrane and this is reversed by Z-DON.**

MCF10DCIS.com cells were plated on a thin layer of Matrigel in the presence of rCLIC3 or rCLIC3 (25 ng/ml) and Z-DON (20  $\mu$ M). These cultures were cultured for 6 days. The cells were then fixed in 2% PFA followed by immunofluorescence staining. The basolateral membrane was visualised using  $\beta 4$  integrin (A, green) and the basement membrane, acini were stained for Laminin-5 (B, green). The cytoskeleton was visualised with Phalloidin-Alexa-Fluor-546 (red) and the nuclei were visualised with DAPI (blue), Scale bar: 50  $\mu$ m. MCF10DCIS.com cells were plated on a thin layer of Matrigel and phase-contrast images were taken from day 3 until day 6. Individual acini were outlined and circularity determined using ImageJ with a value of 1 representing perfect circularity. (C, D) Values are mean  $\pm$  s.e.m,  $n = 3$ , \*\*\* $p < 0.001$ , \*\* $p < 0.01$ , Mann-Whitney test. The data are represented as box and Whisker 5 – 95 % plots (the median are shown with lines and the mean as a plus). (GST day 3  $n = 228$ , CLIC3 day 3  $n = 267$ , CLIC3 Z-DON day 3  $n = 177$ , GST day 5  $n = 141$ , CLIC3 day 5  $n = 180$ , CLIC3 Z-DON day 5  $n = 145$ , GST day 6  $n = 123$ , CLIC3 day 6  $n = 137$ , CLIC3 Z-DON day 6  $n = 129$ ). Phase contrast images were taken every day from day 3 onwards. (D) Representative Phase contrast image of a formed acinus after 6 days in the presence of rCLIC3 (25 ng/ml) and the TG2 inhibitor Z-DON (20 nM), Scale bar: 50  $\mu$ m.

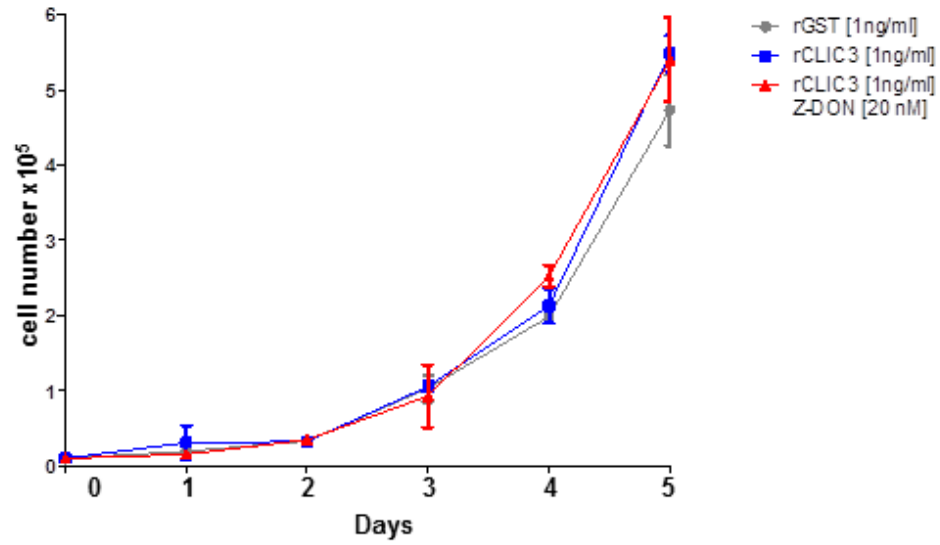


**Figure 4.10: rCLIC3 and Z-DON do not alter the proliferation rate of MCF10DCIS.com cells**  
MCF10DCIS.com were plated at 10,000 cells per well. They were allowed to attach to plastic dishes and the rGST (1 ng/ml) or rCLIC3 (1 ng/ml) in the presence and absence of Z-DON (20 nM) were added. The cells were counted using a CASY® counter at 24 hr intervals following plating, and the treatments were refreshed every two days. Values are mean  $\pm$  s.e.m, n = 2, n.s., Mann-Whitney test.

### 4.3 Discussion

In the first chapter I identified that extracellular CLIC3 drove cancer cell migration and invasion. This chapter has dealt with the role that the multifunctional enzyme TG2 plays in CLIC3's ability to evoke invasive responses from cancer cells. Indeed, my data indicate that expression of TG2 in the ECM producing cells is key to the ability of extracellular CLIC3 to drive invasive responses from tumour cells within that ECM microenvironment. Moreover, I have shown that the pool of TG2 that enables CLIC3 to perform its pro-invasive role is extracellular. Taken together with data indicating that CLIC3 and TG2 interact in a way that depends on the redox environment, these data suggest that CLIC3 may achieve its pro-invasive functions by acting as a redox enzyme to activate TG2.

CLIC proteins were initially described as chloride channels, however, their functions have been extended to act as molecular scaffolds (Littler, Brown et al. 2010). In addition, it becomes more apparent that CLIC proteins function as oxidoreductases. Al Khamici and colleagues have demonstrated that CLIC1, -2 and -4 have glutaredoxin-like activity, with a cysteine in the GST-fold acting as a key catalytic residue (Al Khamici, Brown et al. 2015). Furthermore, compounds such as IAA-94 and A9C, which have been previously considered to be inhibitors of the chloride channel ion conductance activity, have been shown to directly inhibit the oxidoreductase activity of CLICs. I found that CLIC3's putative active site cysteine 22 is necessary for all of its TG2-dependent extracellular functions. Furthermore, there is a requirement for glutathione in CLIC3's ability to influence the binding of TG2 to GTP and to CLIC itself. This supports the view that the pro-invasive capabilities of secreted CLIC3 are associated with its glutathione-dependent oxidoreductase characteristics.

Reactions catalysed by glutaredoxin-like enzymes depend on the redox context of the environment. In the strongly reducing environment of the cytosol, high glutathione concentration (0.5-10 mM) can compromise protein activity by glutathionylation, and CLICs may de-glutathionylate these cysteine residues to restore protein activity (Al Khamici et al., 2015). However, outside the cell, where glutathione concentrations are much lower ( $\mu\text{M}$  range), CLICs would not

need to function as de-glutathionylating enzymes. Certain extracellular enzymes possess cysteine residues which control their activity, and reduction of oxidized cysteines in extracellular proteins is known to be performed by thioredoxins which use FADH as a source of reducing equivalents. Like thioredoxins, glutathione transferases catalyse reduction of cysteine using glutathione as a source of reducing equivalents. We propose that CLIC3 acts in this way to activate extracellular TG2. Although TG2's most well-characterized role outside the cell is to act as a  $\text{Ca}^{2+}$ -dependent transglutaminase, TG2 is a multifunctional protein which can bind directly to integrins to influence their signalling (Akimov, Krylov et al. 2000; Wang, He et al. 2012). Our polarized fluorescence experiments indicate that CLIC3 is clearly capable of altering TG2 association with its ligands, such as GTP. Thus, in addition to acting via TG2's  $\gamma$ -glutamyl cross-linking activity to drive ECM stiffness, CLIC3 may influence its capacity to bind to integrins, which may contribute to the  $\alpha 5\beta 1$ -dependence of CLIC3 driven invasiveness of tumour cells (Figure 4.11).

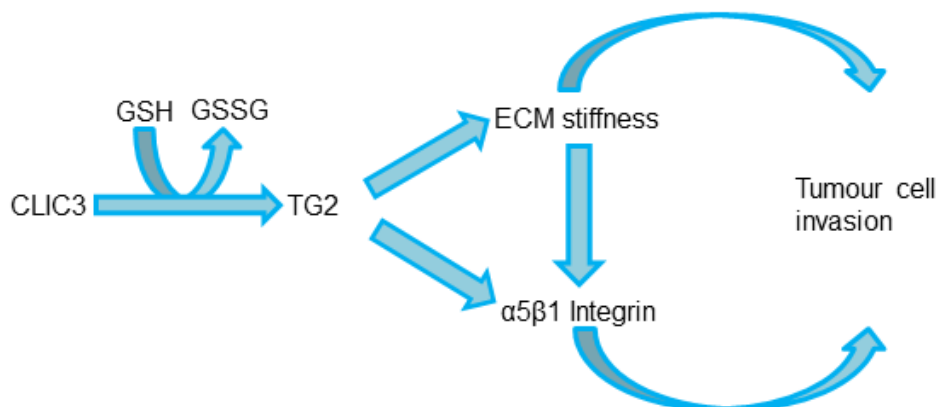


**Figure 4.11: Proposed model for CLIC3's influence on cancer. Adapted from Hernandez, Ruengeler et al., submitted.**

CLIC3 is a protein released from the tumour stroma. In the presence of GSH, CLIC3 converts GSH to GSSG, thereby interacting with TG2 and rendering it active. This reaction increases ECM stiffness and increases tumour cell migration and invasion. Furthermore, the increased ECM stiffness as well as the CLIC3 and TG2 interaction increases  $\alpha 5\beta 1$  integrin binding, thereby increasing tumour cell migration and invasion.

Experiments using Z-DON have shown that CLIC3's ability to drive invasiveness absolutely requires the enzymatic activity of TG2. Moreover, Z-DON is effective

at a concentration that, according to previous reports (Schaertl, Prime et al. 2010), would be expected to selectively target extracellular (and not intracellular) TG2. Despite the fact that A2780 cells express TG2, it is clear that the TG2 activity necessary for CLIC3-driven extension of invasive pseudopods into cell derived matrix is derived from the ECM-generating fibroblasts and not from the A2780 cells. However, in the Matrigel-based invasion assays that I have used - namely the A2780 cell inverted invasion assay and MCF10DCIS.com spheroid assay - the only cell types present are the invading tumour cells. Thus, in these assays the TG2, which is responsible for supporting CLIC3-dependent invasion, must either be secreted by the invading tumour cells (both A2780 and MCF10DCIS.com cells express TG2) or must be present in the Matrigel. The Matrigel-based invasion assays are conducted over a much longer time period than the pseudopod extension assay. Thus, if TG2 were to be slowly secreted by A2780 and MCF10DCIS.com cells, then it is possible that extracellular TG2 may accumulate over the several days during which the Matrigel assays are conducted. Conversely, CLIC3-dependent effects are visible within 4 hours of plating cells onto cell-derived matrix and, as this might be insufficient time to allow accumulation of tumour cell-secreted TG2, then CLIC3-dependent effects would rely on the TG2 present in the fibroblast-derived ECM. Nevertheless, using a range of approaches our study has shown a requirement for a source of extracellular TG2 in CLIC3-driven invasiveness. TG2 is known to be associated with metastasis of a number of cancer types (Erdem, Yegen et al. 2014; Han, Kumar et al. 2014; Kumar, Hu et al. 2014; Kumar, Donti et al. 2014). Thus our data indicate the possibility that targeting the redox-dependent interaction of CLIC3 with TG2 might represent a potential avenue for anti-metastatic therapy.

## 5 General Discussion

### 5.1 Summary

In this thesis, I have shown that CLIC3 is secreted from CAFs as well as from MDA-MB-231 breast cancer cells. CLIC3 has previously been shown to be localised to late endosomal compartments (Dozynkiewicz, Jamieson et al. 2012). I then explored the possible involvement of a mechanism for unconventional secretion, which involves late endosome/multivesicular body (MVB) exocytosis as an export mechanism (Malhotra 2013). However, CLIC3 release is not dependent on Rab GTPases, such as Rab27a/b, which control MVB exocytosis. Therefore, most probably CLIC3 is released via a non-exocytic route. Furthermore, I explored the functions of extracellular CLIC3. I was able to show that it increases  $\alpha 5 \beta 1$  integrin-dependent extension of pseudopods that invade into preparations of the ECM, and induces tumour cell invasion into Matrigel. Extracellular CLIC3 was also able to disrupt the comedo-like non-invasive structures formed by MCF10DCIS.com cells, and to drive the cells to a more invasive phenotype. Moreover, I have shown that extracellular CLIC3 relies on an extracellular source of TG2 in order to drive the invasive processes described above. Because, CLIC3's ability to drive these TG2-dependent invasive processes requires 'active site' cysteine residues in CLIC3' thioredoxin fold, I propose that the role of extracellular CLIC3 acts via a redox mechanism to influence TG2 function to promote integrin-dependent invasion.

### 5.2 The function of extracellular CLIC3 in the tumour stroma

Cancer research is nowadays not only looking at the cancer cells and their genetic and epigenetic changes, but at tumours as a multicellular milieu. The tumour stroma is known to drive tumour cell invasion and angiogenesis (De Wever and Mareel 2003). It comprises several different cell types, such as pericytes, endothelial cells, immune inflammatory cells, cancer cells as well as cancer associated fibroblasts (CAFs) (Ronnov-Jessen, Petersen et al. 1996; De Wever and Mareel 2003). Additionally, the ECM components, which make up the scaffold of the tumour microenvironment, comprise a variety of proteins, such

as for example collagen. Many of the factors secreted by CAFs, including ECM components, render cancer cells more prone to undergo EMT and establish metastasis at different sites (Orimo, Gupta et al. 2005). Therefore, it seemed important to examine these cells in more detail. One possibility was to remove the CAFs from the stroma, thus lessening the secretion of the ECM as well as tumour growth and metastasis at distant sites, due to inherent reduction of stiffness. However, when Özdemir and colleagues removed CAFs from mice in a pancreatic cancer model, the survival was significantly reduced (Ozdemir, Pentcheva-Hoang et al. 2014). Due to removing the CAFs, the ECM was profoundly altered - indeed the collagen I content and stiffness was considerably reduced. Therefore, this study led researchers to look at single secreted factors from CAFs, as well as proteins that CAFs overexpress compared to normal fibroblasts in the healthy ECM. Özdemir and colleagues moreover found that LOX was still expressed, despite the lack of CAFs (which were previously assumed to be the major source of tumour LOX) (Ozdemir, Pentcheva-Hoang et al. 2014). LOX is an extracellular amine oxidase, primarily shown to be important in posttranslationally modifying collagens and elastin in the ECM to catalyse covalent cross-linking, and LOX is involved in tumour progression (Kagan and Li 2003; Butcher, Alliston et al. 2009). Furthermore, it was shown that lysyl oxidase was expressed in the tumour stroma, leading to increased collagen crosslinking. This was shown to enhance breast cancer metastasis (Cox, Bird et al. 2013). Additionally, it was shown by Cox and colleagues that LOX is a secreted factor in hypoxic ER-negative breast cancer cells (Cox, Rumney et al. 2015). Therefore, it is important to identify single proteins that increase primary tumour cell growth and metastatic formation. Using a proteomic screen, which was designed to provide a quantitative comparison between breast cancer CAFs and normal fibroblasts, we have identified CLIC3 as being expressed at high levels and secreted from CAFs (Figure 5.1). I then proceeded to show that CLIC3 expression in CAFs leads to an increased amount of fibrillar collagen I in organotypic matrices and found that this corresponds to increased invasion of PDAC cells into these matrices.

I further established that extracellular CLIC3 drives tumour cell migration and invasion and that this process is  $\alpha 5\beta 1$  integrin dependent (Figure 5.2). Our study is in line with the current literature as, for example, Levental and colleagues have described that integrins are important in responding to microenvironmental

stiffness (Levental, Yu et al. 2009). They have shown that ECM stiffening drives the formation of focal adhesions and increased PI3 kinase signalling which enhances tumour invasion. The next step was to determine how CLIC3 could modify the ECM as well as drive tumour cell migration and invasion.

### **5.3 Secreted CLIC3 regulates ECM remodelling via TG2 to generate a pro-invasive stroma**

I have shown that extracellular CLIC3 requires the activity of TG2 in order to drive tumour cell invasion. Moreover, our data indicate that the pool of TG2 that is required for extracellular CLIC3 to function is also outside the cell. Indeed, not only does a TG2 inhibitor oppose CLIC3-driven invasion when added at a concentration that would not be expected to inhibit intracellular TG2, but experiments in which rTG2 is added to the extracellular milieu clearly show that TG2 acts from outside the tumour cells to support CLIC3's pro-invasive capabilities. TG2 is well-established to act both within and outside the cell. In the high free  $\text{Ca}^{2+}$  concentrations that are found outside the cell, TG2 acts primarily as transglutaminase which is involved with ECM remodelling. However, intracellular TG2 functions as a G-protein (Lorand and Graham 2003), as an ATPase, as a protein kinase (Mishra and Murphy 2004; Mishra, Saleh et al. 2006) or as a transcriptional regulator. An average GTP/calcium ratio in the cell (~150  $\mu\text{M}$ /~100 nM) is thought to ensure that cytosolic TG2 will be in the GTP-bound state, thus maintaining intracellular TG2's transamidase activity at relatively low levels. A GTP-binding defective short isoform of TG2 induced neuroblastoma cell differentiation, but a long isoform inhibited this process (Tee, Marshall et al. 2010). As TG2 inhibitors are able to inhibit neuroblastoma differentiation induced by the short form of TG2, this suggests that differentiation is induced by TG2's transamidating activity (Tee, Marshall et al. 2010). Therefore, to keep the intracellular GTPase function is quite important to reduce neuroblastoma formation. Furthermore, TG2 acts as a regulator of transcription. When stressors, such as intracellular calcium levels rise or hypoxic conditions are present within the cell, TG2 is translocated to the nucleus and controls the transcriptional program. Furthermore, the crosslinking activity of TG2 is calcium dependent as mentioned.  $\text{Ca}^{2+}$  concentrations are generally quite low in the cytosol. Therefore, intracellularly it is not so likely that TG2 will act as a

transglutaminase. However, outside of the cell the calcium concentration is higher and this causes TG2 bound GTP to dissociate and an increased TG2 activity.

TG2 has not only a transamidase activity but it also binds to integrins, which are transmembrane adhesion and signalling receptors that regulate a variety of intracellular signalling processes. Integrins are activated by binding to ECM proteins (Hynes 2002). As described before, TG2 can interact with the ECM, enhancing cell adhesion and integrin-mediated signalling via interaction with  $\beta 1$ ,  $\beta 3$  and  $\beta 5$  integrins (Zemskov, Janiak et al. 2006; Belkin 2011). Additionally, in cancer cells and during metastasis TG2 has been shown to enhance the affinity of certain integrins for fibronectin, which increases cell attachment to the matrix and in turn activates integrin signalling (Satpathy, Cao et al. 2007; Belkin 2011; Piercy-Kotb, Mousa et al. 2012). TG2-induced integrin clustering increases integrin-dependent signalling, such as the activation of FAK, Src and increased levels of GTP-bound RhoA and its downstream target ROCK. The outcome of this can be actin stress fibre formation, which leads to enhanced actomyosin contractility promoting further ECM remodelling (Toth, Garabuczi et al. 2009; Torocsik, Szeles et al. 2010).

This ultimately leads to two possible mechanisms through which CLIC3 may affect TG2, and thereby influence ECM stiffness, cancer cell migration and invasion. One possibility is that CLIC3 might activate TG2's enzymatic activity via a thioredoxin-like mechanism, which leads to increased ECM stiffness followed by integrin activation and signalling. This signalling mechanism in turn could drive pseudopod extension (Figure 5.2 A). TG2 is able to crosslink the  $\gamma$ -carboxamide of the glutamine with the  $\epsilon$ -amino group of the lysine in a calcium dependent mechanism (Fox, Yee et al. 1999). In our studies TG2 drives ovarian carcinoma cell invasion and tumour cell migration. This is probably due to its cross-linking activity as the presence of TG2 drives an increase in the levels of fibrillar collagen in CAF preconditioned matrices. Increased fibrillar collagen would be expected to promote a stiffer microenvironment, which could drive tumour cell invasion. Another possibility is that CLIC3 influences TG2's ability to activate integrins more directly and this then influences matrix deposition and stiffness (Figure 5.2 B).

The mechanism I explored could potentially be used in cancer therapy. CLIC3 and TG2 are upregulated in cancer - TG2 has been shown to be upregulated in several cancers such as pancreatic adenocarcinoma (Verma, Wang et al. 2006), breast carcinoma (Mehta, Fok et al. 2004) and ovarian carcinoma (Satpathy, Cao et al. 2007; Hwang, Mangala et al. 2008). Moreover, CLIC3 upregulation has been shown to lead to a poorer survival in pancreatic and ovarian adenocarcinoma patients (Dozynkiewicz, Jamieson et al. 2012). Furthermore, some studies suggest TG2 may represent an excellent drug target (Szende, Schally et al. 1991), as TG2 has been identified as a negative prognostic marker and has been linked to evasion of apoptosis and drug resistance. This, however, depends on the context, because chemotherapeutic agents have different effects on TG2 and tumours in different tissues (Benedetti, Grignani et al. 1996; Antonyak, McNeill et al. 2003; el-Metwally, Hussein et al. 2005; Joshi, Guleria et al. 2006). Therefore, targeting TG2 alone may evoke both positive and inhibitory effects on tumour growth (Monteagudo, et al., 2015). However, pharmacologically targeting the enzymatic activity of CLIC3 might be a better possibility as it is upstream of TG2 and is only upregulated in cancer tissue and the surrounding tumour stroma.

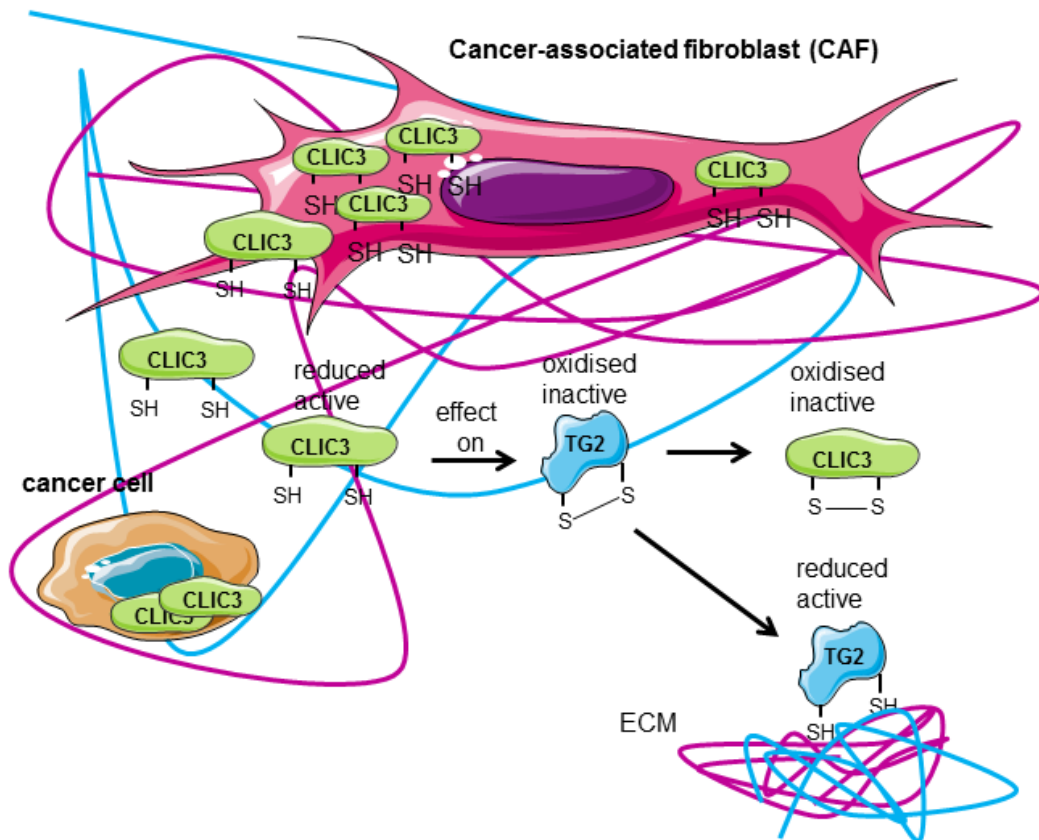


**Figure 5.1: CLIC3 is a secreted factor from cancer-associated fibroblasts and has the potential to activate TG2.**

CLIC3 is secreted from CAFs in the reduced form. It then acts on TG2 to convert the protein from the oxidised (inactive) to the reduced (active) form. In this case TG2 is mostly ECM associated.

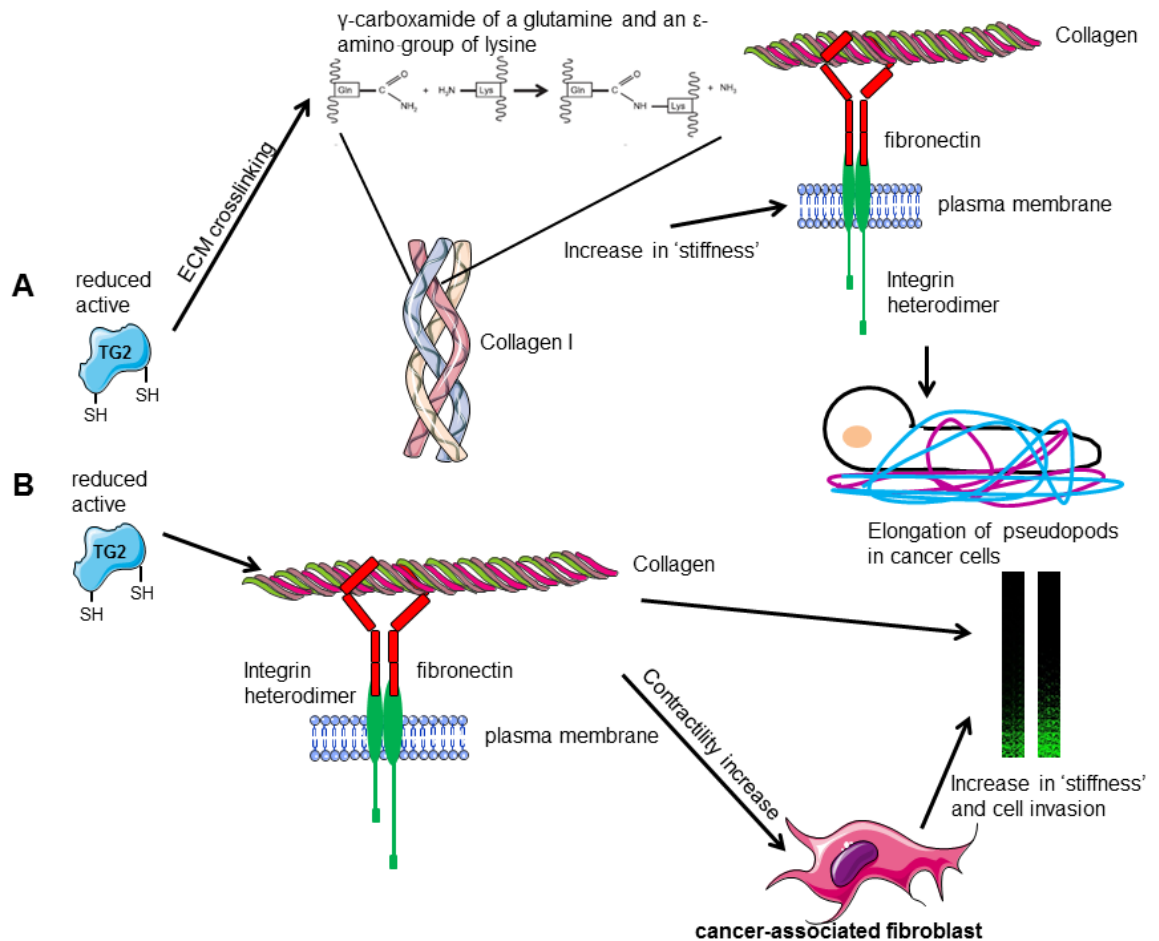


**Figure 5.2: CLIC3 interacts with TG2 and drives invasion via two possible mechanisms.**

(A) TG2 activated by CLIC3 crosslinks glutamine residues in adjacent collagen strands. This leads to an increase in ECM stiffness. Moreover, the affinity to integrins further increases stiffness and leads to elongation of pseudopods in tumour cells. (B) Following activation by CLIC3, TG2 binds to integrins and this leads to activation of integrin signalling, which increases the contractility of the CAFs. This then leads to an increase in ECM stiffness and cell invasion.

## Future Directions

In this thesis, I have determined several characteristics of secreted CLIC3. I have also determined that CLIC3 has, under reducing conditions, the possibility to interact with TG2 and to lead to TG2 dependent ECM remodelling and tumour cell invasion. Despite evidence that these TG2-dependent functions of CLIC3 are sensitive to the redox environment and require CLIC3's 'active site' cysteines (which suggests a role for CLIC3's oxidoreductase activity), further studies are needed to identify and understand the mechanistic details of the interplay between extracellular CLIC3 and TG2. For instance, the possibility that CLIC3 affects proteins other than TG2 to drive tumour cell invasion must be

considered. Furthermore, the unconventional mechanism through which CLIC3 is secreted from CAFs needs to be identified and characterised.

Evidence presented in this thesis suggests that CLIC3 is able to activate TG2 via a redox mechanism. I hypothesise that an intramolecular disulphide bond in CLIC3 is reduced by GSH and this reduced CLIC3 is able, in turn to reduce TG2's disulphide bonds, rendering TG2 in an active conformation. However, this working hypothesis needs further testing in order to be properly ratified. In particular, it is necessary to use enzyme-based assays to formally demonstrate that CLIC3 possesses oxidoreductase activity and that it is capable of activating the enzymatic activity or the integrin-binding capacity of TG2.

This project has been conducted using cell lines and *in vitro* and *ex vivo* assays that report on ECM remodelling and various aspects of tumour cell invasiveness. To fully establish the importance of extracellular CLIC3 to tumour progression, it is necessary to address this question using *in vivo* models of cancer and tissue from human subjects. Preliminary experiments have been conducted to explore the role of extracellular CLIC3 *in vivo*. In one experiment MCF10DCIS.com cells were mixed with Matrigel in the presence and absence of rCLIC3 and injected subcutaneously into the flanks of nude mice. The tumours were harvested after two weeks and examined histologically. In the absence of rCLIC3 the MCF10DCIS.com cells had grown to form tumours that displayed a non-invasive comedo-like morphology that were bounded by a basement membrane and a layer of smooth muscle actin-positive myoepithelial cells. By contrast, when MCF10SDCIS.com cells were mixed with Matrigel that was impregnated with rCLIC3 prior to implantation, these cells grew to form tumours that have an extensively disrupted basement membrane and myoepithelial layer. Furthermore, as mentioned previously, extracellular CLIC3 is able to promote the ability of endothelial cells to form tubules in 3D cultures. We, therefore, used an *in vivo* approach to examine the pro-angiogenic capabilities of extracellular CLIC3. Endothelial cells mixed with Matrigel plugs and implanted subcutaneously into mice in the presence and absence of rCLIC3. This experiment indicated that the ability of the endothelial cells to form functional

blood vessels was significantly enhanced when they were co-injected with Matrigel that had been impregnated with soluble rCLIC3, whereas CLIC3<sup>C22A</sup> was ineffective in this regard. Moreover, the ability of rCLIC3 to promote angiogenesis was opposed by addition of Z-DON, indicating that the ability for extracellular CLIC3 to drive angiogenesis *in vivo* is TG2 dependent - as it is *in vitro*. To use a more controlled system, we are generating a CLIC3 knockout mouse. A CLIC3<sup>-/-</sup> mouse has previously been generated by Kim and colleagues (Kim, Choi et al. 2013). They reported that these mice are viable, but were more susceptible to *Listeria monocytogenes* (LM) infections. Additionally, they have shown that chloride influx and the consequent acidification of endocytic vacuoles containing LM were inhibited in CLIC3<sup>-/-</sup> bone marrow-derived macrophages (Kim, Choi et al. 2013). However, they did not thoroughly characterise the mouse and also do not explore the cancer-associated aspects of CLIC3. Another CLIC3 knock-out mouse was generated at the Beatson Institute. LoxP sites are present before exon 2 and after the exon (CLIC3 has 6 exons) of CLIC3 were present. Once Cre-recombinase was added the gene between the loxP sites was excised and CLIC3 protein expression abolished. So far the mice were crossed to a whole body Cre-recombinase, excising CLIC3 from the genome and abolishing its expression throughout the whole organism. According, to the mentioned paper by Kim and colleagues the mouse should be viable. However, no homozygous offspring has been born thus far - indicating the possibility that CLIC3 knockout may be lethal. Other CLIC knockout mice have been generated previously and all of them were reported to be viable. So far knockout mice of CLIC1 (Chalothorn, Zhang et al. 2009; Qiu, Jiang et al. 2010), CLIC4 (Gagnon, Longo-Guess et al. 2006; Chalothorn, Zhang et al. 2009; Ulmasov, Bruno et al. 2009) and CLIC5 (Gagnon, Longo-Guess et al. 2006; Bradford, Miller et al. 2010) have been generated. However, it seems that the redundancy of the six CLIC proteins is an important aspect overshadowing the experiments in mice. This could be due to the similar structure of the CLIC proteins and thus they can take over functions from the other proteins. Therefore, a more valuable approach would be to cross this mouse with a cancer model known to be associated with CLIC3 overexpression and a tissue specific Cre-recombinase. One valuable cancer model might be breast cancer as it was shown that CLIC3 is highly expressed in breast cancer (Macpherson, Rainero et al. 2014). In this case a possibility would be to use the MMTV-PyMT model. In this mouse the expression of polyoma

middle T antigen (PyMT) is under the control of the Mouse Mammary Tumour Virus promoter (MMTV, driver for oncogene expression). This leads to breast tumours, which metastasise into the lung and lymph nodes (Guy, Cardiff et al. 1992). Additionally, it might be valuable to further evaluate the function of CLIC3 in pancreatic cancer as it was shown to be not expressed in normal tissue but in human pancreatic ductal adenocarcinoma (Dozynkiewicz, Jamieson et al. 2012). Therefore, one possibility would be to cross the CLIC3 knock-out mouse to a *Trp53*<sup>R172H/+</sup>, *KRas*<sup>G12D/+</sup>, *Pdx1-Cre* model of pancreatic adenocarcinoma (Olive, Tuveson et al. 2004; Hingorani, Wang et al. 2005).

To conclude, I have shown that CLIC3, a protein thought previously to be an intracellular protein, which controls the trafficking of integrins and other receptors, is released from stromal fibroblasts. This secreted pool of CLIC3 is able to drive a range of cancer relevant invasive processes and I have shown that it required TG2 activity in order to do so. Further experimentation using *in vivo* and other models will determine the degree to which CLIC3 is secreted by stromal and tumour cells *in vivo* and the relevance that this process has to the progression of cancer in humans.

## Bibliography

- Achilonu, I., S. Fanucchi, et al. (2012). "Role of Individual Histidines in the pH-Dependent Global Stability of Human Chloride Intracellular Channel 1." Biochemistry **51**(5): 995-1004.
- Achyuthan, K. E. and C. S. Greenberg (1987). "Identification of a guanosine triphosphate-binding site on guinea pig liver transglutaminase. Role of GTP and calcium ions in modulating activity." The Journal of biological chemistry **262**(4): 1901-1906.
- Adams, J. M. and S. Cory (2007). "The Bcl-2 apoptotic switch in cancer development and therapy." Oncogene **26**(9): 1324-1337.
- Aeschlimann, D. and M. Paulsson (1994). "Transglutaminases: protein cross-linking enzymes in tissues and body fluids." Thrombosis and haemostasis **71**(4): 402-415.
- Aeschlimann, D. and V. Thomazy (2000). "Protein crosslinking in assembly and remodelling of extracellular matrices: the role of transglutaminases." Connective tissue research **41**(1): 1-27.
- Agnihotri, N., S. Kumar, et al. (2013). "Tissue transglutaminase as a central mediator in inflammation-induced progression of breast cancer." Breast cancer research : BCR **15**(1): 202.
- Ahvazi, B., K. M. Boeshans, et al. (2003). "Roles of calcium ions in the activation and activity of the transglutaminase 3 enzyme." The Journal of biological chemistry **278**(26): 23834-23841.
- Ahvazi, B., K. M. Boeshans, et al. (2004). "Structural basis for the coordinated regulation of transglutaminase 3 by guanine nucleotides and calcium/magnesium." The Journal of biological chemistry **279**(8): 7180-7192.
- Akimov, S. S. and A. M. Belkin (2001). "Cell-surface transglutaminase promotes fibronectin assembly via interaction with the gelatin-binding domain of fibronectin: a role in TGFbeta-dependent matrix deposition." Journal of cell science **114**(Pt 16): 2989-3000.
- Akimov, S. S. and A. M. Belkin (2001). "Cell surface tissue transglutaminase is involved in adhesion and migration of monocytic cells on fibronectin." Blood **98**(5): 1567-1576.
- Akimov, S. S., D. Krylov, et al. (2000). "Tissue transglutaminase is an integrin-binding adhesion coreceptor for fibronectin." The Journal of cell biology **148**(4): 825-838.
- Al Khamici, H., L. J. Brown, et al. (2015). "Members of the chloride intracellular ion channel protein family demonstrate glutaredoxin-like enzymatic activity." PloS one **10**(1): e115699.
- Alonso, S. R., L. Tracey, et al. (2007). "A high-throughput study in melanoma identifies epithelial-mesenchymal transition as a major determinant of metastasis." Cancer research **67**(7): 3450-3460.
- Antonyak, M. A., C. J. McNeill, et al. (2003). "Activation of the Ras-ERK pathway inhibits retinoic acid-induced stimulation of tissue transglutaminase expression in NIH3T3 cells." The Journal of biological chemistry **278**(18): 15859-15866.
- Antonyak, M. A., A. M. Miller, et al. (2004). "Augmentation of tissue transglutaminase expression and activation by epidermal growth factor inhibit doxorubicin-induced apoptosis in human breast cancer cells." The Journal of biological chemistry **279**(40): 41461-41467.

- Apte, M. V. and J. S. Wilson (2012). "Dangerous liaisons: pancreatic stellate cells and pancreatic cancer cells." Journal of gastroenterology and hepatology **27 Suppl 2**: 69-74.
- Assi, J., G. Srivastava, et al. (2013). "Transglutaminase 2 overexpression in tumor stroma identifies invasive ductal carcinomas of breast at high risk of recurrence." PloS one **8(9)**: e74437.
- Bae, S. M., Y. W. Kim, et al. (2004). "Expression profiling of the cellular processes in uterine leiomyomas: omic approaches and IGF-2 association with leiomyosarcomas." Cancer research and treatment : official journal of Korean Cancer Association **36(1)**: 31-42.
- Baker, A. M., D. Bird, et al. (2013). "Lysyl oxidase plays a critical role in endothelial cell stimulation to drive tumor angiogenesis." Cancer research **73(2)**: 583-594.
- Barker, H. E., J. Chang, et al. (2011). "LOXL2-mediated matrix remodeling in metastasis and mammary gland involution." Cancer research **71(5)**: 1561-1572.
- Barrallo-Gimeno, A. and M. A. Nieto (2005). "The Snail genes as inducers of cell movement and survival: implications in development and cancer." Development **132(14)**: 3151-3161.
- Barsky, S. H. and N. J. Karlin (2005). "Myoepithelial cells: autocrine and paracrine suppressors of breast cancer progression." Journal of mammary gland biology and neoplasia **10(3)**: 249-260.
- Bass, M. D., K. A. Roach, et al. (2007). "Syndecan-4-dependent Rac1 regulation determines directional migration in response to the extracellular matrix." The Journal of cell biology **177(3)**: 527-538.
- Begg, G. E., L. Carrington, et al. (2006). "Mechanism of allosteric regulation of transglutaminase 2 by GTP." Proceedings of the National Academy of Sciences of the United States of America **103(52)**: 19683-19688.
- Behbod, F., F. S. Kittrell, et al. (2009). "An intraductal human-in-mouse transplantation model mimics the subtypes of ductal carcinoma in situ." Breast cancer research : BCR **11(5)**: R66.
- Belkin, A. M. (2011). "Extracellular TG2: emerging functions and regulation." The FEBS journal **278(24)**: 4704-4716.
- Belkin, A. M., G. Tsurupa, et al. (2005). "Transglutaminase-mediated oligomerization of the fibrin(ogen) alphaC domains promotes integrin-dependent cell adhesion and signaling." Blood **105(9)**: 3561-3568.
- Bell, C. D. and E. Waizbard (1986). "Variability of cell size in primary and metastatic human breast carcinoma." Invasion & metastasis **6(1)**: 11-20.
- Bendtsen, J. D., L. J. Jensen, et al. (2004). "Feature-based prediction of non-classical and leaderless protein secretion." Protein engineering, design & selection : PEDS **17(4)**: 349-356.
- Bendtsen, J. D., L. Kiemer, et al. (2005). "Non-classical protein secretion in bacteria." BMC microbiology **5**: 58.
- Benedetti, L., F. Grignani, et al. (1996). "Retinoid-induced differentiation of acute promyelocytic leukemia involves PML-RARalpha-mediated increase of type II transglutaminase." Blood **87(5)**: 1939-1950.
- Berry, K. L., H. E. Bulow, et al. (2003). "A C. elegans CLIC-like protein required for intracellular tube formation and maintenance." Science **302(5653)**: 2134-2137.
- Berry, K. L. and O. Hobert (2006). "Mapping functional domains of chloride intracellular channel (CLIC) proteins in vivo." Journal of molecular biology **359(5)**: 1316-1333.

- Berryman, M. and A. Bretscher (2000). "Identification of a novel member of the chloride intracellular channel gene family (CLIC5) that associates with the actin cytoskeleton of placental microvilli." Molecular biology of the cell **11**(5): 1509-1521.
- Berryman, M., J. Bruno, et al. (2004). "CLIC-5A functions as a chloride channel in vitro and associates with the cortical actin cytoskeleton in vitro and in vivo." The Journal of biological chemistry **279**(33): 34794-34801.
- Bershadsky, A., M. Kozlov, et al. (2006). "Adhesion-mediated mechanosensitivity: a time to experiment, and a time to theorize." Current opinion in cell biology **18**(5): 472-481.
- Berx, G. and F. van Roy (2009). "Involvement of members of the cadherin superfamily in cancer." Cold Spring Harbor perspectives in biology **1**(6): a003129.
- Bissell, M. J. and D. Radisky (2001). "Putting tumours in context." Nature reviews. Cancer **1**(1): 46-54.
- Blaser, H., M. Reichman-Fried, et al. (2006). "Migration of zebrafish primordial germ cells: a role for myosin contraction and cytoplasmic flow." Developmental cell **11**(5): 613-627.
- Board, P. G., M. Coggan, et al. (2000). "Identification, characterization, and crystal structure of the Omega class glutathione transferases." The Journal of biological chemistry **275**(32): 24798-24806.
- Board, P. G., M. Coggan, et al. (2004). "CLIC-2 modulates cardiac ryanodine receptor Ca<sup>2+</sup> release channels." The international journal of biochemistry & cell biology **36**(8): 1599-1612.
- Booth, J., E. Boyland, et al. (1961). "An enzyme from rat liver catalysing conjugations with glutathione." The Biochemical journal **79**(3): 516-524.
- Boros, S., E. Ahrman, et al. (2006). "Site-specific transamidation and deamidation of the small heat-shock protein Hsp20 by tissue transglutaminase." Proteins **62**(4): 1044-1052.
- Bosman, F. T. and I. Stamenkovic (2003). "Functional structure and composition of the extracellular matrix." The Journal of pathology **200**(4): 423-428.
- Bradford, E. M., M. L. Miller, et al. (2010). "CLIC5 mutant mice are resistant to diet-induced obesity and exhibit gastric hemorrhaging and increased susceptibility to torpor." American journal of physiology. Regulatory, integrative and comparative physiology **298**(6): R1531-1542.
- Bronisz, A., J. Godlewski, et al. (2012). "Reprogramming of the tumour microenvironment by stromal PTEN-regulated miR-320." Nature cell biology **14**(2): 159-167.
- Bryan, P. N. and J. Orban (2010). "Proteins that switch folds." Current opinion in structural biology **20**(4): 482-488.
- Burkhardt, D. L. and J. Sage (2008). "Cellular mechanisms of tumour suppression by the retinoblastoma gene." Nature reviews. Cancer **8**(9): 671-682.
- Butcher, D. T., T. Alliston, et al. (2009). "A tense situation: forcing tumour progression." Nature reviews. Cancer **9**(2): 108-122.
- Calcagno, A. M., C. D. Salcido, et al. (2010). "Prolonged drug selection of breast cancer cells and enrichment of cancer stem cell characteristics." Journal of the National Cancer Institute **102**(21): 1637-1652.
- Candi, E., S. Oddi, et al. (2002). "Expression of transglutaminase 5 in normal and pathologic human epidermis." The Journal of investigative dermatology **119**(3): 670-677.
- Candi, E., S. Oddi, et al. (2001). "Transglutaminase 5 cross-links loricrin, involucrin, and small proline-rich proteins in vitro." The Journal of biological chemistry **276**(37): 35014-35023.

- Cao, L., M. Shao, et al. (2012). "Tissue transglutaminase links TGF-beta, epithelial to mesenchymal transition and a stem cell phenotype in ovarian cancer." Oncogene **31**(20): 2521-2534.
- Carmichael, D. F., A. Sommer, et al. (1986). "Primary structure and cDNA cloning of human fibroblast collagenase inhibitor." Proceedings of the National Academy of Sciences of the United States of America **83**(8): 2407-2411.
- Cassidy, A. J., M. A. van Steensel, et al. (2005). "A homozygous missense mutation in TGM5 abolishes epidermal transglutaminase 5 activity and causes acral peeling skin syndrome." American journal of human genetics **77**(6): 909-917.
- Caswell, P. T., M. Chan, et al. (2008). "Rab-coupling protein coordinates recycling of alpha5beta1 integrin and EGFR1 to promote cell migration in 3D microenvironments." The Journal of cell biology **183**(1): 143-155.
- Caswell, P. T., H. J. Spence, et al. (2007). "Rab25 associates with alpha5beta1 integrin to promote invasive migration in 3D microenvironments." Developmental cell **13**(4): 496-510.
- Cavallaro, U. and G. Christofori (2004). "Cell adhesion and signalling by cadherins and Ig-CAMs in cancer." Nature reviews. Cancer **4**(2): 118-132.
- Chalothorn, D., H. Zhang, et al. (2009). "Chloride intracellular channel-4 is a determinant of native collateral formation in skeletal muscle and brain." Circulation research **105**(1): 89-98.
- Chang, Y. H., C. C. Wu, et al. (2009). "Cell secretome analysis using hollow fiber culture system leads to the discovery of CLIC1 protein as a novel plasma marker for nasopharyngeal carcinoma." Journal of proteome research **8**(12): 5465-5474.
- Chau, D. Y., R. J. Collighan, et al. (2005). "The cellular response to transglutaminase-cross-linked collagen." Biomaterials **26**(33): 6518-6529.
- Chen, C. D., C. S. Wang, et al. (2007). "Overexpression of CLIC1 in human gastric carcinoma and its clinicopathological significance." Proteomics **7**(1): 155-167.
- Chen, J. S. and K. Mehta (1999). "Tissue transglutaminase: an enzyme with a split personality." The international journal of biochemistry & cell biology **31**(8): 817-836.
- Cheng, K. W., J. P. Lahad, et al. (2004). "The RAB25 small GTPase determines aggressiveness of ovarian and breast cancers." Nature medicine **10**(11): 1251-1256.
- Cho, B. R., M. K. Kim, et al. (2008). "Increased tissue transglutaminase expression in human atherosclerotic coronary arteries." Coronary artery disease **19**(7): 459-468.
- Choi, C. M., S. J. Jang, et al. (2011). "Transglutaminase 2 as an independent prognostic marker for survival of patients with non-adenocarcinoma subtype of non-small cell lung cancer." Molecular cancer **10**: 119.
- Clark, R. A. (2001). "Fibrin and wound healing." Annals of the New York Academy of Sciences **936**: 355-367.
- Collen, A., R. Hanemaaijer, et al. (2003). "Membrane-type matrix metalloproteinase-mediated angiogenesis in a fibrin-collagen matrix." Blood **101**(5): 1810-1817.
- Collighan, R. J. and M. Griffin (2009). "Transglutaminase 2 cross-linking of matrix proteins: biological significance and medical applications." Amino acids **36**(4): 659-670.
- Cox, J. and M. Mann (2008). "MaxQuant enables high peptide identification rates, individualized p.p.b.-range mass accuracies and proteome-wide protein quantification." Nature biotechnology **26**(12): 1367-1372.

- Cox, T. R., D. Bird, et al. (2013). "LOX-mediated collagen crosslinking is responsible for fibrosis-enhanced metastasis." Cancer research **73**(6): 1721-1732.
- Cox, T. R., R. M. Rumney, et al. (2015). "The hypoxic cancer secretome induces pre-metastatic bone lesions through lysyl oxidase." Nature **522**(7554): 106-110.
- Cress, A. E., I. Rabinovitz, et al. (1995). "The alpha 6 beta 1 and alpha 6 beta 4 integrins in human prostate cancer progression." Cancer metastasis reviews **14**(3): 219-228.
- Cromer, B. A., M. A. Gorman, et al. (2007). "Structure of the Janus protein human CLIC2." Journal of molecular biology **374**(3): 719-731.
- Cukierman, E., R. Pankov, et al. (2001). "Taking cell-matrix adhesions to the third dimension." Science **294**(5547): 1708-1712.
- Dammer, U., O. Popescu, et al. (1995). "Binding strength between cell adhesion proteoglycans measured by atomic force microscopy." Science **267**(5201): 1173-1175.
- Datta, S., M. A. Antonyak, et al. (2007). "GTP-binding-defective forms of tissue transglutaminase trigger cell death." Biochemistry **46**(51): 14819-14829.
- De Wever, O., P. Demetter, et al. (2008). "Stromal myofibroblasts are drivers of invasive cancer growth." International journal of cancer. Journal international du cancer **123**(10): 2229-2238.
- De Wever, O. and M. Mareel (2003). "Role of tissue stroma in cancer cell invasion." The Journal of pathology **200**(4): 429-447.
- Debnath, J., S. K. Muthuswamy, et al. (2003). "Morphogenesis and oncogenesis of MCF-10A mammary epithelial acini grown in three-dimensional basement membrane cultures." Methods **30**(3): 256-268.
- Deng, Y. J., N. Tang, et al. (2014). "CLIC4, ERp29, and Smac/DIABLO derived from metastatic cancer stem-like cells stratify prognostic risks of colorectal cancer." Clinical cancer research : an official journal of the American Association for Cancer Research **20**(14): 3809-3817.
- Desmouliere, A., C. Guyot, et al. (2004). "The stroma reaction myofibroblast: a key player in the control of tumor cell behavior." The International journal of developmental biology **48**(5-6): 509-517.
- Docherty, A. J., A. Lyons, et al. (1985). "Sequence of human tissue inhibitor of metalloproteinases and its identity to erythroid-potentiating activity." Nature **318**(6041): 66-69.
- Domcke, S., R. Sinha, et al. (2013). "Evaluating cell lines as tumour models by comparison of genomic profiles." Nature communications **4**: 2126.
- Dozynkiewicz, M. A., N. B. Jamieson, et al. (2012). "Rab25 and CLIC3 collaborate to promote integrin recycling from late endosomes/lysosomes and drive cancer progression." Developmental cell **22**(1): 131-145.
- Dulhunty, A., P. Gage, et al. (2001). "The glutathione transferase structural family includes a nuclear chloride channel and a ryanodine receptor calcium release channel modulator." The Journal of biological chemistry **276**(5): 3319-3323.
- Dulhunty, A. F., P. Pouliquin, et al. (2005). "A recently identified member of the glutathione transferase structural family modifies cardiac RyR2 substate activity, coupled gating and activation by Ca<sup>2+</sup> and ATP." The Biochemical journal **390**(Pt 1): 333-343.
- Duncan, R. R., P. K. Westwood, et al. (1997). "Rat brain p64H1, expression of a new member of the p64 chloride channel protein family in endoplasmic reticulum." The Journal of biological chemistry **272**(38): 23880-23886.

- Dyrskjot, L., M. Kruhoffer, et al. (2004). "Gene expression in the urinary bladder: a common carcinoma in situ gene expression signature exists disregarding histopathological classification." Cancer research **64**(11): 4040-4048.
- Eckert, R. L., M. T. Kaartinen, et al. (2014). "Transglutaminase regulation of cell function." Physiological reviews **94**(2): 383-417.
- Egeblad, M., M. G. Rasch, et al. (2010). "Dynamic interplay between the collagen scaffold and tumor evolution." Current opinion in cell biology **22**(5): 697-706.
- Egeblad, M. and Z. Werb (2002). "New functions for the matrix metalloproteinases in cancer progression." Nature reviews. Cancer **2**(3): 161-174.
- el-Metwally, T. H., M. R. Hussein, et al. (2005). "Natural retinoids inhibit proliferation and induce apoptosis in pancreatic cancer cells previously reported to be retinoid resistant." Cancer biology & therapy **4**(4): 474-483.
- El Fahime, E., Y. Torrente, et al. (2000). "In vivo migration of transplanted myoblasts requires matrix metalloproteinase activity." Experimental cell research **258**(2): 279-287.
- Enterline, H. T. and D. R. Coman (1950). "The ameboid motility of human and animal neoplastic cells." Cancer **3**(6): 1033-1038.
- Erdem, S., G. Yegen, et al. (2014). "The increased transglutaminase 2 expression levels during initial tumorigenesis predict increased risk of metastasis and decreased disease-free and cancer-specific survivals in renal cell carcinoma." World journal of urology.
- Erler, J. T., K. L. Bennewith, et al. (2009). "Hypoxia-induced lysyl oxidase is a critical mediator of bone marrow cell recruitment to form the premetastatic niche." Cancer cell **15**(1): 35-44.
- Erler, J. T. and V. M. Weaver (2009). "Three-dimensional context regulation of metastasis." Clinical & experimental metastasis **26**(1): 35-49.
- Fanucchi, S., R. J. Adamson, et al. (2008). "Formation of an Unfolding Intermediate State of Soluble Chloride Intracellular Channel Protein CLIC1 at Acidic pH." Biochemistry **47**(44): 11674-11681.
- Fisher, M., R. A. Jones, et al. (2009). "Modulation of tissue transglutaminase in tubular epithelial cells alters extracellular matrix levels: a potential mechanism of tissue scarring." Matrix biology : journal of the International Society for Matrix Biology **28**(1): 20-31.
- Fleckenstein, B., O. Molberg, et al. (2002). "Gliadin T cell epitope selection by tissue transglutaminase in celiac disease. Role of enzyme specificity and pH influence on the transamidation versus deamidation process." The Journal of biological chemistry **277**(37): 34109-34116.
- Flores-Tellez, T. N., T. V. Lopez, et al. (2015). "Co-Expression of Ezrin-CLIC5-Podocalyxin Is Associated with Migration and Invasiveness in Hepatocellular Carcinoma." PLoS one **10**(7): e0131605.
- Fok, J. Y., S. Ekmekcioglu, et al. (2006). "Implications of tissue transglutaminase expression in malignant melanoma." Molecular cancer therapeutics **5**(6): 1493-1503.
- Folk, J. E. and J. S. Finlayson (1977). "The epsilon-(gamma-glutamyl)lysine crosslink and the catalytic role of transglutaminases." Advances in protein chemistry **31**: 1-133.
- Forsprecher, J., Z. Wang, et al. (2009). "Enhanced osteoblast adhesion on transglutaminase 2-crosslinked fibronectin." Amino acids **36**(4): 747-753.

- Fox, B. A., V. C. Yee, et al. (1999). "Identification of the calcium binding site and a novel ytterbium site in blood coagulation factor XIII by x-ray crystallography." The Journal of biological chemistry **274**(8): 4917-4923.
- Frantz, C., K. M. Stewart, et al. (2010). "The extracellular matrix at a glance." Journal of cell science **123**(Pt 24): 4195-4200.
- Friedl, P., S. Borgmann, et al. (2001). "Amoeboid leukocyte crawling through extracellular matrix: lessons from the Dictyostelium paradigm of cell movement." Journal of leukocyte biology **70**(4): 491-509.
- Friedl, P. and E. B. Brocker (2000). "The biology of cell locomotion within three-dimensional extracellular matrix." Cellular and molecular life sciences : CMLS **57**(1): 41-64.
- Friedl, P., K. Maaser, et al. (1997). "Migration of highly aggressive MV3 melanoma cells in 3-dimensional collagen lattices results in local matrix reorganization and shedding of alpha2 and beta1 integrins and CD44." Cancer research **57**(10): 2061-2070.
- Friedl, P., P. B. Noble, et al. (1995). "Migration of coordinated cell clusters in mesenchymal and epithelial cancer explants in vitro." Cancer research **55**(20): 4557-4560.
- Friedl, P. and K. Wolf (2003). "Tumour-cell invasion and migration: diversity and escape mechanisms." Nature reviews. Cancer **3**(5): 362-374.
- Friedl, P. and K. Wolf (2010). "Plasticity of cell migration: a multiscale tuning model." The Journal of cell biology **188**(1): 11-19.
- Friedl, P., K. S. Zanker, et al. (1998). "Cell migration strategies in 3-D extracellular matrix: differences in morphology, cell matrix interactions, and integrin function." Microscopy research and technique **43**(5): 369-378.
- Gagnon, L. H., C. M. Longo-Guess, et al. (2006). "The chloride intracellular channel protein CLIC5 is expressed at high levels in hair cell stereocilia and is essential for normal inner ear function." The Journal of neuroscience : the official journal of the Society for Neuroscience **26**(40): 10188-10198.
- Goodchild, S. C., M. W. Howell, et al. (2010). "Metamorphic response of the CLIC1 chloride intracellular ion channel protein upon membrane interaction." Biochemistry **49**(25): 5278-5289.
- Grenard, P., M. K. Bates, et al. (2001). "Evolution of transglutaminase genes: identification of a transglutaminase gene cluster on human chromosome 15q15. Structure of the gene encoding transglutaminase X and a novel gene family member, transglutaminase Z." The Journal of biological chemistry **276**(35): 33066-33078.
- Griffin, M., R. Casadio, et al. (2002). "Transglutaminases: nature's biological glues." The Biochemical journal **368**(Pt 2): 377-396.
- Griffon, N., F. Jeanneteau, et al. (2003). "CLIC6, a member of the intracellular chloride channel family, interacts with dopamine D(2)-like receptors." Brain research. Molecular brain research **117**(1): 47-57.
- Grzegorzolka, J., M. Biala, et al. (2015). "Expression of EMT Markers SLUG and TWIST in Breast Cancer." Anticancer research **35**(7): 3961-3968.
- Gundemir, S., G. Colak, et al. (2012). "Transglutaminase 2: a molecular Swiss army knife." Biochimica et biophysica acta **1823**(2): 406-419.
- Gundemir, S. and G. V. Johnson (2009). "Intracellular localization and conformational state of transglutaminase 2: implications for cell death." PloS one **4**(7): e6123.
- Guy, C. T., R. D. Cardiff, et al. (1992). "Induction of mammary tumors by expression of polyomavirus middle T oncogene: a transgenic mouse model for metastatic disease." Molecular and cellular biology **12**(3): 954-961.

- Han, A. L., S. Kumar, et al. (2014). "Tissue transglutaminase expression promotes castration-resistant phenotype and transcriptional repression of androgen receptor." European journal of cancer **50**(9): 1685-1696.
- Han, B. G., J. W. Cho, et al. (2010). "Crystal structure of human transglutaminase 2 in complex with adenosine triphosphate." International journal of biological macromolecules **47**(2): 190-195.
- Hanahan, D. and J. Folkman (1996). "Patterns and emerging mechanisms of the angiogenic switch during tumorigenesis." Cell **86**(3): 353-364.
- Hanahan, D. and R. A. Weinberg (2000). "The hallmarks of cancer." Cell **100**(1): 57-70.
- Hanahan, D. and R. A. Weinberg (2011). "Hallmarks of cancer: the next generation." Cell **144**(5): 646-674.
- Harrop, S. J., M. Z. DeMaere, et al. (2001). "Crystal structure of a soluble form of the intracellular chloride ion channel CLIC1 (NCC27) at 1.4-Å resolution." The Journal of biological chemistry **276**(48): 44993-45000.
- Hasegawa, G., M. Suwa, et al. (2003). "A novel function of tissue-type transglutaminase: protein disulphide isomerase." The Biochemical journal **373**(Pt 3): 793-803.
- Hayes, J. D., J. U. Flanagan, et al. (2005). "Glutathione transferases." Annual Review of Pharmacology and Toxicology **45**: 51-88.
- Hegerfeldt, Y., M. Tusch, et al. (2002). "Collective cell movement in primary melanoma explants: plasticity of cell-cell interaction, beta1-integrin function, and migration strategies." Cancer research **62**(7): 2125-2130.
- Hennigan, R. F., K. L. Hawker, et al. (1994). "Fos-transformation activates genes associated with invasion." Oncogene **9**(12): 3591-3600.
- Herman, J. F., L. S. Mangala, et al. (2006). "Implications of increased tissue transglutaminase (TG2) expression in drug-resistant breast cancer (MCF-7) cells." Oncogene **25**(21): 3049-3058.
- Hingorani, S. R., L. Wang, et al. (2005). "Trp53R172H and KrasG12D cooperate to promote chromosomal instability and widely metastatic pancreatic ductal adenocarcinoma in mice." Cancer cell **7**(5): 469-483.
- Hiraoka, N., E. Allen, et al. (1998). "Matrix metalloproteinases regulate neovascularization by acting as pericellular fibrinolysins." Cell **95**(3): 365-377.
- Hiratsuka, S., K. Nakamura, et al. (2002). "MMP9 induction by vascular endothelial growth factor receptor-1 is involved in lung-specific metastasis." Cancer cell **2**(4): 289-300.
- Hollosi, P., J. K. Yakushiji, et al. (2009). "Lysyl oxidase-like 2 promotes migration in noninvasive breast cancer cells but not in normal breast epithelial cells." International journal of cancer. Journal international du cancer **125**(2): 318-327.
- Howell, S., R. R. Duncan, et al. (1996). "Identification and characterisation of a homologue of p64 in rat tissues." FEBS letters **390**(2): 207-210.
- Hu, M., J. Yao, et al. (2008). "Regulation of in situ to invasive breast carcinoma transition." Cancer cell **13**(5): 394-406.
- Huijbers, I. J., M. Iravani, et al. (2010). "A role for fibrillar collagen deposition and the collagen internalization receptor endo180 in glioma invasion." PloS one **5**(3): e9808.
- Hwang, J. Y., L. S. Mangala, et al. (2008). "Clinical and biological significance of tissue transglutaminase in ovarian carcinoma." Cancer research **68**(14): 5849-5858.
- Hynes, R. O. (2002). "Integrins: bidirectional, allosteric signaling machines." Cell **110**(6): 673-687.

- Hynes, R. O. (2009). "The extracellular matrix: not just pretty fibrils." Science **326**(5957): 1216-1219.
- Iacobuzio-Donahue, C. A., A. Maitra, et al. (2003). "Exploration of global gene expression patterns in pancreatic adenocarcinoma using cDNA microarrays." The American journal of pathology **162**(4): 1151-1162.
- Ideguchi, H., J. Nishimura, et al. (1990). "A genetic defect of erythrocyte band 4.2 protein associated with hereditary spherocytosis." British journal of haematology **74**(3): 347-353.
- Ilan, N., M. Elkin, et al. (2006). "Regulation, function and clinical significance of heparanase in cancer metastasis and angiogenesis." The international journal of biochemistry & cell biology **38**(12): 2018-2039.
- Jacques, T. S., J. B. Relvas, et al. (1998). "Neural precursor cell chain migration and division are regulated through different beta1 integrins." Development **125**(16): 3167-3177.
- Jalilian, C., E. M. Gallant, et al. (2008). "Redox potential and the response of cardiac ryanodine receptors to CLIC-2, a member of the glutathione S-transferase structural family." Antioxidants & redox signaling **10**(10): 1675-1686.
- Jedezsko, C., B. C. Victor, et al. (2009). "Fibroblast hepatocyte growth factor promotes invasion of human mammary ductal carcinoma in situ." Cancer research **69**(23): 9148-9155.
- Jensen, L. J., R. Gupta, et al. (2002). "Prediction of human protein function from post-translational modifications and localization features." Journal of molecular biology **319**(5): 1257-1265.
- Jensen, L. J., R. Gupta, et al. (2003). "Prediction of human protein function according to Gene Ontology categories." Bioinformatics **19**(5): 635-642.
- Jensen, L. J., M. Skovgaard, et al. (2002). "Prediction of novel archaeal enzymes from sequence-derived features." Protein science : a publication of the Protein Society **11**(12): 2894-2898.
- Jiang, L., K. Salao, et al. (2012). "Intracellular chloride channel protein CLIC1 regulates macrophage function through modulation of phagosomal acidification." Journal of cell science **125**(Pt 22): 5479-5488.
- Jin, X., J. Stammaes, et al. (2011). "Activation of extracellular transglutaminase 2 by thioredoxin." The Journal of biological chemistry **286**(43): 37866-37873.
- Johnson, T. S., A. F. El-Koraie, et al. (2003). "Tissue transglutaminase and the progression of human renal scarring." Journal of the American Society of Nephrology : JASN **14**(8): 2052-2062.
- Joshi, S., R. Guleria, et al. (2006). "Retinoic acid receptors and tissue-transglutaminase mediate short-term effect of retinoic acid on migration and invasion of neuroblastoma SH-SY5Y cells." Oncogene **25**(2): 240-247.
- Kagan, H. M. and W. Li (2003). "Lysyl oxidase: properties, specificity, and biological roles inside and outside of the cell." Journal of cellular biochemistry **88**(4): 660-672.
- Kalinin, A., L. N. Marekov, et al. (2001). "Assembly of the epidermal cornified cell envelope." Journal of cell science **114**(Pt 17): 3069-3070.
- Kalluri, R. and M. Zeisberg (2006). "Fibroblasts in cancer." Nature reviews. Cancer **6**(5): 392-401.
- Kanaoka, Y., H. Ago, et al. (1997). "Cloning and crystal structure of hematopoietic prostaglandin D synthase." Cell **90**(6): 1085-1095.
- Kang, M. K. and S. K. Kang (2008). "Pharmacologic blockade of chloride channel synergistically enhances apoptosis of chemotherapeutic drug-resistant

- cancer stem cells." Biochemical and biophysical research communications **373**(4): 539-544.
- Kaplan, R. N., R. D. Riba, et al. (2005). "VEGFR1-positive haematopoietic bone marrow progenitors initiate the pre-metastatic niche." Nature **438**(7069): 820-827.
- Kass, L., J. T. Erler, et al. (2007). "Mammary epithelial cell: influence of extracellular matrix composition and organization during development and tumorigenesis." The international journal of biochemistry & cell biology **39**(11): 1987-1994.
- Kaupilla, S., F. Stenback, et al. (1998). "Aberrant type I and type III collagen gene expression in human breast cancer in vivo." The Journal of pathology **186**(3): 262-268.
- Kennecke, H., R. Yerushalmi, et al. (2010). "Metastatic behavior of breast cancer subtypes." Journal of clinical oncology : official journal of the American Society of Clinical Oncology **28**(20): 3271-3277.
- Kessenbrock, K., V. Plaks, et al. (2010). "Matrix metalloproteinases: regulators of the tumor microenvironment." Cell **141**(1): 52-67.
- Kim, K. H., B. K. Choi, et al. (2013). "CRLg signals induce anti-intracellular bacterial phagosome activity in a chloride intracellular channel 3-dependent manner." European journal of immunology **43**(3): 667-678.
- Kiraly, R., E. Csoz, et al. (2009). "Functional significance of five noncanonical Ca<sup>2+</sup>-binding sites of human transglutaminase 2 characterized by site-directed mutagenesis." The FEBS journal **276**(23): 7083-7096.
- Klinowska, T. C., J. V. Soriano, et al. (1999). "Laminin and beta1 integrins are crucial for normal mammary gland development in the mouse." Developmental biology **215**(1): 13-32.
- Klymkowsky, M. W. and P. Savagner (2009). "Epithelial-mesenchymal transition: a cancer researcher's conceptual friend and foe." The American journal of pathology **174**(5): 1588-1593.
- Knowles, L. M., J. Zewe, et al. (2013). "CLT1 targets bladder cancer through integrin alpha5beta1 and CLIC3." Molecular cancer research : MCR **11**(2): 194-203.
- Kraus, A. C., I. Ferber, et al. (2002). "In vitro chemo- and radio-resistance in small cell lung cancer correlates with cell adhesion and constitutive activation of AKT and MAP kinase pathways." Oncogene **21**(57): 8683-8695.
- Krusius, T. and E. Ruoslahti (1986). "Primary structure of an extracellular matrix proteoglycan core protein deduced from cloned cDNA." Proceedings of the National Academy of Sciences of the United States of America **83**(20): 7683-7687.
- Kumar, A., C. B. Gilks, et al. (2013). "Patterns of spread of clear cell ovarian cancer: Case report and case series." Gynecologic oncology case reports **6**: 25-27.
- Kumar, A., J. Hu, et al. (2014). "Conformational changes and translocation of tissue-transglutaminase to the plasma membranes: role in cancer cell migration." BMC cancer **14**: 256.
- Kumar, S., T. R. Donti, et al. (2014). "Transglutaminase 2 reprogramming of glucose metabolism in mammary epithelial cells via activation of inflammatory signaling pathways." International journal of cancer. Journal international du cancer **134**(12): 2798-2807.
- Landry, D., S. Sullivan, et al. (1993). "Molecular cloning and characterization of p64, a chloride channel protein from kidney microsomes." The Journal of biological chemistry **268**(20): 14948-14955.

- Lauffenburger, D. A. and A. F. Horwitz (1996). "Cell migration: a physically integrated molecular process." Cell **84**(3): 359-369.
- Le, Q. T., J. Harris, et al. (2009). "Validation of lysyl oxidase as a prognostic marker for metastasis and survival in head and neck squamous cell carcinoma: Radiation Therapy Oncology Group trial 90-03." Journal of clinical oncology : official journal of the American Society of Clinical Oncology **27**(26): 4281-4286.
- Legg-E-Silva, D., I. Achilonu, et al. (2012). "Role of Arginine 29 and Glutamic Acid 81 Interactions in the Conformational Stability of Human Chloride Intracellular Channel 1." Biochemistry **51**(40): 7854-7862.
- Leicht, D. T., T. Kausar, et al. (2014). "TGM2: a cell surface marker in esophageal adenocarcinomas." Journal of thoracic oncology : official publication of the International Association for the Study of Lung Cancer **9**(6): 872-881.
- Lengyel, E. (2010). "Ovarian cancer development and metastasis." The American journal of pathology **177**(3): 1053-1064.
- Levental, K. R., H. Yu, et al. (2009). "Matrix crosslinking forces tumor progression by enhancing integrin signaling." Cell **139**(5): 891-906.
- Li, F., J. Yin, et al. (2010). "The CLIC5 (chloride intracellular channel 5) involved in C2C12 myoblasts proliferation and differentiation." Cell biology international **34**(4): 379-384.
- Li, R. K., J. Zhang, et al. (2012). "Chloride intracellular channel 1 is an important factor in the lymphatic metastasis of hepatocarcinoma." Biomedicine & pharmacotherapy = Biomedecine & pharmacotherapie **66**(3): 167-172.
- Liang, B., P. Peng, et al. (2013). "Characterization and proteomic analysis of ovarian cancer-derived exosomes." Journal of proteomics **80**: 171-182.
- Littler, D. R., N. N. Assaad, et al. (2005). "Crystal structure of the soluble form of the redox-regulated chloride ion channel protein CLIC4." The FEBS journal **272**(19): 4996-5007.
- Littler, D. R., L. J. Brown, et al. (2010). "Structure of human CLIC3 at 2 Å resolution." Proteins **78**(6): 1594-1600.
- Littler, D. R., S. J. Harrop, et al. (2004). "The intracellular chloride ion channel protein CLIC1 undergoes a redox-controlled structural transition." The Journal of biological chemistry **279**(10): 9298-9305.
- Littler, D. R., S. J. Harrop, et al. (2010). "The enigma of the CLIC proteins: Ion channels, redox proteins, enzymes, scaffolding proteins?" FEBS letters **584**(10): 2093-2101.
- Liu, S., R. A. Cerione, et al. (2002). "Structural basis for the guanine nucleotide-binding activity of tissue transglutaminase and its regulation of transamidation activity." Proceedings of the National Academy of Sciences of the United States of America **99**(5): 2743-2747.
- Livak, K. J. and T. D. Schmittgen (2001). "Analysis of relative gene expression data using real-time quantitative PCR and the 2(-Delta Delta C(T)) Method." Methods **25**(4): 402-408.
- Lo, C. M., H. B. Wang, et al. (2000). "Cell movement is guided by the rigidity of the substrate." Biophysical journal **79**(1): 144-152.
- Lochter, A., M. Navre, et al. (1999). "alpha1 and alpha2 integrins mediate invasive activity of mouse mammary carcinoma cells through regulation of stromelysin-1 expression." Molecular biology of the cell **10**(2): 271-282.
- Lopez, J. I., I. Kang, et al. (2011). "In situ force mapping of mammary gland transformation." Integrative biology : quantitative biosciences from nano to macro **3**(9): 910-921.

- Lorand, L. (2001). "Factor XIII: structure, activation, and interactions with fibrinogen and fibrin." Annals of the New York Academy of Sciences **936**: 291-311.
- Lorand, L. and R. M. Graham (2003). "Transglutaminases: crosslinking enzymes with pleiotropic functions." Nature reviews. Molecular cell biology **4**(2): 140-156.
- Lowe, S. W., E. Cepero, et al. (2004). "Intrinsic tumour suppression." Nature **432**(7015): 307-315.
- Lu, P., K. Takai, et al. (2011). "Extracellular matrix degradation and remodeling in development and disease." Cold Spring Harbor perspectives in biology **3**(12).
- Lucero, H. A. and H. M. Kagan (2006). "Lysyl oxidase: an oxidative enzyme and effector of cell function." Cellular and molecular life sciences : CMLS **63**(19-20): 2304-2316.
- Machesky, L. M. and K. L. Gould (1999). "The Arp2/3 complex: a multifunctional actin organizer." Current opinion in cell biology **11**(1): 117-121.
- Macpherson, I. R., E. Rainero, et al. (2014). "CLIC3 controls recycling of late endosomal MT1-MMP and dictates invasion and metastasis in breast cancer." Journal of cell science **127**(Pt 18): 3893-3901.
- Malhotra, V. (2013). "Unconventional protein secretion: an evolving mechanism." The EMBO journal **32**(12): 1660-1664.
- Mangala, L. S. and K. Mehta (2005). "Tissue transglutaminase (TG2) in cancer biology." Progress in experimental tumor research **38**: 125-138.
- Mao, Y., E. T. Keller, et al. (2013). "Stromal cells in tumor microenvironment and breast cancer." Cancer metastasis reviews **32**(1-2): 303-315.
- Mason, B. N., A. Starchenko, et al. (2013). "Tuning three-dimensional collagen matrix stiffness independently of collagen concentration modulates endothelial cell behavior." Acta biomaterialia **9**(1): 4635-4644.
- Massague, J. (2008). "TGFbeta in Cancer." Cell **134**(2): 215-230.
- Mastroberardino, P. G., M. G. Farrace, et al. (2006). ""Tissue" transglutaminase contributes to the formation of disulphide bridges in proteins of mitochondrial respiratory complexes." Biochimica et biophysica acta **1757**(9-10): 1357-1365.
- McConoughey, S. J., M. Basso, et al. (2010). "Inhibition of transglutaminase 2 mitigates transcriptional dysregulation in models of Huntington disease." EMBO molecular medicine **2**(9): 349-370.
- Mehta, K., J. Fok, et al. (2004). "Prognostic significance of tissue transglutaminase in drug resistant and metastatic breast cancer." Clinical cancer research : an official journal of the American Association for Cancer Research **10**(23): 8068-8076.
- Mehta, K., J. Y. Fok, et al. (2006). "Tissue transglutaminase: from biological glue to cell survival cues." Frontiers in bioscience : a journal and virtual library **11**: 173-185.
- Mehta, K., A. Kumar, et al. (2010). "Transglutaminase 2: a multi-tasking protein in the complex circuitry of inflammation and cancer." Biochemical pharmacology **80**(12): 1921-1929.
- Meng, X., G. Wang, et al. (2009). "CLIC2-RyR1 interaction and structural characterization by cryo-electron microscopy." Journal of molecular biology **387**(2): 320-334.
- Miller, F. R., S. J. Santner, et al. (2000). "MCF10DCIS.com xenograft model of human comedo ductal carcinoma in situ." Journal of the National Cancer Institute **92**(14): 1185-1186.

- Milton, R. H., R. Abeti, et al. (2008). "CLIC1 function is required for beta-amyloid-induced generation of reactive oxygen species by microglia." The Journal of neuroscience : the official journal of the Society for Neuroscience **28**(45): 11488-11499.
- Mishra, S. and L. J. Murphy (2004). "Tissue transglutaminase has intrinsic kinase activity: identification of transglutaminase 2 as an insulin-like growth factor-binding protein-3 kinase." The Journal of biological chemistry **279**(23): 23863-23868.
- Mishra, S., A. Saleh, et al. (2006). "Phosphorylation of histones by tissue transglutaminase." The Journal of biological chemistry **281**(9): 5532-5538.
- Miyoshi, N., H. Ishii, et al. (2010). "TGM2 is a novel marker for prognosis and therapeutic target in colorectal cancer." Annals of surgical oncology **17**(4): 967-972.
- Money, T. T., R. G. King, et al. (2007). "Expression and cellular localisation of chloride intracellular channel 3 in human placenta and fetal membranes." Placenta **28**(5-6): 429-436.
- Morton, J. P., P. Timpson, et al. (2010). "Mutant p53 drives metastasis and overcomes growth arrest/senescence in pancreatic cancer." Proceedings of the National Academy of Sciences of the United States of America **107**(1): 246-251.
- Muller, P. A., P. T. Caswell, et al. (2009). "Mutant p53 drives invasion by promoting integrin recycling." Cell **139**(7): 1327-1341.
- Munro, J., K. Steeghs, et al. (2001). "Human fibroblast replicative senescence can occur in the absence of extensive cell division and short telomeres." Oncogene **20**(27): 3541-3552.
- Murtaugh, M. P., K. Mehta, et al. (1983). "Induction of tissue transglutaminase in mouse peritoneal macrophages." The Journal of biological chemistry **258**(18): 11074-11081.
- Murthi, P., J. L. Stevenson, et al. (2012). "Placental CLIC3 is increased in fetal growth restriction and pre-eclampsia affected human pregnancies." Placenta **33**(9): 741-744.
- Murthy, S. N., S. Iismaa, et al. (2002). "Conserved tryptophan in the core domain of transglutaminase is essential for catalytic activity." Proceedings of the National Academy of Sciences of the United States of America **99**(5): 2738-2742.
- Murzin, A. G. (2008). "Biochemistry. Metamorphic proteins." Science **320**(5884): 1725-1726.
- Nabeshima, K., T. Inoue, et al. (1999). "Cohort migration of carcinoma cells: differentiated colorectal carcinoma cells move as coherent cell clusters or sheets." Histology and histopathology **14**(4): 1183-1197.
- Nabeshima, K., T. Inoue, et al. (2000). "Front-cell-specific expression of membrane-type 1 matrix metalloproteinase and gelatinase A during cohort migration of colon carcinoma cells induced by hepatocyte growth factor/scatter factor." Cancer research **60**(13): 3364-3369.
- Nakaoka, H., D. M. Perez, et al. (1994). "Gh: a GTP-binding protein with transglutaminase activity and receptor signaling function." Science **264**(5165): 1593-1596.
- Nelea, V., Y. Nakano, et al. (2008). "Size distribution and molecular associations of plasma fibronectin and fibronectin crosslinked by transglutaminase 2." The protein journal **27**(4): 223-233.
- Nicholas, B., P. Smethurst, et al. (2003). "Cross-linking of cellular proteins by tissue transglutaminase during necrotic cell death: a mechanism for maintaining tissue integrity." The Biochemical journal **371**(Pt 2): 413-422.

- Nickel, W. and M. Seedorf (2008). "Unconventional mechanisms of protein transport to the cell surface of eukaryotic cells." Annual review of cell and developmental biology **24**: 287-308.
- Oh, K., E. Ko, et al. (2011). "Transglutaminase 2 facilitates the distant hematogenous metastasis of breast cancer by modulating interleukin-6 in cancer cells." Breast cancer research : BCR **13**(5): R96.
- Olive, K. P., D. A. Tuveson, et al. (2004). "Mutant p53 gain of function in two mouse models of Li-Fraumeni syndrome." Cell **119**(6): 847-860.
- Orimo, A., P. B. Gupta, et al. (2005). "Stromal fibroblasts present in invasive human breast carcinomas promote tumor growth and angiogenesis through elevated SDF-1/CXCL12 secretion." Cell **121**(3): 335-348.
- Ozdemir, B. C., T. Pentcheva-Hoang, et al. (2014). "Depletion of carcinoma-associated fibroblasts and fibrosis induces immunosuppression and accelerates pancreas cancer with reduced survival." Cancer cell **25**(6): 719-734.
- Page, D. L. and T. J. Anderson (1987). Diagnostic histopathology of the breast. Edinburgh ; New York, Churchill Livingstone.
- Paget, S. (1989). "The distribution of secondary growths in cancer of the breast. 1889." Cancer metastasis reviews **8**(2): 98-101.
- Palermo, C. and J. A. Joyce (2008). "Cysteine cathepsin proteases as pharmacological targets in cancer." Trends in pharmacological sciences **29**(1): 22-28.
- Paradisi, S., A. Matteucci, et al. (2008). "Blockade of chloride intracellular ion channel 1 stimulates Abeta phagocytosis." Journal of neuroscience research **86**(11): 2488-2498.
- Park, D., S. S. Choi, et al. (2010). "Transglutaminase 2: a multi-functional protein in multiple subcellular compartments." Amino acids **39**(3): 619-631.
- Paszek, M. J. and V. M. Weaver (2004). "The tension mounts: mechanics meets morphogenesis and malignancy." Journal of mammary gland biology and neoplasia **9**(4): 325-342.
- Paszek, M. J., N. Zahir, et al. (2005). "Tensional homeostasis and the malignant phenotype." Cancer cell **8**(3): 241-254.
- Paulus, W., I. Baur, et al. (1996). "Diffuse brain invasion of glioma cells requires beta 1 integrins." Laboratory investigation; a journal of technical methods and pathology **75**(6): 819-826.
- Peretti, M., M. Angelini, et al. (2014). "Chloride channels in cancer: Focus on chloride intracellular channel 1 and 4 (CLIC1 AND CLIC4) proteins in tumor development and as novel therapeutic targets." Biochimica et biophysica acta.
- Piercy-Kotb, S. A., A. Mousa, et al. (2012). "Factor XIIIa transglutaminase expression and secretion by osteoblasts is regulated by extracellular matrix collagen and the MAP kinase signaling pathway." Journal of cellular physiology **227**(7): 2936-2946.
- Pinkas, D. M., P. Strop, et al. (2007). "Transglutaminase 2 undergoes a large conformational change upon activation." PLoS biology **5**(12): e327.
- Pisano, J. J., J. S. Finlayson, et al. (1968). "[Cross-link in fibrin polymerized by factor 13: epsilon-(gamma-glutamyl)lysine]." Science **160**(3830): 892-893.
- Pitts, W. C., V. A. Rojas, et al. (1991). "Carcinomas with metaplasia and sarcomas of the breast." American journal of clinical pathology **95**(5): 623-632.

- Polanska, U. M., A. Acar, et al. (2011). "Experimental generation of carcinoma-associated fibroblasts (CAFs) from human mammary fibroblasts." Journal of visualized experiments : JoVE(56): e3201.
- Polanska, U. M. and A. Orimo (2013). "Carcinoma-associated fibroblasts: non-neoplastic tumour-promoting mesenchymal cells." Journal of cellular physiology **228**(8): 1651-1657.
- Polyak, K. and R. A. Weinberg (2009). "Transitions between epithelial and mesenchymal states: acquisition of malignant and stem cell traits." Nature reviews. Cancer **9**(4): 265-273.
- Ponsioen, B., L. van Zeijl, et al. (2009). "Spatiotemporal regulation of chloride intracellular channel protein CLIC4 by RhoA." Molecular biology of the cell **20**(22): 4664-4672.
- Provenzano, P. P., C. Cuevas, et al. (2012). "Enzymatic targeting of the stroma ablates physical barriers to treatment of pancreatic ductal adenocarcinoma." Cancer cell **21**(3): 418-429.
- Provenzano, P. P., K. W. Eliceiri, et al. (2006). "Collagen reorganization at the tumor-stromal interface facilitates local invasion." BMC medicine **4**(1): 38.
- Qian, Z., D. Okuhara, et al. (1999). "Molecular cloning and characterization of a mitogen-activated protein kinase-associated intracellular chloride channel." The Journal of biological chemistry **274**(3): 1621-1627.
- Qiu, M. R., L. L. Jiang, et al. (2010). "Generation and Characterization of Mice With Null Mutation of the Chloride Intracellular Channel 1 Gene." Genesis **48**(2): 127-136.
- Rainero, E., P. T. Caswell, et al. (2012). "Diacylglycerol kinase alpha controls RCP-dependent integrin trafficking to promote invasive migration." The Journal of cell biology **196**(2): 277-295.
- Redhead, C. R., A. E. Edelman, et al. (1992). "A ubiquitous 64-kDa protein is a component of a chloride channel of plasma and intracellular membranes." Proceedings of the National Academy of Sciences of the United States of America **89**(9): 3716-3720.
- Robinson, R. C., K. Turbedsky, et al. (2001). "Crystal structure of Arp2/3 complex." Science **294**(5547): 1679-1684.
- Ronnov-Jessen, L., O. W. Petersen, et al. (1996). "Cellular changes involved in conversion of normal to malignant breast: importance of the stromal reaction." Physiological reviews **76**(1): 69-125.
- Ronnov-Jessen, L., R. Villadsen, et al. (2002). "Differential expression of a chloride intracellular channel gene, CLIC4, in transforming growth factor-beta1-mediated conversion of fibroblasts to myofibroblasts." The American journal of pathology **161**(2): 471-480.
- Roy, I., O. Smith, et al. (2013). "Expression, purification and kinetic characterisation of human tissue transglutaminase." Protein expression and purification **87**(1): 41-46.
- Rozario, T. and D. W. DeSimone (2010). "The extracellular matrix in development and morphogenesis: a dynamic view." Developmental biology **341**(1): 126-140.
- Sahai, E. (2005). "Mechanisms of cancer cell invasion." Current opinion in genetics & development **15**(1): 87-96.
- Sappino, A. P., O. Skalli, et al. (1988). "Smooth-muscle differentiation in stromal cells of malignant and non-malignant breast tissues." International journal of cancer. Journal international du cancer **41**(5): 707-712.
- Satchwell, T. J., D. K. Shoemark, et al. (2009). "Protein 4.2: a complex linker." Blood cells, molecules & diseases **42**(3): 201-210.

- Satpathy, M., L. Cao, et al. (2007). "Enhanced peritoneal ovarian tumor dissemination by tissue transglutaminase." Cancer research **67**(15): 7194-7202.
- Schaertl, S., M. Prime, et al. (2010). "A profiling platform for the characterization of transglutaminase 2 (TG2) inhibitors." Journal of biomolecular screening **15**(5): 478-487.
- Schafer, M. and S. Werner (2008). "Cancer as an overheating wound: an old hypothesis revisited." Nature Reviews Molecular Cell Biology **9**(8): 628-638.
- Schelling, J. R. (2009). "Tissue transglutaminase inhibition as treatment for diabetic glomerular scarring: it's good to be glueless." Kidney international **76**(4): 363-365.
- Schultz, G. S. and A. Wysocki (2009). "Interactions between extracellular matrix and growth factors in wound healing." Wound repair and regeneration : official publication of the Wound Healing Society [and] the European Tissue Repair Society **17**(2): 153-162.
- Seftor, E. A., P. S. Meltzer, et al. (2002). "Molecular determinants of human uveal melanoma invasion and metastasis." Clinical & experimental metastasis **19**(3): 233-246.
- Setti, M., N. Savalli, et al. (2013). "Functional role of CLIC1 ion channel in glioblastoma-derived stem/progenitor cells." Journal of the National Cancer Institute **105**(21): 1644-1655.
- Shanks, R. A., M. C. Larocca, et al. (2002). "AKAP350 at the Golgi apparatus. II. Association of AKAP350 with a novel chloride intracellular channel (CLIC) family member." The Journal of biological chemistry **277**(43): 40973-40980.
- Shukla, A., R. Edwards, et al. (2014). "CLIC4 regulates TGF-beta-dependent myofibroblast differentiation to produce a cancer stroma." Oncogene **33**(7): 842-850.
- Shukla, A., M. Malik, et al. (2009). "TGF-beta signalling is regulated by Schnurri-2-dependent nuclear translocation of CLIC4 and consequent stabilization of phospho-Smad2 and 3." Nature cell biology **11**(6): 777-784.
- Siegel, M., P. Strnad, et al. (2008). "Extracellular transglutaminase 2 is catalytically inactive, but is transiently activated upon tissue injury." PLoS one **3**(3): e1861.
- Simian, M., Y. Hirai, et al. (2001). "The interplay of matrix metalloproteinases, morphogens and growth factors is necessary for branching of mammary epithelial cells." Development **128**(16): 3117-3131.
- Singh, H. (2010). "Two decades with dimorphic Chloride Intracellular Channels (CLICs)." FEBS letters **584**(10): 2112-2121.
- Singh, H. and R. H. Ashley (2006). "Redox regulation of CLIC1 by cysteine residues associated with the putative channel pore." Biophysical journal **90**(5): 1628-1638.
- Singh, H. and R. H. Ashley (2007). "CLIC4 (p64H1) and its putative transmembrane domain form poorly selective, redox-regulated ion channels." Molecular membrane biology **24**(1): 41-52.
- Singh, H., M. A. Cousin, et al. (2007). "Functional reconstitution of mammalian 'chloride intracellular channels' CLIC1, CLIC4 and CLIC5 reveals differential regulation by cytoskeletal actin." The FEBS journal **274**(24): 6306-6316.
- Sinha, A., V. Ignatchenko, et al. (2014). "In-depth proteomic analyses of ovarian cancer cell line exosomes reveals differential enrichment of functional

- categories compared to the NCI 60 proteome." Biochemical and biophysical research communications **445**(4): 694-701.
- Sinkus, R., J. Lorenzen, et al. (2000). "High-resolution tensor MR elastography for breast tumour detection." Physics in medicine and biology **45**(6): 1649-1664.
- Smith, L. A., H. Aranda-Espinoza, et al. (2007). "Neutrophil traction stresses are concentrated in the uropod during migration." Biophysical journal **92**(7): L58-60.
- Smith, M. L., D. Gourdon, et al. (2007). "Force-induced unfolding of fibronectin in the extracellular matrix of living cells." PLoS biology **5**(10): e268.
- So, J. Y., H. J. Lee, et al. (2012). "Differential Expression of Key Signaling Proteins in MCF10 Cell Lines, a Human Breast Cancer Progression Model." Molecular and cellular pharmacology **4**(1): 31-40.
- Song, M. Y., J. W. Tang, et al. (2010). "[Localization and expression of CLIC1 in hepatocarcinoma ascites cell lines with high or low potentials of lymphatic spread]." Zhonghua bing li xue za zhi Chinese journal of pathology **39**(7): 463-466.
- Sood, A. K., E. A. Seftor, et al. (2001). "Molecular determinants of ovarian cancer plasticity." The American journal of pathology **158**(4): 1279-1288.
- Spiekerkoetter, E., C. Guignabert, et al. (2009). "S100A4 and bone morphogenetic protein-2 codependently induce vascular smooth muscle cell migration via phospho-extracellular signal-regulated kinase and chloride intracellular channel 4." Circulation research **105**(7): 639-647, 613 p following 647.
- Spurlin, T. A., K. Bhadriraju, et al. (2009). "The treatment of collagen fibrils by tissue transglutaminase to promote vascular smooth muscle cell contractile signaling." Biomaterials **30**(29): 5486-5496.
- Stamnaes, J., B. Fleckenstein, et al. (2008). "The propensity for deamidation and transamidation of peptides by transglutaminase 2 is dependent on substrate affinity and reaction conditions." Biochimica et biophysica acta **1784**(11): 1804-1811.
- Stamnaes, J., D. M. Pinkas, et al. (2010). "Redox regulation of transglutaminase 2 activity." The Journal of biological chemistry **285**(33): 25402-25409.
- Stoychev, S. H., C. Nathaniel, et al. (2009). "Structural Dynamics of Soluble Chloride Intracellular Channel Protein CLIC1 Examined by Amide Hydrogen-Deuterium Exchange Mass Spectrometry." Biochemistry **48**(35): 8413-8421.
- Suh, K. S., J. M. Crutchley, et al. (2007). "Reciprocal modifications of CLIC4 in tumor epithelium and stroma mark malignant progression of multiple human cancers." Clinical cancer research : an official journal of the American Association for Cancer Research **13**(1): 121-131.
- Suh, K. S., M. Malik, et al. (2012). "CLIC4 is a tumor suppressor for cutaneous squamous cell cancer." Carcinogenesis **33**(5): 986-995.
- Szajnik, M., M. Derbis, et al. (2013). "Exosomes in Plasma of Patients with Ovarian Carcinoma: Potential Biomarkers of Tumor Progression and Response to Therapy." Gynecology & obstetrics Suppl **4**: 3.
- Szauter, K. M., T. Cao, et al. (2005). "Lysyl oxidase in development, aging and pathologies of the skin." Pathologie-biologie **53**(7): 448-456.
- Szende, B., A. V. Schally, et al. (1991). "Immunocytochemical demonstration of tissue transglutaminase indicative of programmed cell death (apoptosis) in hormone sensitive mammary tumours." Acta morphologica Hungarica **39**(1): 53-58.

- Takano, K., D. Liu, et al. (2012). "An X-linked channelopathy with cardiomegaly due to a CLIC2 mutation enhancing ryanodine receptor channel activity." Human molecular genetics **21**(20): 4497-4507.
- Takeuchi, Y., H. Ohashi, et al. (1998). "Nuclear translocation of tissue type transglutaminase during sphingosine-induced cell death: a novel aspect of the enzyme with DNA hydrolytic activity." Zeitschrift fur Naturforschung. C, Journal of biosciences **53**(5-6): 352-358.
- Tan, T. T. and L. M. Coussens (2007). "Humoral immunity, inflammation and cancer." Current opinion in immunology **19**(2): 209-216.
- Tang, H. Y., L. A. Beer, et al. (2012). "A xenograft mouse model coupled with in-depth plasma proteome analysis facilitates identification of novel serum biomarkers for human ovarian cancer." Journal of proteome research **11**(2): 678-691.
- Tang, H. Y., L. A. Beer, et al. (2013). "Protein isoform-specific validation defines multiple chloride intracellular channel and tropomyosin isoforms as serological biomarkers of ovarian cancer." Journal of proteomics **89**: 165-178.
- Tee, A. E., G. M. Marshall, et al. (2010). "Opposing effects of two tissue transglutaminase protein isoforms in neuroblastoma cell differentiation." The Journal of biological chemistry **285**(6): 3561-3567.
- Thiery, J. P. (2002). "Epithelial-mesenchymal transitions in tumour progression." Nature reviews. Cancer **2**(6): 442-454.
- Timpson, P., E. J. McGhee, et al. (2011). "Organotypic Collagen I Assay: A Malleable Platform to Assess Cell Behaviour in a 3-Dimensional Context." (56): e3089.
- Timpson, P., E. J. McGhee, et al. (2011). "Organotypic collagen I assay: a malleable platform to assess cell behaviour in a 3-dimensional context." Journal of visualized experiments : JoVE(56): e3089.
- Tonini, R., A. Ferroni, et al. (2000). "Functional characterization of the NCC27 nuclear protein in stable transfected CHO-K1 cells." FASEB journal : official publication of the Federation of American Societies for Experimental Biology **14**(9): 1171-1178.
- Torocsik, D., L. Szeles, et al. (2010). "Factor XIII-A is involved in the regulation of gene expression in alternatively activated human macrophages." Thrombosis and haemostasis **104**(4): 709-717.
- Torres, S., R. A. Bartolome, et al. (2013). "Proteome profiling of cancer-associated fibroblasts identifies novel proinflammatory signatures and prognostic markers for colorectal cancer." Clinical cancer research : an official journal of the American Association for Cancer Research **19**(21): 6006-6019.
- Toth, B., E. Garabuczi, et al. (2009). "Transglutaminase 2 is needed for the formation of an efficient phagocyte portal in macrophages engulfing apoptotic cells." Journal of immunology **182**(4): 2084-2092.
- Tringali, C., B. Lupo, et al. (2012). "The plasma membrane sialidase NEU3 regulates the malignancy of renal carcinoma cells by controlling beta1 integrin internalization and recycling." The Journal of biological chemistry **287**(51): 42835-42845.
- Tsujino, T., I. Seshimo, et al. (2007). "Stromal myofibroblasts predict disease recurrence for colorectal cancer." Clinical cancer research : an official journal of the American Association for Cancer Research **13**(7): 2082-2090.

- Tulk, B. M., S. Kapadia, et al. (2002). "CLIC1 inserts from the aqueous phase into phospholipid membranes, where it functions as an anion channel." American journal of physiology. Cell physiology **282**(5): C1103-1112.
- Tung, J. J., O. Hobert, et al. (2009). "Chloride intracellular channel 4 is involved in endothelial proliferation and morphogenesis in vitro." Angiogenesis **12**(3): 209-220.
- Ulmasov, B., J. Bruno, et al. (2009). "Chloride intracellular channel protein-4 functions in angiogenesis by supporting acidification of vacuoles along the intracellular tubulogenic pathway." The American journal of pathology **174**(3): 1084-1096.
- Valenzuela, S. M., D. K. Martin, et al. (1997). "Molecular cloning and expression of a chloride ion channel of cell nuclei." The Journal of biological chemistry **272**(19): 12575-12582.
- Valenzuela, S. M., M. Mazzanti, et al. (2000). "The nuclear chloride ion channel NCC27 is involved in regulation of the cell cycle." The Journal of physiology **529 Pt 3**: 541-552.
- Velnar, T., T. Bailey, et al. (2009). "The wound healing process: an overview of the cellular and molecular mechanisms." The Journal of international medical research **37**(5): 1528-1542.
- Verma, A., S. Guha, et al. (2008). "Tissue transglutaminase regulates focal adhesion kinase/AKT activation by modulating PTEN expression in pancreatic cancer cells." Clinical Cancer Research **14**(7): 1997-2005.
- Verma, A., H. Wang, et al. (2006). "Increased expression of tissue transglutaminase in pancreatic ductal adenocarcinoma and its implications in drug resistance and metastasis." Cancer research **66**(21): 10525-10533.
- Verma, A., H. M. Wang, et al. (2006). "Increased expression of tissue transglutaminase in pancreatic ductal adenocarcinoma and its implications in drug resistance and metastasis." Cancer research **66**(21): 10525-10533.
- Vial, E., E. Sahai, et al. (2003). "ERK-MAPK signaling coordinately regulates activity of Rac1 and RhoA for tumor cell motility." Cancer cell **4**(1): 67-79.
- Vicente-Manzanares, M., D. J. Webb, et al. (2005). "Cell migration at a glance." Journal of cell science **118**(Pt 21): 4917-4919.
- Vona-Davis, L., D. P. Rose, et al. (2014). "Breast cancer pathology, receptor status, and patterns of metastasis in a rural appalachian population." Journal of cancer epidemiology **2014**: 170634.
- Walker, R. A. (2001). "The complexities of breast cancer desmoplasia." Breast cancer research : BCR **3**(3): 143-145.
- Wang, J. W., S. Y. Peng, et al. (2009). "Identification of metastasis-associated proteins involved in gallbladder carcinoma metastasis by proteomic analysis and functional exploration of chloride intracellular channel 1." Cancer letters **281**(1): 71-81.
- Wang, L., S. He, et al. (2012). "Elevated expression of chloride intracellular channel 1 is correlated with poor prognosis in human gliomas." Journal of experimental & clinical cancer research : CR **31**: 44.
- Warton, K., R. Tonini, et al. (2002). "Recombinant CLIC1 (NCC27) assembles in lipid bilayers via a pH-dependent two-state process to form chloride ion channels with identical characteristics to those observed in Chinese hamster ovary cells expressing CLIC1." The Journal of biological chemistry **277**(29): 26003-26011.

- Wegner, B., A. Al-Momany, et al. (2010). "CLIC5A, a component of the ezrin-podocalyxin complex in glomeruli, is a determinant of podocyte integrity." American journal of physiology. Renal physiology **298**(6): F1492-1503.
- Wilce, M. C. and M. W. Parker (1994). "Structure and function of glutathione S-transferases." Biochimica et biophysica acta **1205**(1): 1-18.
- Williams-Ashman, H. G., A. C. Notides, et al. (1972). "Transamidase reactions involved in the enzymic coagulation of semen: isolation of -glutamyl- -lysine dipeptide from clotted secretion protein of guinea pig seminal vesicle." Proceedings of the National Academy of Sciences of the United States of America **69**(8): 2322-2325.
- Wojciak-Stothard, B., V. B. Abdul-Salam, et al. (2014). "Aberrant chloride intracellular channel 4 expression contributes to endothelial dysfunction in pulmonary arterial hypertension." Circulation **129**(17): 1770-1780.
- Wolf, K., I. Mazo, et al. (2003). "Compensation mechanism in tumor cell migration: mesenchymal-amoeboid transition after blocking of pericellular proteolysis." The Journal of cell biology **160**(2): 267-277.
- Wood, S., Jr. (1958). "Pathogenesis of metastasis formation observed in vivo in the rabbit ear chamber." A.M.A. archives of pathology **66**(4): 550-568.
- Wozniak, M., A. Fausto, et al. (2000). "Mechanically strained cells of the osteoblast lineage organize their extracellular matrix through unique sites of alphavbeta3-integrin expression." Journal of bone and mineral research : the official journal of the American Society for Bone and Mineral Research **15**(9): 1731-1745.
- Wulfkuhle, J. D., D. C. Sgroi, et al. (2002). "Proteomics of human breast ductal carcinoma in situ." Cancer research **62**(22): 6740-6749.
- Wushou, A., J. Hou, et al. (2014). "Twist-1 up-regulation in carcinoma correlates to poor survival." International journal of molecular sciences **15**(12): 21621-21630.
- Yakubov, B., B. Chelladurai, et al. (2013). "Extracellular Tissue Transglutaminase Activates Noncanonical NF-kappa B Signaling and Promotes Metastasis in Ovarian Cancer." Neoplasia **15**(6): 609-+.
- Yang, J. Y., J. Y. Jung, et al. (2009). "Chloride intracellular channel 1 regulates osteoblast differentiation." Bone **45**(6): 1175-1185.
- Yokoyama, K., N. Nio, et al. (2004). "Properties and applications of microbial transglutaminase." Applied microbiology and biotechnology **64**(4): 447-454.
- Yoshida, K. and T. Soldati (2006). "Dissection of amoeboid movement into two mechanically distinct modes." Journal of cell science **119**(Pt 18): 3833-3844.
- Yu, Q., B. P. Toole, et al. (1997). "Induction of apoptosis of metastatic mammary carcinoma cells in vivo by disruption of tumor cell surface CD44 function." The Journal of experimental medicine **186**(12): 1985-1996.
- Yu, Y., C. H. Xiao, et al. (2014). "Cancer-associated fibroblasts induce epithelial-mesenchymal transition of breast cancer cells through paracrine TGF-beta signalling." British Journal of Cancer **110**(3): 724-732.
- Zemskov, E. A., A. Janiak, et al. (2006). "The role of tissue transglutaminase in cell-matrix interactions." Frontiers in bioscience : a journal and virtual library **11**: 1057-1076.
- Zhong, J., X. Kong, et al. (2012). "Inhibition of CLIC4 enhances autophagy and triggers mitochondrial and ER stress-induced apoptosis in human glioma U251 cells under starvation." PloS one **7**(6): e39378.

Zhu, G. G., L. Risteli, et al. (1995). "Immunohistochemical study of type I collagen and type I pN-collagen in benign and malignant ovarian neoplasms." Cancer **75**(4): 1010-1017.